



**ROBERT GORDON
UNIVERSITY • ABERDEEN**

OpenAIR@RGU

The Open Access Institutional Repository at Robert Gordon University

<http://openair.rgu.ac.uk>

Citation Details

Citation for the version of the work held in 'OpenAIR@RGU':

LABOVITIADI, O., 2011. Antimicrobial wafers as a novel technology for infection control in chronic wounds. Available from *OpenAIR@RGU*. [online]. Available from: <http://openair.rgu.ac.uk>

Copyright

Items in 'OpenAIR@RGU', Robert Gordon University Open Access Institutional Repository, are protected by copyright and intellectual property law. If you believe that any material held in 'OpenAIR@RGU' infringes copyright, please contact openair-help@rgu.ac.uk with details. The item will be removed from the repository while the claim is investigated.

ANTIMICROBIAL WAFERS AS A NOVEL TECHNOLOGY
FOR INFECTION CONTROL IN CHRONIC WOUNDS

OLGA LABOVITIADI

PhD

2011

ANTIMICROBIAL WAFERS AS A NOVEL TECHNOLOGY
FOR INFECTION CONTROL IN CHRONIC WOUNDS

OLGA LABOVITIADI

Thesis submitted in partial fulfilment of the
requirements of the
Robert Gordon University
for the degree of Doctor of Philosophy

September 2011

DECLARATION

This thesis has been composed by myself and has not been submitted in any previous application for a higher degree. The work that is documented was carried out by myself. All verbatim extracts have been distinguished by quotation marks and the source of information specifically acknowledged.

Olga Labovitiadi

Abstract

Bacterial contamination and persistent infection is a common cause of impaired wound healing. Generally, non-healing wounds display similar physiological features with regards to mixed bacterial flora, ischemia and production of exudate. The application of topical, broad spectrum antimicrobial compounds embedded in absorbent dressings has been shown to control bioburden and improve healing. Lyophilised, biopolymeric antimicrobial wafers can offer a contemporary, user-friendly, self-adhesive and effective approach for the management of suppuration and polybacterial contamination in a wide range of non-healing wounds.

Cohesive, non-friable, porous, disc shape wafers were successfully produced with sodium alginate (SA) (18.17 ± 0.70 Pa.s), guar gum (GG) (82.21 ± 5.41 Pa.s; 95.87 ± 2.31 Pa), xanthan gum (XG) (2.86 ± 0.12 Pa.s; 23.61 ± 0.68 Pa), karaya gum (KAG) (12.89 ± 0.93 Pa.s) and an original gel consisting of a blend of a synergistic SA-KAG (7.75 ± 0.64 Pa.s; 86.34 ± 5.19 Pa) (1:1 ratio). Clinical concentrations of the broad spectrum, topical, antimicrobial compounds, neomycin sulphate (0.5 % w/v NS), chlorhexidine digluconate (0.5 % v/v CHD), povidone iodine (1.0 % v/v PVP-I) and silver sulfadiazine (1.0 % w/v SS) were mixed with compatible biopolymers and appeared to alter the rheological properties of the biopolymers. Rheological analysis of pre-lyophilised gels was undertaken to quantify the flow properties of the gels. The necessity of producing sterile wafers was investigated by exposing all biopolymer-antimicrobial combinations to 25 and 40 kGy of gamma irradiation. Gamma-rays caused total degradation of GG, KAG, SA and SA-KAG, while XG appeared to withstand irradiation.

A novel free standing dissolution raft (FSDR) was designed and used to quantify the CHD released from both gels and wafers. CHD released from wafers ranged from 3.5 ± 0.01 to 17.4 ± 0.39 %. Gels and wafers released CHD in a sustained manner and the release profile of wafers was similar to the respective gels, with the exception of GG. Neither gels nor wafers released 100 % of the incorporated antimicrobial indicating that drug-polymer interactions governed the general performance of antimicrobial wafers, in terms of adhesion, expansion ratio (ER), inhibition ratio (IR), water uptake capacity (WUC) and antimicrobial delivery. Molecular modelling studies

undertaken for KAG-antimicrobial complexes demonstrated an unusual 'Z-shape' geometry for cationic CHD. The charge and geometry of CHD was plausibly responsible for the antimicrobial's entrapment within biopolymeric networks.

The efficacy of antimicrobial wafers was demonstrated *in vitro* under simulated conditions of an exuding wound using modified disc diffusion and an original antimicrobial diffusion cell (ADC). All wafers were effective *in vitro* against common chronic wound pathogens of such as methicillin-resistant *Staphylococcus aureus* (MRSA), methicillin-sensitive *Staphylococcus aureus* (MSSA), *E. coli* and *P. aeruginosa*. Antimicrobial activity depended on the sensitivity of the microorganisms to a specific antimicrobial compound and the presence of organic material. Data obtained demonstrated that the presence of protein (BSA) in the pseudo-exudate inhibited the antimicrobial activity of CHD and PVP-I, while enhancing the antimicrobial activity of SS and NS against MRSA.

The general findings summarised in this thesis conclude that factors such as protein content, electrolyte content and pH of exudate play a key role in the efficacy of self-adhesive, absorbent formulations intended for the topical delivery of antimicrobial compounds to non-healing, infected wounds. Drug-polymer interactions developed between biopolymers and incorporated antimicrobial compounds have a profound effect on the general performance of lyophilised antimicrobial wafers.

Acknowledgments

I would like to thank and to acknowledge all the people that helped, supported and encouraged me over the four years of my PhD. In particular, I am thankful to:

My principal supervisor, Dr. Kerr H Matthews, for his useful advice, support, patience, help and guidance on formulation and material science and scientific writing.

My second supervisor, Dr. Andrew J Lamb, for being always supportive and optimistic and for his valuable advice and help in the microbiological part of the project.

Prof. Donald Cairns for his time, help, advice and guidance on the molecular modelling work.

Dr. Colin J Thomson and Dr. Alberto Di Salvo for their much appreciated help with the TA and NMR, respectively.

Dr. Hector Williams and Dr. Martin O'Driscoll for their guidance and valuable help with statistics.

Miss Vivienne Hamilton for her valuable assist, guidance and technical support in the microbiology labs. I would like to express my gratitude to the other technicians, Moira Innes, Liz Hendrie, Laurie Mearns-Smith, Dorothy Moir, Margaret Brown, Brain De Jonckheere. I would like also to thank the engineering workshop staff, Martin and Steve, for their help in constructing of the FSDR.

Dr. Noëlle O'Driscoll for being always supportive for good and bad days. I would like to express my gratitude to her for the wonderful times we spent together in the lab, for her valuable advice, philosophical chats, discussions and laughs during lunch and tea breaks. I am thankful, also, to Dr. Ania Gryka and Dr. Pramod Gadad for the enjoyable Research Student Association days and all the events that we organised and enjoyed together.

Konstantine Chalatsopoulos for being a great friend and partner. I would like to thank him from the bottom of my heart for his profound love, support and faith in me. I am also deeply appreciative of my family and relatives for always being supportive in all my endeavours.

To my Mother Vasiliki

List of publications/presentations/awards

2010 UK-PharmSci–Nottingham, Podium presentation/Abstract:

LABOVITIADI, O., LAMB, A., MATTHEWS, K., 2010. Sustained release of Chlorhexidine from lyophilized wafers. *Journal of Pharmacy and Pharmacology*, 62 (10), pp. 1303.

2010 EWMA-Geneva, Podium presentation/Abstract/First Time International Presenter's Prize:

LABOVITIADI, O., LAMB, A., MATTHEWS, K., 2010. Formulation and evaluation of antimicrobial wafers as a novel technology for infection control in chronic wounds. *European Wound Management Journal*, 70 (Supplement).

2009 Royal Pharmaceutical Society of Great Britain, London, Podium presentation/Abstract:

LABOVITIADI, O., CAIRNS, D., LAMB, A., MATTHEWS, K., 2010. Molecular modelling study on the components of antimicrobial wafers. Recent developments in wound management: intelligent biomaterials to novel antimicrobials.

2009 British Pharmaceutical Conference, Manchester, Podium presentation/Abstract:

LABOVITIADI, O., LAMB, A., MATTHEWS, K., 2009. Modified Franz diffusion for the *in vitro* determination of the efficacy of antimicrobial wafers against methicillin-resistant *Staphylococcus aureus* (MRSA). *Journal of Pharmacy and Pharmacology*, 61(Supplement), A19, 27.

2009 Society for General Microbiology, Spring Meeting, Harrogate, UK, Podium presentation/Abstract:

LABOVITIADI, O., LAMB, A., MATTHEWS, K., 2009. Novel antimicrobial wafers for topical drug delivery against *Staphylococcus aureus*. (Har12/05, 42).

2008 British Pharmaceutical Conference, Manchester, Abstract:

MATTHEWS, K., LABOVITIADI, O., LAMB, A., 2008. Rheological investigation of some common polymer gels and their synergistic combinations. *Journal of Pharmacy and Pharmacology*, 60 (Supplement 1), A42, 105.

2008 British Pharmaceutical Conference, Manchester, Podium presentation/Abstract/ Poster First Prize:

LABOVITIADI, O., LAMB, A., MATTHEWS, K., 2008. Microbiological (MRSA) and rheological testing of antimicrobial karaya wafers. *Journal of Pharmacy and Pharmacology*, 60 (Supplement), A-15, 36.

Table of Contents

Abstract.....	iv
Acknowledgments	vi
List of publications/presentations/awards.....	viii
List of Tables	xiii
List of Figures.....	xvi
Abbreviations	xxi
Chapter 1 Introduction to Chronic Wounds.....	1
1.1 Prevalence of chronic wounds	2
1.2 The healing process.....	3
1.3 Pathophysiology of three major categories of non-healing wounds.....	10
1.3.1 Burns	10
1.3.2 Pressure ulcers.....	11
1.3.3 Neuropathic (diabetic) ulcers.....	11
1.4 Exudate profile of non-healing wounds.....	12
1.5 Ischemia	15
1.6 Bacterial infection.....	15
1.7 Chronic wounds in both hospital and community acquired MRSA	19
1.8 Control of bacterial bio-burden (systemic or topical treatment)	21
1.9 Debridement.....	21
1.10 The role of topical antimicrobials	22
1.11 The role of growth factors in the treatment of non-healing wounds...	27
1.12 Other popular and supplementary treatments	28
1.12.1 Honey	28
1.12.2 Vitamin and mineral supplements	30
1.13 Wound management.....	31
1.14 Existing topical applications	31
1.14.1 Alginate dressings.....	34

1.14.2 Hydrogel dressings.....	35
1.14.3 Hydrocolloid dressings	36
1.15 Advanced and innovative applications	37
1.15.1 Lyophilised wafers as innovative potential dressings	39
1.16 Project design	40
1.16.1 Aims	41
Chapter 2 Formulation of lyophilised antimicrobial wafers	42
2.1 Aim	43
2.2 Introduction	43
2.3 Materials and methods.....	44
2.3.1 Materials	44
2.3.2 Methods	44
2.3.3 Preparation of silver sulfadiazine (SS) gels.....	44
2.3.4 Binary gel synergies.....	45
2.3.5 Rheological measurements	45
2.3.6 Freeze drying process	46
2.3.6.1 Batches of lyophilised formulations.....	46
2.3.7 Thermogravimetric (TGA) analysis of the lyophilised wafers	46
2.3.8 Scanning electron microscopy (S.E.M).....	47
2.3.9 <i>In vitro</i> determination of adhesive properties of lyophilised wafers to a model agar surface.....	47
2.4 Statistical analysis.....	48
2.5 Results	49
2.6 Discussion	63
Chapter 3 <i>In vitro</i> evaluation of the efficacy of lyophilised antimicrobial wafers.....	72
3.1 Aim	73
3.2 Introduction	73
3.3 Materials and Methods	75

3.3.1 Materials	75
3.3.2 Methods	75
3.3.2.1 Bacterial storage and preparation.....	75
3.3.2.2 Determination of minimum inhibitory concentration (MIC) and minimum bactericidal concentration (MBC) of antimicrobials.....	76
3.3.2.3 Modified disc diffusion assay as a simple model of an exuding surface	76
3.3.2.4 <i>In vitro</i> assessment of the efficacy of antimicrobial wafers using a diffusion cell	78
3.4 Statistical analysis.....	80
3.5 Results	81
3.6 Discussion	90
Chapter 4 Release studies of chlorhexidine digluconate (CHD) from lyophilised wafers and gels	102
4.1 Aim	103
4.2 Introduction	103
4.3 Materials and methods.....	104
4.3.1 Materials	104
4.3.2 Methods	104
4.3.2.1 <i>In vitro</i> release of CHD from lyophilised wafers and gels	104
4.3.2.2 Calculation of the water uptake capacity (WUC) (%) for lyophilised wafers in NaCl-CaCl ₂ dissolution medium.....	106
4.3.2.3 Analysis of drug release kinetics.....	106
4.4 Data analysis.....	107
4.5 Results	108
4.6 Discussion	115
Chapter 5 Physicochemical and antimicrobial properties of gamma- irradiated lyophilised wafers	122
5.1 Aim	123
5.2 Introduction	123

5.3 Materials and methods.....	124
5.3.1 Materials	124
5.3.2 Methods	124
5.3.1 Gamma-irradiation sterilisation of lyophilised wafers	124
5.3.2 Microbiological validation of sterility of irradiated products	124
5.3.3 Structural validation of antimicrobial compounds	125
5.3.4 Rheological analysis of irradiated polymers and lyophilised formulations as reconstituted gels.....	125
5.3.5 Antimicrobial properties of irradiated lyophilised formulations	126
5.3.6 Release profile, swelling properties and kinetics of CHD release from gamma-irradiated SA-CHD wafers.....	126
5.4 Data analysis.....	127
5.5 Results	128
5.6 Discussion	157
Chapter 6 <i>In silico</i>, molecular modelling studies on the components of karaya (KAG) antimicrobial wafers.....	168
6.1 Aim	169
6.2 Introduction	169
6.3 Materials and methods.....	171
6.4 Results	176
6.5 Discussion	183
Chapter 7 General discussion	189
7.1 General discussion and future work	190
7.2 Conclusions and future work.....	200
7.2.1 Conclusions.....	200
7.2.2 Future work	200
REFERENCES.....	202

List of Tables

Chapter 1 Introduction to chronic wounds

1.1	Main ECM components and their function.....	5
1.2	Phases of wound healing.....	9
1.3	Constituents of exudate and their function in wound healing.....	14
1.4 (a)	Aerobic and facultative aerobic isolates from chronic wounds with varied aetiology	16
1.4 (b)	Anaerobic isolates from chronic wounds with varied aetiology....	17
1.5	Main characteristic of some modern dressings based on their ability to handle exudate.....	34

Chapter 2 Formulation of lyophilised antimicrobial wafers

2.1	Qualitative analysis of physical compatibility (pre-lyophilisation) and friability (post-lyophilisation) between combinations of natural polymers and antimicrobials.....	49
2.2	Viscosity coefficient and yield stress for four natural polymers and their mixtures in aqueous solution.....	51
2.3	Viscosity coefficient of KAG in combination with clinical concentrations of antimicrobials.....	52
2.4	Viscosity coefficients and yield stresses of pre-lyophilised gels (controls) and CHD-containing gels of GG, SA, XG and the binary mixture of SA-KAG.....	55
2.5	TGA of water content of KAG lyophilised wafers.....	56
2.6	Adhesion properties of KAG lyophilised wafers impregnated with clinical concentrations of antimicrobial compounds.....	60
2.7	Adhesion properties of lyophilised wafers prepared with different biopolymers impregnated with clinical concentrations of CHD....	60

Chapter 3	<i>In vitro</i> evaluation of the efficacy of lyophilised antimicrobial wafers	
3.1	MIC and MBC values of antimicrobial compounds tested against common pathogens of chronic wounds.....	81
Chapter 4	Release studies of chlorhexidine digluconate (CHD) from lyophilised wafers and gels	
4.1	Values of the diffusion exponent and solute drug release mechanism of cylindrical shaped polymeric systems.....	109
4.2	Stability of CHD aqueous solutions at different temperatures...	109
4.3	Accumulation of CHD from gels and wafers impregnated.....	111
4.4	Values of the release exponent and the correlation coefficient of CHD released from gels and wafers.....	114
Chapter 5	Physicochemical and antimicrobial properties of gamma-irradiated lyophilised wafers	
5.1	Microbiological validation of raw polymers.....	128
5.2	Microbiological validation of control lyophilised wafers.....	128
5.3	Microbiological validation of KAG antimicrobial wafers.....	129
5.4	Microbiological validation of lyophilised CHD wafers prepared with different biopolymers.....	129
5.5	Viscosity coefficients and yield stresses of non-irradiated and irradiated pre-lyophilised gels.....	139
5.6	Viscosity coefficient of KAG pre-lyophilised antimicrobial gels and irradiated and non-irradiated post-lyophilised KAG gels.....	141
5.7	Rheological properties of irradiated non-irradiated, antimicrobial-free, post-lyophilised gels, prepared from different biopolymers.....	144

5.8	Rheological properties, of non-irradiated and irradiated, CHD-loaded, post-lyophilised gels, prepared from different biopolymers.....	145
5.9	Accumulation of CHD released from irradiated SA-CHD wafers and values of the release exponent and the correlation coefficient.....	156
Chapter 6	<i>In silico</i>, molecular modelling studies on the components of karaya (KAG) antimicrobial wafers	
6.1	Optimal docking energies of KAG with the incorporated drugs.....	179
6.2	Binding enthalpies of compounds and complexes calculated at 300 K.....	180
6.3	Binding enthalpies of compounds and complexes calculated at 500 K.....	180
6.4	Sugars present in karaya gum.....	181

List of Figures

Chapter 1 Introduction to chronic wounds

1.1	A diagrammatical cross-section through human skin.....	3
1.2	Chemical structure of chlorhexidine.....	23
1.3	Chemical structure of silver sulfadiazine.....	24
1.4	Chemical structure of polyvinylpyrrolidone-iodine complex.....	25

Chapter 2 Formulation of lyophilised antimicrobial wafers

2.1	Particle size distribution curve for SS suspension, prepared in distilled water with non-ionic surfactant pluronic F68.....	50
2.2	Rheological analysis of pre-lyophilised gels of flow curves of SA, KAG and the synergistic combination of SA-KAG.....	51
2.3	Rheological analysis of flow curves of KAG control and antimicrobial gels.....	52
2.4	Rheological analyses of pre-lyophilised gels of CHD embedded in GG, XG, SA and binary gel synergy of SA-KAG.....	54
2.5	Temperature profile of the freeze-drying process.....	56
2.6	S.E.M images of wafer matrices top surfaces of different biopolymeric wafers controls and CHD-loaded.....	57
2.7 (a)	S.E.M images of KAG, KAG-NS, KAG-CHD and KAG-(PVP-I).....	59
2.7 (b)	S.E.M images of KAG-SS of top and bottom surfaces.....	59
2.8	Tensile stress of KAG lyophilised wafers.....	61
2.9	Tensile stress of GG, XG, SA and SA-KAG lyophilised wafers controls and CHD-loaded.....	62

Chapter 3	<i>In vitro</i> evaluation of the efficacy of lyophilised antimicrobial wafers	
3.1	Aerial view of disc diffusion measurements.....	77
3.2	Schematic of the ADC assembly.....	79
3.3	Expansion ratio of KAG wafers prepared with clinical concentrations of NS, PVP-I, CHD and SS.....	82
3.4	Inhibition ratio of KAG wafers prepared with clinical concentrations of NS, PVP-I, CHD and SS.....	83
3.5	Expansion ratios of wafers prepared with different biopolymers impregnated with CHD.....	84
3.6	Inhibition ratios of wafers prepared with different biopolymers and impregnated with CHD tested against <i>P. aeruginosa</i>	85
3.7	Correlation of ER/IR for CHD impregnated wafers.....	86
3.8	Viability of MRSA in the ADC suspended in PBS.....	87
3.9	Viability of MRSA in the ADC suspended in NaCl-CaCl ₂	88
3.10	Viability of MRSA in the ADC suspended in NaCl-CaCl ₂ enriched with BSA as a model organic material.....	89
Chapter 4	Release studies of chlorhexidine digluconate (CHD) from lyophilised wafers and gels	
4.1	Configuration of the free standing dissolution raft (FSDR) device.....	105
4.2	Determination of UV wavelengths of CHD solution.....	108
4.3	Standard UV calibration curve of CHD in NaCl-CaCl ₂ solution at 254 nm.....	108

4.4	Dissolution profiles of CHD- impregnated biopolymeric gels and wafers.....	110
4.5	Water uptake capacity of re-hydrated wafers within 24 hours, placed on the FSDR.....	112
4.6	Linear regression of released CHD from gel and wafers.....	113
Chapter 5	Physicochemical and antimicrobial properties of gamma-irradiated lyophilised wafers	
5.1	Typical images taken after 24 hours incubation of KAG-SS wafers (non-irradiated and irradiated) tested on a modified disc diffusion assay.....	127
5.2	¹³ C NMR spectra of CHD.....	131
5.3	UV analysis of gamma-irradiated aqueous solutions of chlorhexidine digluconate.....	132
5.4	¹³ C NMR spectra of NS.....	134
5.5 (a)	¹ H NMR spectra and HSQC of SS.....	135-136
5.6	Plots of natural logarithm of shear stress as a function of ln shear rate for non-irradiated and irradiate pre-lyophilised gels of GG, KAG, SA, XG and SA-KAG.....	138
5.7	Plots of natural logarithm of shear stress as a function of ln shear rate of non-irradiated and irradiated post-lyophilised KAG gels containing different antimicrobials.....	141
5.8	Plots of natural logarithm of shear stress as a function of ln shear rate for non-irradiated and irradiated post-lyophilised gels of controls SA and XG and CHD-loaded respectively.....	143
5.9	Expansion and inhibition ratios of irradiated KAG antimicrobial wafers tested with a modified disc diffusion assay against common bacterial strains of infected, non-healing wounds.....	147

5.10	Images of irradiated KAG wafers impregnated with clinical concentrations of broad spectrum antimicrobials, tested against MRSA in the modified disc diffusion assay.....	148
5.11	Linear regression analysis of IR vs. ER of KAG wafers (non-irradiated and irradiated) containing of NS.....	149
5.12	Linear regression analysis of IR vs. ER of KAG wafers (non-irradiated and irradiated) containing of CHD.....	150
5.13	Linear regression analysis of IR vs. ER of KAG wafers (non-irradiated and irradiated) containing of PVP-I.....	151
5.14	Linear regression analysis of IR vs. ER of KAG wafers (non-irradiated and irradiated) containing of SS.....	152
5.15	Expansion and inhibition ratios of irradiated wafers prepared with a clinical concentration of CHD incorporated within different biopolymers matrices against <i>P. aeruginosa</i>	153
5.16	Linear regression analysis of IR vs. ER of CHD wafers (non-irradiated and irradiated) prepared with different biopolymers, when tested against <i>P. aeruginosa</i>	154
5.17	Dissolution profiles of SA wafers irradiated impregnated with a clinical concentration of CHD in NaCl-CaCl ₂ dissolution medium.....	155
5.18	Water uptake of rehydrated SA-CHD wafers irradiated at 24 hours, placed on the FSDR.....	155
5.19	Linear regressions of CHD released from irradiated SA-CHD as analysed with the Korsmeyer-Peppas model.....	156
Chapter 6	<i>In silico</i>, molecular modelling studies on the components of karaya (KAG) antimicrobial wafers	
6.1	Summarised work diagram of the molecular modelling stages.....	172

6.2	A schematic one-dimensional energy surface of small molecules and folding-energy landscape of biological heterogeneous polymer.....	174
6.3	Schematic folding pathways of polymers, used to reach a global minimum energy conformation.....	175
6.4	Molecular modelling CPK configurations of minimised structures of KAG polymer and selected antimicrobials.....	176
6.5	Molecular modelling of minimised CPK configurations of KAG – antimicrobial complexes.....	178
6.6	Proposed model for <i>Sterculiaceae</i> gelation.....	182
6.7	A plausible block configuration of karaya gum.....	182
 Chapter 7 General discussion and future work		
7.1	A plausible block configuration of sodium alginate interlinked with CHD.....	195

Abbreviations

ADC	antimicrobial diffusion cell
BSA	bovine serum albumin
Ca²⁺	calcium ion
CA-MRSA	community associated MRSA
cff91	consistent family of force fields
cfu	colony forming unit
CHD	chlorhexidine digluconate
Cl⁻	chloride ion
CMC	carboxymethylcellulose
CPK	Corey-Pauling-Koltum
cvff	consistent valence force field
D₂O	deuterium oxide
DNA	deoxyribonucleic acid
DSC	differential scanning calorimetry
DVA	dynamic vapour sorption
ECM	extracellular matrix
EGF	epidermal growth factor
EMC	equilibrium moisture content
ER	expansion ratio
F68	pluronic F68
FGF-β	fibroblast growth factors beta
FSDR	free standing dissolution raft
FTIR	fourier transform infrared spectroscopy
FTRS	fourier transform Raman spectroscopy
GG	guar gum
HA	hyaluronic acid
HAI	hospital acquired infection
hGH	human growth hormone
HIV	human immunodeficiency virus
HSQC	heteronuclear single quantum coherence
IGF-1	insulin-like growth factor one
INF	infinity (∞)
IR	inhibition ratio

K	Kelvin
K⁺	potassium ion
KAG	karaya gum
KC	kappa-carrageenan
kGy	kilo Gray
log	logarithm
ln	natural logarithm
MBC	minimum bactericidal concentration
MC	methylcellulose
MD	molecular dynamics
MIC	minimum inhibitory concentration
MMPs	metalloproteinase enzymes
MRSA	methicillin resistant <i>S. aureus</i>
MSSA	methicillin sensitive <i>S. aureus</i>
Na⁺	sodium ion
NCCLS	National Committee of Clinical Laboratory Standards
NCTC	National Collection of Type Culture
NHS	National Health Service
NINSS	Nosocomial Infection National Surveillance Service
NMR	nuclear magnetic resonance
NS	neomycin sulphate
OH	hydroxyl group
PDGF	platelet-derived growth factors
PEO	polyethylene oxide
PM3	parametric method three
PVP-I	poly (vinyl pyrrolidone) iodine
RCLSM	rapid confocal laser scanning microscopy
RCPE	Royal College of Physicians Edinburgh
SAL	sterility assurance level
SA	sodium alginate
SDA	sabouraud dextrose agar
SEM	standard error of mean
S.E.M	scanning electron microscopy
SS	silver sulfadiazine
T_g	glass transition temperature

TGA	thermogravimetric analysis
TGF-β	transforming growth factor beta
TFA-d	deuterium trifluoroacetic acid
TIMPs	tissue inhibitors of metalloproteinases
TNF-α	tumour necrosis factor alpha
TNF-β	tumour necrosis factor beta
TSA	tryptone soya agar
UK	United Kingdom
USA	United States of America
UV	ultraviolet
VEGF	vascular endothelial growth factor
VRE	vancomycin-resistant enterococci
WUC	water uptake capacity
XG	xanthan gum

Chapter 1

Introduction to Chronic Wounds

1.1 Prevalence of chronic wounds

In the United Kingdom (UK), chronic wounds are a considerable burden to patients and the National Health Service (NHS). It has been estimated that around 200,000 patients suffer from a chronic wound, where the most affected population is over the age of 65. In particular, the prevalence of venous leg ulcer ranges from 1.2 - 3.2 per 1000 people. The number of patients who develop pressure ulcers in the UK is estimated to be around 400,000 annually. In addition, around 64,000 individuals suffer from an active foot ulcer as a common complication of diabetes. Apart from the fact that chronic wounds are a major source of pain and disability for patients, their treatment involves a considerable economic budget. The cost absorbed for the treatment of patients with chronic wounds has been estimated as £ 2.3 – 3.1 billions per year, which was around 3 % of the total expenditure on health during 2005 - 2006. Future trends in the UK population are likely to lead to a significant increase in the incidence of chronic wounds over the next 20 years. This increase in numbers of chronic wounds in the UK will be associated mainly with a 36 % increase in population aged over 65 and also due to an increase of lifestyle diseases, including diabetes, obesity and cardiovascular diseases (Posnett and Franks 2008).

With this in mind, this introductory review, aims to provide background information on wound healing and key factors that delay or prevent it. In addition, it will discuss the impact of chronic wounds in hospitals, community acquired infections and the use and role of antibiotics or antimicrobials. It will also focus on existing therapies and topical delivery of therapeutic compounds via polymeric biomaterials, where emphasis will be given to the delivery of antimicrobial compounds in a sustained fashion. Furthermore, it will discuss and provide information on the formulation of novel delivery systems, such as lyophilised wafers, and their potential role as contemporary formulations in wound management.

1.2 The healing process

Human skin is a complex and uniquely constructed organ consisting of approximately 10 % of the body mass of an average person. The functions of healthy skin are vital and include protection, thermoregulation and preservation of body fluids. In addition, intact skin plays a key role in metabolic functions such as the vitamin D metabolism, neurosensory and immunological functions (Church et al. 2006; Williams 2003). For the purposes of transdermal and topical drug delivery, the structure and function of human skin can be classified into four main parts as presented in Figure 1.1 (Williams 2003):

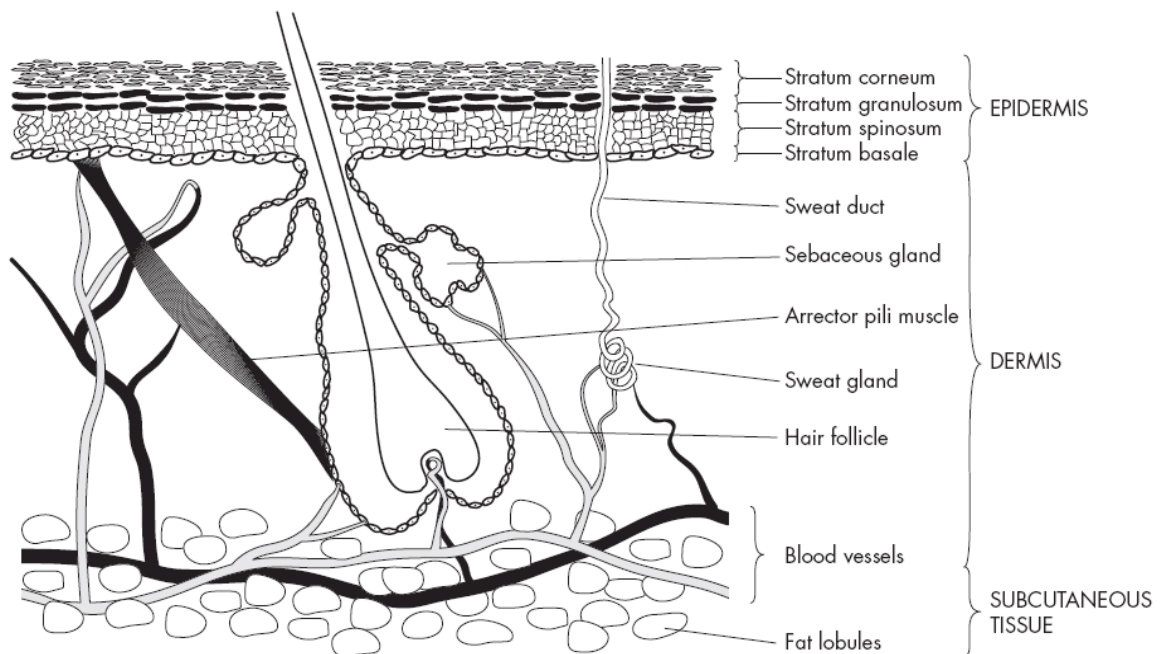


Figure 1.1 A diagrammatical cross-section through human skin (Adapted from Williams 2003)

- the stratum corneum is the exterior, non-viable epidermal layer.
- the epidermis is a viable, but non-vascular layer that varies in thickness (0.06 - 0.8 mm) over different body surfaces.
- the dermis is the vital layer of the human skin (3 - 5 mm thick) which consists of connective tissue such as collagen fibrils and elastine, blood and lymphatic vessels, sebaceous glands, nerve endings and sweat glands. The largest component of the dermis is the extracellular matrix (ECM), which is composed of a variety of polysaccharides and collagen proteins that provide strength, elasticity and compressibility to the skin. In addition, this layer is capable of regenerating new epithelial cells to replace the lost and/or damaged ones and therefore plays an important role in wound healing (Schultz et al. 2005). Table 1.1 summarizes the main component molecules and their function in the properties of the dermal skin and their role in the healing process.
- the hypodermis is the inner subcutaneous fat layer which mainly provides insulation and physical protection.

Table 1.1 Main ECM components and their function (Schultz et al. 2005)

ECM Components	Function
Collagen type I (80 – 85 %) and collagen type III (8 – 11 %)	Tensile strength and stability
Elastin	Elasticity (resilience to recoil after stretching)
Fibronectin (glycoprotein of both plasma and tissue)	Interacts with different types of ECM molecules stimulating cell signalling and promoting cell attachment, migration and differentiation
Hyaluronic acids (HA)	HA increases in damaged tissue stimulating cytokine production of macrophages and promoting angiogenesis
Proteoglycans	Facilitate the lubrication around and between cells. Prolongs the inflammatory response by binding chemokine molecules on the surface of endothelial cells

Wounds occur when the integrity of the skin tissue is disrupted. The most common causes of tissue trauma which can lead to skin wounds are as follows: physical and chemical traumas; pressure sores (vascular compromised, arterial, venous or mixed); neuropathic and metabolic diseases including diabetes; neoplastic malignancies; immunodeficiency (HIV patients); autoimmune and haematologic diseases and skin infections from bacterial, fungal and viral organisms (Keast and Orsted 1998).

Tissue injury triggers a cascade of events between ECM and blood molecules aimed at quick repair (Table 1.2). Wound healing is generally considered to be a complicated but very orderly process, which includes four overlapping phases: haemostasis, inflammation, proliferation and remodelling. Each phase is mediated by specific biological markers and has a certain time limit during the normal healing process. Cell-ECM and cell-cell interactions are essential at all stages of this process and are mediated by different cytokines and growth factors. Each cytokine is responsible for multiple actions at the various phases of the healing process and their effect is almost never restricted to one single phase of healing (Jurjus et al. 2006).

Immediately after injury, formation of a fibrin plug (coagulation) consisting of platelets, provide an instant protection to the external environment and a temporary wound coverage. At the same time, the aggregations of platelets within the fibrin plug are also needed for the initiation of haemostasis (Falanga 2005). During haemostasis, blood platelets, the main mediators of the process, come into contact with collagen and other components of the extracellular matrix (Diegelmann and Evans 2004). This contact activates the platelets to produce clotting factors, essential growth factors such as platelet-derived growth factor (PDGF), transforming growth factor beta (TGF- β), insulin-like growth factor 1 (IGF-1), epidermal growth factor (EGF) and other cytokines. These growth factors start the wound healing cascade by the activation of polymorpho-nuclear leucocytes (PMNLs), macrophages and fibroblasts. In addition, the triggered platelets release vasoactive amines such as serotonin that increase the microvascular permeability. An overlap between haemostasis and inflammation occurs as the neutrophils then enter the wound site and phagocytosis (removal of foreign materials, bacterial and damaged tissue) begins (Diegelmann and Evans 2004). This process is completed by the presence of macrophages, which are

the most important cells in the late inflammatory (42 - 72 hours) phase, and not only by continuing phagocytosis and the production of growth factors such as TGF- β and PDGF, but also by acting as key regulatory cells for proliferation, producing tumour necrosis factor alpha (TNF- α) and matrix metalloproteinase enzymes (MMPs) (Enoch and Price 2004).

Proliferation commences at about 72 hours after injury, and is characterised by the migration of fibroblasts activated by TGF- β and PDGF. Fibroblasts have the main role in the formation and regeneration of ECM. They are responsible for the production of the main proteins of ECM such as fibronectin, hyaluronan and later on, collagen and proteoglycans. In addition, proliferation is completed with collagen synthesis, angiogenesis, granulation tissue formation and epithelialisation. Collagen synthesis and granulation tissue formation occur as the result of fibroblast migration. Angiogenesis is the process during which new blood vessels are formed and occurs during all stages of the healing process. The macrophages, in particular, play a major role in angiogenesis by releasing a number of angiogenic factors such as TNF- α , TNF- β , PDGF and fibroblast growth factor beta (FGF- β) (Enoch and Price 2004).

The remodelling phase and matrix synthesis start simultaneously with the development of granulation tissue and continues over a prolonged period of time. The cross-linked collagen results from continuously ongoing collagen synthesis and its breakdown as ECM is continually remodelled. The equilibrium between reconstruction and degradation of collagen matrix is maintained by specific matrix metalloproteinases (MMPs) and tissue inhibitors of metalloproteinases (TIMPs) (Enoch and Price 2004).

The family of MMPs are produced by many cells during the healing process such as macrophages, fibroblasts and endothelial cells (Mannelo and Raffetto 2011). The most important of these MMPs are: MMP-1 (collagenase); MMP-2 and MMP-9 (gelatinase); and MMP-3 (stromelysin), which cut intact collagen at a single site, degrade partially denatured collagen and multiply protein substrate in the ECM, respectively. The role of the MMPs is important in the remodelling phase as they facilitate specific interactions between collagen molecules that result in the formation of new, strong collagen fibrils (Schultz et al. 2005). As remodelling in the wound site continues, MMP activity decreases and the activity of tissue inhibitors of metalloproteinases (TIMPs)

increases (Enoch and Price 2004). However, this process is carefully controlled and equilibrium is maintained by TGF- β , which promotes matrix accumulation (Diegelmann and Evans 2004).

Although most dermal wounds heal in an uncomplicated fashion following the aforementioned process, there are a large number of non-healing wounds that fall into three major categories: burns, pressure ulcers and diabetic ulcers. In these types of wounds, the normal healing has been disrupted in more than one stage, where the type, size and depth of the wound influences the continuation of healing phases at both cellular and molecular levels (Falanga 2005). Despite the differences in origin of non-healing wounds, these wound types display common clinical features which include: the presence of necrotic and unhealthy tissue, excess exudate and slough, lack of adequate blood supply, absence of healthy granulation tissue, failure of re-epithelialisation, cyclical and persistent pain, recurrent wound breakdown and clinical and sub-clinical infection. However, each category also presents specific dissimilarities that have to be appreciated for effective therapy (Enoch and Price 2004).

Table 1.2 Phases of wound healing (Adapted from Falanga 2005).

Time	Phase	Main cell type	Specific event
<p style="text-align: center;">↓</p> <p style="text-align: center;">Hours</p> <p style="text-align: center;">↓</p> <p style="text-align: center;">Days</p> <p style="text-align: center;">↓</p> <p style="text-align: center;">Weeks to months</p>	<p style="text-align: center;">Coagulation</p> <p style="text-align: center;">Fibrin plug formation, release of growth factors, cytokines, hypoxia</p> <p style="text-align: center;">↓</p>	Platelets	Platelet aggregation and release of fibrinogen fragments and other proinflammatory mediators
	<p style="text-align: center;">Inflammation</p> <p style="text-align: center;">Cell recruitment and chemotaxis, wound debridement</p> <p style="text-align: center;">↓</p>	Neutrophils, monocytes	Selectins slow down blood cells and binding to integrins – diapedesis
	<p style="text-align: center;">Migration/proliferation</p> <p style="text-align: center;">Epidermal resurfacing, fibroplasia, angiogenesis, ECM deposition, contraction</p> <p style="text-align: center;">↓</p>	Macrophages	Hemidesmosome breakdown – keratinocyte migration
	<p style="text-align: center;">Remodelling</p> <p style="text-align: center;">Scar formation and revision, ECM degradation, further contraction and tensile strength</p>	Keratinocytes, fibroblasts, endothelial cells	Cross-talk between MMPs, integrin cells, cytokines – cell migration, ECM production
			Myofibroblasts

1.3 Pathophysiology of three major categories of non-healing wounds

1.3.1 Burns

Serious thermal injury resulting from a burn causes total loss of the skin surface over large areas of the body. This results in cellular damage, alteration of molecular conformation and disruption of intermolecular bonds to the skin (Church et al. 2006). High temperatures applied to the skin surface lead to cell membrane dysfunction, protein denaturation and eventually death of the cell, with the formation of burn eschar. These dysregulations result in increased capillary leakage. Significant thermal injuries are characterised by electrolyte imbalance, significant protein loss, circulatory insufficiency and immuno-deficiencies that predispose burn patients to infection complications (Joneidi-Jafari et al. 2009). The large, damaged and necrotic areas of extracellular matrix (ECM), which produce excessive amounts of exudate, with considerable loss of intravascular proteins, lead to inefficient cell-matrix and intracellular interactions resulting in non-healing wounds (Church et al. 2006). Under these circumstances the exposed wounded surface (partial or full-thickness) provides an ideal environment for bacterial growth.

Thermo-resistant pathogens such as *Staphylococcus* ssp. heavily colonise the wound surface within the first 48 hours. The open wounded skin is eventually further infected (5 - 7days) with other pathogens that include Gram-positive, Gram-negative bacteria and yeast derived from external and/or internal sources, where *P. aeruginosa* is the most common cause of burns infection. Chronic burn wounds are considered to be a host niche for resistant bacterial strains such as methicillin resistant *S. aureus* (MRSA), increasing the risk of spreading the antibiotic-resistant strains in health care units and between health care workers, enhancing cross contamination between other patients and exacerbating the treatment of chronic burn wounds (Church et al. 2006).

1.3.2 Pressure ulcers

This kind of chronic ulcer is caused by constant pressure, usually over a bony prominence that results in destruction to underlying tissue. Elderly people between the ages of 70 - 80 years are worst affected. The pressure ulcer is characterized by non-blanced erythema of intact skin. However, the clinical features of pressure ulcers depend on several characteristics of each ulcer such as the ulcer size and depth, the colour and the necrotic tissue mass involved. As such a comprehensive assessment of an ulcer includes four phases. General symptoms of phases I and II are partial thickness of skin loss from epidermis and/or dermis. The ulcer in the IIIrd and the IVth phase is characterized by further destruction and tissue devitalisation, or damage of muscles and bones. Generally, pressure ulcers promote infections by pathogens such as *P. aeruginosa*, staphylococci and enterococci and anaerobes such as *Clostridium* spp., that lead to a prolonged delay of the healing process. In addition, further complications such as cellulitis and osteomyelitis can occur as a result of bacterial colonization (Dhamarajan and Ugalino 2002).

1.3.3 Neuropathic (diabetic) ulcers

Diabetic ulcers result from a combination of vascular and neurological abnormalities of the disease. Continuous studies have shown that diabetic patients have an excessive thickness of the basement membrane in the muscle. Compared to healthy people, the thickness of the basement membrane is up to 2-fold greater in diabetics (Falanga 1993). This 2-fold increase of the basement membrane can lead to further complications in dermal capillaries and other physiological, microvascular abnormalities, which are demonstrated by increased perivascular localization of albumin. Poor blood supply results in low oxygen tension (hypoxia), which constitutes a well established phenomenon in chronic wounds. Tissue hypoxia results in cell death and tissue necrosis. This physio-biochemical change generally leads to failure of autonomic nerves and results in neuropathy (Falanga 1993). As a result of sensory insufficiency in diabetic patients, breakdown of the skin after prolonged pressure occurs and the initiation of trauma leads to ulceration

(Falanga 2005). Ischemia and infection also play a critical role in impaired healing of diabetic patients. The combination of factors described above leads to polybacterial (aerobes and anaerobes) infection. The additional presence of biofilms, generally leads to further complications and failure of the healing process (Falanga 2005).

All the above examples of chronic wounds contribute to the fact that a non-healing injury can be the result of discontinuation of the normal healing process at one or more points in the main stages of haemostasis, inflammation, proliferation or remodelling. In addition, disruption of the healing process results from the coexistence of both endogenous and exogenous factors. Endogenous factors include the presence of neuropathy and metabolic disease (diabetes), neoplastic malignancies, immunodeficiency, autoimmune and/or haematologic diseases, while exogenous factors include post-injury consequences such as bacterial, fungal and viral infections. Although, endogenous factors can lead to a diverse pathophysiology of chronic wounds, which vary from patient to patient, generally the main clinical features that result after wounding are similar and include abnormal exudation, ischemia (poor blood supply) and bacterial infection.

1.4 Exudate profile of non-healing wounds

Exudate production from open wounds is essential for moist wound healing. In acute wounds, exudate is an essential fluid in the wound bed, containing all the necessary components for healing. Table 1.3 lists the components of wound fluid and their function in the healing process. Production of excessive wound fluid occurs as a result of uncontrolled expression of inflammatory mediators such as histamine and bradykinin. The presence of such mediators increase vascular permeability and consequently increase the amount of extracellular fluid. When wounds produce inadequate or excessive exudate and infection becomes established, the composition of the wound fluid takes an abnormal guise. This will result in problematic conditions that ultimately delay or prevent healing and generate clinical challenges (White and Cutting 2006).

Assessment of abnormal wound fluid, in terms of volume, colour, odour and consistency can provide useful information on the status of the wound (Cutting 2003). Although, there is little published information with regards to the volume of exudate that chronic wounds produce, non-healing wounds are traditionally categorised as light, moderate and heavy exudative (Thomas et al. 1996). It has been reported that the amount of fluid produced by non-healing wounds varies from 3.4 – 10 grams /m²/day, where leg ulcers and burns are the most exudative wounds (Thomas 2007). Based on colour and odour, exudates have been categorised as bloody, serosanguineous, serous, purulent and foul purulent indicating the level of suppuration and the amount of pus present (Cutting and White 2002). However, the aforementioned characterizations of exudate are subjective, while different types of wounds produce various types and volumes of exudates during the non-healing period (Cutting 2003).

Analysis of wound fluid with regards to biochemical and cellular examination can provide useful information and a complete picture of the non-healing environment. Exudate produced from non-healing wounds is, in its essence, a modified and anomalous serum which contains electrolytes (e.g. Na⁺, K⁺, Ca²⁺, Cl⁻), lactate, urea, glucose and high protein content with a specific gravity greater than 1.020 (White and Cutting 2006, Cutting 2003). Estimation of the protein level in wound fluid has shown a total amount higher than 40 g/l, of which approximately 60 % is albumin (Clough and Noble 2003). In non-healing wounds, in particular during inflammation, the exudate presents an environment with an increased number of neutrophil and leukocyte counts, which result in production of proteases and oxidants that degrade the ECM and inhibit cell migration, hence prevent wound closure (Mustoe 2004). *In vitro* studies have shown that the elevated levels of MMPs and serine proteases degrade growth factors and fibronectin (essential mediators of the remodelling phase) (Enoch and Price 2004). Recently, Rayment *et al.* (2008) have reported that there is an excessive protease activity in the exudate of chronic wounds compared with both human serum and acute wound fluids. The latter authors have also shown that MMP-9 was the predominant protease in chronic wounds that was correlated with a clinically worse wound. In addition, TIMPs (TIMP-1 in particular) levels were lower in chronic wounds than in healing wounds (Bullen et al. 1995).

Consequently, the lost balance between proteolytic enzymes and their inhibitors contributes to failure of new tissue deposition, preventing healing in open wounds.

Table 1.3 Constituents of exudate and their function in wound healing
(Adapted from White and Cutting 2006)

Components	Function
Fibrin	Clotting
Platelets	Clotting
Polymorpho-nuclear neutrophils (PMNs)	Immune defence, production of growth factors
Lymphocyte	Immune defence
Macrophage	Immune defence, production of growth factors
Plasma proteins, albumin, globulin, fibrinogen	Maintain osmotic pressure, immunity, transport of macromolecules
Lactic acid	Product of cellular metabolism and indicating biochemical hypoxia
Glucose	Cellular energy source
Inorganic salts	pH buffering of hydrogen ions in solution
Growth factors	Protein controlling specific healing activities
Wound debris/dead cells	No function
Proteolytic enzymes	Enzymes that degrade protein, including serine, cysteine, aspartic protease and MMPs
Tissue inhibitors of metalloproteinases (TIMPs)	Controlled inhibition of MMPs

1.5 Ischemia

Ischemia is considered another serious contributing factor to the non-healing process. A deficiency in blood supply prevents the progress of healing due to continued tissue injury. From a clinical point of view, ischemia is usually associated with aggravating factors such as diabetes, malnutrition and age (Schäffer et al. 2002). Most examples of chronic wounds are associated with elderly people suffering from diabetes, pressure and arterial ulcers. The cellular characteristics of non-healing wounds generally include low mitotic activity, impaired fibroblast proliferation and migration, lack of response of fibroblasts to growth factors in conjunction with impaired venous arterial blood flow (Enoch and Price 2004). These cellular features of chronic wounds are further impaired with advancing age. Aged skin presents essential differences to young skin and appears to have decrease mobility of fibroblasts, reduced turnover of keratinocytes to epidermis and low response to stimulatory growth factors. This impaired cellular activity leads to reduced rates of formation of granulation tissue and epithelisation, hence preventing or delaying healing. Consequently, elderly patients suffering from non-healing ulcers present another clinical challenge in the treatment of chronic wounds (Enoch and Price 2004).

1.6 Bacterial infection

As previously mentioned, the condition of injured, non-healing skin promotes bacterial contamination within the first 24 hours. The sources of contamination arise from the patient's surrounding skin, gastrointestinal and respiratory flora (internal sources), as well as from the local hospital environment and health care workers (external sources) (Church et al. 2006). As a consequence, the microbiological profile of a wound bed often presents a complex polymicrobial environment. In addition, the protein rich environment provided by the excessive production of wound fluids serves as a suitable niche for bacterial contamination and growth in the wound bed.

The most predominant bacterial species are *Staphylococcus aureus* and *Staphylococcus epidermidis*, which colonize wounds within the first hours. *Pseudomonas aeruginosa*, *Escherichia coli*, *Streptococcus* spp and other Gram-

positive and Gram-negative aerobes and anaerobes, will further colonize the injured, exposed tissue after an average of 4 - 7 days. Recent studies using molecular techniques have emphasised the complex microbiological flora of non-healing wounds (Howell-Jones et al. 2005). A longitudinal study performed in patients with persisting venous leg ulcers demonstrated that the most common bacteria found were *S. aureus*, *Enterococcus faecalis*, *P. aeruginosa*, coagulase-negative staphylococci, *Proteus* species and anaerobic bacteria (Gjødsbøl et al. 2006). Tables 1.4 (a) and (b) list all the pathogens that have been found in chronic wounds.

Table 1.4 (a) Aerobic and facultative aerobic isolates from chronic wounds with varied aetiology (Adapted from Bowler et al. 2001)

Aerobic and facultative bacteria	
Gram-positives	Gram-negatives
*Coagulase-negative staphylococci	* <i>Enterobacter cloacae</i>
* <i>Staphylococcus aureus</i>	<i>Enterobacter aerogenes</i>
Beta-haemolytic <i>Streptococcus</i> (group G)	* <i>Escherichia coli</i>
* <i>Streptococcus</i> spp. (<i>faecal</i>)	* <i>Klebsiella pneumoniae</i>
* <i>Streptococcus</i> spp. (<i>viridans</i>)	* <i>Klebsiella oxytoca</i>
* <i>Acinetobacter calcoaceticus</i>	<i>Serratia liquefaciens</i>
<i>Corynebacterium xerosis</i>	* <i>Pseudomonas aeruginosa</i>
* <i>Corynebacterium</i> spp.	* <i>Proteus mirabilis</i>
<i>Micrococcus</i> spp.	<i>Proteus vulgaris</i>
	<i>Citrobacter freundii</i>
	<i>Morganella morganii</i>
	<i>Sphingobacterium multivorum</i>

(* Isolates also present in acute wounds)

Table 1.4 (b) Anaerobic isolates from chronic wounds with varied aetiology
(Adapted from Bowler et al. 2001)

Anaerobic bacteria	
Gram-positives	Gram-negatives
<i>Streptococcus intermedius</i>	*Gram-negative pigmented bacillus
* <i>Clostridium perfringens</i>	* <i>Prevotella oralis</i>
* <i>Clostridium clostridioforme</i>	<i>Prevotella oris</i>
* <i>Clostridium cadaveris</i>	<i>Prevotella bivia</i>
* <i>Clostridium histolyticum</i>	<i>Prevotella buccae</i>
<i>Clostridium ramosum</i>	* <i>Prevotella corporis</i>
* <i>Clostridium sporogenes</i>	<i>Prevotella melaninogenica</i>
<i>Clostridium difficile</i>	* <i>Bacteroides fragilis</i>
* <i>Peptostreptococcus asaccharolyticus</i>	* <i>Bacteroides ureolyticus</i>
* <i>Peptostreptococcus anaerobius</i>	* <i>Bacteroides uniformis</i>
* <i>Peptostreptococcus magnus</i>	<i>Bacteroides stercoris</i>
* <i>Peptostreptococcus micros</i>	<i>Bacteroides capillosus</i>
* <i>Peptostreptococcus prevotii</i>	<i>Bacteroides thetaiotaomicron</i>
<i>Peptostreptococcus indolicus</i>	<i>Bacteroides caccae</i>
* <i>Peptostreptococcus</i> sp.	<i>Fusobacterium necrophorum</i>
* <i>Propionibacterium acnes</i>	* <i>Porphyromonas asaccharolytica</i>
<i>Eubacterium limosum</i>	

(* Isolates also present in acute wounds)

The presence of pathogens in chronic wounds has been traditionally classified in four levels: contamination, colonization, critical colonization and wound infection (Collier 2004). Only, recently, the term 'wound infection' was subcategorized into local and systemic infection (Healy and Freedman 2007). A variety of techniques such as swab culture and tissue cultures, obtained from biopsies of the chronic wound environment, have been used in order to estimate the number of pathogens responsible for infection. Research studies have demonstrated a correlation of the number of bacteria found between the two methods used, and experimentally have shown that a bacterial density of 1×10^5 colony forming units (cfu)/g tissue is equivalent to 1×10^3 cfu/ml (Bowler et al. 2001). This bacterial density has been generally defined as an infective population (Cutting 2003). However, in a poly-contaminated niche such as a chronic wound bed, the established infection would depend on the expressed pathogenicity of each bacterium rather than density of microorganisms, where the interaction between the host and the pathogens would better classify the levels of wound infection. For instance, for an organism such as haemolytic *Streptococcus*, a lower tolerance is accepted due to its high virulence (Kirketerp-Møller et al. 2011).

Concurrently, wound care research studies have emphasized the ability of pathogens to harvest the sustainable nutrition provided from the inflamed wound bed in order to produce and surround themselves in a protective polysaccharide cover defined as a biofilm (Wolcott et al. 2008). James *et al.* (2008) have investigated the microbiological profile of 50 chronic and 16 acute wounds and demonstrated that 60 % of chronic wounds contain bacteria in the composite state of biofilms. As such, investigators have accentuated the critical role that biofilms may play in persistence of chronicity of infection, and prevention of healing (Kirketerp-Møller et al. 2011). Additionally, it has been shown that the host response is often not effective against biofilms. It has been suggested that the community of bacteria assembled in biofilms are able to release planktonic seeds of bacteria, which confuse the host immune response permitting biofilms to withstand phagocytosis (Wolcott et al. 2008). This mechanism of biofilms, however, is not fully understood and further investigations are being undertaken. Another major concern in the management of infected wounds is the fact that bacteria in a composite state such as biofilms become more tolerant and consequently resistant to

antimicrobial therapies when compared with their unicellular existence (Widgerow 2008). For example, both mupirocin cream and the triple antibiotic ointment containing cetrimide, bacitracin and polymyxin B sulphate were effective in decreasing planktonic *S. aureus* cells, while the same applications had reduced antimicrobial activity against *S. aureus* biofilms (Widgerow 2008).

The role of bacteria in non-healing wounds has detrimental effects and bacterial infection is undoubtedly considered to be a common reason for impaired wound healing and chronicity. In addition, the complex polymicrobial environment of the infected wound bed, with regards to density, diversity, virulence and biofilm formation, present a major challenge for the treatment and therapy of infected chronic wounds.

1.7 Chronic wounds in both hospital and community acquired MRSA

Chronic wounds have an important impact on patients' health and their quality of life. This results from the fact that non-healing wounds are a major source of pain, disability, psychiatric morbidity and even mortality for patients (Franks and Moffat 1999). Apart from the fact that the infected and non-healing profile of wounds represent a significant burden to both patients and healthcare workers, their hospitalisation appear to be an important risk factor in the spread and/or acquisition of pathogens, including antibiotic resistant organisms such as methicillin resistant *S. aureus* (MRSA) (Weber et al. 1999).

The Nosocomial Infection National Surveillance Service (NINSS) has reported that in 2002 the prevalence of hospital acquired infections (HAI) related to surgical wounds was 10 % (Collier 2004). The Royal College of Physicians of Edinburgh (RCPE) has reported that health care workers are passive contributors to the spread of MRSA. Cross contamination amongst patients may occur by the transfer of organisms via hands and lab coat sleeves. Also, poor hand hygiene can spread contamination in the environment (equipment, dissemination while bed-making etc). In addition, healthcare workers may also act as active distributors of MRSA if they themselves are carriers of the pathogen (Baird et al. 2006).

Bearing this in mind, it's not difficult to believe that the majority of chronic wounds are found to be colonised with multi-drug resistant organisms, including MRSA (Landis 2008). The main risk factor that predisposes acquisition of MRSA is the prolonged hospitalisation of patients suffering from a non-healing wound and MRSA has been found to be the most prevalent pathogen in UK hospitals and worldwide (Elston and Barlow 2009). In addition, it has been reported that MRSA is the most common pathogen of hospitalised patients in emergency departments with skin and soft tissue infections (Frazee et al. 2005). Other factors such as previous antibiotic misuse and transfer between hospital facilities may also increase the likelihood of acquiring multi-drug resistant infection (Landis 2008).

Recently, concerns have also been raised with regards to the prevalence of community associated MRSA infection (CA-MRSA), as an increased number of wounds are infected with CA-MRSA strains (Landis 2008). Genetic screening and antimicrobial susceptibility tests have demonstrated that CA-MRSA strains are different from MRSA strains in hospitals, with regards to both genetic and phenotypic profiles. Although CA-MRSA strains are found to be susceptible to a broader range of anti-staphylococcus drugs, they appear to be more virulent than the hospital associated MRSA strains (Frazee et al. 2005). It has been reported that the acquisition of CA-MRSA infections is mainly associated with increased transmission and hospitalisation of patients suffering from skin and soft tissue infections. Moreover, CA-MRSA strains are rapidly spreading worldwide. In the UK, although infection with such strains have been rarely reported, the prevalence of CA-MRSA infections is showing an increasing trend (Elston and Barlow 2009). The prevalence of resistant strains in emergency departments in the USA, where CA-MRSA stains were found to be the dominant isolates, have concerned research communities, who recommend a change in the empirical way that skin and soft tissue infections are treated (Elston and Barlow 2009).

1.8 Control of bacterial bio-burden (systemic or topical treatment)

There is a ubiquitous debate regarding how an infected, non-healing wound should be treated, what therapeutic agents should be used, and whether systemic or topical antimicrobial therapy should be applied. As previously described, the presence of bacteria in chronic wounds is categorized as contamination, colonization, critical colonization and wound infection (local and systemic). This classification of wound bioburden was mainly established as a guideline for diagnostic purposes and determination of suitable treatments, however, this classification is arguable and remains controversial with regards to the density of pathogens present in an infected, non-healing wound.

Established infection is clinically defined as the situation where the non-healing wound appears discoloured, presents friable granulation tissue, produces non-purulent exudate and abnormally foul odour (Lipsky and Hoey 2009). Under these circumstances, it has been suggested that clinically infected wounds could benefit from systemic antibiotic treatment, especially in cases of advanced deeper tissue infections. However, it is well known, that antibiotics are compounds that usually kill or inhibit one or very few specific groups of pathogens, in other words they demonstrate a narrow spectrum of activity. Moreover, they have been found to have decreased activity against the polysaccharide shield of biofilms formed around bacterial pathogens and consequently lose their effectiveness. As discoloured tissue is related to poor blood circulation and ischemic conditions, their efficacy at the infected wound site is questionable.

1.9 Debridement

Traditionally, prior to the application of any suitable therapy, debridement is one of the principle stages in the treatment of non-healing wounds. It has been suggested that all non-healing wounds can only benefit from effective debridement, since removing devitalised tissue, suppuration and foreign materials results in the reduction of bacterial load (Bowler et al. 2001). In addition, debridement is considered to play an important role in cleaning

the wound bed from bacterial biofilms while revealing the healthy tissue required for wound healing (Kirketerp-Møller et al. 2011).

There are several available methods for debridement, which include: surgical (performed with scissors, scalpels and recently lasers); autolytic (performed with occlusive and semi-occlusive dressings, which soften the eschar and allow the proteolytic enzymes within the wound fluid to digest the devitalised tissue); mechanical (performed with irrigation fluids baths and removal of tissue from wet to dry dressings); enzymatic (include the use of topical enzymes, such as collagenase, papain and urea, to digest necrotic tissue); and biological debridement (include the use of maggots) (Ayello and Cuddigan 2004).

A clinical guide to debridement decisions suggests that surgical and enzymatic debridement could be used for wounds that present all levels of bacterial loads, particularly in advanced tissue sepsis. Autolytic and mechanical debridement could be used with caution in wounds with less bacterial load, before the stage of local extended infection (Ayello and Cuddigan 2004). The use of maggot larvae in wound debridement is however, controversial. Although this method of debridement, involves mainly the secretion of proteolytic enzymes and ammonia in conjunction with antimicrobial substances from maggots (Chan et al. 2007), their use is found to be ineffective in wounds heavily colonised with *P. aeruginosa*. Additionally, recent experimental research with maggots has shown that these, at least initially, benefit biofilm formation for *S. aureus* and *P. aeruginosa* (Kirketerp-Møller et al. 2011).

1.10 The role of topical antimicrobials

Non-healing, chronic wounds have been treated topically since ancient times. Potential advantages that topical approaches provide include: adequate and sustained concentrations of therapeutic agent at the site of infection, avoidance of using systemic antibiotics that usually lead to development of antibiotic resistance strains and easy application in outpatients (Lipsky and Hoey 2009). Nowadays, topical antimicrobial compounds are grouped as antiseptics and antibiotics. Replacement of systemic antibiotics with topical

broad spectrum antimicrobials (mostly antiseptics), in the absence of advanced cellulitis, bacteraemia and fever is thought to offer the most useful first line of treatment (Bowler et al. 2001). Antiseptics are antimicrobial compounds usually limited to external application which possess a broad spectrum of activity against pathogens and often demonstrate cytotoxicity against main cell mediators of the healing process.

The most effective and widely used topical antimicrobials include chlorhexidine, ionic silver and its sulfadiazine salt and iodophores (iodine-carriers). These antimicrobials have demonstrated rapid bactericidal properties against a wide range of Gram-positive and Gram-negative bacteria, fungi and even viruses and cases of developed resistance by pathogens are less evident than for topical antibiotics (Lipsky and Hoey 2009). It has been suggested that the exceptional antimicrobial properties of these compounds are likely due to multi-targeted mechanisms of action against bacteria. For example, the bactericidal activity of chlorhexidine (Figure 1.2) is mediated by the ability of this cationic compound to damage the outer cell layers as well as cytoplasmic targets of the microorganism, inducing leakage of cellular components. Despite the fast bactericidal activity of chlorhexidine, cases of acquired resistance for MRSA have been documented (Cooper 2004).

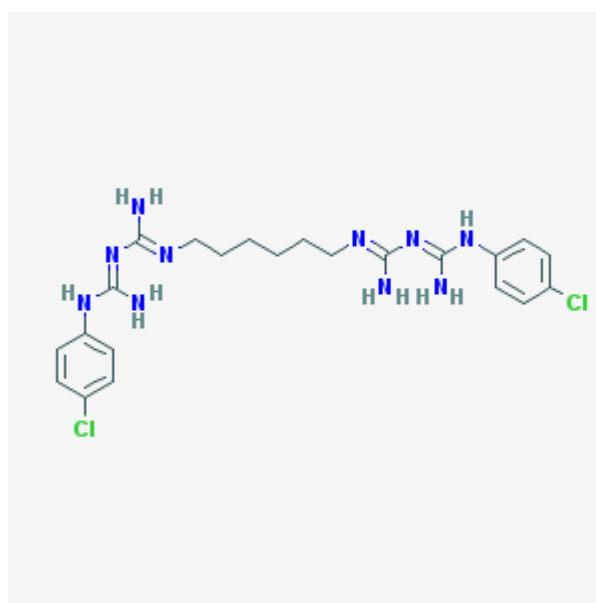


Figure 1.2 Chemical structure of chlorhexidine (Adapted from PubChem).

Antimicrobial properties of silver have been reported for over a century. Usually this compound is used as ionic silver, silver sulfadiazine (Figure 1.3) and/or silver nitrate (White and Cooper 2005). Although this antimicrobial compound has been widely used, its mechanism of action is still not well defined. It has been suggested that silver ions have an affinity for thiol groups and also interact with carboxylates, phosphates, hydroxyls, imidazoles, indoles and amines. As such, silver ions bind to proteins and nucleic acids, thus inducing structural alterations in bacterial cell walls, membranes and nucleic acids. Hence, its dynamic antimicrobial nature is likely due to multi-targeted antimicrobial events, which appear to simultaneously cause damage to bacterial cells and affect the viability of a wide variety of pathogens (Cooper 2004). Despite the dynamic antimicrobial activity of silver, resistance to this antimicrobial has been reported from both clinical and environmental isolates (Woods et al. 2009).

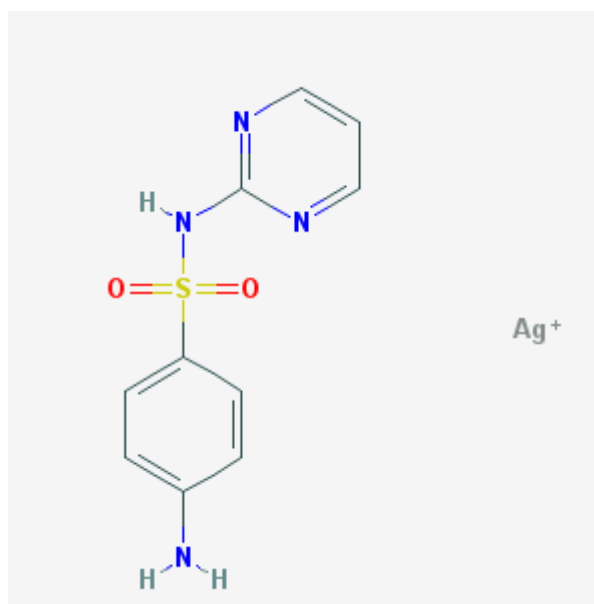


Figure 1.3 Chemical structure of silver sulfadiazine (Adapted from PubChem)

Iodine has been extensively used for over 150 years either as an alcohol solution of potassium iodide salt or incorporated in iodophores such as polyvinylpyrrolidone-iodine complex (PVP-I) (Figure 1.4) and cadexomer iodine formulations. *In vitro* experiments have shown broad bactericidal properties against bacteria, fungi, protozoa and viruses (Cooper 2004) and despite its prolonged application, only one case of resistant MRSA has been clinically reported (Mycock 1985). As with silver, iodine's mechanism of action is not yet fully understood. It has been suggested that iodine may possess multiple mechanisms of action, which can induce multiple lethal cellular effects (Cooper 2004). These modes of action include the ability of iodine to bind to key groups of proteins (e.g. free sulphur amino acids, cysteine and methionine), nucleotides (adenine, cytosine and guanine) and fatty acids (McDonnell and Russell 1999).

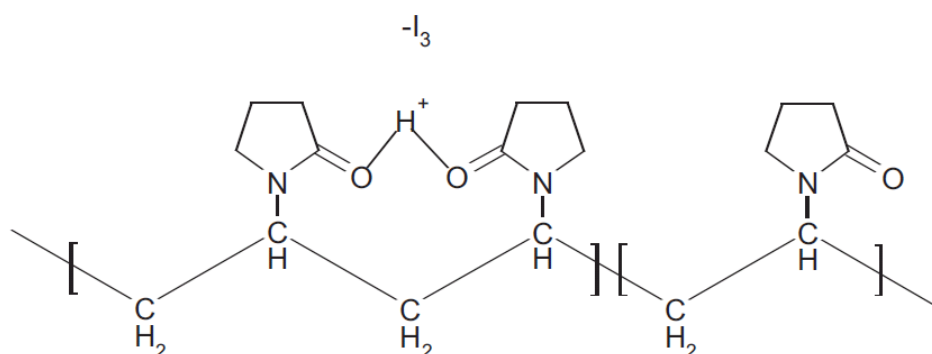


Figure 1.4 Chemical structure of polyvinylpyrrolidone-iodine complex
(Adapted from International Speciality Products 2004).

In vitro, topical antimicrobials, in particular antiseptics, have demonstrated broad and rapid bactericidal properties against a wide variety of microorganisms. However, a considerable limitation of such compounds is that their aggressive cidal properties may also be toxic to different mammalian cells which construct the skin tissue. A significant amount of *in vitro* research has shown that most of these agents are highly cytotoxic to different cell lines. For example, silver has been shown to be highly toxic to both keratinocytes and fibroblasts in monolayer cultures (Poon and Burd 2004). Giannelli *et al.* (2008) showed that chlorhexidine digluconate demonstrates different degrees of cytotoxicity as tested on osteoblastic, endothelial and fibroblastic cell lines. Povidone iodine solutions (Betaisodona and Braunol) have also demonstrated an ability to decrease cell viability for keratinocytes and fibroblasts (Hirsch *et al.* 2010).

Other *in vitro* studies have tried to link the cytotoxic potential of topical antimicrobials, in respect to their antimicrobial effect against common chronic wound pathogens, in order to establish a clinical, therapeutic and less toxic concentration of topical antimicrobial (Kautzky *et al.* 1996; Hirsch *et al.* 2010). However, the *in vitro* results, with regards the role of antiseptics in infection control and promotion of healing in chronic wounds, remains controversial when compared to clinical trials. There are a significant number of published works referring to the therapeutic role of antiseptics in infection control and closure of non-healing wounds in humans. For example, a clinical investigation of the antimicrobial effect and healing rates of chronic leg ulcers treated with chlorhexidine digluconate, silver sulfadiazine or PVP-I, demonstrated that all three antimicrobials decreased the microbial load. Silver sulfadiazine and chlorhexidine digluconate caused slight improvements in the healing rate of leg ulcers, altering the microvessels and dendrocyte population. In addition, PVP-I significantly increased the healing rate and induced less histological changes (Fumal *et al.* 2002). Another study has reported that 1 % silver sulfadiazine (Flamazine) showed a significant improvement in antimicrobial activity in treatment of burn patients compared to povidone iodine (Hadjiiski and Lesseva 1999).

Scientists have indicated that despite the fact that antiseptic agents have been applied to treat infected wounds for centuries, their proper role in wound healing remain unclear. The contradictory and confusing evidence with

regards to the efficacy of antiseptics in wound management originates from different sources. Firstly, the difficulty in realistically modelling non-healing wounds *in vitro* or in wounded animal models is a major disadvantage. Secondly, the lack of specific *in vitro* standardised tests and methods for the evaluation of the efficacy of topical therapies (Lipsky and Hoey 2009). Many factors such as temperature, bacterial species, concentration, number of organisms and the presence of organic material and electrolytes may influence the results obtained (Cooper 2004). Thirdly, there is insufficient evidence provided from limited and incomparable clinical trials (Lipsky and Hoey 2009).

1.11 The role of growth factors in the treatment of non-healing wounds

Growth factors are the essential mediators of the healing process, as they are directly involved in the active physiological processes of haemostasis, inflammation, proliferation and remodelling. Molecules such as epidermal growth factor (EGF), platelet-derived growth factor (PDGF), transforming growth factor beta (TGF- β) and fibroblast growth factor (FGF) have been considered as the most important mediators of the healing process (Sullivan et al. 2001; Pierce and Mustoe 1995). It is not known whether the topical application of specific growth factors or a mixture of growth factors would facilitate healing.

Several *in vivo* studies, involving wounded small animals, have produced positive results. For example, investigations by Lee and colleagues (2005) have showed that *in vivo* wound healing accelerated when EGF was applied in combination with silver sulfadiazine. In addition, EGF has shown clear stimulation of epidermal and dermal repair in an animal wound model (Lee et al. 2005). The role of TGF- β was tested in small mammals, but results obtained were contradictory. Although TGF- β is a potent inducer of fibronectin and inhibitor of MMPs, experiments with wounded animal models demonstrated that its effect depends on the dose applied. This growth factor could also act as an inhibitor of cell growth when applied in increased doses. As such, further *in vivo* and eventually clinical investigations are required to

elucidate its role in treatment of non-healing wounds (Pierce and Mustoe 1995).

PDGF, isolated from human platelets, mediates many processes required for tissue repair including chemotaxis (neutrophils, macrophage, monocytes and fibroblasts), proliferation, angiogenesis and wound remodelling. Preclinical studies have been conducted in patients suffering from diabetic foot ulcers and pressure sores, where PDGF was applied daily to non-healing wounds for 28 days. The results obtained demonstrated an accelerated rate of healing, however this was not significant compared to the control groups (Pierce and Mustoe 1995). Further preclinical studies of PDGF delivered via a gel formulation to diabetic foot ulcers, daily for 20 weeks, showed significant healing and complete ulcer closure compared to the untreated patients (Pierce and Mustoe 1995). These encouraging results obtained from preclinical studies, led a few years later to a definitive clinical trial using Regranex (PDGF gel, Ortho-McNeil Pharmaceutical, Inc, Raritan, NJ). The results generated from over 1000 patients with diabetic ulcers, revealed that only a 10 % increase in total wound closure was achieved (Mustoe 2005). Although, this low percentage in wound closure could be considered as a failure of the PDGF product in treating diabetic ulcers, the latter author considered it debatable that other critical factors, such as debridement and elimination of ischemia reperfusion injury, probably influenced the final results (Mustoe 2005). Consequently, the role of topically applied growth factors in wound healing is not totally understood and further investigations are required to elucidate their multi-functional roles as mediators of the healing process.

1.12 Other popular and supplementary treatments

1.12.1 Honey

Topical antimicrobials and growth factors are undoubtedly the main compounds whose roles have been extensively discussed and investigated in chronic wound treatment. However, in the last decade, there has been an increased interest in the antimicrobial and therapeutic properties of honey. Curative properties of honey vary with floral sources, origin and processing

(Molan 2001). Antimicrobial properties of honey are associated with high osmolarity, release of hydrogen peroxide and methylglyoxal, cationic antimicrobial peptide (bee-defencin-1), phytochemical components such as flavonoids and antioxidants (Kwakman et al. 2010; Molan 2001; Cushnie and Lamb 2005).

In vitro research has demonstrated that honey possesses remarkable antimicrobial properties against a wide range of Gram-positive and Gram-negative bacteria, such as *S. aureus* and *P. aeruginosa*, including antibiotic resistant strains such as MRSA and vancomycin-resistant enterococci (VRE) (Molan 2001). In addition, dilutions of 2 - 4 % of pasture honey and manuka honey have shown to inhibit the growth of 58 coagulase-positives *S. aureus* strains isolated from patients with infected wounds (Cooper et al. 1999). Recently, it was discovered that in particular, manuka honey and Sird honey from Yemen, demonstrated *in vitro* bacteriocidal properties against biofilms of *S. aureus* and *P. aeruginosa* (Alandejani et al. 2009).

Although honey's antimicrobial mechanism of action has not been determined yet, its therapeutic role in accelerating healing is thought to be related to its anti-inflammatory properties. Similarly, *in vitro* studies were undertaken using immuno-competent monocytic MM6 cell lines treated with different honey solutions. Results obtained indicated that all honey types significantly stimulated the release of inflammatory cytokines, such as TNF- α , IL- β and IL-6, when compared to untreated and artificial honey-treated cells (Tonks et al. 2003). The healing properties of honey were further supported by *in vivo* studies undertaken on wounded animal models, where the application of 5 ml pure honey improved epithelialisation and tissue strength, indicating acceleration of healing (Oryan and Zaker 1998).

A recent review aimed to evaluate the therapeutic effect of honey applied on the mixed aetiology of both acute and chronic wounds (Jull et al. 2009). The author's conclusion from the data analysis of 19 randomised and quasi-randomised trials (n = 2,554), summarized that "honey may improve healing time in mild to moderate superficial and partial thickness burns compared with some conventional dressings". However, "honey dressings as an adjuvant to compression do not significantly increase leg ulcer healing at 12 weeks", where additionally, adverse side effects such as pain, deterioration of ulcer and increased exudate were observed (Jull et al. 2009; Jull et al.

2008). In conclusion, these results indicate that the remedial properties of honey and its role in wound healing will continue to be of interest.

1.12.2 Vitamin and mineral supplements

Vitamins and minerals, such as A, C, E, zinc and copper, are considered adjuvant compounds in treatment of non-healing wounds. Vitamins are actively involved at different stages of cellular activities including tissue development. For example, the role of vitamin A is associated with epithelisation, collagen synthesis, fibroplasia, angiogenesis and rapid inflammatory response (Keller and Fenske 1998).

The active form of vitamin C (L-ascorbic acid) is one of the most important compounds in biological processes and cellular activities. Ascorbic acid has a pivotal role in wound healing as this compound acts as a co-factor for several enzymes during collagen synthesis and other intracellular activities of matrix tissue, including bones, capillary walls and connective tissues (Keller and Fenske 1998, Boateng et al. 2007). In addition, ascorbic acid possesses anti-oxidative activities by quenching free radicals and also acts as a regenerator of vitamin E from its radical form (Keller and Fenske 1998).

Free D-alpha tocopherol is the main active fraction of vitamin E. The role of this compound is associated with antioxidant and anti-inflammatory activity, angiogenesis and/or reduction of scars (Boateng et al. 2007). However, effects of vitamin E tested in pre-clinical and clinical trials have been controversial and usually associated with adverse local effects such as papular and follicular dermatitis (Keller and Fenske 1998). Thus, the aid of this vitamin in improving healing by topical application requires further investigation (MacKey and Miller 2003).

Zinc is an important trace mineral, which is required for approximately 300 enzymatic activities during tissue repair including DNA synthesis, cell division and protein synthesis. Although zinc deficiency is usually associated with poor wound healing and decreased collagen deposition in wounded tissue, there is insufficient clinical data to support the supplementary role of this mineral in improved wound healing. Further investigation is needed to confirm

the efficacy of zinc supplements in the healing process (MacKey and Miller 2003).

1.13 Wound management

General principles of local wound management apply in a wide variety of chronic wounds. Management of non-healing wounds can be characterised as a multi-operational process, which includes debridement, control of exudate, inhibition of infection, optimal conditions of moisture, temperature, oxygen, blood circulation and protection (Werdin et al. 2009). Based on these principles of wound management, the ideal properties of a topical application were determined. The ideal dressing could be characterised as the one which could provide continued and consistent delivery and activity of therapeutic compounds over the entire surface of the wound; absorbs and restrains the exudate, maintaining moisture balance in the wound bed; conformable and comfortable, providing thermo-insulation; protects the wounded skin from external contamination and foreign materials while being non-adherent, non-toxic, oxygen permeable and pain-free on removal (Werdin et al. 2009).

1.14 Existing topical applications

Traditionally, therapeutic compounds used for topical applications have been prepared as liquid formulations, such as solutions, suspensions and/or emulsions or semi-solid preparations such as ointments (occlusive) and creams (less occlusive) (Boateng et al. 2007). Generally, such preparations were incorporated into cotton wool bandages and gauzes, in order to inhibit infection and protect the open wound from the external environment. This way of wound care is also referred as traditional wound management. Traditional wound management relies on the application of non-extensible, extensible, adhesive/cohesive, tubular and medicated paste bandages (Thomas 1990). Although the majority of these categories of dressing are still in use, mainly as secondary dressings, the application of such materials, especially as primary dressings, are associated with major disadvantages.

Firstly, non-extensible bandages were found to be not particularly comfortable and difficult to apply correctly (Thomas 1990). Secondly, the materials from which they were made were unsuitable in providing a moist wound bed as the outer surface gets easily moistened by wound fluids. The application of a gauze dressing was associated with adhesion at the wound site and their use was associated with painful removal and patient discomfort (Boatang et al. 2007). There was also the necessity of incorporating therapeutic and/or antimicrobial compounds in a practical and comfortable formulation that had a suitably long residence time in the wound bed. Liquid or semi-liquid dosage forms had a limited residence time in the wound bed, particularly when wounds produced significant amount of fluids.

The use of novel, natural, hydrophilic and non-toxic polymeric materials was associated with innovations in administering therapeutic compounds in order to achieve an effective therapy with minimal toxicity. The concept of continued and controlled rates of delivery of therapeutic compounds, also known as sustained drug delivery, was initially based on the hydration of polymers and their ability to retain absorbed liquids and consequently swell (swelling behaviour). During this process, the incorporated compounds were released either by diffusion or degradation of the polymeric vehicle (Boateng et al. 2007). The use of polymeric formulations on broken wound tissue offered additional advantages with regard to maintaining and providing optimal healing conditions and concentrations of topical therapeutic agents.

The properties of wound dressings depend on the materials used. Advantages and/or disadvantages are discussed, and categorised according to the materials from which modern dressings are prepared. Table 1.5 summarizes the main characteristics of the most applicable and well known modern dressings based on exudate-holding capacity.

Table 1.5 Main characteristic of some modern dressings based on their ability to handle exudate (Adapted from Ayello and Cuddigan 2004)

None	Low	Moderate	Heavy
<p>-----></p> <p>Films</p> <p>Impermeable to water and microorganisms</p> <p>Used for wounds with little exudate</p> <p>Available as adhesive and non-adhesive</p> <p>Long wear times</p>			
<p>-----></p> <p>Hydrogels</p> <p>High water content</p> <p>Add moisture to wounds, used for dry or low exudative wounds</p> <p>Cooling and smoothing effect; good for burn and painful wounds</p> <p>Available as amorphous gels and sheets</p> <p>Need a secondary dressing to hold in place</p>			
<p>-----></p> <p>Hydrocolloids</p> <p>Maintain moist environment in partial thickness wounds</p> <p>Used in wounds with low or moderate amounts of exudate</p> <p>Flexible, mouldable, some are non-adhesive</p> <p>Available in many shapes and sizes</p> <p>Long wear times, 2-7 days</p>			
<p>-----></p> <p>Alginates and Foams</p> <p>Absorb large amount of exudate</p> <p>Provide thermal insulation</p> <p>Used in infected wounds</p> <p>Need a secondary dressing</p>			

1.14.1 Alginate dressings

Alginic acid was discovered in 1882 by Stanford during extraction experiments with kelp seaweeds in Scotland (Blaine 1946). Since then, the utilisation of haemostatic and non-toxic properties of alginate and its sodium and/or calcium salts in preparation of surgical dressings (Blaine 1946) initiated a new epoch of wound management. Additional conspicuous advantages of alginates such as moisture-holding capacity, biodegradability and compatibility with several antibacterial substances were originally observed by Blaine (1946). These favourable properties of alginates were embraced by the application of alginate dressings in a wide variety of wound types. In particular, alginates were most appreciated for their high absorbance capacity and their rapid and harmless transformation into gels when contacting wound fluids (Boateng et al. 2007; Agren 1996). The transformation of alginate fibres into gel occur via an exchange reaction between calcium ions present in wound exudate and sodium ions present in alginate fibres, which result in a crosslinked sodium/calcium degradable gel (Boateng et al. 2007; Agren 1996). Thus, the application of alginate materials has been more suitable in moderate/heavy exuding wounds rather than in dry or low exuding ones. Alginate dressings available in the UK market include antimicrobial free formulations such as ActiHeal[®] Alginate (MedLogic), Algisite[®] M, Algosteril[®] (Smith & Nephew), Kaltostat[®] (ConvaTec), Melgisorb[®] (Mölnlycke), SeaSorb[®] (Coloplast), Sorbalgon[®] (Hartmann) and antimicrobial loaded formulations such as Acticoat[®] Absorbent (Smith & Nephew) impregnated with silver and Alvigon[®] (Advancis) impregnated with medical grade manuka honey.

The hydrophilic, non-toxic and haemostatic properties of alginates provide favourable moist conditions in the wound bed, desirable for epithelisation and eventually wound healing. Furthermore, it was suggested that alginates may have a biological effect, acting as direct modulators of different cellular activities occurring during healing. Experimental studies undertaken with human histiocytic lymphoma cell lines U937, treated with several alginate-containing dressings, demonstrated that Kaltostat[®] (ConvaTec) induced a significant release of macrophage activator TNF- α (Thomas et al. 2000). Recent research studies conducted in wounded rats treated with alginates demonstrated that alginates increased expression of

collagen-I, while significantly suppressing expression of TGF- β 1, fibronectin and vascular endothelial growth factor (VEGF) (Lee et al. 2009). This data indicated that some particular alginate dressings may possess the potential of inducing pro-inflammatory response by activating macrophages (Thomas et al. 2000) and/or simultaneously act as cellular modulators in increasing collagen deposition in wounded tissue (Lee et al. 2009). It is difficult to conclude whether the physiological properties of alginates i.e. their properties as ideal dressings, or their effect on the physiology of wound healing, is more important.

1.14.2 Hydrogel dressings

Hydrogel dressings consist of insoluble synthetic or semi-synthetic polymers or an appropriate combination, which possess hydrophilic properties and moderate ability to absorb and retain fluids (swelling behaviour) (Thomas 1990; Boateng et al 2007). Currently, there is a plethora of dressings available in the UK market including antimicrobial free and antimicrobial impregnated formulations. Some of the antimicrobial free dressings include ActiFormCool[®] (Activa), ActivHeal Hydrogel[®] (MedLogic), Coolie[®] (Tyco), IntraSite[®] Gel (Smith & Nephew) etc. Hydrogel dressings impregnated with antimicrobials include Iodoflex[®], Iodosorb[®] (Smith & Nephew) prepared with 0.9 % cadexomer iodine in a paste or ointment base, and Mesitran[®] (Mölnlycke) prepared with medical grade honey.

Hydrogels fulfil many of the criteria that an ideal dressing should display. They are non-adherent, non-toxic, painless to remove and oxygen permeable. *In vitro* testing of Derma-Gel[®] and IntraSite Gel[®] has demonstrated that these particular hydrogels also possess bacteriostatic and fungistatic properties against *S. aureus*, *P. aeruginosa* and *Candida albicans* (Jones and Vaughan 2005). Although their ability to absorb fluids is limited due to the fact that hydrogels contain 70 - 90 % water, they provide a moist wound environment in dry and low exudative wounds (Boateng et al. 2007). In addition, their high water content can rehydrate the necrotic tissue, while promoting autolytic debridement in the devitalised tissue present in dry chronic wounds (Jones and Vaughan 2005). A recent review by Jones and

Vaughan (2005) based on the analysis of available published literature on clinical trials and case studies performed with hydrogel dressings since 1982, concluded that the use of hydrogels on burns was associated with soothing and cooling effects. All the above properties possessed by hydrogels rank them as functional and applicable dressings for a wide variety of shallow and deep wounds including burns. Limitations of hydrogels are restricted to low absorbance capacity of fluids in moderate and heavy suppurating wounds, and with respect to allergenicity and maceration in long term wound care (Jones and Vaughan 2005; Boateng et al. 2007).

1.14.3 Hydrocolloid dressings

Hydrocolloids constitute the third major group of most practical and widely used dressings. As with alginates and hydrogels, hydrocolloids include both antimicrobial free and antimicrobial loaded dressings. Some of them available on the UK market are: Aquacel[®], ConviDerm[®], DuoDerm[®], Granuflex[®], Versiva[®] (ConvaTec), Contreet[®] (Coloplast), and Silvercel[®] (J & J) impregnated with silver.

Hydrocolloids include a large variety of dressings, as they are produced from the combination of gel-forming materials such as carboxymethylcellulose (CMC) or other polysaccharides with elastomers and adhesives (Thomas 1990; Boateng et al. 2007). The amalgamation of different materials into a flexible and absorbent layer of either foams or films, enable hydrocolloids to suit a wide range of non-healing wounds. Although they adhere to both dry and moist surfaces, hydrocolloid dressings are mainly applied to low and moderately exuding wounds. Generally, hydrocolloids can be characterised as “multifunctional” dressings, as they help maintain moisture in the wound bed and facilitate autolytic debridement of dry, necrotic tissue whilst promoting granulation. The permeability of hydrocolloids to water and oxygen increases with the amount of exudate produced and they can be designed to manage different volumes of exudate (Thomas et al. 1996; Boatang et al. 2007). Generally, hydrocolloids provide a moist wound bed, a protective barrier from the external environment, are user friendly and comfortable products.

A comparative *in vivo* study performed with wounded domestic swine demonstrated that different hydrocolloid dressings had dissimilar impacts on the treatment of full-thickness wounds that depended on their composition (Agren et al. 1997). The latter authors reported that the application of hydrocolloids showed different histological features, which were likely related to the different levels of adherence displayed. A randomised clinical trial performed with 31 patients suffering from venous ulcers helped evaluate the clinical efficacy of two hydrocolloid dressings. The results revealed significant differences in epithelialisation, adhesion, conformability, application and patient comfort for each hydrocolloid (Limova and Troyer-Caudle 2002). Testing of hydrocolloids is often controversial due to variations in wound aetiologies, selection of control groups and differences from one animal model to another.

1.15 Advanced and innovative applications

The complex nature of non-healing wounds has necessitated the employment of a wide variety of materials, including biomaterials such as collagen and hyaluronic acid (HA), which are physiologically involved in the construction of healthy tissue. This group of materials, also known as bioactive, constitute another category of dressings referred to as biological or advanced dressings (Boateng et al. 2007). Collagen and HA are thought to have a pharmacological role in wound healing. Other advantages attributed to bioactive materials include biocompatibility, biodegradability and lack of toxicity. Collagen in particular is thought to be active in the healing process, stimulating fibroblast and macrophage production (Mian et al. 1992). In addition, collagen and HA can be used as carriers of different therapeutic compounds such as antimicrobials and/or growth factors (Boateng et al. 2007).

In the last two decades, there has been an increased interest in the investigation of pharmacological properties of either collagen or HA, or their binary combination, as carriers of therapeutic agents. The use of technologies such as freeze drying in the field of formulation science contributed to the formulation and combination of such materials. Park *et al.* (2003) have

investigated the role of collagen-HA matrices on human fetal dermal fibroblasts and their *in vivo* effect on wounded animals. Experimental data demonstrated that the presence of HA enhanced the proliferation of fibroblasts, but did not effect significantly their migration. In addition, the application of collagen and/or collagen-HA sponges on full-thickness wounds induced in guinea swine, increased epithelialisation, collagen synthesis and eventually wound healing, while the incorporation of HA did not significantly have an additional effect (Park et al. 2003). Recent *in vitro* and *in vivo* experiments performed with oligosaccharide-HA formulations on acute dermal wounds in small animal models, demonstrated that such formulations enhanced angiogenesis, granulation, fibroblast proliferation and collagen deposition. In addition, oligosaccharide-HA formulations promoted the repair of injured tissue (Gao et al. 2010).

Other authors support that the application of collagen itself, may likely not promote healing in the presence of bacterial contamination, as collagen can rather serve as a substrate for pathogens, because it is in its essence a large protein (Kumar et al. 2010). As such, the incorporation of therapeutic compounds into collagen matrices could facilitate better healing rates. *In vivo* experiments performed with wounded mice demonstrated that the application of collagen films impregnated with human growth hormone (hGH) significantly reduced the wounded area after 21 days, while the application of either collagen film or powdered hGH alone, had no effect compared to the untreated controls (Maeda et al. 2001). Recent *in vivo* investigative data, performed in wounded albino mice, demonstrated that the incorporation of an antioxidant with antimicrobial properties, such as triphala, in collagen matrices can induce tissue regeneration, collagen deposition and faster wound closure, while also having an impact on reducing the activity of MMP-8 and MMP-9, compared to collagen and gauze controls.

1.15.1 Lyophilised wafers as innovative potential dressings

The use of natural polymers, also known as biopolymers, in conjunction with the application of the freeze drying process in formulation of dressings possessing a high absorbency, led to innovative technologies in the field of wound management. Lyophilised wafers as a topical drug delivery system for the treatment and management of a wide range and types of non-healing exudative wounds have been developed by Matthews *et al.* (2005). The philosophy behind the design of wafers relies on the ability of a three-dimensional, porous and regular matrix structure to turn into high viscosity, physical gels. The technology which supports the formulation of such structures is a sophisticated process, in terms of temperature and pressure, known as freeze drying or lyophilisation. In other words, wafers are shape-adaptive or mouldable formulations as they take shape from the containers where the gels are placed prior to lyophilisation.

The term 'wafer' originated as the initial lyophilised polymers were relatively thin and porous. Lyophilised wafers can be suitable formulations for topical drug delivery on every moist biological membrane as they can be self-adhesive. Adhesion at the site of delivery can provide targeted delivery of the appropriate therapeutic compounds. Porosity and hydrophilicity have been considered as the most dominant parameters which govern the swelling behaviour of drug-loaded, hydrophilic polymers as the drug is being released as the polymer swells (Vlachou *et al.* 2001). Lyophilised wafers can be considered as ideal carriers of therapeutic agents, including antimicrobials and therefore are thought to be efficient systems to deliver antimicrobial treatment on a wide range of suppurating chronic wounds.

1.16 Project design

As outlined above, treatment of chronic non-healing wounds addresses major medical concerns with regard to selection of appropriate therapy, application of effective formulations and desirable quantities of therapeutic agents in a poly-contaminated site of infection. As previously discussed, there are many factors that can result in non-healing, broken skin tissue. Undoubtedly, the presence of different types and populations of pathogens in an open skin injury stimulates inflammation, leading to persistent infection and inevitably to non-healing conditions. The topical delivery of antimicrobials on a contaminated chronic wound bed is considered an optimal choice of treatment. The application of such compounds via materials which can simultaneously absorb the excess exudate providing optimal moist conditions, sustained drug delivery while being self-adhesive, harmless and practical, present additional advantages. Contemporary formulations such as lyophilised wafers impregnated with broad spectrum antimicrobial compounds are thought to possess all the aforementioned properties.

This project has therefore been designed to investigate formulations and microbiological issues that need to be considered in the development of a lyophilised antimicrobial wafer as a potential wound dressing for non healing exudating wounds. Additionally, the experimental work contained in this project, is multidisciplinary in nature, combining the disciplines of materials science, drug delivery, wound management and microbiology. Importantly, emphasis has been placed on attempting to mimic the contaminated and exuding profile of a chronic wound and to investigate the role of lyophilised antimicrobial wafers under those simulated conditions.

1.16.1 Aims

- 1.** To formulate cohesive lyophilised antimicrobial wafers using hydrophilic biopolymers which can be physically compatible with the embedded broad spectrum topical antimicrobial compounds.
- 2.** To evaluate the antimicrobial properties of lyophilised wafers using suitable *in vitro* wound models.
- 3.** To quantify the release of antimicrobials from lyophilised wafers under simulated condition of exuding wounds.
- 4.** To investigate the physicochemical and antimicrobial properties of gamma-irradiated lyophilised wafers.

Chapter 2

Formulation of lyophilised antimicrobial wafers

2.1 Aim

To formulate cohesive, non friable lyophilised antimicrobial wafers using hydrophilic biopolymers which are physically compatible with the embedded broad spectrum topical antimicrobial compounds.

2.2 Introduction

Natural polymers are materials which have been extracted from natural sources, such as plants, algae and/or bacterial biofilms. The exceptional properties, in terms of gelling in the presence of water and low cost, ranked them as broadly used thickeners, stabilisers or emulsifiers in the food industry. Simultaneously, the hydrophilic and non-toxic properties are also utilised in the pharmaceutical and cosmetic industries. Sodium alginate (SA) and xanthan gum (XG) are two of the most used biopolymers in both food and pharmaceutical manufacturing, while the use of karaya gum (KAG) and guar gum (GG) was initially restricted to food additives. Recently, there has been an increased interest in investigating their properties as drug delivery vehicles.

Brannon-Peppas (1997) has characterised the ideal delivery system as the one which should be "inert, biocompatible, mechanically strong, comfortable for the patient, capable of achieving high drug loading, safe from accidental release, simple to administer and remove, and easy to fabricate and sterilise". Interestingly, most of these properties have been found in materials displaying a polymeric nature. Although polymer gels are simply characterised as 'soft' and 'wet' materials (Kavanagh and Ross-Murphy 1998), their multi-clustered structure present different challenges in understanding their physicochemical behaviour in terms of gelling, swelling, flowing and interacting with other polymeric or non-polymeric compounds.

In the present chapter, biopolymers such as XG (*Xanthomonas campestris*), GG (*Cyamopsis tetragonolobus*), SA and KAG (*Sterculia urens*) were selected for the formulation of lyophilised matrices, to contain clinical concentrations of selected, commonly used, broad spectrum topical antimicrobial compounds such as neomycin sulphate (NS), chlorhexidine digluconate (CHD), povidone iodine (PVP-I) and silver sulfadiazine (SS). Physicochemical properties of biopolymeric carriers will be investigated in

terms of biocompatibility, flow behaviour, lyophilisation and adhesive properties.

2.3 Materials and methods

2.3.1 Materials

Neomycin trisulphate (powder), chlorhexidine digluconate (20 % w/v solution), silver sulfadiazine (SS) (98 % purity of powder), pluronic F68 (non-ionic surfactant), sodium alginate, guar gum, karaya gum and xanthan gum were purchased from Sigma-Aldrich, Gillingham, UK. Povidone iodine (10 % w/v standardised aqueous solution) and 12-well polystyrene culture plates were purchased from Seaton Healthcare Group, Oldham and Costar Ltd., UK, respectively. Bacteriological agar was purchased from Oxoid Ltd., UK.

2.3.2 Methods

Initially, in order to establish a workable concentration for polymers and physical compatibility between the biopolymers and antimicrobials, combinations of different natural polymers and antimicrobial compounds were prepared as gels in distilled water at approximately 25 °C with continuous stirring at 1000 – 2000 rpm, using an overhead mechanical stirrer fitted with a 70 mm (*RZR 2102*, Heidolph) propeller shaft. Clinical concentrations of antimicrobials used ranged from 0.5 % – 1 % (w/v or v/v depending on the nature of the antimicrobial) while concentrations of polymers ranged from 1.5 – 5 % (w/v). Table 2.1 presents a summary of the antimicrobial gels prepared.

2.3.3 Preparation of silver sulfadiazine (SS) gels

Silver sulfadiazine was prepared as a suspension using 0.2 % (w/v) of a non-ionic surfactant (pluronic F68). The suspension was prepared using a turbine mixer (*DIAX 900*, Heidolph) at maximum speed for 5 minutes. Analysis of the particle size distribution of SS suspensions prepared with pluronic F68 was undertaken using a MastersizerS laser light scattering instrument. A 300 mm

lens focused the scattered beam ($\lambda = 633 \text{ nm}$) onto a multi diode detector. The size-range of the detector was $0.1 - 1000 \mu\text{m}$. The results of particle size distribution were obtained as the computed value for particle abundance (%) as a function of mean particle size, based on the statistics of polydisperse systems. The volume mean diameter $D [4, 3]$ (derived from the statistical analysis of the distribution) was used, Figure 2.1.

2.3.4 Binary gel synergies

Binary polymer mixtures were prepared by the addition of small concentrations of powdered gums (XG, SA, GG and KAG) to distilled water warmed at approximately $25 \text{ }^{\circ}\text{C}$ and stirred continuously at $1000 - 2000 \text{ rpm}$. Gels were prepared by combining two polymer gels/solutions at concentrations ranging from $0.5 - 1.5 \%$ for individual polymers. All possible combinations of two polymers were prepared. Table 2.2 presents the rheological analysis of the flow properties of each polymer and their binary mixtures as analysed with the Herschel-Bulkley mode (Aulton 2002).

2.3.5 Rheological measurements

The analysis of flow and deformation of all polymeric gels prepared was investigated by rheological measurements. At least three fresh samples of each polymer solution (with and without antimicrobial) were characterised by continuous flow rheometry at 25°C . A cone and plate geometry was used ($40 \text{ mm}/2^{\circ}$ steel) and flow measurements were conducted at continuous shear rates from 0 to 600 s^{-1} using a dynamic rheometer (*AR1000, TA Instrument*). Analysis of the descending flow curves was undertaken with the system software using the Herschel-Bulkley model, viz:

$$\sigma = \eta' \gamma^n + \sigma_0$$

where, σ = shear stress (Pa), η' = viscosity coefficient or 'consistency' (Pa.s), γ = shear rate (s^{-1}), n = rate index of pseudoplasticity and σ_0 = yield stress (Pa), Figures 2.2-2.4 and Tables 2.3 - 2.4.

2.3.6 Freeze drying process

Aliquots (1.5 ± 0.02 g) of each batch of gel formulation were cast to the individual compartments of 12-well polystyrene culture plates and lyophilised in a laboratory-scale freeze drier (Virtis, Advantage 2.0) for 26 hours. Figure 2.5 shows the temperature profile for sample and shelf during the lyophilisation cycle. The lyophilisation process used was identical for all the wafer batches. Samples were slowly cooled to approximately -55 °C and then heated in a series of thermal ramps to room temperature under reduced pressure, ranging from 3525 mTorr to a minimum of 52 mTorr during the programmed cycle. Ice was removed by sublimation during the primary drying phase and residual non-freezing water was removed by desorption to the gas phase during the secondary drying cycle. The lyophilised wafers produced were stored in a dry place at room temperature in the sealed polystyrene plates in which they were cast.

2.3.6.1 Batches of lyophilised formulations

Two main groups of lyophilised wafers were prepared as presented in Table 2.1 (grey boxes). The first group includes the combination of 3 % (w/v) solution of KAG with clinical concentrations of 0.5 % (w/v) NS, 0.5 % (v/v) CHD, 1.0 % (v/v) PVP-I and 1.0 % (w/v) SS. The second group of lyophilised antimicrobial wafers consists of three different polymer formulations, namely XG, SA, GG and the binary gel of SA-KAG in combination with 0.5 % (v/v) CHD. Control wafers (wafers with no antimicrobials added) were prepared for each group of antimicrobial wafers. For the KAG-SS wafer, an extra control wafer (KAG-F68) containing 0.2 % (w/v) pluronic F68 was included, as silver sulfadiazine was prepared as a suspension with pluronic F68 as surfactant.

2.3.7 Thermogravimetric (TGA) analysis of the lyophilised wafers

Thermogravimetric analysis was undertaken to determine the water content of the lyophilised wafers. All wafer samples were manually compressed to fit on the pre-tarred platinum sample pan. Powder-free, latex gloves were worn to avoid external contamination from skin moisture/sweat. Mean sample weights of 9.8 ± 2.4 mg were used. The residual water content of lyophilised wafers

was analysed as the weight loss of the sample during a heating ramp from 25 °C – 200 °C at a heating rate of 10 °C/min. A *TA Q500 Instrument* was used for all measurements. Table 2.5 summarises the results of the thermogravimetric analysis for both control and antimicrobial KAG wafers.

2.3.8 Scanning electron microscopy (S.E.M)

A *Leo S430* digital scanning electron microscope was used to image the microstructure of control and drug-loaded wafers. Samples for imaging were coated with gold and palladium for four minutes. Images of the wafer surfaces (top and bottom) were taken at magnifications of 200x and 500x, Figure 2.6 and 2.7.

2.3.9 *In vitro* determination of adhesive properties of lyophilised wafers to a model agar surface

The adhesive properties of lyophilised wafers to a model surface were measured using a texture analyser with a 5 kg load cell attached (TA-XT2i, Stable Micro System Surrey, UK). A 0.8 % (w/v) agar plate was prepared using a salt solution (142 mmol.l⁻¹ of sodium ions, 2.5 mmol.l⁻¹ of calcium ions) representative of sodium/calcium levels found in wound fluid (Thomas 2007). A wafer was attached to the base of an aluminium probe (20.0 mm) using double-sided adhesive tape and the probe fixed to the mobile arm of the texture analyser. The wafer was lowered at a rate 2.0 mm s⁻¹ until contact with the moist agar surface was made. A contact force of 0.05 N was maintained for 30 seconds for KAG, NS, CHD, SS, F68, GG, XG and 90 seconds for SA, SA/CHD, SA-KAG, SA-KAG/CHD, until approximately 1 mm of a gel layer was formed, after which the probe was withdrawn from the agar surface at a rate of 5.0 mm s⁻¹. Clearly, wafers containing SA took slightly longer to swell. The peak detachment force was noted and the work of adhesion calculated using the area under the force/distance curve, Table 2.6 and 2.7. The tensile stress (N cm⁻²) was calculated as the peak detachment force divided by the surface area of the wafer (approximately 3.463 cm² at 25 °C).

2.4 Statistical analysis

Data are presented as the mean value of three samples \pm standard error of the mean (SEM). Statistical analysis of adhesion data was performed using GraphPad Prism 4 software. The normality of data was analysed with the Skewness-Kurtosis Omnibus test for variable sampling plans. Normality of data was determined by 95 % confidence of the normal distribution of the data. When normal distribution was proven, a parametric test such as one way analysis of variance (ANOVA), followed by post hoc Tukey's multiple comparison test was used to compare more than two groups. A nonparametric Mann-Whitney test was used for the comparison of two groups when the data did not show normal distribution. A p-value less than 0.05 was considered a significant difference.

2.5 Results

Table 2.1 Qualitative analysis of physical compatibility (pre-lyophilisation) and friability (post-lyophilisation) between combinations of natural polymers and antimicrobials. NC- not compatible, C- compatible; +, ++, +++ indicate the visualised degree of friability and integrity for a disc of lyophilised polymer impregnated with antimicrobial compound. Formulated combinations are marked as grey boxes.

Polymers (w/v)	Antimicrobials			
	NS (0.5 % w/v)	CHD (0.5 % v/v)	PVP-I (1.0 % v/v)	SS (1.0 % w/v)
KAG (3.0 %) pH = 4.5	C	C	C	C
GG (2.0 %) pH = 6.1	C ⁺	C	C ⁺⁺⁺	C
XG (1.5 %) pH = 6.2	NC	C	C ⁺⁺	C ⁺
SA (5.0 %) pH = 8.3	NC	C	C ⁺⁺⁺	C ⁺

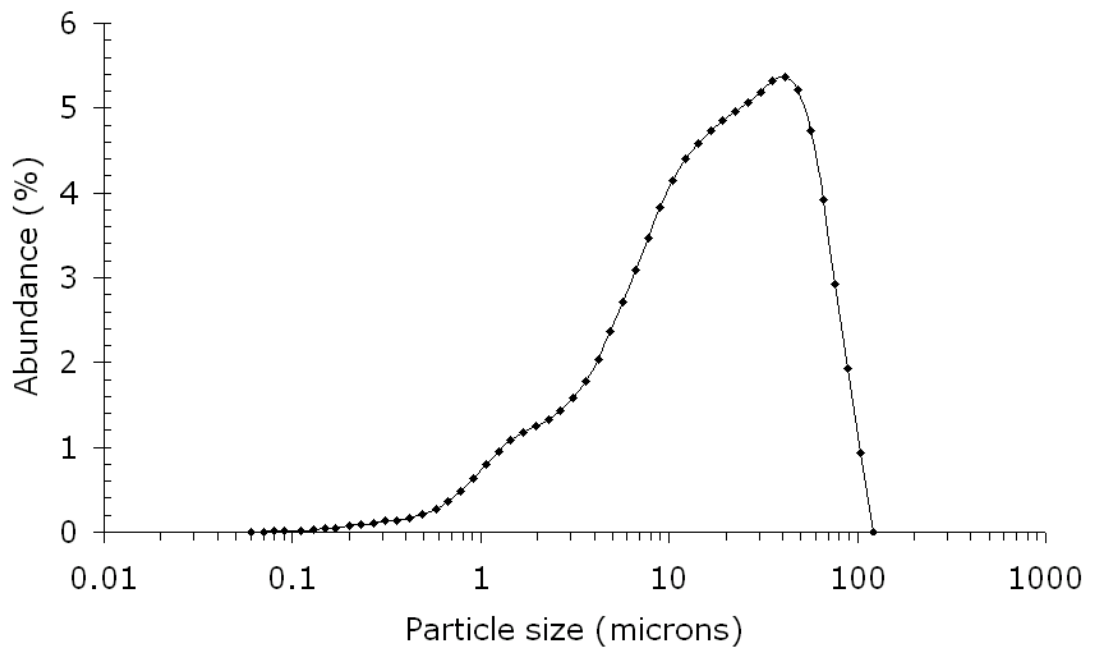


Figure 2.1 Particle size distribution curve for 1.0 % (w/v) silver sulfadiazine suspension, prepared in distilled water with 0.2 % (w/v) non-ionic surfactant pluronic F68. Mean particle size = 23.63 μm .

Table 2.2 Viscosity coefficient or 'consistency', η' (Pa.s) and yield stress σ_0 (Pa), for four natural polymers and their mixtures in aqueous solution as analysed with the Herschel-Bulkley model. Note the particularly large yield stress of the SA-KAG combination.

Polymer (w/v)	SA η' (σ_0)	XG η' (σ_0)	GG η' (σ_0)	KAG η' (σ_0)
SA (1.5 %)	0.61 (0.00)	-	-	-
XG (0.5 %)	2.00 (0.00)	0.17 (6.09)	-	-
GG (0.5 %)	6.89 (0.00)	2.35 (21.29)	0.16 (4.58)	-
KAG (1.5%)	9.03 (96.45)	0.94 (20.38)	3.15 (22.60)	0.50 (0.00)

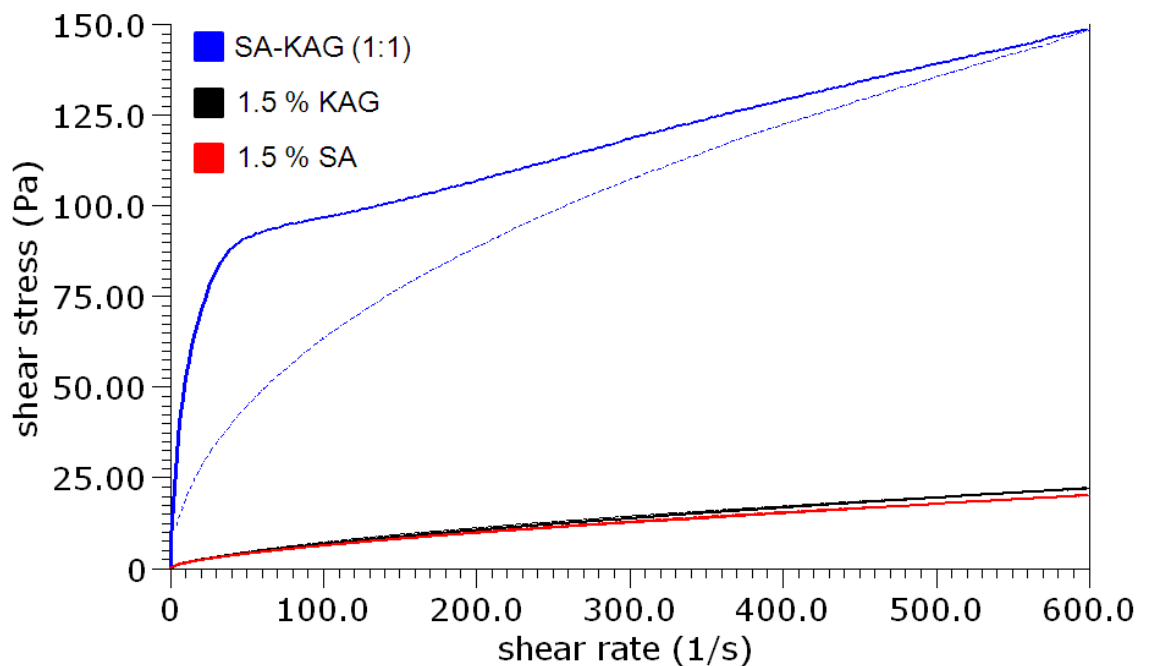


Figure 2.2 Rheological analysis of pre-lyophilised gels. Flow curves of 1.5 % SA, 1.5 % KAG and the combination of SA-KAG (1:1) ratio. (—) ascending, (----) descending.

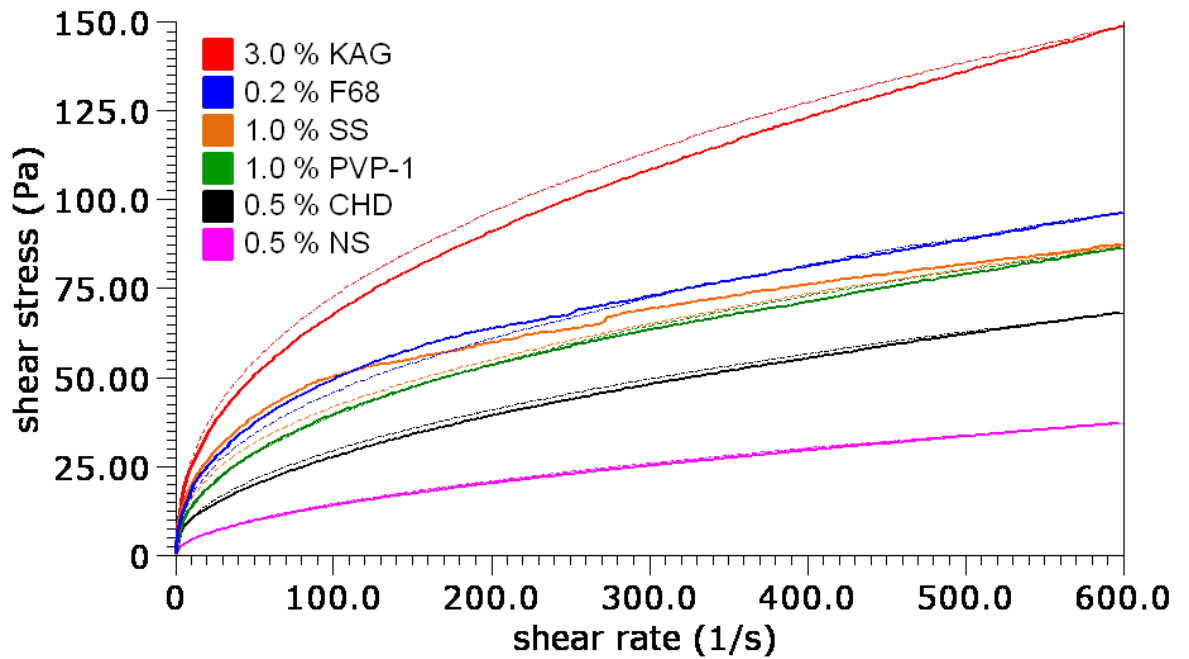
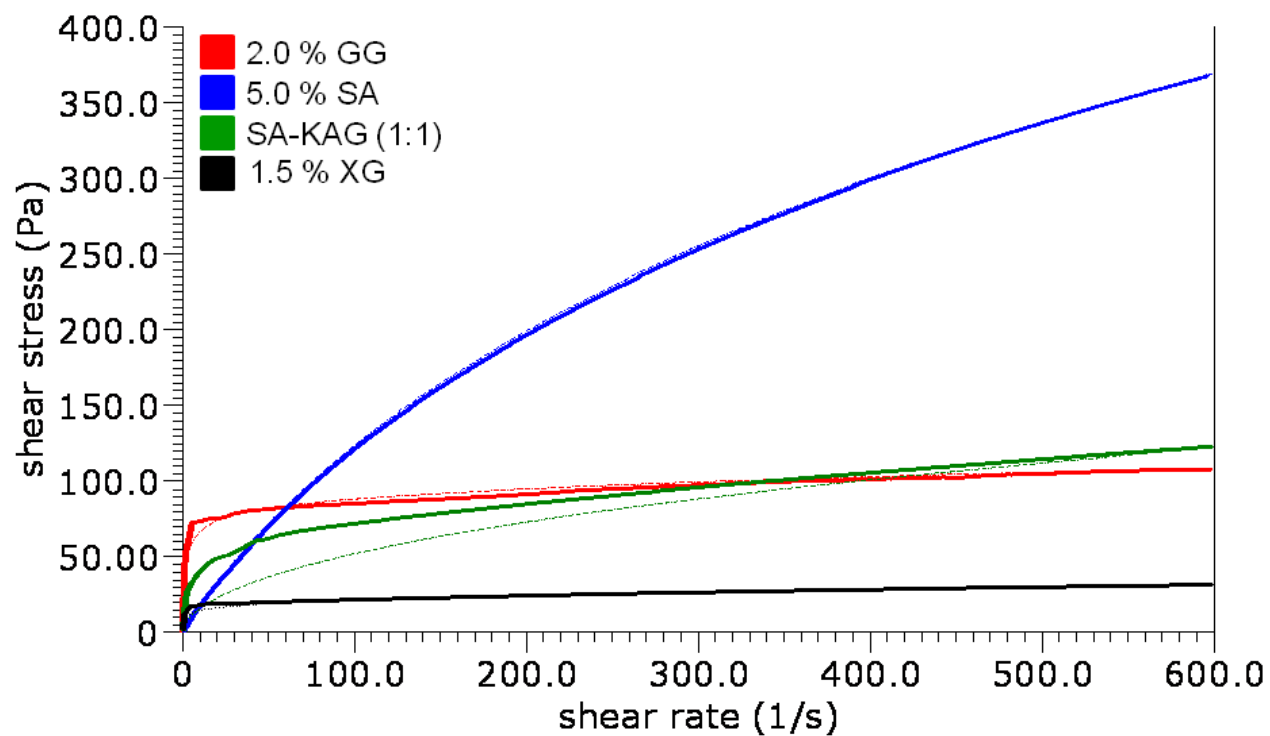


Figure 2.3 Rheological analysis of flow curves of KAG control and antimicrobial gels; (—) ascending, (----) descending.

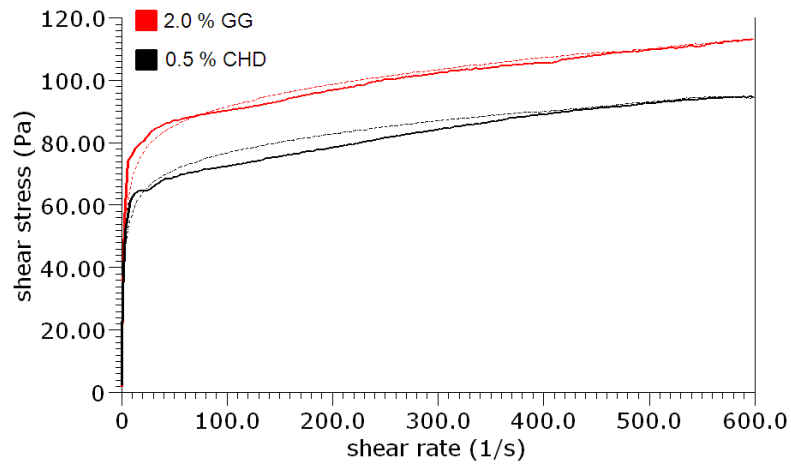
Table 2.3 Viscosity coefficient of 3 % (w/v) KAG in combination with clinical concentrations of antimicrobials as obtained using the Herschel-Bulkley model. Values represent the mean value of three samples \pm the standard error of mean (n=3, SEM)

Pre-lyophilised gel (3.0 % KAG w/v)	Viscosity coefficient (Pa.s)
Control (3.0 % KAG)	12.89 \pm 0.93
0.5 % NS	1.56 \pm 0.10
1.0 % PVP-I	4.09 \pm 0.34
0.5 % CHD	3.79 \pm 0.30
1.0 % SS (0.2 % F68)	6.48 \pm 0.33
0.2 % F68	7.40 \pm 0.55

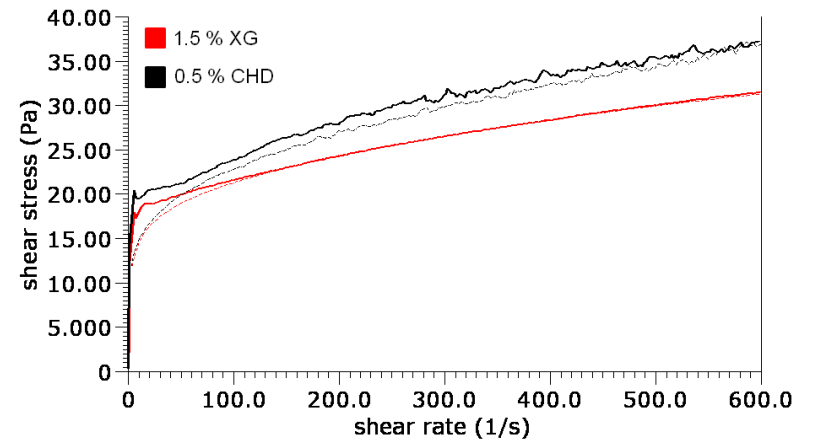
Figure 2.4 Rheological analyses of pre-lyophilised control gels. Below [Figures (a), (b), (c) and (d)]: Flow curves of control gels (—) and 0.5 % CHD (—); (a) 2.0 % GG, (b) 1.5 % XG, (c) 5.0 % SA and (d) binary gel synergy of SA-KAG; Note the difference in scale of the 'y' axis. (—) ascending, (----) descending.



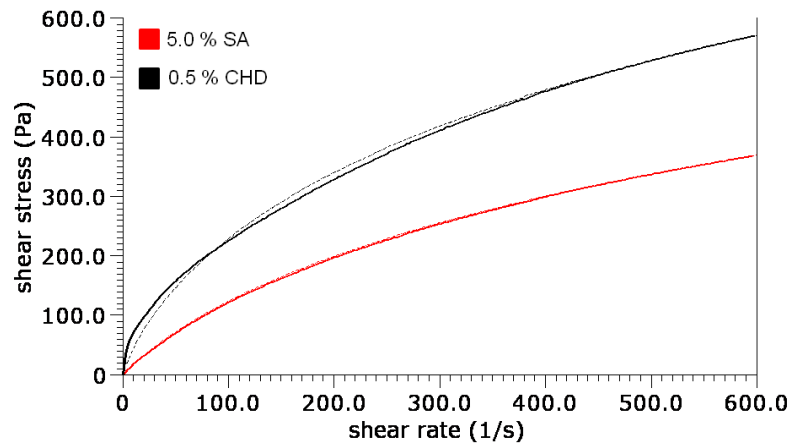
(a)



(b)



(c)



(d)

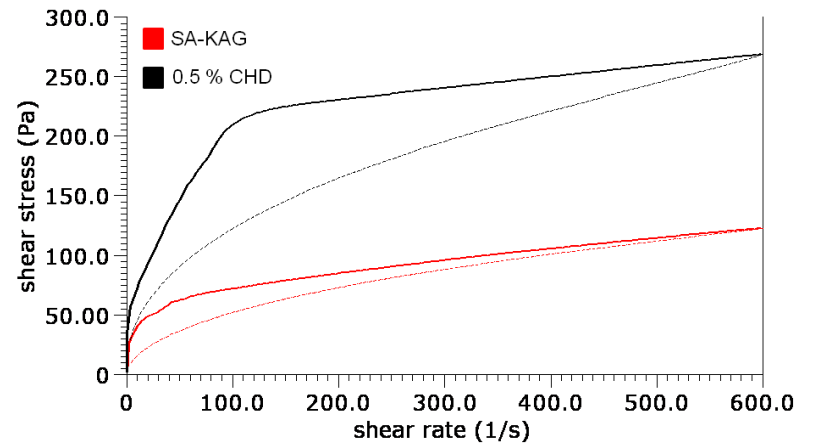


Table 2.4 Viscosity coefficients and yield stresses of pre-lyophilised gels (controls) and 0.5 % CHD-containing gels of 2 % GG, 5 % SA, 1.5 % XG and the binary mixture of SA-KAG, as obtained with the Herschel-Bulkley model. Values represent the mean value of three samples \pm the standard error of mean (n=3, SEM)

Pre-lyophilised gels (w/v)	(η') Viscosity coefficient (Pa.s) [(σ_0) Yield stress (Pa)]	
	Control	0.5 % (v/v) CHD
2 % GG	82.21 \pm 5.41 (95.87 \pm 2.31)	65.49 \pm 6.64 (93.63 \pm 9.50)
5 % SA	18.17 \pm 0.70 (00.00 \pm 0.00)	43.36 \pm 6.48 (00.00 \pm 00.00)
1.5 % XG	2.86 \pm 0.12 (23.61 \pm 0.68)	2.56 \pm 0.37 (31.71 \pm 2.43)
1.5 % - 1.5 % SA - KAG	7.75 \pm 0.64 (86.34 \pm 5.19)	13.71 \pm 0.8 (155.43 \pm 12.08)

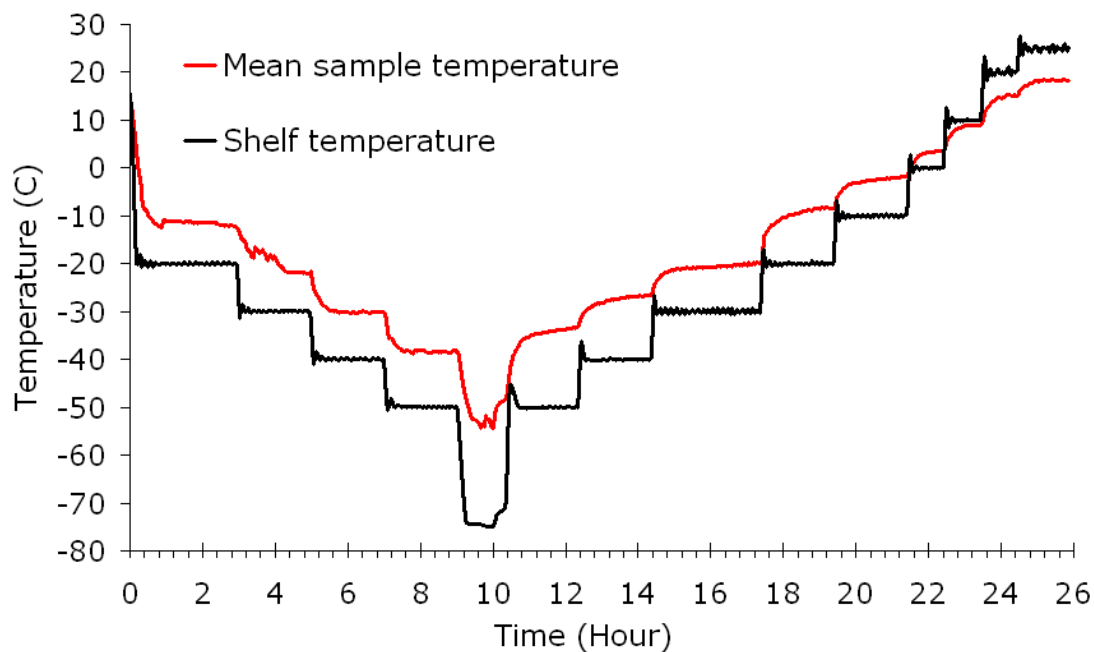


Figure 2.5 Temperature profile of the freeze-drying process

Table 2.5 Thermogravimetric analysis (TGA) of water content of KAG lyophilised wafers.

Wafers	Water content (%)
KAG	15.22
NS	16.77
CHD	16.12
PVP-I	13.87
SS	15.54
F68	18.49

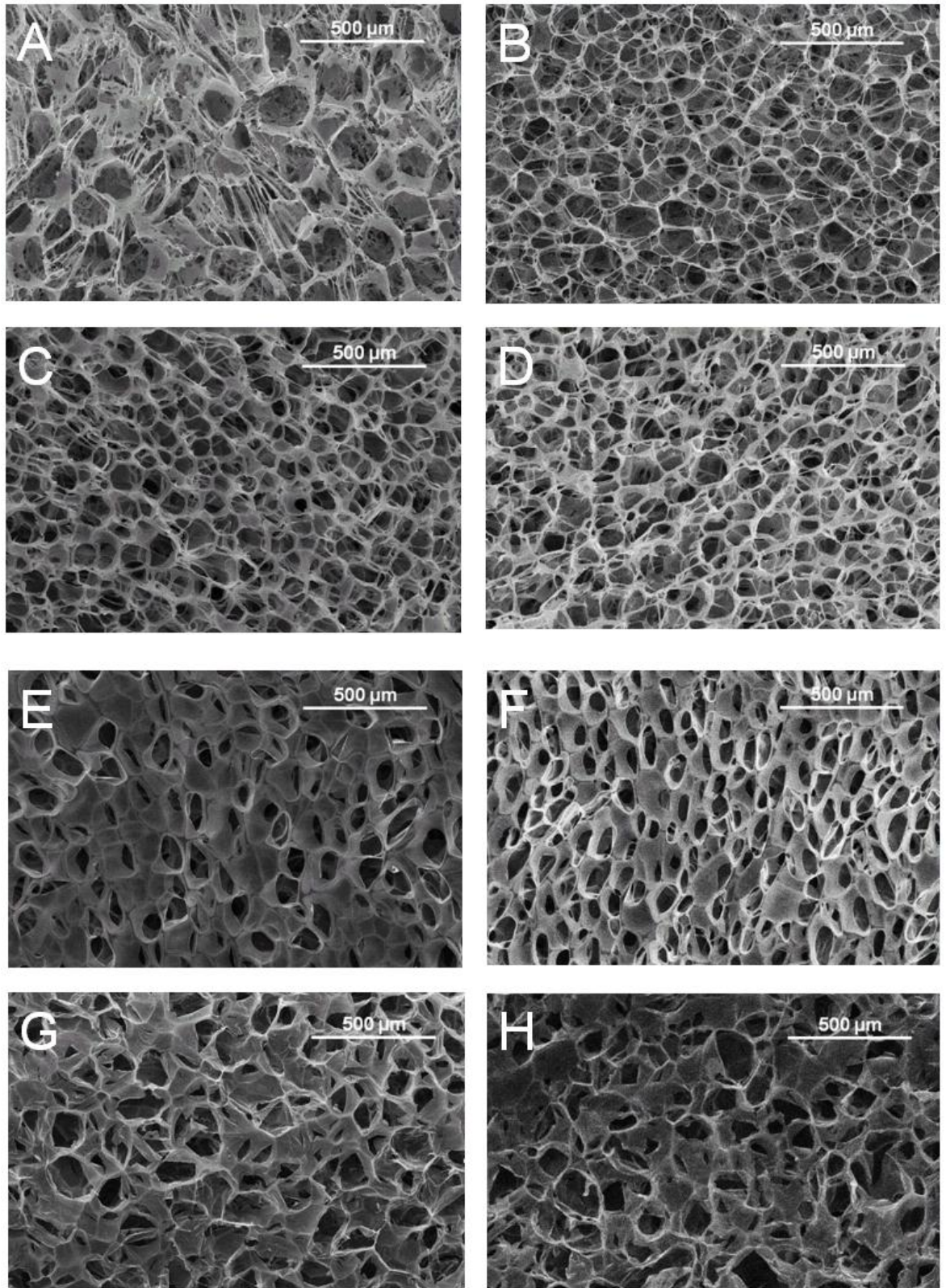
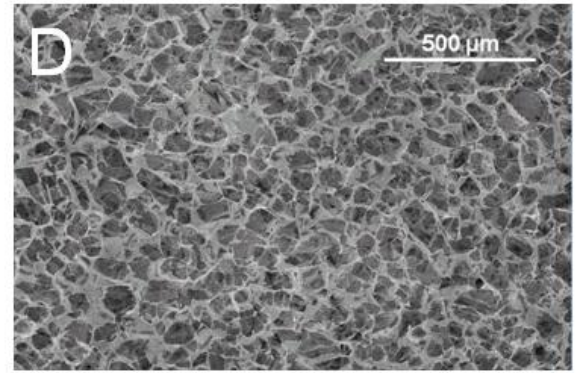
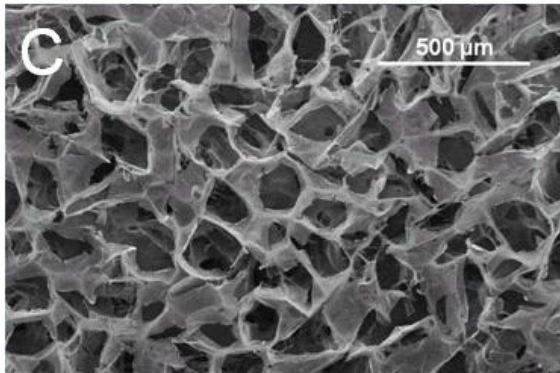
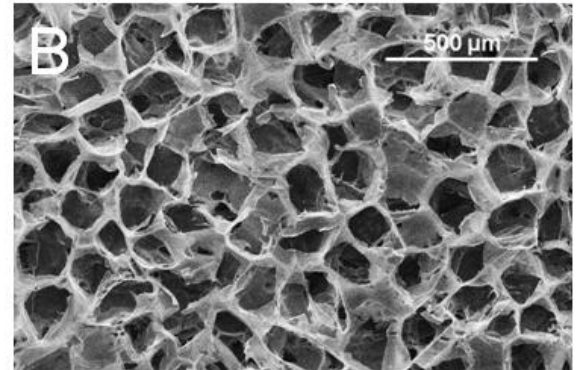
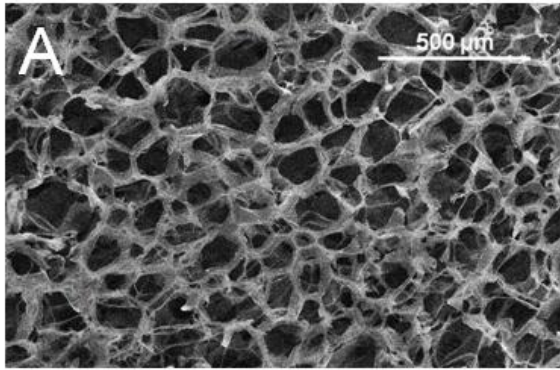


Figure 2.6 Scanning electron microscopy (S.E.M) images of wafer matrices top surfaces taken at 200x magnification. Image **A** – GG, **B** – GG-CHD; **C** - XG, **D** – XG-CHD; **E** – SA, **F** – SA-CHD; **G** – SA-KAG, **H** – SA-KAG-CHD.

Figure 2.7 (a) S.E.M images taken at 200x magnification, **A** – KAG (control wafer) **B** – KAG-NS, **C** – KAG-CHD and **D** – KAG- PVP-I.
(b) S.E.M images of KAG/SS. Images **A** and **C** taken at 200x magnification, **B** and **D** taken at 500x magnification. Images **A** and **B** - top surface of the wafer, **C** and **D** - bottom surface of the wafer. (Note the differences in pore size and shape between the top and bottom surfaces).

(a)



(b)

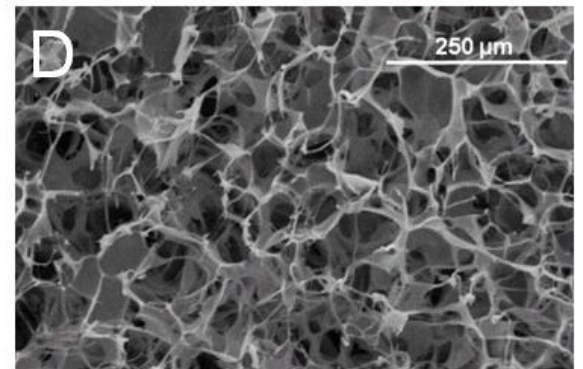
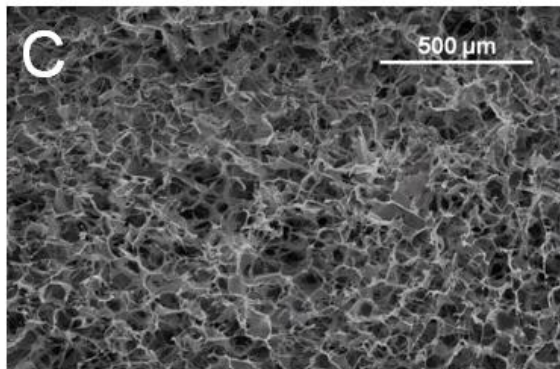
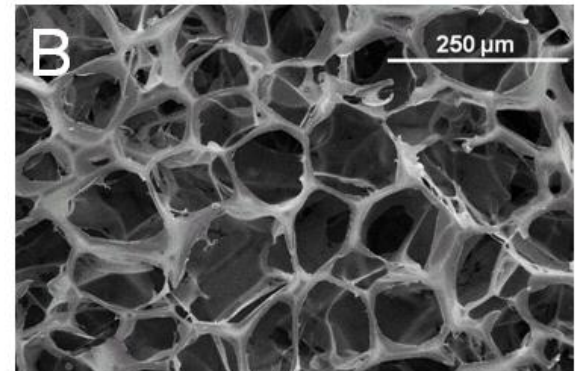
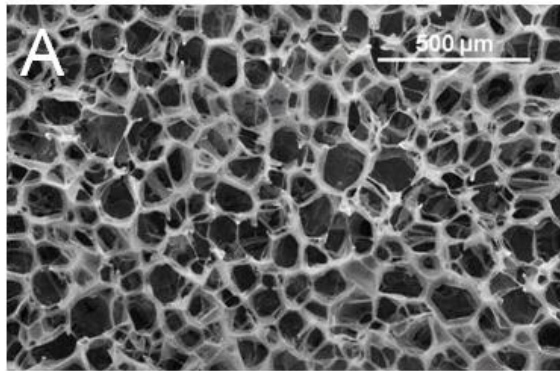


Table 2.6 Adhesion properties (peak detachment force and work of adhesion) of KAG lyophilised wafers impregnated with clinical concentrations of antimicrobial compounds. Statistical analysis of data was performed using one-way analysis of variance (ANOVA), followed by Tukey's post hoc test. A $p < 0.05$ was considered a significant difference. (n = 3, SEM) (* $p < 0.05$, ** $p < 0.01$, *** $p < 0.001$)

Lyophilised wafers	Peak detachment force (N)	Work of adhesion (N. mm)
KAG (Control)	0.88 ± 0.018	0.33 ± 0.023
NS	0.68 ± 0.026*	0.30 ± 0.010
PVP-I	0.36 ± 0.035***	0.31 ± 0.009
CHD	0.52 ± 0.049***	0.27 ± 0.016
SS	0.78 ± 0.038	0.30 ± 0.026
F68 (Control for SS)	0.78 ± 0.048	0.37 ± 0.022

Table 2.7 Adhesion properties (peak detachment force and work of adhesion) of lyophilised wafers prepared with different biopolymers impregnated with clinical concentrations of CHD. Statistical analysis of data was performed using a two-tailed, nonparametric Mann-Whitney test. A $p < 0.05$ was considered a significant difference. (n = 3, SEM)

Lyophilised wafers	Peak detachment force (N)		Work of adhesion (N. mm)	
	Control	0.5 % CHD	Control	0.5 % CHD
GG	0.86 ± 0.032	0.82 ± 0.028	0.48 ± 0.037	0.41 ± 0.009
XG	0.93 ± 0.077	0.79 ± 0.034	0.55 ± 0.028	0.49 ± 0.028
SA	1.05 ± 0.101	0.90 ± 0.024	0.45 ± 0.044	0.32 ± 0.023
SA-KAG	0.56 ± 0.026	0.31 ± 0.003	0.18 ± 0.004	0.12 ± 0.014

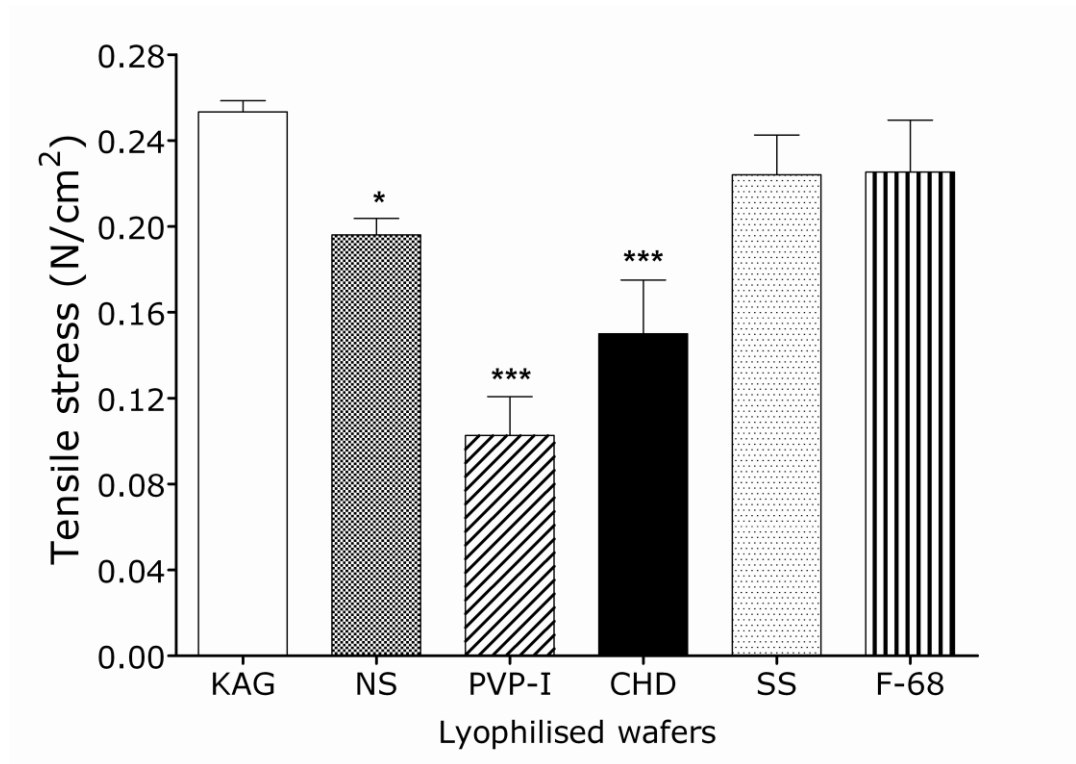


Figure 2.8 Tensile stress of KAG lyophilised wafers, control and antimicrobial-loaded, was calculated as the stress applied over the contact surface area of the wafer. The effect of embedded antimicrobials in the KAG matrix was compared to the control (KAG) matrix. Statistical analysis was performed using one way analysis of variance (ANOVA) followed by Tukey’s post hoc test. A $p < 0.05$ was considered a significant difference. ($n=3$, SEM) (* $p < 0.05$, ** $p < 0.01$, *** $p < 0.001$)

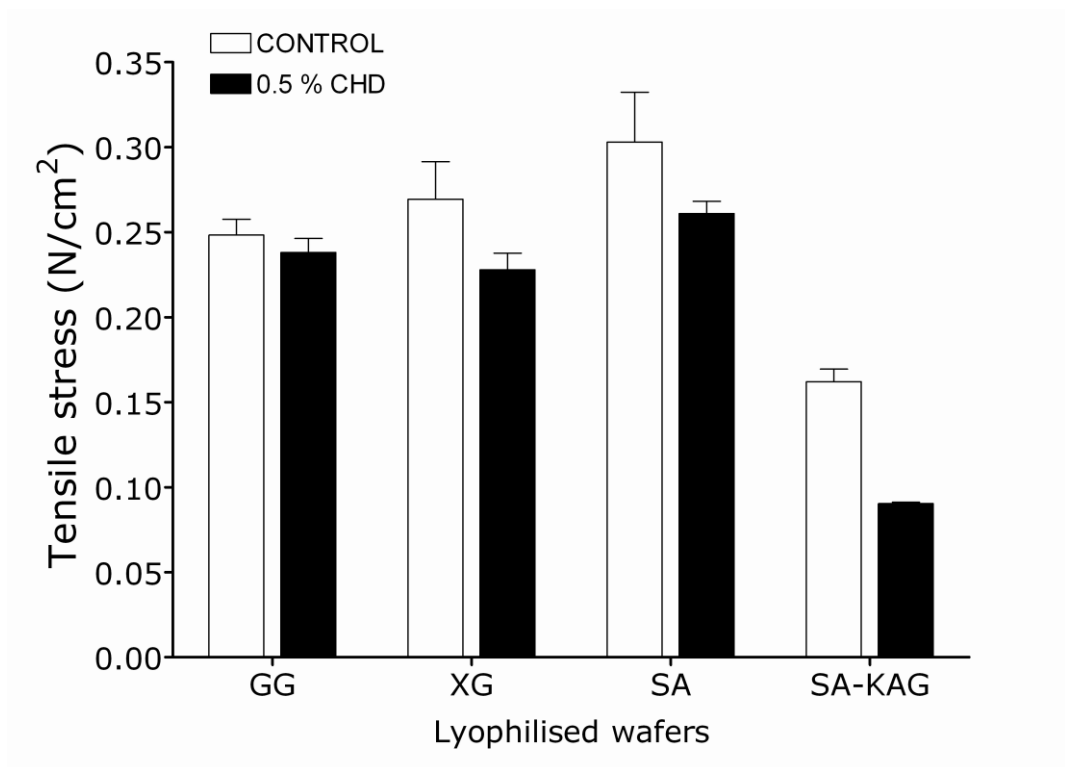


Figure 2.9 Tensile stress of GG, XG, SA and SA-KAG lyophilised wafers was calculated as the stress applied over the contact surface area of the wafer. The effect of embedded 0.5 % CHD in lyophilised matrices of different biopolymers was compared to the control. Statistical analysis was performed using a nonparametric Mann-Whitney test. A $p < 0.05$ was considered a significant difference. (n=3, SEM)

2.6 Discussion

The formulation and physicochemical characterisation of novel antimicrobial wafers containing clinical concentrations of the broad spectrum topical antimicrobials neomycin sulphate (NS), chlorhexidine digluconate (CHD), povidone iodine (PVP-I) and silver sulfadiazine (SS) form the basis of this chapter. Several issues are discussed with regard to the utilisation of natural polymers such as sodium alginate (SA), xanthan gum (XG), guar gum (GG), karaya gum (KAG) and the binary combination of SA-KAG used as carrier of the selected antimicrobials.

Based on the results obtained from the qualitative assessment of physical compatibility between polymers and antimicrobials (Table 2.1), only certain combinations were selected for further development as cohesive and non friable antimicrobial wafers. KAG was the biopolymer which was found physically compatible with all of the antimicrobials and produced intact lyophilised wafers. In addition, CHD was miscible with all the polymers tested, also producing cohesive lyophilised wafers. As a result, two main groups of lyophilised antimicrobial wafers were prepared. This led to the investigation and evaluation of carrier (KAG) loaded with different antimicrobial compounds and different carriers loaded with the same antimicrobial compound (CHD).

A brief investigation was also undertaken on the analysis of the rheological properties of binary combinations of biopolymeric gels presented in Table 2.2. In the present study, rheological investigation has clearly shown that several binary combinations of biopolymers demonstrated a notable increase in viscosity and yield stress compared to the respective homopolymer gels. A distinctive example of this synergistic interaction is the combination of KAG with SA in a 1:1 ratio. Figure 2.2 clearly shows that the gel mixture of SA-KAG exhibits different and improved flow behaviour with regards to increased viscosity (9.03 Pa.s), yield stress (96.45 Pa) and thixotropy (reversible isothermal transformation of gels induced by applied stress), compared to homopolymers of SA (0.61 Pa.s) and KAG (0.5 Pa.s). This may be due to interactive interconnections between polymeric chains of KAG and SA and formations of hyperentanglement. The water soluble salt of alginic acid, sodium alginate, is weakly basic (pH = 8.3) while KAG has free carboxylic acid groups (pH = 4.5). The synergistic interaction exhibited by the

combination of SA with KAG is likely to be attributed to the overriding acidic effect of karaya residues upon sodium alginate. However, further investigation will be required to explain the complex intermolecular interactions between both materials. This novel synergistic combination between KAG and SA has been used in this project as a lyophilised matrix impregnated with 0.5 % CHD and appears to be original.

Analysis of the flow behaviour (rheology) of the pre-lyophilised gels (miscible complexes of biopolymers with antimicrobials) was performed under controlled conditions of geometry and temperature. Rheological characterization of pre-lyophilised gels plays an essential role in quantification of flow properties of the gels (antimicrobial-loaded and/or antimicrobial-free). Flow properties of pre-lyophilised gels provide necessary information with regards to performance and flow behaviour (expansion) of the re-hydrated lyophilised wafers. Rheological analysis of 3 % (w/v) KAG gels (antimicrobial-free and antimicrobial-loaded) indicated pseudoplastic flow behaviour with no yield stress as presented in Figure 2.3. However, the rheological behaviour of pre-lyophilised KAG gel mixed with antimicrobials demonstrated decreased viscosity compared to the control KAG gel.

Flow curves of pre-lyophilised KAG gels (Figure 2.3) clearly display the effect of each antimicrobial on the polymer network of KAG. Table 2.3 summarises the values of viscosity coefficients of all KAG gels, as analysed with the Herschel-Bulkley model. The viscosity coefficient or consistency for KAG pre-lyophilised gels ranged from 1.56 – 12.89 Pa.s, where KAG-NS had the lowest value of consistency and KAG control gel revealed the highest. Apparently, the presence of antimicrobials such as NS and CHD had a major influence on the consistency of KAG gel, as they reduced the consistency of KAG gel by approximately 8 and 3.4 times, respectively.

Gelation of a branched, partly acetylated biopolymer such as KAG is complex. Silva *et al.* (2003) have reported that *Sterculiaceae* forms a gel network mainly due to opposite ionic interconnections between galacturonic acid residues of the main chain and glucuronic acid branching residues. In addition, junction zones may also form from hydrogen bonding created between rhamnose segments. The later authors suggest that interaction between homogalacturonic residues between different chains (the 'egg-box model') may also occur, however, to a small extent. De Brito *et al.* (2005)

have analysed the flow behaviour of karaya gum in aqueous solution and have shown that the presence of salt, such as NaCl (0.1 M), decreased the gel strength of karaya. The latter authors suggest that the presence of salt may partition the ionic strength of KAG and decrease cross-linking between polymer chains. It is proposed that disruption of junction zones is more likely to happen for counter ion interaction between galacturonic and glucuronic acid segments (De Brito et al. 2005; Silva et al. 2005). Therefore, it is very likely that the presence of antibacterial compounds such CHD, NS, PVP-I and SS may disrupt the gel network of karaya, resulting in a reduced gel consistency. However, further investigation is required to elucidate the drug-polymer interactions occurring and the effect of specific ions having a detrimental influence in the gel network of KAG.

Rheological analysis was also undertaken for pre-lyophilised gels (control and 0.5 % CHD-loaded) of GG, XG, SA and SA-KAG (Figure 2.4, Table 2.4). Different rheological behaviours of pre-lyophilised control gels were attributed to inherent differences in the molecular configuration of biopolymer chains. Rheological analysis of 2 % GG and 1.5 % XG gels displayed plastic flow behaviour with a clear yield stress, while the gel prepared with 5 % SA demonstrated pseudoplastic flow properties with no apparent yield stress. In addition, the gel prepared with SA-KAG (1:1 ratio) demonstrated plastic and thixotropic flow behaviour with high values of yield stress. Incorporation of cationic CHD notably affected the flow behaviours of XG, SA and SA-KAG. Complexes of SA and SA-KAG with CHD both displayed a substantial increase in consistency and yield stress. CHD enhanced the consistency of SA gel by approximately 2.4 times and doubled the yield stress of SA-KAG gel. The consistency of XG was not affected considerably by the addition of CHD, whereas the yield stress was increased from 23.61 – 31.71 Pa. The non-ionic polymeric structure of GG did not exhibit notable qualitative alterations to its rheological behaviour in the presence of CHD, however, the analysis of the flow curves of GG gels showed a slightly decreased yield stress and consistency. In conclusion, the antimicrobials NS and CHD incorporated in KAG, SA, XG and SA-KAG gel networks, influenced the rheological properties of the gels and would be expected to influence the *in vitro* performance of reconstituted wafers.

Disc-shaped, lyophilised wafers were produced by casting gels in the circular wells of polystyrene plates and freeze drying. The freeze drying process consists of a triple-stage operation, starting with freezing, followed by primary drying and secondary drying. All stages play a definitive role in the quality, micro and macro morphology of the final lyophilised product. During freezing, materials are cooled to low temperatures (e.g. $-60\text{ }^{\circ}\text{C}$). The high water content of the gel will result in ice crystals, the size of which will depend on the cooling rate, while the polymers will form highly concentrated solutions that display amorphous and glassy properties below their glass transition temperature (T_g). Consequently, the freezing gel will yield a combination of an amorphous and a crystalline phase. On freezing, the pressure is reduced and primary drying begins. During primary drying, the ice is removed by sublimation and the endothermic phase transition from solid to gas is driven by a gradual increase in the process temperature. Water vapour is collected as ice on a condenser that is at a lower temperature than the sample. It is important that during this stage, the freeze concentrate is maintained at a process temperature below its glass transition temperature (T_g) to maintain the cast shape. Upon complete removal of ice, residual amounts of non-freezing water contained within the freeze concentrate, must be removed by desorption. This is achieved by a careful increase in the process temperature under continuous low pressure/high vacuum conditions. As the non-freezing water is removed, the T_g of the freeze concentrate increases (Beddu-Addo 2004).

The temperature profile of the freeze drying process presented in Figure 2.5 demonstrates that the mean sample temperature followed the shelf temperature with an approximate $+15 - 20\text{ }^{\circ}\text{C}$ difference. The recorded difference of the mean sample temperature was attributed to the insulating properties of the polystyrene plates used as moulds. In addition, the freeze drying cycle used for the lyophilisation of the biopolymeric gels (with or without antimicrobials), involved a slow cooling rate of approximately $10\text{ }^{\circ}\text{C}/2.5\text{ hours}$ (Figure 2.5), whereas the lowest temperature reached by the sample was approximately $-55\text{ }^{\circ}\text{C}$. The freezing cycle is decisive for the morphology of the lyophilised product, in particular the size of the pore formed by the ice crystals. It is observed that the freezing rate influences the mean size of the ice crystals. A rapid freezing process develops small and numerous

crystals, whereas slow freezing develops large and less numerous ice crystals, affecting the microstructure and the appearance of the matrix of the final lyophilised formulation (Faydi et al. 2001).

Such micro structural dissimilarities were observed between top and bottom surfaces of lyophilised wafers. Although, the cast gel had a depth of approximately 5 mm, there was an apparent variance in the cooling rate of the bulk. S.E.M pictures taken at two magnifications (200x and 500x) presented in Figure 2.7(b) show the distinctive micro structure of top and bottom surfaces of a KAG-SS wafer. The top surface of KAG-SS (Images A and B) is notably different from that of the bottom surface (Images C and D), the pore size of the top surface being much larger ($\approx 100 \mu\text{m}$) than that of the underside ($< 50 \mu\text{m}$). These differences can be attributed to different crystal sizes resulting from bulk variations in cooling rate during the freezing process.

The network microstructure of KAG-NS, KAG-CHD and KAG-SS (Figure 2.7 (a) Images B, C and Figure 2.7 (b) Image A, respectively) did not display distinctive morphological differences compared to the control (KAG) matrix, Figure 2.7 (a) Image A. However, notable alterations were presented in the matrix morphology of KAG-(PVP-I) (Figure 2.7 (a) Image D) as the matrix microstructure of KAG impregnated with 1 % PVP-I demonstrated a two-fold reduced pore size and semi-formed pore shapes compared to the control (KAG). It appears that the incorporation of PVP-I, which was used as a standardized liquid formulation (containing: 100 mg/g PVP-I, glycerol, nonoxynol-9, sodium phosphate, sodium hydroxide, potassium iodate, citric acid and water), affected the thermal properties of the KAG-(PVP-I) mixture. Although it is difficult to precisely conclude which of the ingredients of the PVP-I solution affected the micro morphology of the KAG-(PVP-I) formulation, the presence of compounds possessing cryoprotective properties such as glycerol may be the more likely candidate. The presence of glycerol molecules during the freezing stage of lyophilisation have a strong effect on ice formation in the bulk, resulting in partial ice nucleation (Inaba and Anderson 2007). Therefore, the development of semi-formed, non-maturated ice crystals in the presence of small amounts of glycerol within the bulk of KAG-(PVP-I) mixture likely led to the formation of small and rounded pore morphologies in the final lyophilised structure.

The microstructures of lyophilised polymers impregnated with 0.5 % CHD were also observed and compared to the control samples. S.E.M analysis of CHD-polymer lyophilised complexes presented in Figure 2.6 demonstrate similarities between controls and CHD impregnated wafers, indicating that the presence of CHD had no apparent effect on the morphology of the lyophilised matrix. The same was also true of wafers formed from GG, XG and SA-KAG (Images A, B, C, D, G and H). CHD incorporated in SA wafers did not appear to affect the microstructure. The matrix morphology of lyophilised SA appeared to form a denser interconnected network with an elongated, 'melted-looking' porous structure (Figure 2.8, Images E and F). The microstructure of a SA wafer is similar to the one reported recently by Boateng *et al.* (2010). The matrix morphology of SA wafers might be attributed to the process temperature exceeding the T_g of SA during the primary or secondary drying cycles. Thermal analysis of the freeze/thaw behaviours of polymer gels could give a definitive explanation of 'melt-back' in terms of the T_g of the glassy freeze concentrate, however, the notoriously weak nature of these thermal events made detection extremely difficult. Despite many efforts to detect this weak but critical thermal event using differential scanning calorimetry (DSC), no clear transition in the frozen state were unambiguously detected. The small amounts of polymer contained in the frozen gels relative to the amount of water requires a much larger gel sample than is commonly possible with the standard aluminium pans. As a result, chances of detecting the T_g of polymer/antimicrobial freeze concentrates may require the use of large volume steel sample pans. Alternatively, use of modulated DSC may enhance the resolution (Flikkema *et al.* 1998).

The determination of residual moisture in a lyophilised formulation is important for two main reasons: firstly, to assess the quality of the final lyophilised product and secondly, to establish the appropriate storage conditions, in terms of moisture content, for the lyophilised articles (Franks 1990). Thermogravimetric analysis (TGA) of KAG wafers showed that the residual water content varied from 13.87 – 18.49 %, where the KAG-(PVP-I) wafer exhibited the lowest percentage and KAG-F68 the highest (Table 2.5). Equilibrium moisture content (EMC), post-lyophilisation, is related to the hygroscopicity (affinity to water) of both polymer and contained compounds. EMC will generally vary with changes to temperature and relative humidity. A

typical example is the incorporation of minimal amounts of highly hygroscopic surfactant such as pluronic F68, which is highly hydrophilic and contributes to a slightly increased moisture content. Also, the moisture content of KAG-NS and KAG-CHD wafers were slightly increased compared to the antimicrobial-free control (KAG), indicating the likely hygroscopic nature of NS and CHD. It is difficult to precisely determine the exact quantity of moisture, as external parameters such as storage temperature and percentage of room humidity on the day of examination have an effect on the final water content.

Lyophilised wafers (with and without antimicrobial compounds), intended for topical application on damaged and exuding skin, were further analysed for adhesive properties *in vitro* using a model exuding surface. The method used to mimic this environment was a soft, moist agar gel prepared with the same concentrations of electrolytes as found in wound exudate. Adhesion in its essence is an interfacial phenomenon resulting from chemical and mechanical attraction (or repulsion) of molecules of dissimilar materials in contact (Peppas and Buri 1985). Attractive forces usually consist of Van der Waals interactions, hydrogen bonding and polymeric chain entanglement that develops during hydration of the formulation from the moist surface with which it is in contact. At this polymer-polymer interface, penetration of polymer chains from the formulation to the substrate and vice versa occurs (Bredenberg and Nystrom 2003). The breakdown of these bonds, also known as debonding behaviour, is usually calculated as the work of adhesion, where the peak detachment force represents the maximum force required to disconnect the tested article from the interacting surface.

Tensile stress (ratio of maximum force with the contact surface area) values generated from the analysis of KAG wafers, impregnated with clinical concentrations of antimicrobial compounds, demonstrated that the incorporation of 0.5 % NS ($p < 0.05$), 1.0 % PVP-I ($p < 0.001$) and 0.5 % CHD ($p < 0.001$) had a significant effect. The incorporation of an iodophore, such as PVP, into the matrix of KAG would generally be expected to improve adhesion properties of the formulation; however, other authors have reported the 'anti-tack' action of PVP. Karavas *et al.* (2006) have demonstrated that PVP displayed *in vitro* a negligible mucoadhesive force equal to 0.006 N/cm^2 . In addition, dynamic adhesive evaluation of lyophilised nasal formulations

prepared with 1 % PVP showed that the incorporation of PVP significantly reduced bioadhesion (McInnes et al. 2007).

Although the incorporation of 1.0 % SS prepared as a suspension with 0.2 % pluronic F68 decreased the tensile stress of the lyophilised formulation, it didn't apparently affect it significantly (Figure 2.8). However, while the adhesive properties of antimicrobial wafers displayed a tendency for a decreased tensile stress, compared to control samples (KAG), the work of adhesion showed similar values for all the KAG wafers tested. This paradox may be related to the wettability of antimicrobial wafers. Although the interfacial contact time was similar (30 seconds) for all the lyophilised formulations tested, the presence of antimicrobials may restrain the hydration ability of lyophilised matrices. In addition, other dispersive forces such as polymeric chain entanglement, apart from hydrogen bonding, were likely developed during contact of KAG with the agar surface, and this increases the difficulty of precisely interpreting the debonding behaviour of lyophilised formulations.

The incorporation of CHD into biopolymer matrices with different rheological behaviours, demonstrated a small and insignificant decrease in tensile stress and work of adhesion compared to CHD-free wafers (Figure 2.9). It is apparent, however, that different polymeric materials displayed different adhesive properties. The work of adhesion of CHD-free wafers ranged from 0.18 – 0.55 N.mm, where the dual synergistic wafer of SA-KAG was the least adhesive and XG the most. The peak detachment force of CHD free wafers ranged from 0.56 – 1.05 N, where the matrix of SA-KAG had the lowest and SA the highest. Generally, the SA-KAG matrix (antimicrobial free or loaded) exhibited weak adhesive properties with respect to both work of adhesion and tensile strength. However, with the exception of SA-KAG, the peak detachment force of different biopolymeric wafers was not proportional to the work of adhesion, as wafers displaying increased values of work of adhesion displayed moderate values of detachment force. This phenomenon is likely related to different polymer hydration abilities. In addition, the incorporation of CHD influenced negatively the adhesive properties of biopolymeric wafers. Further investigations are required to elucidate the molecular behaviours of miscible compounds.

While the examination of the physicochemical characteristics of different natural polymers as lyophilised carriers of antimicrobials was undertaken, the antimicrobial activity of these formulations was also tested *in vitro* against selected and common pathogens of chronic, non-healing wounds. Chapter 3 describes the effect of antimicrobial compounds released upon swelling of the wafers. In addition, the influence of the rheological and adhesive properties of antimicrobial wafers on their flow behaviour is further discussed.

Chapter 3
***In vitro* evaluation of the efficacy of lyophilised
antimicrobial wafers**

3.1 Aim

To evaluate the antimicrobial properties of lyophilised wafers using a modified disc diffusion assay and an antimicrobial diffusion cell (ADC) to simulated conditions of an exuding wound.

3.2 Introduction

Bacterial infection is considered a common reason for impaired wound healing. The presence of diverse types and populations of pathogens, often assembled in the form of biofilms, represent a major difficulty in controlling contamination and/or infection in the wounded skin. As previously mentioned (Chapter 1), an optimal treatment of infection is considered to be the topical application of broad spectrum antimicrobials such as silver, iodophores, chlorhexidine etc. Despite the plethora of commercially available antimicrobial formulations, the complex nature of non-healing infected wounds with regards to microbial flora, tissue pathophysiology and surface abnormalities, present a real challenge in establishing a universal *in vitro* antimicrobial wound assay.

Generally, *in vitro* testing of antimicrobial formulations has been performed using different assays, which were essentially based on the established method of diffusion of antimicrobials within an agar substrate. For instance, Bhende and Spangler (2004) have tested, *in vitro*, the antimicrobial activity of chlorhexidine gluconate impregnated foam, against common pathogens associated with wound infections, using inoculated agar plates. Grzybowski *et al.* (1996) modified the use of an agar substrate by creating circular wells for bacteria carriers, where formulations to be tested were placed on top of the agar surface. Recently, Bowler *et al.* (2010) modified further the agar surface to represent a shallow wound microbial model.

A paper disc wetted with an antimicrobial solution and placed on the inoculated agar surface, also known as the disc diffusion technique, has been used successfully to determine bacterial susceptibility to soluble antimicrobial compounds. The antimicrobial diffuses from the saturated disc, which represents a drug reservoir, resulting in the formation of a clear and visible circular area, known as the zone of inhibition. The inhibition zone is formed from the synchronised events of drug diffusion and bacterial growth, until the

accumulation of the antimicrobial within the agar substrate reaches a critical inhibitory concentration. Consequently, the diameter of the inhibition zone reflects the degree of susceptibility of the tested bacterium against the drug, when all other variable parameters are kept constant (i.e. drug concentration, bacterial density, depth of agar, diameter of paper disc, temperature) (Barry 1986). One major limitation of the method is considered to be that the diffusion rate of the drug depends on the molecular weight, solubility and the likelihood of drug interacting with the agar; factors that should be considered when interpreting and comparing any data obtained.

The assessment of the antimicrobial activity of formulations impregnated with antimicrobial, designed for application in a suppurating wound bed, represents another challenge, in terms of interference occurring between antimicrobial compounds and organic matter present, such as serum, blood and pus. Previous investigations have shown that many antimicrobial compounds are reversibly bound to serum proteins, as structures of proteins possess several interactive groups. Albumin, in particular, has approximately 100 acidic and 86 basic groups ionised at pH 7.4 (Craig and Suh 1986). The interaction of organic matter with antimicrobials can lead to substantial alterations to the antimicrobial activities of certain antimicrobial compounds.

The experimental work summarised in this chapter is undertaken in order to investigate, *in vitro*, the performance of antimicrobial formulations, such as lyophilised antimicrobial wafers, using an inoculated agar surface. In addition, an antimicrobial diffusion cell assay was developed and optimised in order to assess the activity of released antimicrobials from the slowly rehydrating matrix of lyophilised formulations. Moreover, emphasis has been given in assessing the activity of released antimicrobials in the presence of electrolytes (e.g. Na^+ , Ca^{2+} and Cl^-) and protein, present in chronic wound exudate.

3.3 Materials and Methods

3.3.1 Materials

Antimicrobial wafers prepared as described in Chapter 2 (2.2.2) were used. Neomycin trisulphate (powder), chlorhexidine digluconate (20 % w/v solution), silver sulfadiazine (SS) (98 % purity of powder) were purchased from Sigma-Aldrich, Gillingham, UK. Povidone iodine (10 % w/v standardised aqueous solution) was purchased from Seaton Healthcare Group. Nutrient agar and broth were purchased from Oxoid, UK. Phosphate buffer tablets (PBS), bovine serum albumin (BSA), sodium chloride (NaCl), calcium chloride (CaCl₂) were purchased from Sigma-Aldrich, Gillingham, UK. Cellulose membrane (12-14 kDa) was obtained from Medicell Int. Ltd., UK. Triple vented Petri dishes of 90 mm diameter and sterile syringes and needles were purchased from Fisher Scientific. Franz diffusion apparatus was purchased from Copley Scientific and a Spectrophotometer Cecil CE 3021 was used to determine the optical densities of the bacterial strains used.

National Collection of Type Culture (NCTC) methicillin-resistant *Staphylococcus aureus* (11940), methicillin-sensitive *Staphylococcus aureus* (6571), *Escherichia coli* (4174) and *Pseudomonas aeruginosa* (6750) strains, were used for microbiological assays.

3.3.2 Methods

3.3.2.1 Bacterial storage and preparation

The bacterial stock cultures of methicillin-resistant *S. aureus* (MRSA), methicillin-sensitive *S. aureus* (MSSA), *E. coli* and *P. aeruginosa* were stored at -80 °C using Protect Bacterial Preservation beads (Technical Service Consultants Ltd., Haywood, UK). Fresh bacterial cultures were prepared at 37 °C by transferring a single bead unit to 10 ml of nutrient broth and incubating for 24 hours. A loop full of bacterial culture was streaked onto a nutrient agar plate and incubated at 37 °C for 24 hours to yield separate colonies. The plates were subsequently stored in a refrigerator (4 °C) and agar plates sub-cultured weekly using a representative single colony.

Broth cultures were prepared by inoculating 100 ml of a nutrient broth in a 250 ml flask with one discrete colony and incubating with orbital agitation (100 rpm) at 37 °C for 24 hours. Overnight bacterial cultures (40 ml) were centrifuged at 4000 rpm for 10 minutes in an MSE Centaur 1 centrifuge. The sitting supernatant was discarded and the bacterial pellet re-suspended in 20 ml of sterile 0.9 % (w/v) NaCl solution. Bacterial density was determined spectrophotometrically by measurement of a dilute suspension at a wavelength of 500 nm.

3.3.2.2 Determination of minimum inhibitory concentration (MIC) and minimum bactericidal concentration (MBC) of antimicrobials

Antimicrobial susceptibility of MRSA, MSSA, *E. coli* and *P. aeruginosa* were determined by establishing the MIC using a standard 2-fold macro-broth dilution method in 10 ml volumes of nutrient broth inoculated with 5×10^5 cfu/ml. Suitable controls incorporating a non-inoculated bottle of nutrient broth (negative) and an inoculated bottle of nutrient broth (positive) were included in all assays. After 24 hours incubation at 37 °C, the presence or not of bacterial growth was determined optically comparing each dilution to the negative and positive controls.

The MBC values were determined by plating duplicate samples of 100 μ l (20 μ l x 5 volumes) taken from each MIC dilution on agar plates and incubated at 37° C for further 24 hours. The absence of bacterial colonies was determined as the MBC value of the tested antimicrobial against the bacterial strains. All MIC/MBC determinations for each antimicrobial were performed twice in duplicate.

3.3.2.3 Modified disc diffusion assay as a simple model of an exuding surface

A modified disc diffusion assay was used to determine initially the bacterial susceptibility to the antimicrobial compounds incorporated within the matrix structure of lyophilised wafers. The method was optimized according to the protocol of the National Committee of Clinical Laboratory Standards (NCCLS) and Barry (1986). Triple vented sterile Petri dishes (90 mm) were

prepared by pouring 20 ml of molten nutrient agar (1.5 %) containing yeast extract (20 g/l), peptone (5.0 g/l), sodium chloride (5.0 g/l). Each plate was inoculated with 5×10^5 cfu/ml of either MRSA, MSSA, *E. coli* or *P. aeruginosa*. Individual circular (diameter ≈ 20 mm) antimicrobial wafers, including controls, were placed onto solidified, seeded agar plates and incubated at 37°C for 24 hours. The diameter of inhibition of the antimicrobial wafers was measured from one edge of the circular zone of inhibition to the other (Figure 3.1). Zones of inhibition (calculated from the average of two measurements of the diameter of the inhibition zone taken at intervals of 0° and 90°) and the swollen diameter of wafers (D_t) were measured after incubation using a rigid steel engineering rule (*Mitutoyo*). The initial diameters of the wafers (D_0) were measured with a digital calliper (*Mitutoyo*) prior to being placed on the centre of the seeded agar plate. Wafer expansion was calculated as the ratio of D_t/D_0 (Matthews et al. 2005). Antimicrobial activity was determined as an inhibition ratio $\text{IR} = D_i/D_0$, where D_i = mean diameter of inhibition zone.

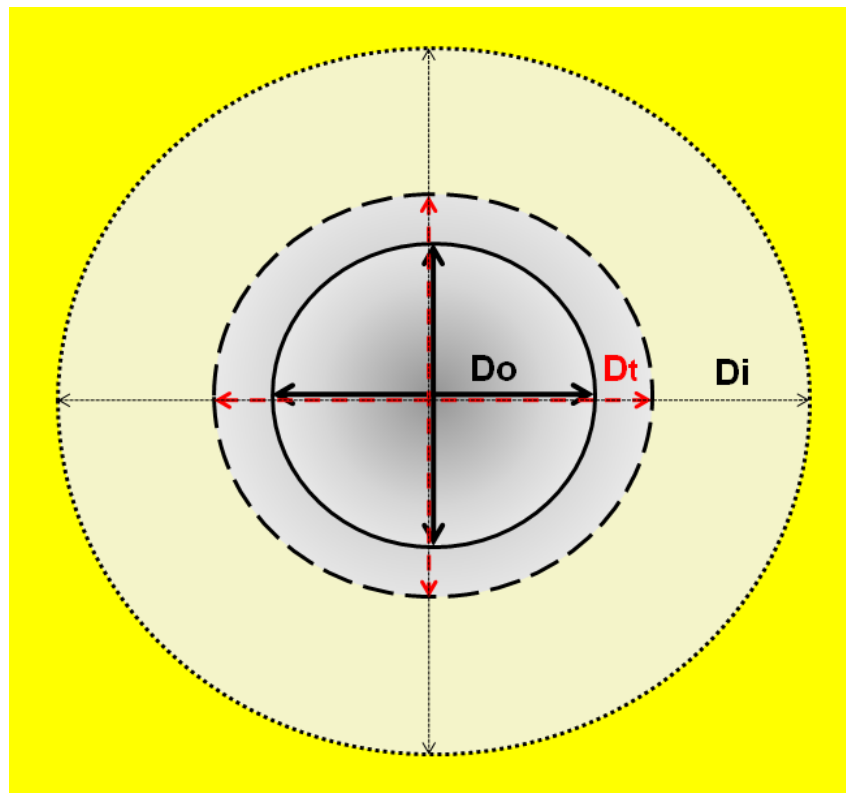


Figure 3.1 Aerial view of disc diffusion measurements

3.3.2.4 *In vitro* assessment of the efficacy of antimicrobial wafers using a diffusion cell

The use of a Franz diffusion apparatus was altered in order to assess the antimicrobial activity of loaded wafers as they slowly rehydrated in contact with the dissolution medium. For the purposes of this project the modified and optimised method is referred to as an antimicrobial diffusion cell (ADC). This original term is used to characterize the precise use of the diffusion apparatus, as both chambers (donor and receptor) were filled with media inoculated with known concentrations of MRSA (Figure 3.2).

The effective diffusion area of the receptor chamber was 3.46 cm², matching perfectly with the surfaces of lyophilised formulations and had a total volume of 20 ml. The receptor chamber kept at 25 ± 0.5 °C was inoculated to yield a final bacterial cell density of 5×10⁵ cfu/ml of MRSA. An antimicrobial wafer was placed on top of a cellulose membrane (12 - 14 kDa) in contact with the inoculated medium. The system was sealed in order to maintain a continuous volume of medium in the receptor chamber (20 ml) and to keep the membrane and wafer constantly hydrated. A maximal volume of 200 µl was withdrawn at each time point in order to minimize the introduction of untreated bacterial cells into the receptor chamber. The sample was withdrawn using a sterile syringe and needle. Samples (200 µl) of the dissolution medium were taken at 0, 2, 4, 6, 8 and 24 hour intervals and each diluted to sub-inhibitory levels, ten-fold down to 10⁻⁵, in 0.9% (w/v) NaCl solution. Dilutions were plated in duplicate on nutrient agar plates (5 µl × 20 volumes) and incubated at 37 °C for 24 hours. After incubation, bacterial colonies were counted and the original cell count (cfu/ml) calculated. The lowest detectable limit of the method was 100 cfu/ml.

Different dissolution media were used and inoculated with the same MRSA densities, in order to compare the activity of released antimicrobials from the re-hydrated matrices of antimicrobial wafers. The dissolution media of the chambers were stirred at 1200 rpm and consisted of either:

a) phosphate buffer solution (PBS) containing 0.2 % potassium chloride (KCl) and 0.8 % sodium chloride (NaCl) (pH 7.4),

b) sodium/calcium chloride solution (pH 6.5) containing 142 mmol/litre of sodium ions (0.82 %) and 2.5 mmol/litre of calcium ions (0.027 %), typical of those found in wound exudate Thomas (2007),

c) pseudo-exudate containing sodium/calcium chloride solution enriched with 3 % (w/v) BSA (pH 7.4), similar to protein levels found in wound exudate (Clought and Noble 2003).

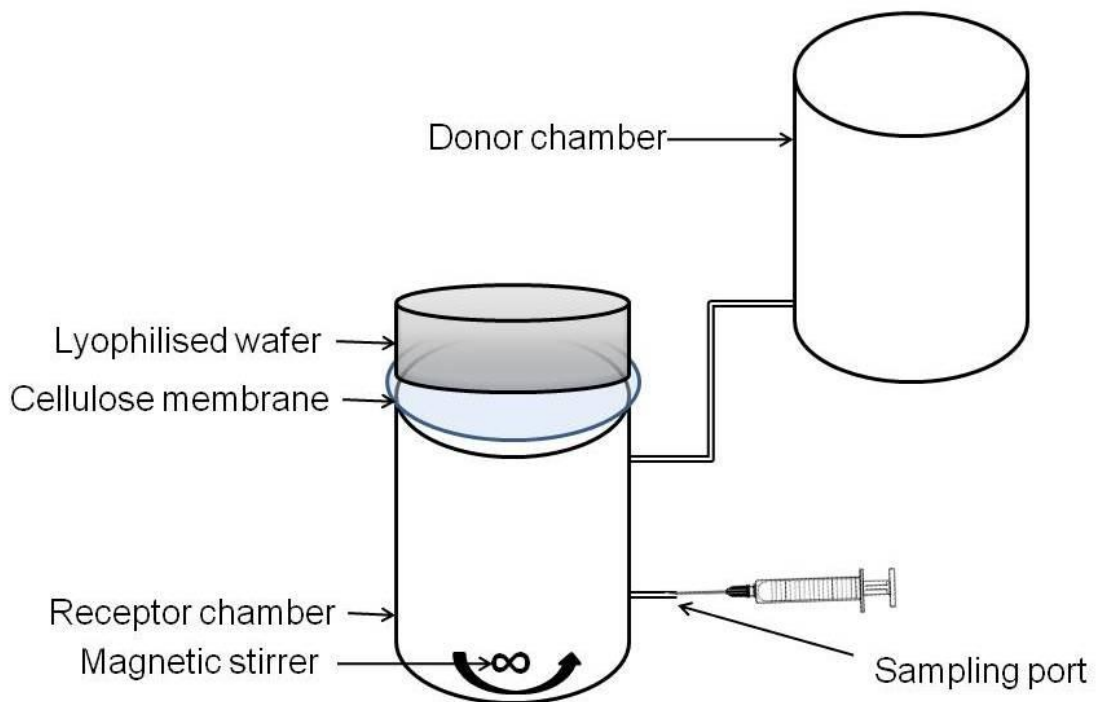


Figure 3.2 Schematic of antimicrobial diffusion cell (ADC) assembly used for *in vitro* determination of antimicrobial measurements

3.4 Statistical analysis

Data are presenting as the mean value of three samples \pm standard error of the mean (SEM). Statistical analysis of data obtained from the expansion and inhibition ratios was performed using GraphPad Prism 4 software. The normality of data was analysed with the Skewness-Kurtosis Omnibus test for variable sampling plans. Normality of data was determined by 95 % confidence of normal distribution. When normal distribution was proven, a parametric test such as one way analysis of variance (ANOVA), followed by post hoc Tukey's multiple comparison test was used to compare more than two groups. A p-value less than 0.05 was considered a significant difference.

3.5 Results

Table 3.1 MIC and MBC values of antimicrobial compounds tested against a bacterial density of 5×10^5 cfu/ml. PVP-I* is used as a standardised aqueous formulation containing 100 mg/g PVP-I, where the exact concentration of antimicrobial iodine compound is not given. Silver sulfadiazine was poorly soluble in distilled water and the determination of MIC /MBC values for this antimicrobial compound was not possible (ND – not determined).

Bacterial strains	Antimicrobials MIC – MBC ($\mu\text{g/ml}$)			
	NS	CHD	PVP-I*	SS
MRSA	3.0 – 6.0	0.2 – 0.4	625	ND
MSSA	2.0 – 6.0	0.2 – 0.4	625	ND
<i>E. coli</i>	6.0 - 18	0.6 - 14	1256	ND
<i>P. aeruginosa</i>	8.0 - 20	4.0 - 20	1256	ND

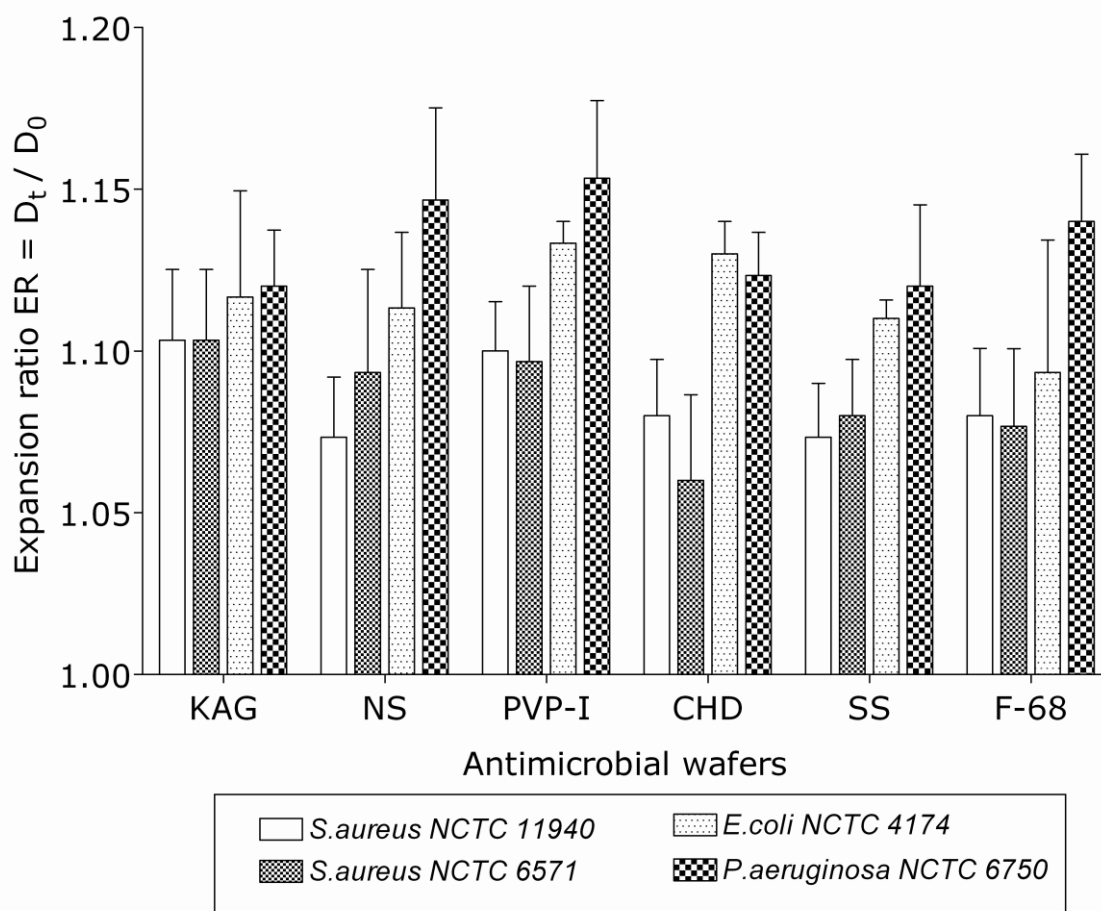


Figure 3.3 Expansion ratio (ER) of 3 % (w/v) KAG wafers prepared with 0.5 % (w/v) NS, 1.0 % (v/v) PVP-I, 0.5 % (v/v) CHD, 1.0 % (w/v) SS, 0.2 % (w/v) pluronic F68. Data were statistically analysed using one way analysis of variance (ANOVA), followed by Tukey’s post-hoc test. Statistical analysis was performed comparing the same formulation tested against four different bacterial strains, and also comparing different antimicrobial formulations to the control (KAG). A $p < 0.05$ was considered a significant difference ($n=3$, SEM). (Please note that the large error bars are due to the small scale of the y axis).

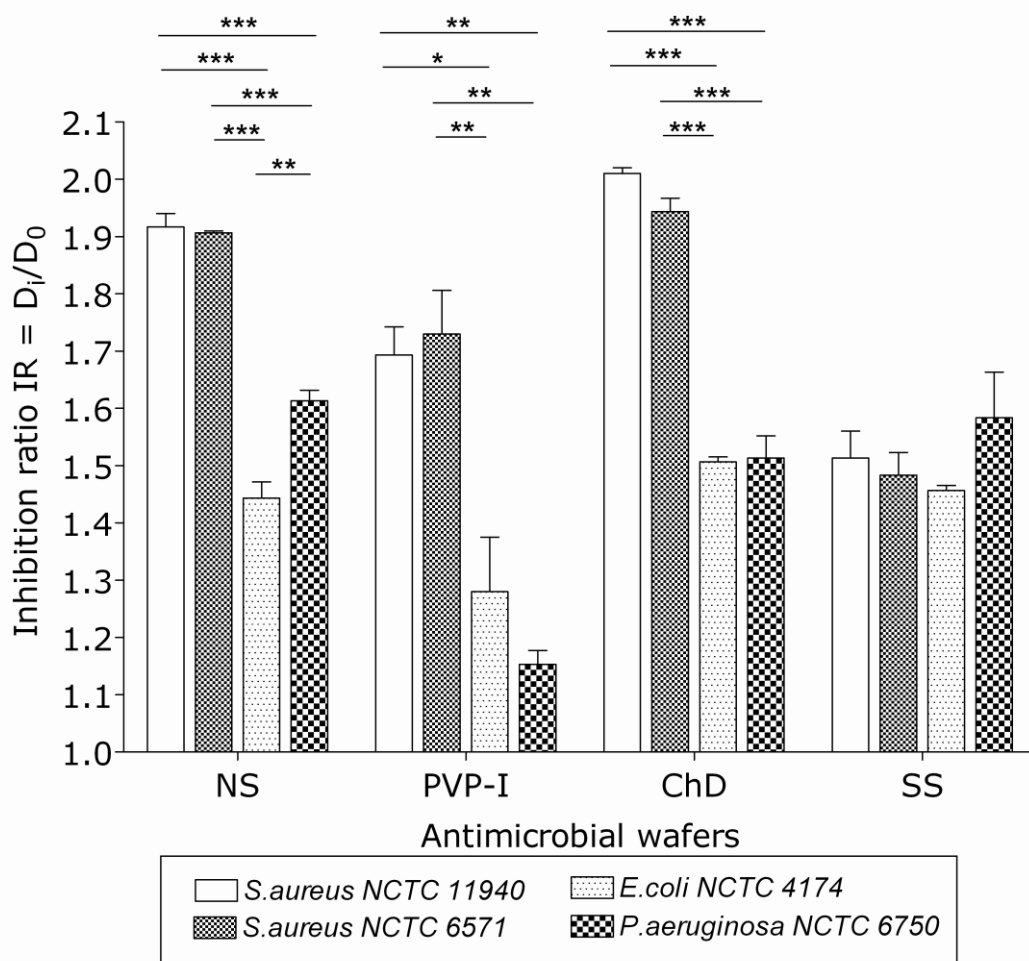


Figure 3.4 Inhibition ratio (IR) of 3 % (w/v) KAG wafers prepared with 0.5 % (w/v) NS, 1.0 % (v/v) PVP-I, 0.5 % (v/v) CHD, 1.0 % (w/v) SS. Control wafers (KAG) and 0.2 % (w/v) pluronic F68, did not show zones of inhibition. Data were statistically analysed using one way analysis of variance (ANOVA), followed by Tukey's post-hoc test. A $p < 0.05$ was considered a significant difference ($n=3$, SEM). (* $p < 0.05$, ** $p < 0.01$, *** $p < 0.001$)

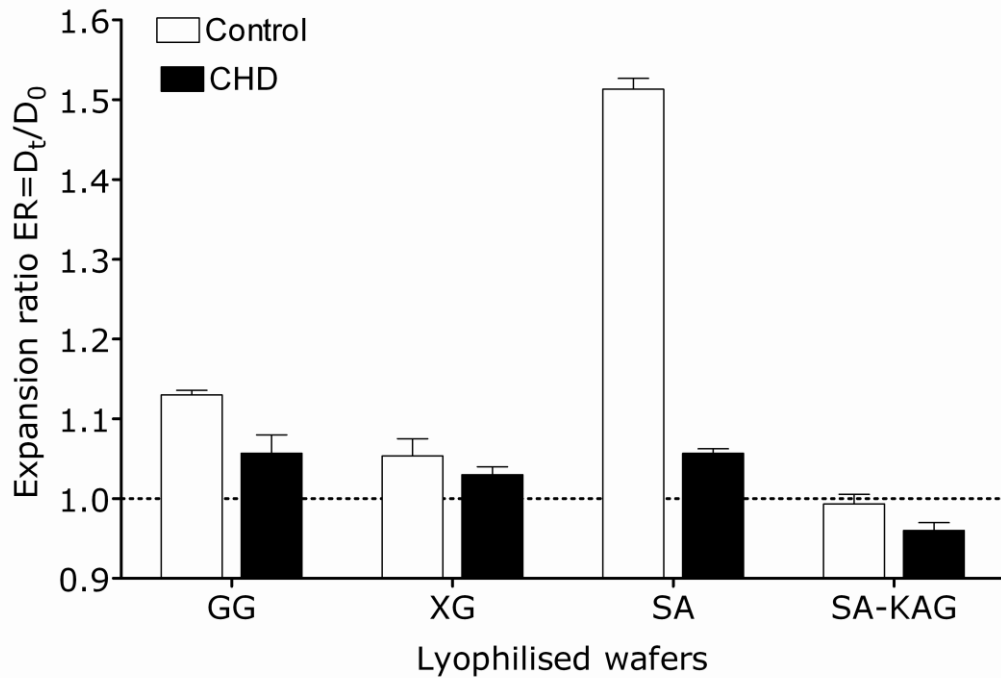


Figure 3.5 Expansion ratios of wafers prepared with different biopolymers [guar gum (GG), xanthan gum (XG), sodium alginate (SA) and blend of SA with karaya gum (KAG) (1:1) ratio] impregnated with 0.5 % (v/v) CHD. Measurements were taken testing lyophilised wafers against *P. aeruginosa* NCTC 6750. (n=3, SEM).

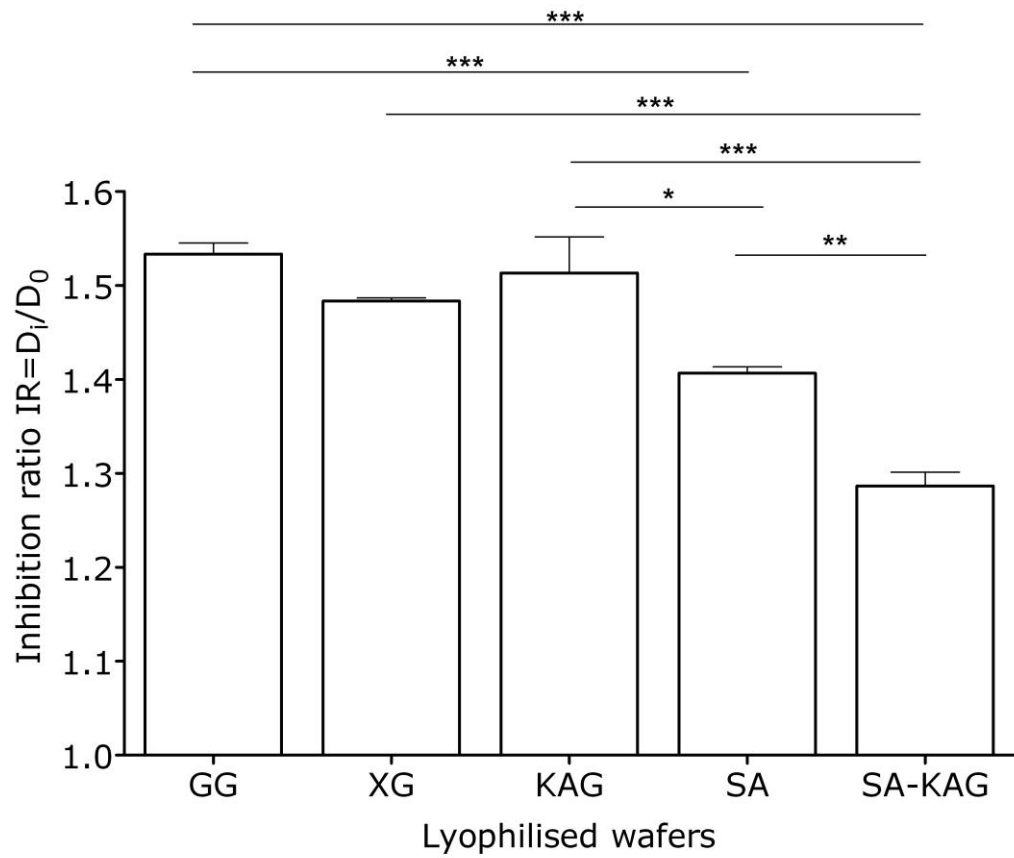


Figure 3.6 Inhibition ratios of wafers prepared with different biopolymers [guar gum (GG), xanthan gum (XG), sodium alginate (SA), karaya gum (KAG) and blend of SA with KAG (1:1) ratio], impregnated with 0.5 % CHD, tested against *P. aeruginosa* NCTC 6750. Data were statistically analysed using one way analysis of variance (ANOVA), followed by Tukey's post-hoc test. (n=3, SEM). (*p<0.05, **p<0.01, ***p<0.001)

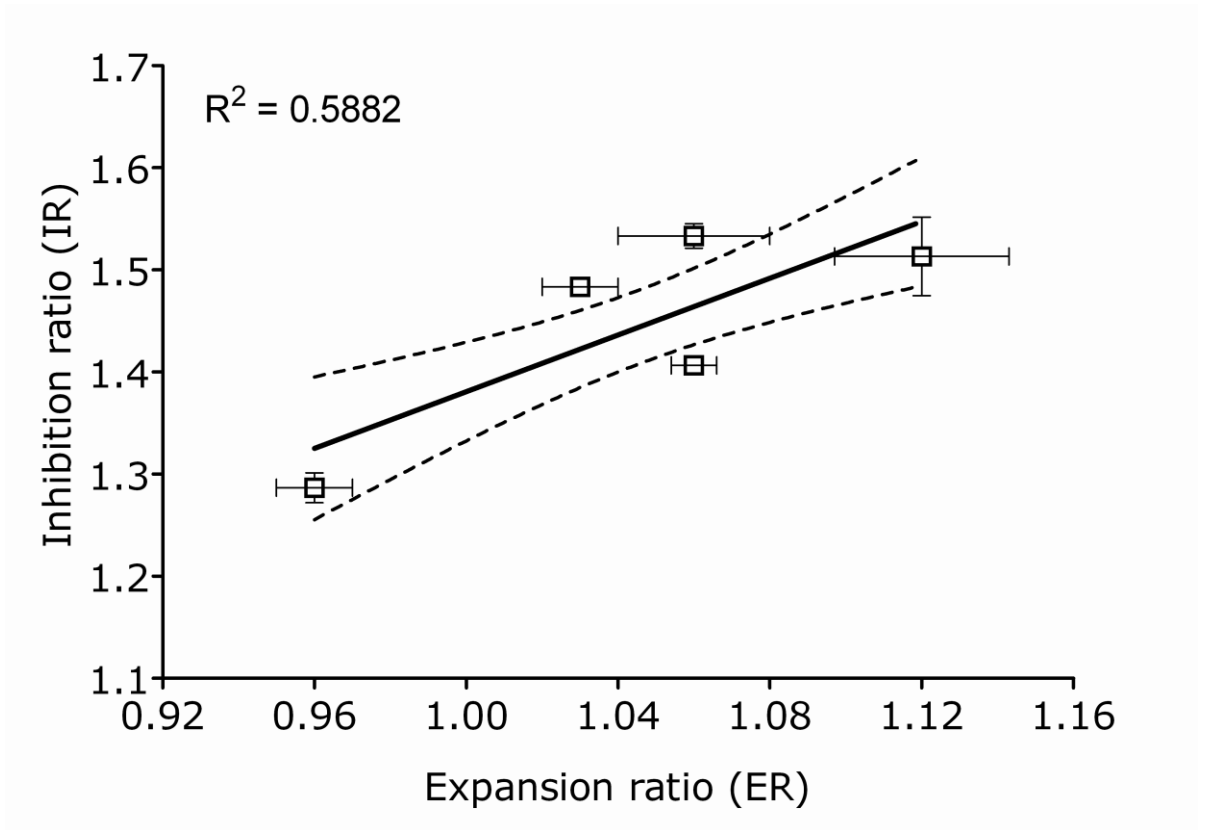


Figure 3.7 Correlation of ER/IR for 0.5 % CHD impregnated wafers. Significant linear regression between ER and IR values of CHD wafers is apparent. (---) represent 95 % confidence intervals. (n=3, SEM)

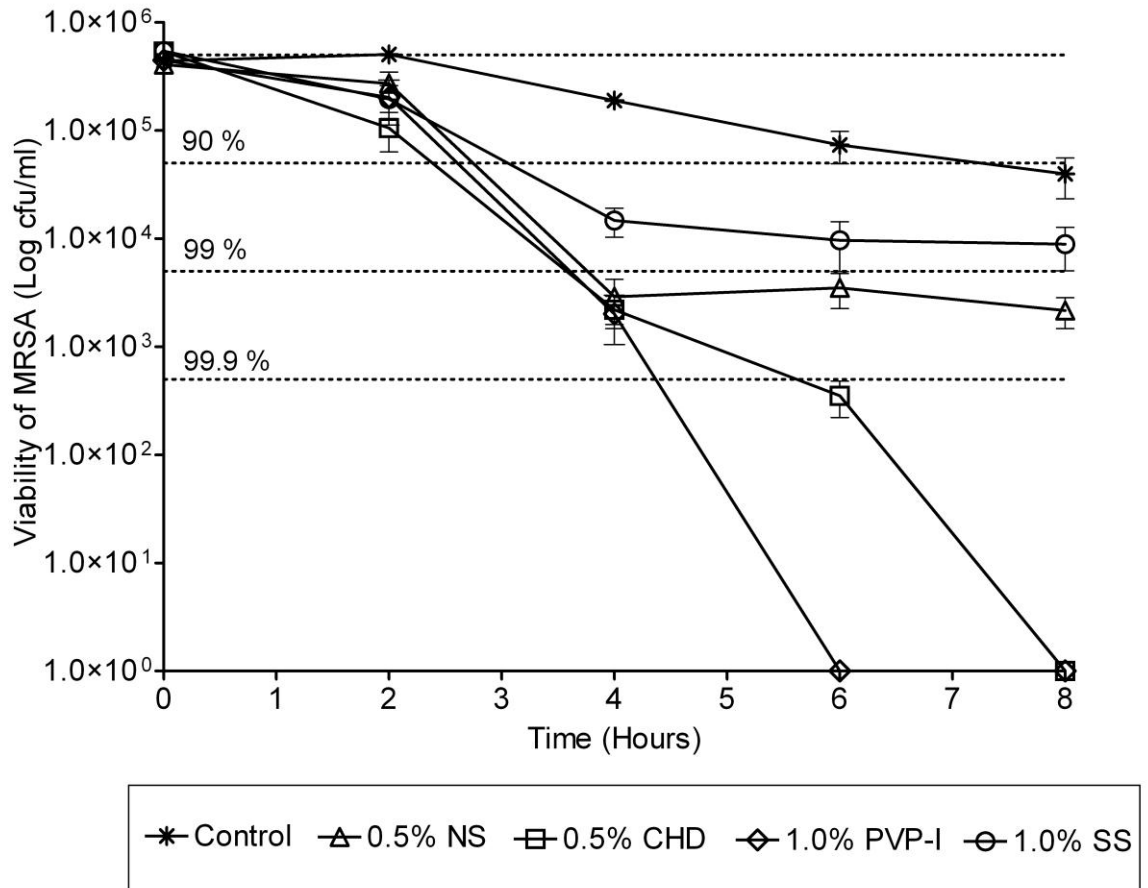


Figure 3.8 Viability of MRSA in the antimicrobial diffusion cell (ADC) suspended in PBS, containing 0.02 % KCl and 0.8 % NaCl, adjusted to the same pH of the nutrient agar/broth medium (pH 7.4). The experiment was performed over 24 hours, however, the above graph presents the viability of MRSA over 8 hours. There is a natural > 2-log powers decrease in the number of cells (control) in this period. NS killed all MRSA cells at 24 hours, while the antimicrobial profile of SS remained constant. The values represent the mean of three independent experiments \pm standard error of mean. (---) represent the loss of viability of MRSA populations at each log division, in percentage terms, compared to the initial MRSA population (n=3, SEM).

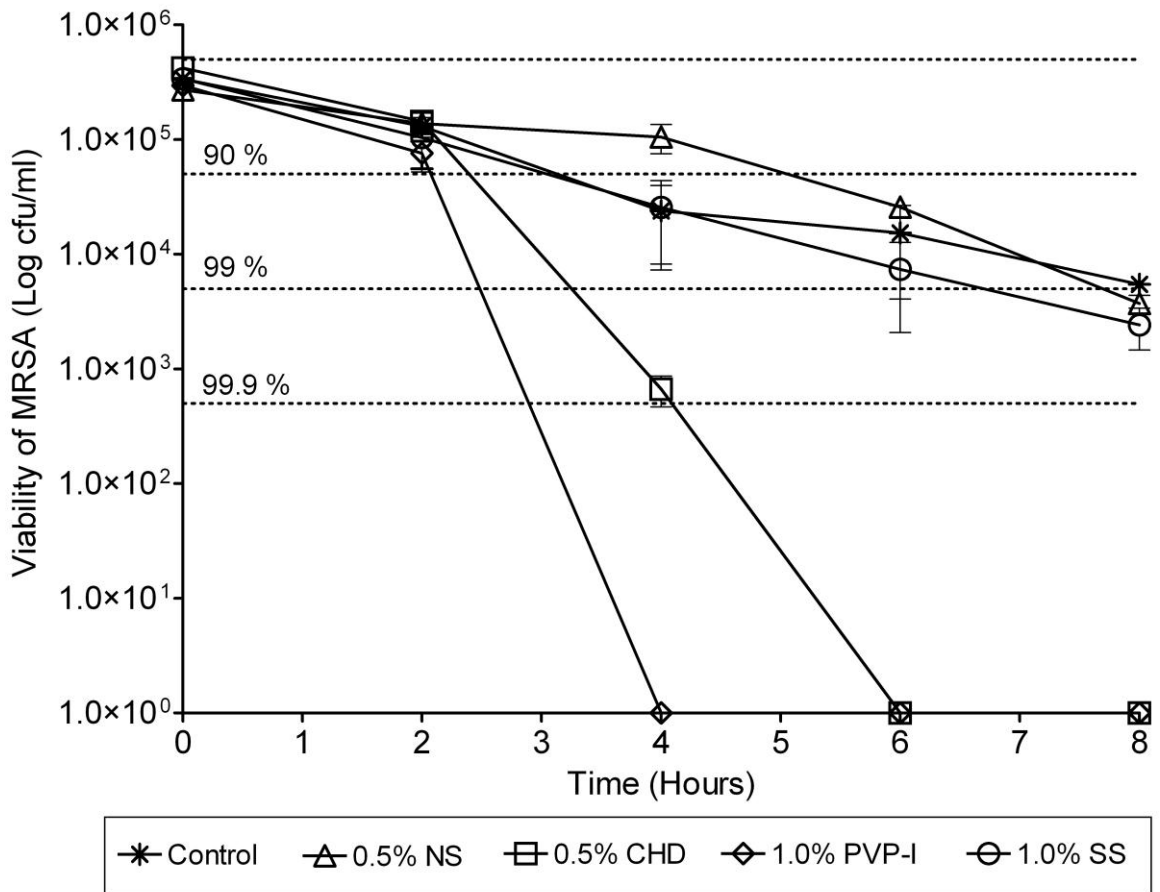


Figure 3.9 Viability of MRSA in the antimicrobial diffusion cell (ADC) suspended in NaCl-CaCl₂, containing 0.027 % CaCl₂ and 0.82 % NaCl, (pH 6.5). The experiment was performed over 24 hours, however, the above graph presents the viability of MRSA over 8 hours. There is a natural > 2-log powers decrease in the number of cells (control) in this period. NS killed all MRSA cells at 24 hours, while antimicrobial profile of SS remained constant. The values represent the mean of three independent experiments ± standard error of mean. (---) represent the loss of viability of MRSA populations at each log division, in percentage terms, compared to the initial MRSA population (n=3, SEM).

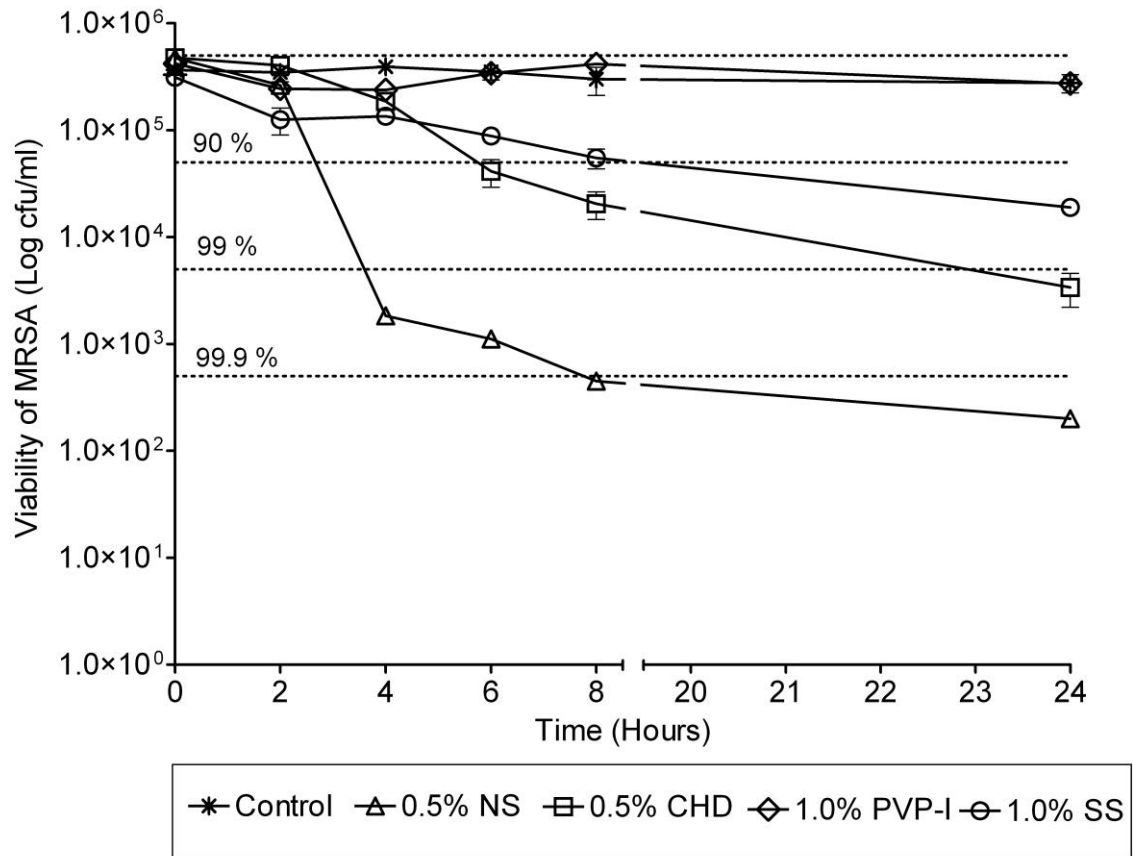


Figure 3.10 Viability of MRSA in the antimicrobial diffusion cell (ADC) suspended in NaCl-CaCl₂ enriched with organic material, containing 0.027 % CaCl₂, 0.82 % NaCl and 3 % (w/v) BSA, (pH 7.4). The prepared solution simulates chronic wound exudate. The presence of one model protein does not necessarily reflect an infected wound. The values represent the mean of four independent experiments ± standard error of mean. (---) represent the loss of viability of MRSA populations at each log division, in percentage terms, compared to the initial MRSA population (n=4, SEM).

3.6 Discussion

Initially, the minimum inhibitory and bactericidal concentrations, MIC and MBC, respectively, of selected topical antimicrobial compounds were determined for known densities of common bacterial strains found associated with infected, non healing wounds. Table 3.1 summarises the obtained values of MICs and MBCs. It is apparent that CHD displayed, *in vitro*, the lowest inhibitory/bactericidal concentration against all bacterial strains, in particular against MRSA and MSSA (0.2 - 0.4 µg/ml). *E. coli* and *P. aeruginosa* showed 3 times and 20 times increased MIC values, respectively compared to *S. aureus* strains. MBC values of CHD against *E. coli* and *P. aeruginosa* were 23 times and 5 times higher, respectively than MIC values. The antimicrobial activity of NS tested against all bacterial strains demonstrated moderately increased values of MIC compared to CHD, whereas the MBC concentrations of NS against *E. coli* and *P. aeruginosa* were similar to those of CHD. MBC values for NS and CHD against *E. coli* and *P. aeruginosa* were notably higher than the respective MICs, indicating that the growth of such strains can be easily inhibited, but a considerably higher lethal concentration of drug is required.

PVP-I demonstrated equal values for both MIC and MBC against all bacterial strains tested, indicating that this compound possesses a rapid lethal mechanism of action, however, *E. coli* and *P. aeruginosa* demonstrated a higher tolerance to the activity of PVP-I (1256 µg/ml) compared to MRSA and MSSA (625 µg/ml). Previous research studies have also reported the tolerant nature of *Pseudomonas* spp against iodophoric solutions, whereas the production of a protein coat from such species was the most likely explanation for the inefficacy of PVP-I (Berkelman et al. 1984). A decade later, Hardegger *et al.* (1994) proved by using molecular techniques that *P. aeruginosa* produces a 16-kDa extracellular protein, encoded by the *pra* gene present in *P. aeruginosa* genome. These data suggest that the antimicrobial activity of PVP-I is challenged in the presence of organic matter. It is apparent that the inhibitory/bactericidal concentrations demonstrated by PVP-I, against tested pathogens, were notably higher compared to NS and CHD. Although PVP-I is generally reported as one of the broadest spectrum, rapidly acting bactericidal antimicrobial compounds (Burks 1998), *in vitro*, under certain circumstances, PVP-I displayed relatively high values for MIC/MBC. This paradox most

probably results from a combination of factors related to both instability of this formulation and antimicrobial deactivation of PVP-I occurring during *in vitro* testing conditions.

The macro dilution assay undertaken to determine the MIC/MBC values of antimicrobials, including PVP-I, was performed at 37 °C, using a nutrient broth as a culture medium. However, the 10 % aqueous standardised formulation of PVP-I is stable at temperatures ≤ 25 °C, as suggested by the manufacturer. The elevated temperature, 12 °C above the stability requirements during the 24 hours of examination, led to decreased activity of the antimicrobial compound (iodine). Simultaneously, the presence of organic material such as peptone and/or beef extracts in the growth medium acted as quencher for PVP-I resulting in decreased antimicrobial activity and increased values of MIC/MBC. Messenger *et al.* (2001) have also reported the neutralising capacity of organic matter such as bovine albumin (1 g/l) to antimicrobial activity of 2 % (w/v) PVP-I.

Silver sulfadiazine (SS) is a non-ionised antimicrobial compound which is poorly soluble in water (White and Cooper 2005). Despite the numerous efforts of investigating SS solubility in other solvents, harmless to microorganisms, the insoluble nature of this compound made it unfeasible to determine the MIC/MBC values, using the macro dilution assay. Previous studies conducted by Hamilton-Miller and Shah (1996) have assessed the susceptibility of clinical isolates against SS. The latter authors tested the MIC of SS, prepared as a suspension, and demonstrated that the inhibitory levels of suspended SS against MRSA isolates were notably higher (32 - 128 mg/ml) compared to *E. coli* and *P. aeruginosa* (16 - 32 mg/ml). It is clear that *in vitro*, Gram-negative strains are more sensitive to the antimicrobial activity of SS, than Gram-positive ones; however, the MIC values of SS were relatively high for a powerful and effective, *in vivo*, antimicrobial compound.

It has been suggested that the oligodynamic antimicrobial profile of SS shown *in vitro* can be enhanced *in vivo* by the presence of electrolytes and/or thiol groups of proteins that biological fluids (e.g. wound exudate) contain. The continuous contact of SS molecules with wound fluids leads to solubilisation of silver sulfadiazine, therefore release of sulfadiazine and additional antimicrobial activity (White and Cooper 2005). Tsipouras *et al.* (1995) have investigated the solubility of SS in a synthetic electrolyte solution

(containing NaCl, NaHCO₃, Na₂HPO₄ and Na₂SO₄), artificial exudate and human serum. They demonstrated that the disassociation of SS was greatly increased in the presence of biological fluids containing chlorides, peptides and proteins.

The assessment of antimicrobial activity of antimicrobial wafers was undertaken, *in vitro*, using a slightly modified disc diffusion method. The nutritional, polymeric surface inoculated with known densities of bacteria, represented a suitable *in vitro* wound model for the initial assessment of antimicrobial properties of lyophilised wafers. In addition, the application of circular antimicrobial formulations on a moist surface was indicative of the swelling during rehydration of the specimens, which was calculated as the ratio of expansion. Figure 3.3 presents the expansion ratios of KAG wafers tested against MRSA, MSSA, *E. coli* and *P. aeruginosa*. The decreased consistency of KAG (Table 2.3, Chapter 2) induced from the incorporation of clinical concentrations of drugs into the biopolymeric matrix, would generally be expected to increase the expansion of antimicrobial formulations. However, such a trend was not observed. The expansion ratio of KAG wafers varied from 1.05 – 1.15, where a non significant intra-batch variation was noted (Figure 3.3) for all antimicrobial/polymer combinations.

While the expansion of wafers resulted from the flow properties of the rehydrated polymer on a moist surface, the inhibition zone was the effect of diffused antimicrobial within the inoculated agar substrate during hydration. As such, the visible, clear and circular area of inhibition observed depended on the susceptibility of the bacterial strain tested against selected antimicrobials. However, other secondary parameters may influence the inhibition zone formed from the diffusion of antimicrobial compounds. Molecular weight of the tested drugs, solubility and the degree of interaction between the diffused drug and the agar substrate are considered as the main secondary parameters which may influence the rate of diffusion of antimicrobial compounds. Consequently, these parameters will likely affect, indirectly, the zone of inhibition obtained for an antimicrobial compound against a selected bacterium.

Figure 3.4 presents the antimicrobial activity of tested antimicrobial formulations, calculated as the inhibition ratio (IR), where the control wafer of plain KAG or KAG impregnated with 0.2 % (w/v) F68 (control for the SS wafer) did not demonstrate inhibition zones. The antimicrobial activity of

loaded wafers was compared between the bacterial species, as the antimicrobial compounds tested possess different molecular weights and solubility profiles. Diffused CHD demonstrated the largest IR against MRSA and MSSA, whereas the susceptibility of *S. aureus* strains to CHD was significantly higher compared to *E. coli* and *P. aeruginosa* ($p < 0.001$). The antimicrobial effect of diffused CHD appeared to be lower against *E. coli* and *P. aeruginosa*; however, there was no significant difference for CHD between Gram-negative strains.

Diffused neomycin sulphate (NS) demonstrated a similar antimicrobial activity to CHD when tested against MRSA, MSSA, *E. coli* and *P. aeruginosa*. NS showed a similar IR against Gram-positive strains of MRSA and MSSA and a significantly higher IR compared with *E. coli* and *P. aeruginosa* ($p < 0.001$). The antimicrobial activity of NS was reduced when tested against Gram-negative strains. In addition, *P. aeruginosa* appeared to be more susceptible to NS than *E. coli* ($p < 0.01$). Moreover, it is worth noting that although NS is a broad spectrum topical antibiotic, its antimicrobial activity, *in vitro*, calculated as the IR, appeared to be notably higher compared to the broad spectrum, rapidly lethal antiseptic compounds of PVP-I and SS.

The antimicrobial activity of PVP-I varied between the bacterial strains tested. Similar to NS and CHD, PVP-I appeared to be more effective against Gram-positive strains of MRSA and MSSA. The IR with both *S. aureus* strains was similar, but significantly greater than those with *E. coli* ($p < 0.05$, $p < 0.01$) and *P. aeruginosa* ($p < 0.01$). *P. aeruginosa* demonstrated the highest tolerance to PVP-I compared to all antimicrobials and bacterial strains tested. The antimicrobial activity of PVP-I against *P. aeruginosa* obtained from the disc diffusion assay, was in agreement with previous research studies, already discussed, indicating the deactivation of antimicrobial properties of iodophors by *Pseudomonas* spp. In addition, other factors such as the temperature exceeding the stability requirements of PVP-I and the presence of organic matter (e.g. peptone/beef extract) in the cultivated nutrient can affect the size of the inhibition area created over 24 hours for this antimicrobial.

Antimicrobial wafers impregnated with 1.0 % of SS (w/v) prepared as a suspension with 0.2 % (w/v) pluronic F68, were also tested using the inoculated, moist agar surface. Interestingly, all species were similarly susceptible to the small, soluble amount of SS diffused from the hydrated

matrix of KAG. *P. aeruginosa* demonstrated slightly increased susceptibility to SS, however not significantly different compared to MRSA, MSSA and *E. coli*. In addition, SS showed reduced antimicrobial activity, in general, compared to NS, CHD and PVP-I, indicating that the poor solubility of this compound probably had a major effect on the diffusion of SS particles within the agar substrate.

The disc diffusion assay was used as a simple model surface for exuding wounds for assessment of the antimicrobial activity of CHD-loaded wafers prepared with different biopolymers (e.g. GG, XG, SA and SA-KAG). The expansion properties were investigated along with the antimicrobial activity of wafers when tested against *P. aeruginosa*. Expansion of CHD-free specimens was compared to CHD-loaded lyophilised formulations. Figure 3.5 presents the expansion profiles of controls and CHD-loaded lyophilised wafers calculated as the expansion ratio (ER). It is apparent that the incorporation of CHD into the biopolymeric matrices generally decreased the expansion of re-hydrated wafers compared to controls. SA-CHD matrix, in particular, demonstrated the most notable decrease in ER compared to respective control specimen by approximately 1.5 times.

The antimicrobial-free matrix of SA displayed the highest value of ER, indicating that the re-hydrated SA wafer extended its diameter 1.51 ± 0.03 times the original diameter. These results are in total agreement with Matthews *et al.* (2005), where the lyophilised wafers ($D_0 = 34$ mm) prepared with 5 % of a low viscosity grade SA displayed an ER of 1.6 ± 0.01 within 24 hours. The addition of CHD into the SA matrix induced a notable decrease in the expansion ratio. The decreased ER of SA-CHD wafers was likely to be due to a considerable increase in consistency induced from the incorporation of CHD in the gel network of SA, reported in Chapter 2 (Table 2.4, Figure 2.4). Earlier work by Matthews *et al.* (2005) had produced a similar decrease in the ER of SA wafers by the addition of small amounts of methylcellulose (MC) which acted as a viscosity modifier. It was suggested that the viscosity of pre-lyophilised gels determined the flow behaviour of re-hydrated wafers. These observations were based on truly pseudoplastic flow behaviour i.e. no apparent yield stress.

In the case of formulations prepared with gels displaying pseudoplastic flow with an apparent yield stress (e.g. GG and XG), the expansion behaviour

of re-hydrated wafers, appeared to be more complex. It is apparent that such polymers show a restricted expansion; however, it is not clear if the increased yield stress is proportionally related to decreased expansion of the respective re-hydrated formulations. For instance, the expansion ratio of XG was smaller than GG; however, the pre-lyophilised gel of GG demonstrated a higher viscosity and yield stress than XG (Table 2.4, Chapter 2). Therefore, the degree of wettability may play a primary role in the expansion behaviour of polymers displaying a plastic flow.

The phenomenon of expansion of a swollen polymer becomes more complicated and indecipherable when the drug incorporated into the polymer network acts as a 'viscosity modifier'. As reported in Chapter 2 (Table 2.4, Figure 2.4), the combination of CHD with biopolymers notably affected the rheological behaviour of pre-lyophilised gels. The CHD-impregnated wafers of GG, XG and SA demonstrated similar expansion behaviours, where the expansion ratio varied from 1.02 - 1.07, indicating slightly increased swollen diameters and no appreciable flow. On the other hand, the wafer prepared as a dual synergistic carrier of SA-KAG, did not expand within 24 hours of re-hydration, whereas the diameter of CHD-loaded SA-KAG specimens displayed a decreased diameter conducive with shrinkage.

It is difficult to precisely conclude which factors have a primary influence in the expansion/shrinkage behaviours of re-hydrated wafers, either alone or as carriers of antimicrobial compounds, as this behaviour is strongly related to both external factors such as temperature and humidity conditions created within the Petri dish, and internal factors such as the inherent hydrophilic properties of individual biopolymers. In other words, expansion and/or shrinkage of each specimen is the result of an equilibrium during water uptake (rate of re-hydration) and water restraint (rate of evaporation), where hydrophilic properties of individual biopolymers most probably play the key role. However, other external factors such as adhesive, polymeric chain entanglements developed at the polymeric interface between polymeric carriers and the agar surface may also have an additional impact (Shenoy et al. 2005).

The antimicrobial activity of CHD-loaded wafers was measured after 24 hours of re-hydration when in contact with a nutrient agar surface inoculated with known densities of *P. aeruginosa*. The inhibition zones were calculated as

the inhibition ratio (IR) and are presented in Figure 3.6. It is apparent that although antimicrobial wafers were prepared with an equal concentration of CHD, i.e. similar weights of drug ($7434 \pm 98.0 \mu\text{g}$), the inhibition ratios were significantly different. GG, XG and KAG demonstrated significantly higher values of IR compared to SA and/or SA-KAG ($p < 0.001$, $p < 0.01$ and $p < 0.05$). Plotted values of ER versus IR of antimicrobial wafers (Figure 3.7) indicated that there is a significant, yet moderate correlation ($R^2 = 0.5882$) between the expansion and inhibition ratios resulting within 24 hours of swelling. The data obtained indicate that for inhibition zones developed during gradual expansion of re-hydrated wafers, the bigger the expansion the larger the inhibition area. Although inhibition ratios were calculated as the ratio of the diameter of the inhibition zone (D_i) to the initial diameter of the wafer (D_0), these estimations do not characterise the absolute antimicrobial activity of CHD-loaded formulations. In addition, the significant correlation between ER vs. IR indicated that the diffusion of CHD is part of a dynamic process, where the diameters of the saturated discs are variable with time. It was concluded that the disc diffusion assay is a reliable, yet semi-quantitative control method for the initial investigation of the flow and antimicrobial properties of antimicrobial wafers.

It is not a simple matter to quantify the antimicrobial efficacy of formulations intended for topical application in a variety of suppurating wounds. The complex nature of infected non-healing wounds with regards to both polycontamination and continuous production of exudate represent a complex environment to mimic *in vitro*. The efficacy of antimicrobial dressings in terms of determining the killing rates of released antimicrobials during hydration of the formulation has normally been undertaken using the conventional kill-time assay (Ip et al. 2006; Rossi et al. 2007). However, under such conditions, the formulation under test will eventually totally disintegrate and dissolve in the presence of substantial amounts of dissolution medium. Usually, contemporary formulations prepared for topical drug delivery in exuding wounds aim to absorb the exudate while maintaining a swollen intact state. Therefore, testing the antimicrobial properties of dressings using time-kill studies, is likely to demonstrate the accelerated rate of killing of antimicrobials released from their carriers, possibly a desirable

property for effective topical application. Importantly, however, it does not resemble the real conditions of exuding wounds.

The antimicrobial diffusion cell (ADC) was developed in order to quantify the effect of antimicrobials released slowly from the matrices of KAG wafers as the antimicrobial formulations continuously hydrated and swelled, but did not disintegrate. These conditions were mediated by placing the antimicrobial formulation in permanent contact with a wetted hydrophilic membrane. The antimicrobial effect of released antimicrobials was tested against planktonic cells of MRSA, a common pathogen of chronic wounds. In addition, in order to overcome the potential quenching affect of organic matter present in nutrient agar/broth, bacterial cells were initially suspended in phosphate buffer solution (PBS) containing KCl (0.02 %) and NaCl (0.8 %), adjusted to pH 7.4. Figure 3.8 presents the killing behaviour of the tested antimicrobials against MRSA over 8 hours. Although PBS buffer was adjusted to a similar pH to the growth medium, the lack of nutrition led to gradual death of MRSA cells by approximately 1-log power (90 %) within 8 hours and 2-log powers (99 %) at 24 hours.

The data obtained demonstrated that all the antimicrobials decreased the viability of MRSA by approximately 2-log powers (99 %) over 4 hours. At that stage the untreated cells (control) were still at a considerable and viable density. The release of iodine from its PVP carrier showed the fastest killing rate, where this potent antimicrobial killed all the MRSA cells within 6 hours. CHD demonstrated the second fastest killing rate against MRSA as there were no detectable bacterial cells within 8 hours. NS demonstrated a slower killing rate compared to PVP-I and CHD, however the release of NS decreased by > 2-log powers (> 99 %) the viability of MRSA over 8 hours, and totally killed the presence of the bacterium at 24 hours. SS demonstrated a similar killing pattern to NS within 8 hours, however in the case of SS, its sparing solubility should also be considered. The SS particles entrapped in the lyophilised matrix of KAG, were unable to pass through the cellulose membrane, resulting in a slower, yet considerable decrease of MRSA population. However, the change in colour from white to light purple-blue for the SS wafer, at 24 hours, consistent with the formation of silver chloride, indicated that the chloride ions present in the PBS solution enhanced the solubilisation of the silver salt producing

sulfadiazine. These results are in agreement with previous studies on solubilisation of silver sulfadiazine undertaken by Tsipouras *et al.* (1995).

The antimicrobial activity of antimicrobials released from the swollen matrix of KAG was further assessed by suspending similar densities of MRSA cells in a salt solution containing 142 mmol/l NaCl (0.82 %) and 2.5 mmol/l CaCl₂ (0.027 %), typical values to those found in wound exudate (Thomas 2007). This experimental condition aimed to investigate the antimicrobial activity of selected antimicrobial compounds only in the presence of certain electrolytes such as Na⁺, Ca²⁺ and Cl⁻ at a lower pH. The pH of the prepared solution was slightly acidic (pH 6.5) and the absence of nutrients led to considerable reduction of untreated MRSA cells (Figure 3.9). There was a notable decrease in the viability of MRSA cells [(> 1 -log power, (> 90 %)] over 4 hours, suggesting that the salt solution did not present a suitable niche for the viability of planktonic cells. The killing rate of PVP-I and CHD were faster than in PBS, however, this was probably due to a reduced MRSA population in the NaCl-CaCl₂ solution, rather than potentiation of CHD and/or iodine in the presence of Na⁺, Ca²⁺ and Cl⁻ electrolytes. On the other hand, the antimicrobial effect of released NS and SS upon the viability of MRSA was notably inhibited compared to the untreated control, despite the apparent reduction of the MRSA population in the control medium. This paradox was likely related to inhibited antimicrobial activity of NS in a slightly acidic environment. NS is a bactericidal, antimicrobial compound which induces lethal reaction in bacteria by inhibiting protein synthesis. However, the antimicrobial effect of this aminoglycoside depends on the extracellular pH. It has been reported that antimicrobial activity of NS is reduced significantly in the presence of cations (e.g. Ca²⁺ and Mg²⁺) and in solutions of pH ≤ 6.5 (www.greatvistachemicals.com).

The antimicrobial activity of SS upon the viability of MRSA was also reduced compared to the antimicrobial-free control (KAG) wafer. Although it has been reported that the anionic content of exudate, in particular chloride ions, influence the solubility of sulfadiazine salt and increase its antimicrobial activity (Tsipouras *et al.* 1995) the effect of chloride ions, present in the prepared salt solution, was probably inhibited by the slightly acidic pH displayed. White and Cooper 2005 have also reported that disassociation of silver salts is a pH dependent reaction. The results obtained indicated that the

pH of the environment where antimicrobial compounds are released plays a decisive role in antimicrobial activity.

To simulate further the conditions existing in exudates of infected, non healing wounds, the salt solution of NaCl-CaCl₂, containing similar values of electrolytes to those found in human exudates, was enriched with 3 % w/v bovine serum albumin (BSA). The concentration of protein varies with wound aetiology and clinical healing stage, however, the selected concentration of BSA represents an average value of protein found in exudates of chronic wounds (Clought and Noble 2003). Figure 3.10 presents the antimicrobial effect of antimicrobial compounds released in the presence of BSA over 24 hours. The antimicrobial profiles of topical antimicrobials released from the swollen KAG matrix were notably altered in the presence of BSA. The BSA supplement increased the pH of the solution to 7.4 and provided sufficient nutrient for a viable population of MRSA to survive over 24 hours, maintaining the initial bacterial density. Under these conditions, the comparison of antimicrobial effect to the untreated control was more meaningful.

The presence of BSA totally deactivated the antimicrobial effect of iodine released from its carrier. These results are in agreement with previous research studies indicating the quenching activity of BSA upon the antimicrobial activity of PVP-I (Messenger et al. 2001). The presence of organic matter appeared to inhibit moderately the antimicrobial activity of CHD, as the CHD released decreased the viability of MRSA by less than 1-log power (< 90 %) after 4 hours. In contrast, the same antimicrobial led to more than a 2-log powers (> 99 %) reduction of MRSA cells in the absence of organic mater, at similar pH values, in PBS. Pitten *et al.* (2003) has also reported the inhibition effect of organic matter such as 10 % albumin, 10 % sheep blood or 1% mucin on the antimicrobial activity of chlorhexidine and/or PVP-I.

While the presence of organic material represents a challenge for the antimicrobial activity of PVP-I or CHD, for other topical antimicrobials such as SS and NS, the presence of BSA acts as a potentiator. SS decreased the viability of MRSA by 1-log power (90 %) after 4 hours. The viability of bacterial cells was further decreased after 24 hours by >1-log power (> 90 %), however, not considerably compared to SS wafers in the presence of PBS. Fox and Modak (1974) and Tsipouras *et al.* (1995) have also indicated that dissociation of SS is similar in both electrolyte solutions containing chloride

ions and in the presence of human serum. Solubility of the sulfadiazine salt of silver appeared to be moderate in such solutions, where the addition of protein does not enhance significantly the antimicrobial activity of SS (Fox and Modak 1974).

In contrast, the presence of BSA and the elevated pH of the pseudo-exudate enhanced notably the antimicrobial activity of NS. Under such conditions, NS released showed a maximum antimicrobial activity and the fastest killing rate by decreasing the viability of MRSA cells more than 3-log powers (> 99 %) within 8 hours. It is difficult to precisely identify the enhanced effect of BSA upon the antimicrobial properties of NS in a complex solution such as the pseudo exudate. However, a plausible interpretation may be achieved by elucidating the interaction occurring between the molecules present in the medium. Although it is well known that the majority of proteins of human serum bind to antimicrobials/antibiotics and deactivate their antimicrobial effect, recently, it has been reported that NS binds weakly to BSA (Keswani et al. 2010). In addition, it has been reported that small ions such as Na^+ and Ca^{2+} do appreciably bind to the structures of BSA (Doremus and Johnson 1958). This favourable interaction between BSA and Na^+ and Ca^{2+} results in two simultaneously favourable effects towards enhancement of the antimicrobial activity of NS; elevated values of pH (from 6.5 to 7.4) and the elimination of free Ca^{2+} inhibitors of NS.

In conclusion, it is apparent that the use of the ADC represented a superior *in vitro* microbiological assay, compared to disc diffusion, for evaluating the efficacy of antimicrobial formulations, such as antimicrobial wafers, intended as topical delivery systems for suppurating, non healing wounds. There are several advantages of the ADC to conventional time-kill studies and disc diffusion. Firstly, ADC represents an *in vitro* model that resembles relatively well the swollen yet intact state of dressings when applied in moderately exuding wound beds. Secondly, it demonstrates the antimicrobial effect, with time, of sustained release of antimicrobials from slowly re-hydrating wafers upon the common bacterial population present in chronic wounds. Thirdly, the different media used either alone, or enriched with organic material, provide a picture of how antimicrobial activity of well-known and widely used antimicrobial compounds can be considerably altered by the presence of electrolytes and proteins found in wound exudates. In

addition, interaction between topically applied antimicrobials and compounds present in human serum should be elucidated prior to application of any antimicrobial formulation to suppurating wound beds, as inhibition of the antimicrobial effect can lead to poor therapy and perhaps to an increased likelihood of acquired bacterial resistance.

Limitations of the developed ADC model are recognised, two main drawbacks being apparent. Firstly, the use of an inert, hydrophilic membrane would be considered a better choice, as cellulose was reported recently to favourably interact with cationic compounds such as chlorhexidine (Gimenez-Martin et al. 2009); however, these recent facts were not known at the time of experimentation. Secondly, samples taken at 2-hour intervals introduced untreated planktonic MRSA cells from the donor chamber into the receptor chamber (Figure 3.2). However, this untreated bacterial population was calculated to be a maximum of 5 % of the total volume of the receptor chamber and did not exceed 1 ml over 24 hours.

Chapter 4
Release studies of chlorhexidine digluconate
(CHD) from lyophilised wafers and gels

4.1 Aim

To analyse the release profiles and to quantify released CHD from lyophilised and pre-lyophilised gels prepared with biopolymers displaying different flow behaviours.

4.2 Introduction

Lyophilised antimicrobial wafers intended for targeted drug delivery in contaminated and exuding non healing wounds, were analysed for the ability to release a broad spectrum antimicrobial compound such as CHD. Quantification of the amount of delivered antimicrobial compound in a poly-contaminated niche, such as the non-healing chronic wound bed, is an important parameter for the efficacy of an antimicrobial formulation. It is well known that quantities of antimicrobial delivered must exceed the MIC/MBC values for selected bacteria for the treatment to be effective. In contrast, sub-inhibitory antimicrobial concentrations of active agents will lead to continued growth of pathogens in a wound bed, persistent infection and poor control of bacterial bioburden.

The quantification of released antimicrobial compound from a polymeric antimicrobial dressing is not a simple matter, as many factors can influence the release of the drug from its carrier. Factors such as the rate of exudate production from the damaged skin (external factor) and the degree of water uptake of the polymeric carrier (internal factor) are two of the most important. There is restricted information with regards to quantification of exudate produced from non healing wounds as exudation varies with wound aetiology and clinical healing stage. Different levels of suppuration are difficult to reproduce *in vitro*, however, in the present study, an enclosed dissolution apparatus that roughly resembles the exuding wound environment is used to quantify and further understand the release profiles of CHD from lyophilised polymeric carriers. In addition, the release profiles of CHD from lyophilised wafers have been compared to those of pre-lyophilised gels.

The release of CHD from the biopolymeric vehicles was assessed in a dissolution medium containing 142 mmol/litre of sodium ions and 2.5 mmol/litre of calcium ions, similar values of electrolytes found in wound

exudate (Thomas 2007). The same dissolution medium is used to assess moisture vapour permeability, fluid handling properties and absorbance capacity of commercial polymeric dressings (www.dressings.org). Additional water uptake estimations were undertaken for re-hydrated antimicrobial wafers, under the conditions created in the enclosed dissolution apparatus. Kinetics of release profiles of CHD from both wafers and gels were also analysed using an appropriate diffusion model.

The *in vitro* simulated conditions of an exuding environment were facilitated by placing antimicrobial formulations (wafers and/or gels) on a constantly hydrated cellulose membrane. Recently, published studies revealed that chlorhexidine digluconate is absorbed by cellulosic fibres (Gimenez-Martin et al. 2009). The experiments performed for the purposes of this chapter were scheduled and undertaken, prior the publication of this information, however, the sorption of chlorhexidine on cellulose will be taken into account during discussion of the obtained data.

4.3 Materials and methods

4.3.1 Materials

Gels and wafers were used and produced as previously described in Chapter 2 (2.2.2). Sodium chloride (NaCl) and calcium chloride (CaCl₂) were purchased from Sigma-Aldrich, Gillingham, UK. Cellulose membrane (12-14 kDa) was obtained from Medicell Int. Ltd., UK. UV spectrophotometer Cecil CE 3021 was used. Quartz cuvettes (3 ml volume) were purchased from Fischer Scientific Ltd. UK. The free standing dissolution raft was designed by the author and constructed by the workshop engineers of the Robert Gordon University.

4.3.2 Methods

4.3.2.1 *In vitro* release of CHD from lyophilised wafers and gels

Six identical free standing dissolution rafts (FSDR) were constructed as indicated in Figure 4.1. CHD lyophilised wafers and freshly prepared CHD gels (1.5 ± 0.2 g) were placed on top of the cellulose membrane (12-14 kDa) in contact with the dissolution medium for 24 hours at 36 ± 0.5 °C. The FSDR

was placed in 20 ± 2 ml of dissolution medium (NaCl-CaCl_2) in a glass container topped with a lid to avoid evaporation during the experiment. The enclosed dissolution system was placed in an agitating water bath (Fischer Scientific) at 145 rpm. Samples (3 ml) were taken, analysed and returned to the glass container at hourly intervals for eight hours and after 24 hours, in order to maintain a constant volume of dissolution medium with time. The presence of CHD was detected by UV analysis at 254 nm and the concentration determined from the regression equation generated from the calibration curve in NaCl-CaCl_2 solution ($y = 0.0306x$, $R^2 = 0.9995$).

Two controls containing known amounts of CHD in the dissolution medium were included. The first contained $46 \mu\text{g/ml}$ of CHD and was placed under the same conditions with the tested CHD-polymeric carriers (36 ± 0.5 °C). The second control contained $30 \mu\text{g/ml}$ CHD, and a dissolution raft with no CHD-wafers/gel was placed at 20 ± 0.5 °C. Samples (3 ml) were taken every hour for 8 hours and at 24 hours and analysed as described above. The absorbance indicated the amount of CHD in the solution over 24 hours.

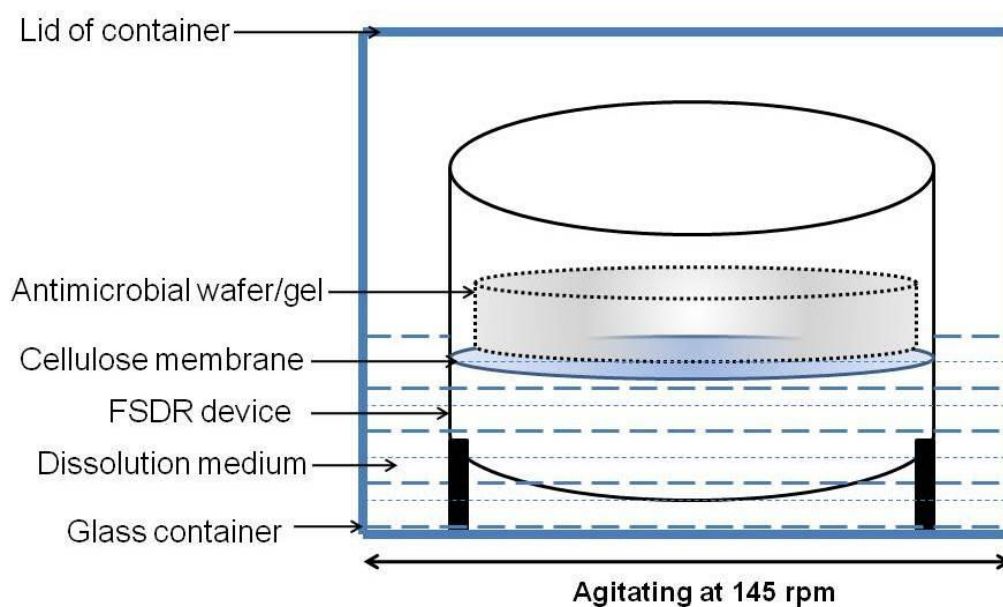


Figure 4.1 Configuration of the free standing dissolution raft (FSDR)

4.3.2.2 Calculation of the water uptake capacity (WUC) (%) for lyophilised wafers in NaCl-CaCl₂ dissolution medium

The water uptake capacity of different lyophilised controls and CHD loaded wafers when placed on top of a constantly hydrated cellulose membrane for 24 hours, as presented in Figure 4.1, was determined. Wafer weights were recorded prior to being placed on the membrane (W_0) and after 24 hour of water uptake (W_t), using an analytical balance, Mettler AE 50. Water uptake (WU) was calculated in percentage terms (%) using the simple formula: $WU = (W_t / W_0) \times 100$, where W_t = weight of swollen wafer after 24 hours of hydration and W_0 = weight of lyophilised wafer at time zero.

4.3.2.3 Analysis of drug release kinetics

The kinetics of CHD released from re-hydrated wafers and gels in NaCl-CaCl₂ dissolution media were determined by analysing the curves based on a simple, yet comprehensive model of Korsmeyer-Peppas [Equation (1)], which is based on the Higuchi theory of diffusion (Lao et al. 2011).

$$M_t / M_{inf} = kt^n \quad (1)$$

$$\log_{10}(M_t / M_{inf}) = \log_{10}(kt^n) \quad (2)$$

$$\log_{10}(M_t / M_{inf}) = n \log_{10}t + \log_{10}k \quad (3)$$

M_t = the concentration of CHD released at a given time (t), M_{inf} = the concentration of CHD present initially, k = constant of structural and geometrical characteristic of the formulation and n = the diffusion exponent. The diffusion exponent (n) was calculated as the slope of the linear regression line, by plotting the mean value of three samples [$\log_{10}(M_t / M_{inf})$] against ($\log_{10}t$) [Equation (2) and (3)]. Table 4.1 presents the values of the release exponent (n) and drug release mechanism of the polymeric delivery system formulated as a cylindrical shape (Lao et al. 2011).

Table 4.1 Values of the diffusion exponent (n) and solute drug release mechanism of cylindrical shaped polymeric systems (Lao et al. 2011; Cox et al. 1999; Tang et al. 2009).

Diffusion exponent (n)	Drug release mechanism
≤ 0.45	Fickian diffusion
$0.45 < n < 0.89$	Anomalous (non-Fickian) transport
0.89	Case-II transport
$n > 0.89$	Super case-II transport

4.4 Data analysis

Data are presented as the mean value of three samples \pm standard error of the mean (SEM). Regression analysis of the data was performed using GraphPad Prism 4 software.

4.5 Results

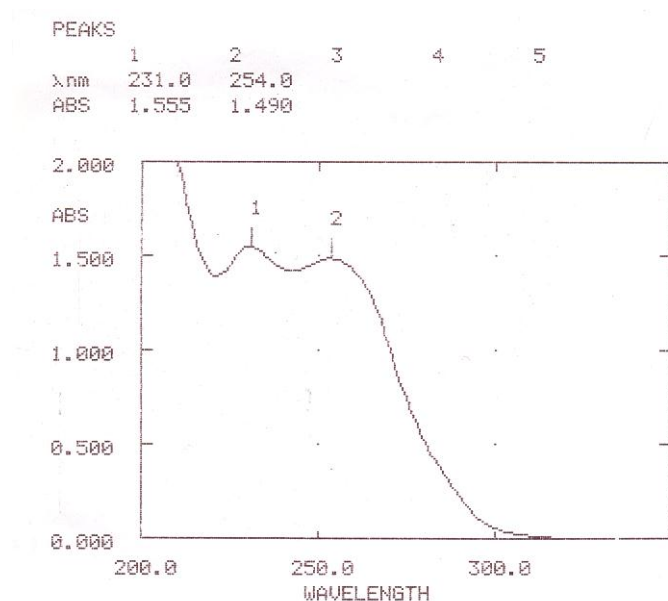


Figure 4.2 Determination of UV wavelengths of CHD solution, using a ThermoSpectronic Biomate 5 spectrophotometer. Note that CHD has two peak maxima in the wavelength region at 231 and 254 nm. UV measurements for the purposes of this project were undertaken at 254 nm.

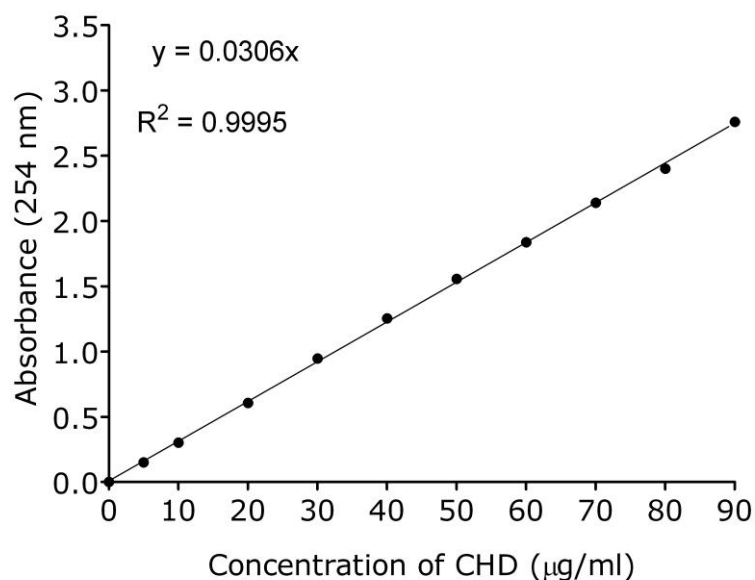


Figure 4.3 Standard UV calibration curve of CHD in NaCl-CaCl₂ solution at 254 nm ($R^2 = 0.9995$).

Table 4.2 Control solutions of CHD containing 46 and 30 $\mu\text{g/ml}$ CHD, respectively, tested at 36 ± 0.5 and 20 ± 0.5 $^{\circ}\text{C}$. Please, note that there is a decrease in the concentration of CHD (control 1) at 36 ± 0.5 $^{\circ}\text{C}$ by approximately 4 %, indicating degradation of CHD after 24 hours incubation. CHD solution tested at 20 ± 0.5 $^{\circ}\text{C}$ remained at a steady concentration, indicating that the presence of cellulose membrane did not affect the concentration of CHD.

Time (Hours)	Control 1 (36 ± 0.5 $^{\circ}\text{C}$)		Control 2 (20 ± 0.5 $^{\circ}\text{C}$)	
	CHD ($\mu\text{g/ml}$)	CHD (%)	CHD ($\mu\text{g/ml}$)	CHD (%)
0	46.30	100	29.68	100
1	45.57	98	30.76	104
2	45.74	99	30.05	101
3	45.98	99	30.66	103
4	45.49	98	29.76	100
5	46.05	99	29.74	100
6	46.32	100	29.67	100
7	46.16	100	29.42	99
8	46.33	100	-	-
24	44.29	96	30.16	102

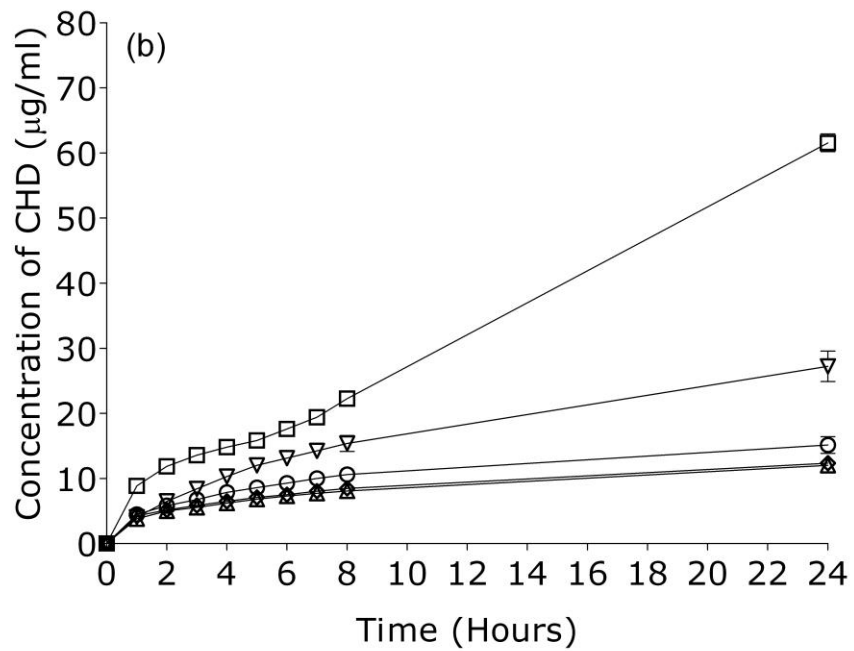
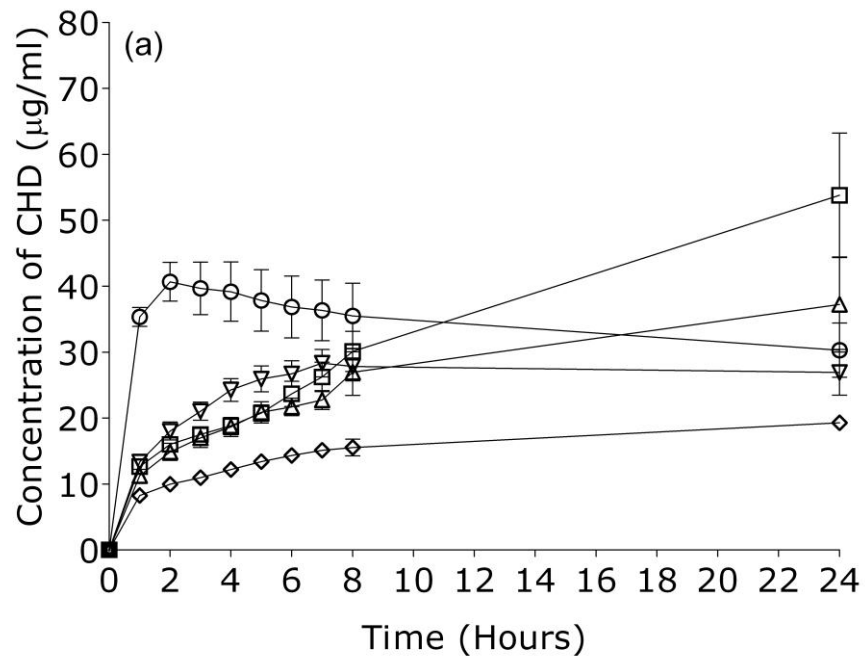


Figure 4.4 Release profiles of CHD- impregnated biopolymeric carriers (pre-lyophilised gels and lyophilised wafers) in NaCl-CaCl₂ dissolution medium, (a) gels (b) wafers (n = 3, SEM)

Table 4.3 Accumulation of CHD (%) in NaCl-CaCl₂ dissolution medium, from gels and wafers impregnated with clinical concentrations (0.5 % v/v) CHD, at 24 hours (n = 3, SEM).

Polymer type (w/v)	Accumulation of CHD (%) in NaCl-CaCl₂	
	Gel	Wafer
2.0 % GG	8.5 ± 1.15	4.2 ± 0.21
1.5 % XG	7.5 ± 0.97	7.6 ± 0.66
3.0 % KAG	14.7 ± 2.59	17.4 ± 0.39
5.0 % SA	10.7 ± 2.07	3.5 ± 0.04
1.5 % - 1.5 % SA-KAG	5.5 ± 0.21	3.5 ± 0.01

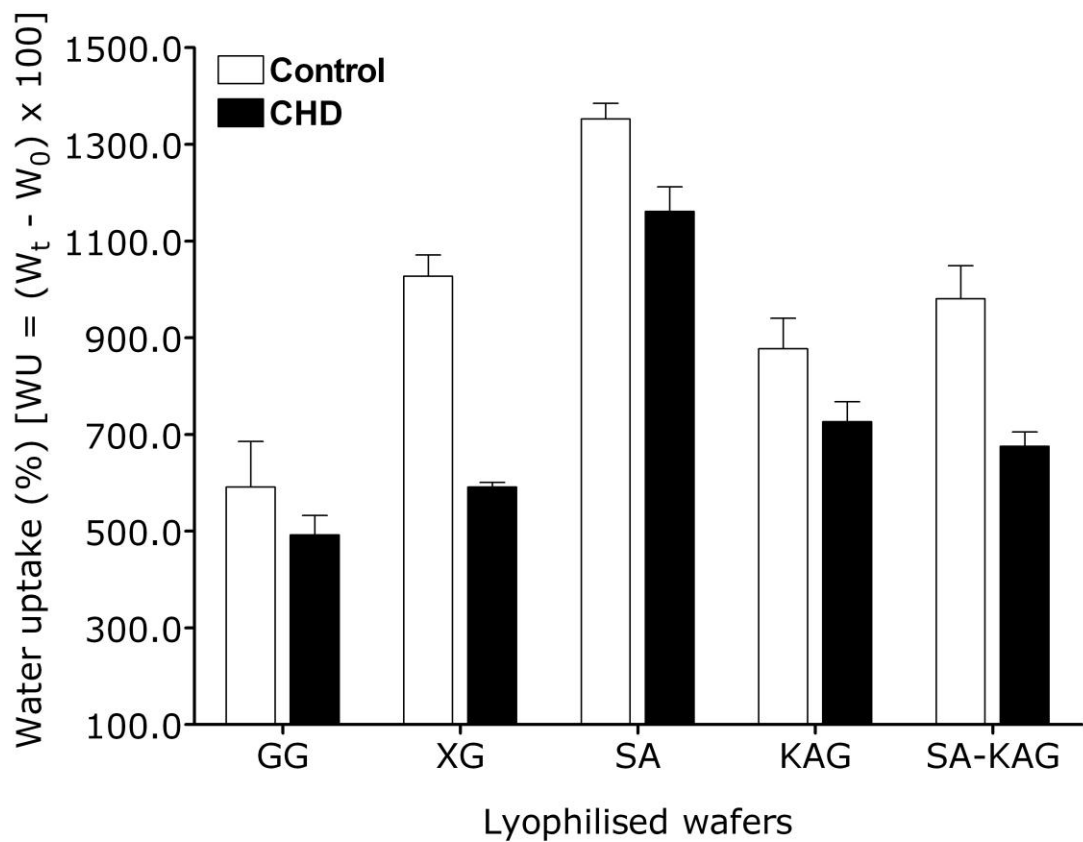


Figure 4.5 Water uptake capacity (WUC) (%) of re-hydrated wafers within 24 hours, placed on the FSDR. (n=3, SEM).

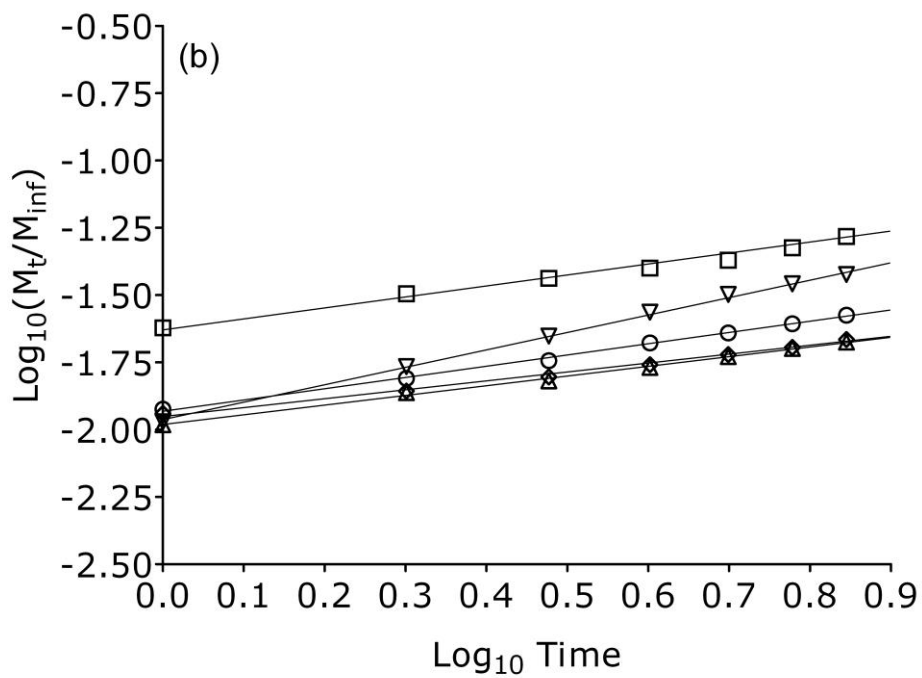
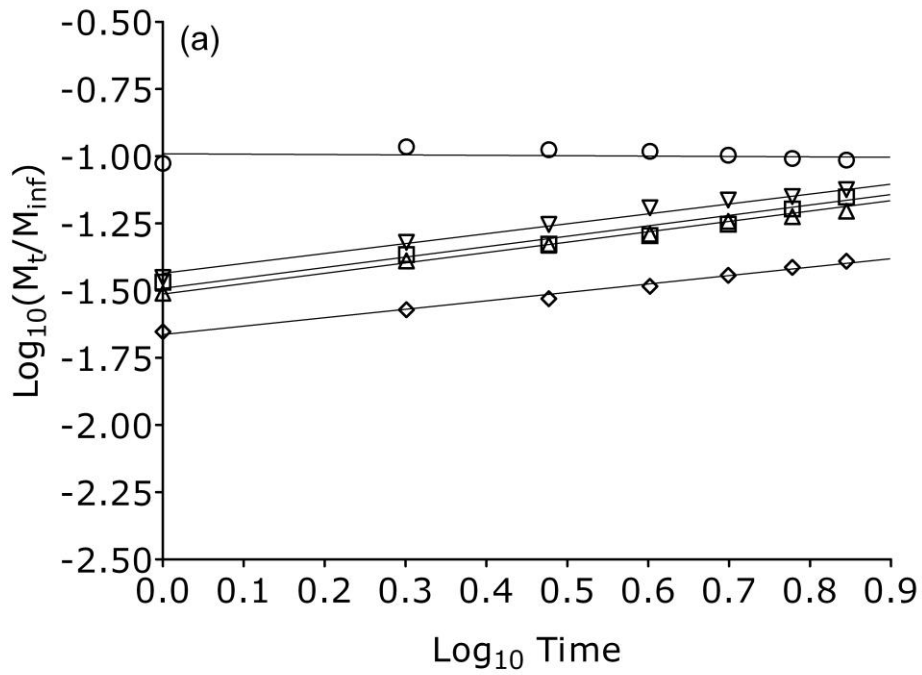


Figure 4.6 Linear regression of released CHD from polymeric systems in NaCl-CaCl₂, as analysed with the Korsmeyer-Peppas model; (a) gels (b) wafers

Table 4.4 Values of the release exponent (n) and the correlation coefficient (R^2) of CHD released from gels and wafers, in NaCl-CaCl₂, as analysed with the Korsmeyer-Peppas model; F (Fickian diffusion), NF (non-Fickian diffusion).

Polymeric systems impregnated with CHD (w/v)	n (R^2)	
	Gel	Wafer
GG	0.0 (0.0359)	0.36 ^F (0.9974)
XG	0.37 ^F (0.9791)	0.65 ^{NF} (0.9981)
KAG	0.39 ^F (0.9413)	0.41 ^F (0.9752)
SA	0.39 ^F (0.9819)	0.36 ^F (0.9974)
SA-KAG	0.31 ^F (0.9914)	0.33 ^F (0.9935)

4.6 Discussion

Antimicrobial loaded biopolymers, studied either as lyophilised wafers or pre-lyophilised gels, showed varied release profiles (Figure 4.4). The concentrations of CHD detected in NaCl-CaCl₂ after eight hours varied from 15.5 ± 1.250 µg/ml for SA-KAG gel to 35.5 ± 4.934 µg/ml for GG gel. The accumulated CHD after eight hours released from rehydrating wafers varied from 8.1 ± 0.183 µg/ml for SA and 22.3 ± 0.958 µg/ml for KAG. The rate of released CHD after eight hours varied between gel types, where GG > KAG > XG > SA > SA-KAG, where the synergistic combination showed the lowest rate of release and GG the highest, respectively. The release patterns of CHD from rehydrating wafers differ between wafers, where KAG > XG > GG > SA-KAG > SA. It is apparent that the rate of released CHD was not similar for polymeric carriers consisting of the same biopolymer in the pre-lyophilised or lyophilised state; however, generally SA and SA-KAG (gel and/or wafer) showed the slowest rate of release. The apparent decrease of CHD, from 8-24 hours, observed in the case of GG gels, was attributed to degradation of CHD with time, at 36 ± 0.5 °C (Table 4.2).

The diffusion of a soluble compound from a polymeric network is mediated via complex mechanisms that depends on both external (nature of the aqueous environment) and internal (inherited properties of polymeric molecules) factors. Hydrophilic biopolymers 'biohydrogels' used as carriers of a cationic antimicrobial compound, CHD, are large molecules, linear and/or branched, ionic and/or non-ionic, which possess an inherent ability to form a three-dimensional, cross-linked network in the presence of water. Cross-linking of such molecules is facilitated through ionic, hydrogen bonds, van der Waals forces and/or physical entanglements (Singh et al. 2010). The compartments formed within the 3-D polymeric network are filled with water, which contains the soluble molecules of CHD. Solute transport within the biohydrogels occurs, initially, within the water-filled areas in the structure depicted by the polymeric chains. Alteration in space of these regions will eventually influence the movement of the entrapped solute. The main factors that effect the diffusivity of solute entrapped in compartments between polymeric chains include, solute concentration, solute size in relation to the size of compartments created between polymeric chains, degree of swelling,

molecular weight between crosslinks, degree of crystallinity, pore size, mobility of polymeric chains and drug-polymer interactions (Amsden 1998).

The amount of CHD within the polymeric carriers was similar and the weight of drug was estimated at $7434.4 \pm 98.0 \mu\text{g}$ per $1.5 \pm 0.02 \text{ g}$ of gel (pre-lyophilised and/or lyophilised). However, the polymer concentration varies from 1.5 - 5 % (w/v), where XG had the lowest and SA the highest concentration. The slower diffusivity of CHD from the SA gel, compared to that from the XG gel, may simply be due to an increased polymer concentration for SA. According to Amsden (1998) "the diffusivity of a solute through a physically cross-linked hydrogel decreases as cross-linked density increases". However, based on the rheological results, XG appear to be more prone to forming a weak gel network (with a yield stress) than SA (with no yield stress, even at 5 % w/v). The release of CHD from GG however, does not appear to fit this picture.

As previously mentioned (Chapter 2), the presence of CHD in the biopolymer network induced notable changes to the flow properties of the gels. Rheological analysis of CHD-loaded gels demonstrated that the addition of CHD increased the values of consistency and/or yield stress for SA, XG and SA-KAG, while GG gel showed negligible alterations (Table 2.4, Figure 2.4). These results indicate that the entrapment of CHD in the water-filled compartments of cross-linked biohydrogels was likely interacting with the surrounding polymeric chains. Drug-polymer interactions led to permanent entrapment of drug within the cross-linked network, and restrained diffusivity through the gel network. It is apparent that most gels and/or wafer samples released CHD at a decreasing rate, indicating that the developed interactions between CHD and polymer carriers played a key role in the delivery of the antimicrobial compound.

GG gel demonstrated a different pattern of CHD release compared to all other gels. Diffusivity of CHD from GG gel showed a burst release that reached a maximum concentration of $40.7 \pm 2.922 \mu\text{g/ml}$ at 2 hours. This pattern of release of CHD from the pre-lyophilised gel of GG was clearly dissimilar compared with release of CHD from the lyophilised wafer of GG. These results suggest that this lyophilised wafer can deliver in a sustained release manner; however, the rate of delivery of impregnated compounds varies with nature of the biopolymeric carrier. The total accumulated concentrations of CHD at 24

hours (Table 4.3) provide a rough indication of such influence, however, these values do not represent absolutely the accumulated concentration at 24 hours, as some of CHD is degraded (approximately 4 %). Although it was reported that CHD interacts with cellulose fibres, this interaction did not play a considerable effect on the total accumulation of CHD in the dissolution medium (Table 4.2).

The total accumulation of CHD at 24 hours varied from 3.5 ± 0.01 % to 17.4 ± 0.39 % for wafers, where SA-KAG and KAG demonstrated the lowest and the highest accumulation, respectively. The accumulation of CHD from gels was slightly increased compared to wafers and ranged from 5.5 ± 0.21 % to 14.7 ± 2.59 % for SA-KAG and KAG, respectively. Although the concentration of accumulated CHD from biopolymeric carriers is minimal and did not exceed 17.5 %, the accumulated concentrations of CHD from gel and wafers were generally similar, except in the case of GG and SA. It is apparent that the amount of CHD released from GG gels was 2-times higher than from GG wafers. Interestingly, both gels and wafers of XG and KAG released similar amounts of CHD within 24 hours. Although wafers of SA and SA-KAG released similar amounts of CHD at 24 hours, these gels increased the release of CHD by 3 and 1.5 times respectively. This data indicates that lyophilised wafers can provide a controlled release of the impregnated therapeutic compound.

The majority of polymeric systems (gels and/or wafers), displayed similar patterns of release of CHD. Although the pre-lyophilised gels were expected to show a faster release of CHD compared to the respective wafers, this was only apparent for GG gel. The mechanism of drug transport through a polymeric gel is governed by the rules already discussed, however in the case of water absorbent formulations the level of water uptake will also have an impact on the pattern of release of the incorporated drug. According to Vlachou *et al.* (2001) "the overall delivery rate from a polymeric specimen is expected to be a function of both swelling and disintegration (erosion)". In the case of rehydrated lyophilised wafers, water uptake only led to swelling of the matrix.

Water uptake capacity (WUC) of lyophilised wafers, (antimicrobial-free or loaded) varied from 492 ± 56.65 % to 1161 ± 87.55 %, where GG showed the lowest and SA the highest water uptake capacity, respectively (Figure

4.5). These results suggest that lyophilised wafers can absorb and retain a substantial amount of water, approximately 5 - 11 times their initial weight; however, the ability to absorb water will depend on the inherent hygroscopicity of each polymer. The equilibrium swelling will be a balance between available water, relative humidity and temperature. All these biopolymers will have a particular water uptake capacity in the conditions created in the FSDR. Antimicrobial-free wafers demonstrated a slightly increased water uptake capacity, compared to CHD-loaded wafers. XG-CHD wafers in particular demonstrated approximately 2 times decreased WUC, compared to XG CHD-free control. The decreased capacity to retain water is due to altered properties of the gels mediated from the CHD-polymer interactions.

Water uptake capacity of CHD-loaded wafers varied with biopolymer type in the following order SA > KAG > SA-KAG > XG > GG, where SA had the highest water uptake and GG the lowest. Diffusion of CHD from swelling wafers, however was in the order KAG > XG > GG > SA-KAG > SA. It is apparent that diffusion of CHD was not proportional to water uptake capacity as the most swollen wafer (SA) released the lowest quantity of CHD. This paradox may be explained by consideration of the polymer content (solid content) of individual wafers. Presumably, increased polymer content determines the water uptake capacity. SA (5 % w/v) has a much higher capacity than XG (1.5 % w/v). Diffusion of CHD on the other hand, is determined by polymer-drug interactions.

Kinetic analyses of diffused solute were undertaken using a comprehensive model of Korsmeyer-Peppas in order to understand further the drug release mechanism from cylindrical shaped matrices (Figure 4.6). This model is thought to represent the kinetics of drug/solute released as controlled by polymer swelling, where the value of the release exponent (n) is indicative of the mechanism of diffusion. The amorphous polymer matrix is initially in a glassy state, but as the lyophilised system absorbs water, the glass transition temperature (T_g) of the matrix is reduced, as water acts as a plasticiser for the polymer network. The swollen lyophilised matrix possesses an increased mobility of polymeric chains, which eventually lead to diffusion of the solute and an increased matrix volume (Perrie and Rades 2010). Diffusion

of solute from a swollen polymeric carrier can be explained by four mechanisms, depending on the diffusion exponent value (Table 4.1).

Fickian diffusion represents steady-state diffusion that occurs due to a chemical potential gradient, where the flux goes from regions with high concentration to regions with low concentration (Lao et al. 2011). Anomalous (non-Fickian) transport refers to the abridgement of both diffusion and dissolution of released solute (Reza et al. 2003). Case II and super case II transport generally refer to solute release mechanisms associated with state-transitions in hydrophilic, glassy matrices which swell in water or biological fluids (Cox et al. 1999). This state presents polymer disentanglement and erosion (Danarao et al. 2011). Table 4.4 presents the release exponents (n) and correlation coefficients (R^2) for CHD diffused from both rehydrated wafers and gels. It is apparent that the Korsmeyer-Peppas model was generally a good-fit for the diffused CHD within 8 hours of dissolution, as the majority of R^2 values ranged from 0.9413 to 0.9981. The only exception was the case of burst release of CHD from GG gel.

The release mechanism of CHD from polymeric carriers was generally Fickian, indicating that gel structures in pre-lyophilised form or swollen wafers were not completely relaxed at 8 hours. In the majority of cases, the diffusion mechanism was the same for gels and rehydrated wafers. XG gels demonstrated Fickian diffusion of CHD, while re-hydrated wafers showed non-Fickian transport of CHD, indicating that the presence of electrolytes likely had an effect on the XG network. Samples of KAG, SA and SA-KAG all demonstrated Fickian diffusion of CHD, indicating that drug-polymer interactions played a key role in the diffusivity of the incorporated drug from the polymeric matrix.

It is very difficult to precisely elucidate the mechanism of drug diffusion from a polymeric carrier as many factors interplay during transportation of solute. Interestingly, the majority of both gel and re-hydrated wafers had similar patterns of diffusivity of CHD. The rehydrated matrices absorbed a substantial amount of water, which did not reach the initial amount of water in the pre-lyophilised gel, mainly due to equilibrium conditions created in the enclosed FSDR. Clearly, gels or re-hydrated wafers of GG, XG, SA, KAG and SA-KAG did not result in complete relaxation of polymer chains hence the diffusion of CHD was governed by considerable drug-polymer interactions.

However, further research is required to decipher the intermolecular interactions taking place within the biopolymer network.

As mentioned previously, the quantification of a released antimicrobial compound is essential for effective treatment and therapy of bacterial infection. Applied antimicrobial concentrations which exceed the MIC/MBC values at the site of application against common pathogens are considered to be effective for the treatment of bacterial contamination. Although CHD is a broad spectrum antimicrobial, the estimated values of MIC and MBC against common pathogens of chronic wounds varied with the type of bacterial strain (Chapter 3, Table 3.1). MRSA and MSSA showed the lowest values of MIC and MBC (0.2 - 0.4 $\mu\text{g/ml}$) indicating that low concentrations of CHD are required to kill the growth of *S. aureus*. CHD demonstrated moderate values of MIC (0.6 $\mu\text{g/ml}$) and MBC (14 $\mu\text{g/ml}$), when tested against *E. coli*, where the MBC was 23 times higher than MIC, indicating that increased doses of CHD are required to totally kill the viability of such a pathogen. *In vitro* antimicrobial activity of CHD against *P. aeruginosa* demonstrated increased values of both MIC/MBC, indicating that the latter pathogen can withstand the antimicrobial activity of CHD below 20 $\mu\text{g/ml}$. Estimated values of MIC (4 $\mu\text{g/ml}$) and MBC (20 $\mu\text{g/ml}$) indicated that a concentration of CHD higher than 20 $\mu\text{g/ml}$ is required to totally kill the viability of *P. aeruginosa*.

The release profiles of CHD-containing wafers and gels demonstrated that the bulk of the antimicrobial compound remained in the gel network. All gels released quantities of CHD greater than the MBC of all bacterial strains tested. All wafers released CHD in a sustained fashion, where the concentration of CHD accumulated from XG, GG, SA and SA-KAG did not exceed 15.4 ± 1.218 $\mu\text{g/ml}$ within 8 hours. Quantities of CHD released from wafers of GG, SA and SA-KAG at 24 hours were still lower (15.13 ± 0.738 $\mu\text{g/ml}$) than the estimated MBC value of CHD against *P. aeruginosa*.

It is well known that suppurating chronic wounds have a mixed polymicrobial flora, where more than one species of pathogen can contaminate the wound bed. Although it was clear from these measurements that most of the antimicrobial remains within the swollen biopolymer network, that in itself did not undermine the utility of antimicrobial wafers to be used as effective antimicrobial dressings. Antimicrobial wafers are formulations intended to provide controlled and sustained delivery of therapeutic compounds, by

adhering to a suppurating wound bed. This includes the ability to absorb wound fluids and maintain a moist wound bed. It has been reported that the exudate of infected chronic wounds contains a variety and high densities of common bacterial species (White and Cutting 2006). Dressings with a high absorbance capacity are able to absorb and retain bacteria within their matrix (Newman et al. 2006). Walker *et al.* (2003) have visualized the encapsulation and immobilisation of *P. aeruginosa* and *S. aureus* in alginate and carboxymethyl cellulose dressings (Aquacel®). Recently, Newman *et al.* (2006) examined the antimicrobial activity of Hydrofyber® dressings where bacterial populations of *S. aureus* and *P. aeruginosa* were entrapped. They concluded that the ability of polymeric dressings to sequester and immobilise bacterial pathogens may provide a beneficial environment for wound healing. In addition, antimicrobial-loaded dressings, containing ionic silver, killed the entrapped microorganism, demonstrating a favourable behaviour for dressings which aim to control wound bioburden. Moreover, minimal release of broad spectrum antimicrobials may prove less cytotoxic for skin cells.

Porous, adhesive and absorptive formulations, such as lyophilised wafers, are very likely to encapsulate bacterial species within their swollen structure. However, it is currently unknown how entrapped pathogens will behave within the swollen network of antimicrobial free and/or loaded biopolymers. Additional research is required to quantify the microorganisms absorbed by wafers and to investigate the antimicrobial activity of swollen antimicrobial wafers containing entrapped pathogens associated with chronic wounds.

Chapter 5
**Physicochemical and antimicrobial properties of
gamma-irradiated lyophilised wafers**

5.1 Aim

To investigate the physicochemical and antimicrobial properties of gamma-irradiated lyophilised wafers prepared with different natural polymers and clinical concentrations of broad spectrum topical antimicrobial compounds.

5.2 Introduction

Medical products, including dressings, which aim to provide protection and treatment of injured and infected skin, must be prepared as sterile products. Based on the constituent materials, dressings have been sterilised by different methods including autoclaving, dry heat, ethylene oxide and ionising radiation (Ford 2004). Gamma irradiation in particular, is broadly utilised for the sterilisation of pharmaceutical products and surgical materials including polymeric and antimicrobial dressings. This sterilising method has been usually the choice for heat-sensitive materials and/or compounds, as there is only a minimal increase in temperature during the sterilising process performed with gamma-rays. However, gamma-irradiation has been reported to affect the structures of some polymeric materials. Structural alterations of polymers are due to either chain scission or cross-linking which ultimately lead to decreased and/or increased molecular weight, respectively. Matthews *et al.* (2006) has reported both phenomena occurring on irradiated biopolymers such as xanthan gum and sodium alginate by analysing the rheological properties post-irradiation. In addition, increased doses of gamma-irradiation have been reported to induce colour alteration in alginate solutions, turning them brown (Lee et al. 2003).

The present chapter includes work undertaken to investigate the rheological properties of gamma-irradiated, selected natural polymers (SA, KAG, GG and XG) and the structural stability of broad spectrum antimicrobial compounds (NS, CHD, PVP-I and SS). In addition, the performance of lyophilised wafers with and without antimicrobial, were also investigated, in terms of expansion and inhibition ratios. Moreover, antimicrobial release properties and swelling properties will be assessed for some of the irradiated formulations and compared to non-irradiated lyophilised wafers.

5.3 Materials and methods

5.3.1 Materials

Neomycin trisulphate (powder), chlorhexidine digluconate (20 % w/v solution), silver sulfadiazine (98 % purity of powder), pluronic F68 (non-ionic surfactant) karaya gum, sodium alginate, guar gum and xanthan gum, deuterium oxide (99.9 % D₂O) and trifluoroacetic acid deuterated (TFA-d) were purchased from Sigma-Aldrich, Gillingham, UK. Povidone iodine (10 % standardised aqueous solution) and 12-well polystyrene culture plates were purchased from Seaton Healthcare Group and Costar Ltd., UK, respectively. Tryptone soya agar and sabouraud dextrose agar were purchased from Oxoid, Ltd. UK.

5.3.2 Methods

5.3.1 Gamma-irradiation sterilisation of lyophilised wafers

Irradiation sterilisation of lyophilised wafers was carried out by Isotron Ltd. UK, using gamma rays generated from a radioactive Cobalt-60 source with an approximate dose rate of 5 kGy/hour. Two lots from each batch of formulated wafers (antimicrobial loaded and antimicrobial free) were irradiated with 25.0 kGy \pm 10 % and 40.0 kGy \pm 10 % doses, respectively. Lyophilised wafers were sterilised within the polystyrene plates in which they were cast. Polystyrene is reported to have excellent radiation resistance (Isotron Ltd, UK). Samples of raw polymers and antimicrobials were irradiated within glass vials under the same conditions. The prescribed doses of irradiation are typically used for sterilising medical devices (Matthews et al. 2006).

5.3.2 Microbiological validation of sterility of irradiated products

Validation of the sterility of irradiated polymeric products was undertaken using aseptic microbiological examination of a minimum number of samples taken from each irradiated lot. Samples were placed on tryptone soya agar (TSA) and sabouraud dextrose agar (SDA) plates, incubated at 37 °C for 24 - 48 hours and at 25 °C for 4-5 days, respectively. TSA plates were composed of 15 g/l tryptone, 5 g/l soyapeptone, 5 g/l sodium chloride and 15 g/l agar to

test for the presence of aerobic bacterial species and SDA plates were composed of 10 g/l mycological peptone, 40 g/l glucose and 15 g/l agar to test for the presence of fungi. Both growth media were autoclaved at 121 °C for 15 minutes prior to use to ensure sterility. Controls of non-irradiated samples were also included and were tested under the same conditions. Growth and/or absence of either bacterial or fungal species was recorded after 48 hours and 5 days incubation, respectively. The presence of visible growth was recorded as '+' and the lack of growth was recorded as '-'.

5.3.3 Structural validation of antimicrobial compounds

A 400 MHz nuclear magnetic resonance (NMR) spectrometer (Bruker, Biospin UK) was used to investigate the chemical configuration of irradiated antimicrobial compounds. NS (80 mg) and CHD (50 µl of 20 % stock aqueous solution) were dissolved in deuterium oxide, D₂O (0.5 ml). SS (30 mg) was dissolved in deuterium trifluoroacetic acid, TFA-d, (0.5 ml). Changes in the positioning or ordering of resonances detected may indicate changes to the chemical configuration induced by gamma-irradiation.

Both proton (¹H) and/or carbon 13 (¹³C) NMR were used to characterise irradiated and non-irradiated PVP-I, with no success. This was essentially due to the presence of additives such as glycerol, nonoxynol-9, sodium phosphate, sodium hydroxide, potassium iodate and citric acid, which complicated the spectra in the 10 % (w/v) standardised solution (obtained commercially), the complex structure of the iodophor(e) arguably being the main reason.

5.3.4 Rheological analysis of irradiated polymers and lyophilised formulations as reconstituted gels

Rheological characterisation of gels prepared from irradiated raw polymers was performed as previously described in Chapter 2, Section 2.3.5. Rheological analysis was also performed for irradiated lyophilised wafers as reconstituted gels. Lyophilised formulations (with and without antimicrobial) were reconstituted to gels by adding precise volumes of distilled water until reaching the pre-lyophilised weight of the initial cast gels (1.5 ± 0.02g). The

rheological properties of at least three samples for each prepared gel were analysed with the Herschel-Bulkley model.

For the purposes of this project the gels prepared from irradiated raw polymers will be referred to as pre-lyophilised irradiated gels. The gels prepared from reconstituted irradiated wafers will be referred to as post-lyophilised irradiated gels. The gels prepared from non-irradiated raw polymers and/or reconstituted wafers will be referred to as pre-lyophilised gels and post-lyophilised gels, respectively.

5.3.5 Antimicrobial properties of irradiated lyophilised formulations

A modified disc diffusion method (as previously described in Chapter 3, Section 3.3.2.3) was used to investigate the performance and antimicrobial properties of irradiated wafers. Measurements of the of initial diameter of the wafers (D_0), the swollen diameter of the wafers (D_t) and diameter of the inhibition zone (D_i) were taken at intervals of 0° and 90° using a digital calliper and steel engineering ruler (*Mitutojo*). Only in the case of karaya (KAG) wafers (with and without antimicrobial), was the swollen diameter (D_t) and diameter of the inhibition zone (D_i) measured in one direction as indicated in Figure 5.1-B, due to a total erosion of the disc shape of KAG wafers after 24 hours incubation at 37°C . Expansion and inhibition ratios were calculated as $ER = D_t/D_0$ and $IR = D_i/D_0$, respectively.

5.3.6 Release profile, swelling properties and kinetics of CHD release from gamma-irradiated SA-CHD wafers

Release profiles of irradiated wafers of sodium alginate (SA) impregnated with clinical concentrations of chlorhexidine digluconate (CHD) were investigated using the free standing dissolution raft (FSDR) as previously described in Chapter 4 (Section 4.3.2.1). The same diffusion model and associated formula were used to calculate the diffusion mechanism of CHD from irradiated wafers of SA-CHD. In addition, the same formula as indicated in Chapter 4 (Section 4.3.2.1), was used to calculate the water uptake (WU) of swollen wafers at 24 hours in the conditions created in the FSDR.

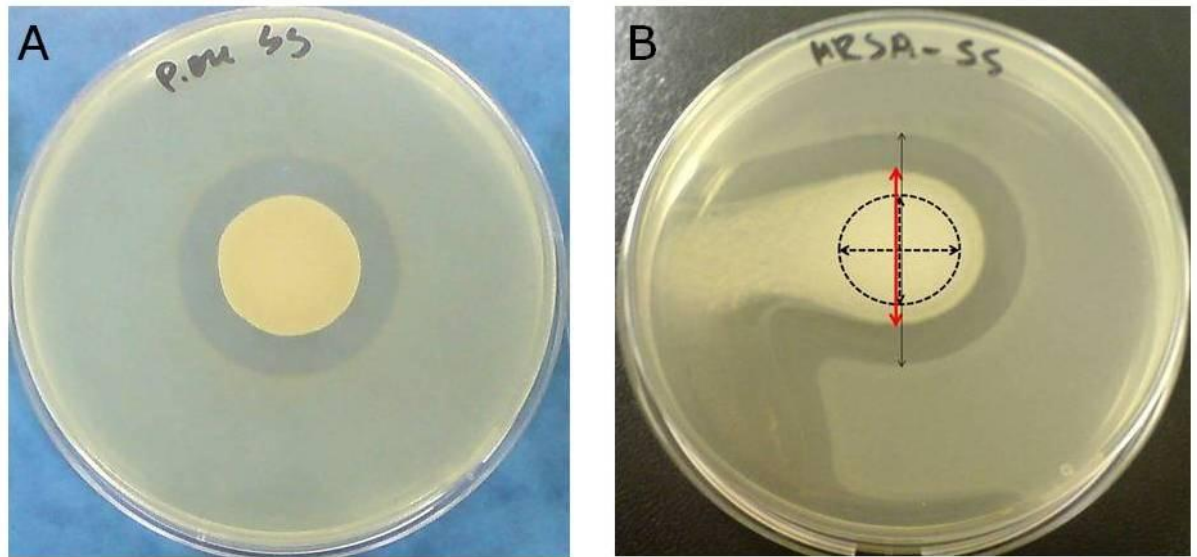


Figure 5.1 Typical images taken after 24 hours incubation of karaya (KAG) wafer impregnated with 1 % (w/v) silver sulfadiazine (SS), tested against bacterial strains using a modified disc diffusion assay. **A** - Non-irradiated and **B** - irradiated antimicrobial wafer. The same behaviour was observed for all KAG loaded and non-loaded, irradiated wafers.

5.4 Data analysis

Data are presented as the mean value of three samples \pm standard error of the mean (SEM). Regression analysis of data was performed using GraphPad Prism 4 software.

5.5 Results

Table 5.1 Microbiological validation of raw polymers tested for the presence of bacterial and/or fungal contamination. (+) presence of bacterial/fungal growth, (-) lack of bacterial/fungal growth.

Raw polymers	Bacterial growth			Fungal growth		
	Non-irradiated	Irradiated doses		Non-irradiated	Irradiated doses	
	0 kGy	25 kGy	40 kGy	0 kGy	25 kGy	40 kGy
KAG	-	-	-	-	-	-
GG	+	-	-	-	-	-
XG	+	-	-	+	-	-
SA	-	-	-	-	-	-

Table 5.2 Microbiological validation of control (antimicrobial free) lyophilised wafers tested for the presence of bacterial and/or fungal contamination. (+) presence of bacterial/fungal growth, (-) lack of bacterial/fungal growth.

Control wafers	Bacterial growth			Fungal growth		
	Non-irradiated	Irradiated doses		Non-irradiated	Irradiated doses	
	0 kGy	25 kGy	40 kGy	0 kGy	25 kGy	40 kGy
KAG	-	-	-	-	-	-
GG	-	-	-	-	-	-
XG	+	-	-	+	-	-
SA	-	-	-	-	-	-
SA-KAG	-	-	-	-	-	-

Table 5.3 Microbiological validation of KAG (3 % w/v) lyophilised antimicrobial wafers tested for the presence of bacterial and/or fungal contamination.

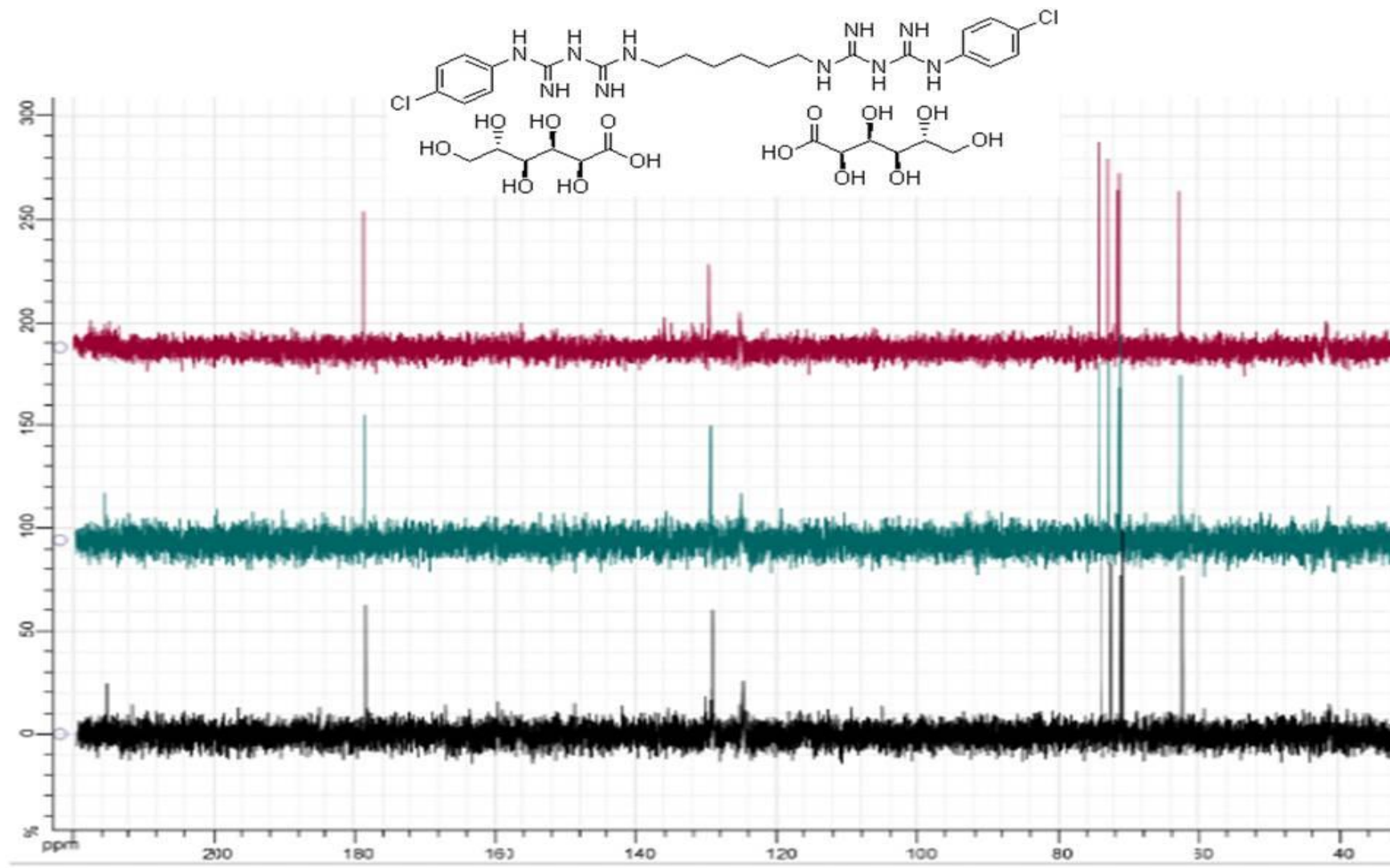
(+) presence of bacterial/fungal growth, (-) lack of bacterial/fungal growth.

KAG antimicrobial wafers	Bacterial growth			Fungal growth		
	Non-irradiated	Irradiated doses		Non-irradiated	Irradiated doses	
	0 kGy	25 kGy	40 kGy	0 kGy	25 kGy	40 kGy
0.5 % (w/v) NS	-	-	-	-	-	-
0.5 % (v/v) CHD	-	-	-	-	-	-
1.0 (v/v) PVP-I	-	-	-	-	-	-
1.0 % (w/v) SS	-	-	-	-	-	-
0.2 % (w/v) F68	+	-	-	-	-	-

Table 5.4 Microbiological validation of lyophilised antimicrobial wafers prepared with the incorporation of a clinical concentration of CHD (0.5 % v/v) into matrices of different biopolymers. (+) presence of bacterial/fungal growth, (-) lack of bacterial/fungal growth.

CHD lyophilised wafers	Bacterial growth			Fungal growth		
	Non-irradiated	Irradiated doses		Non-irradiated	Irradiated doses	
	0 kGy	25 kGy	40 kGy	0 kGy	25 kGy	40 kGy
2 % GG	-	-	-	-	-	-
1.5 % XG	-	-	-	-	-	-
5.0 % SA	-	-	-	-	-	-
SA-KAG (1:1)	-	-	-	-	-	-

Figure 5.2 ^{13}C NMR spectra of chlorhexidine digluconate (CHD) diluted in D_2O . (—) non-irradiated compound, (—) irradiated with $25.0 \text{ kGy} \pm 10 \%$ and (—) irradiated with $40.0 \text{ kGy} \pm 10 \%$.



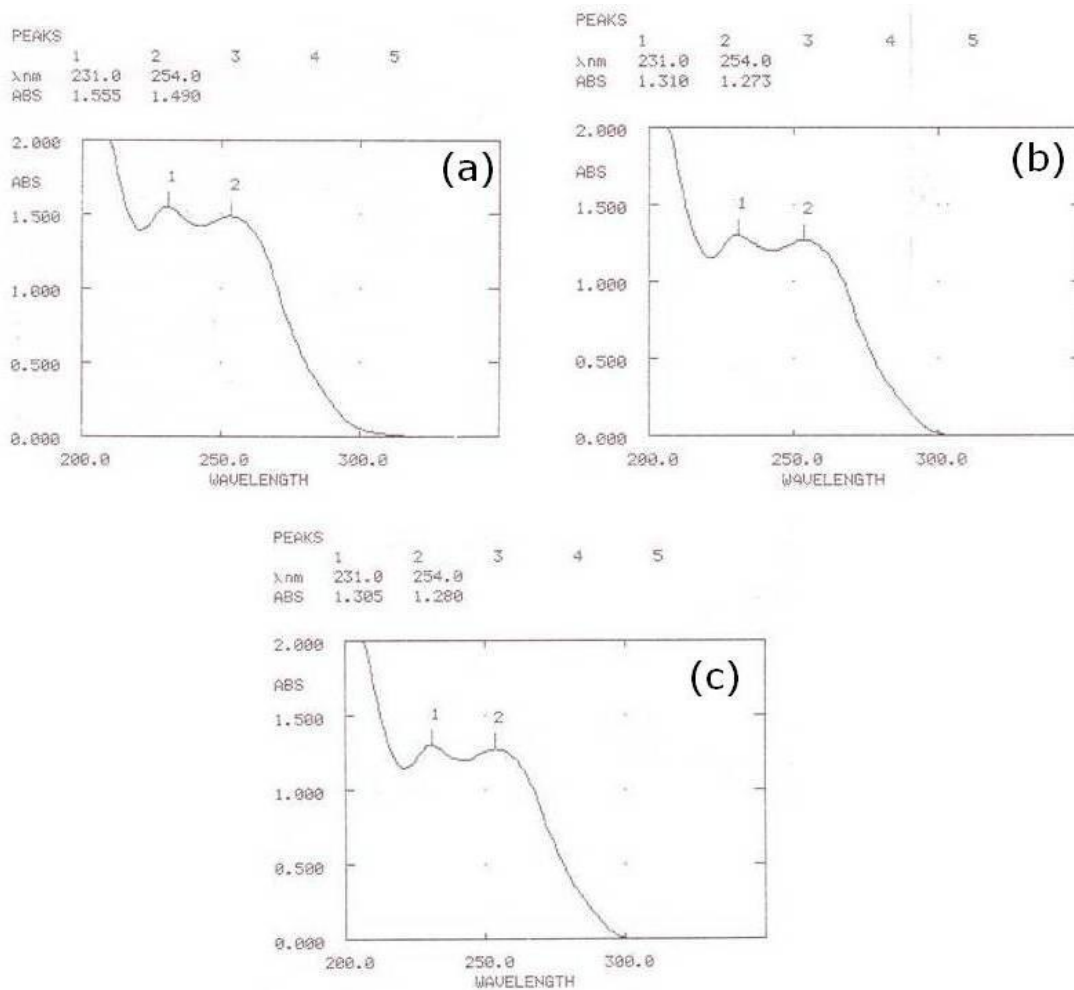


Figure 5.3 UV analysis of gamma-irradiated chlorhexidine digluconate (CHD) aqueous solutions containing the same concentrations of CHD (40 $\mu\text{g}/\text{ml}$), using a ThermoSpectronic Biomate 5 spectrophotometer. Note that both chromophores (chlorobenzene rings) are visible at identical wave lengths (231 and 254 nm) for all solutions; however the intensity of absorbance is lower in the irradiated samples by approximately 15 %. (a) Non-irradiated sample, (b) Irradiated sample with 25.0 kGy \pm 10 %, (c) Irradiated sample with 40.0 kGy \pm 10 %

Figure 5.4 ^{13}C NMR spectra of neomycin sulphate (NS) dissolved in D_2O . (—) non-irradiated compound, (—) irradiated with $25.0 \text{ kGy} \pm 10 \%$ and (—) irradiated with $40.0 \text{ kGy} \pm 10 \%$.

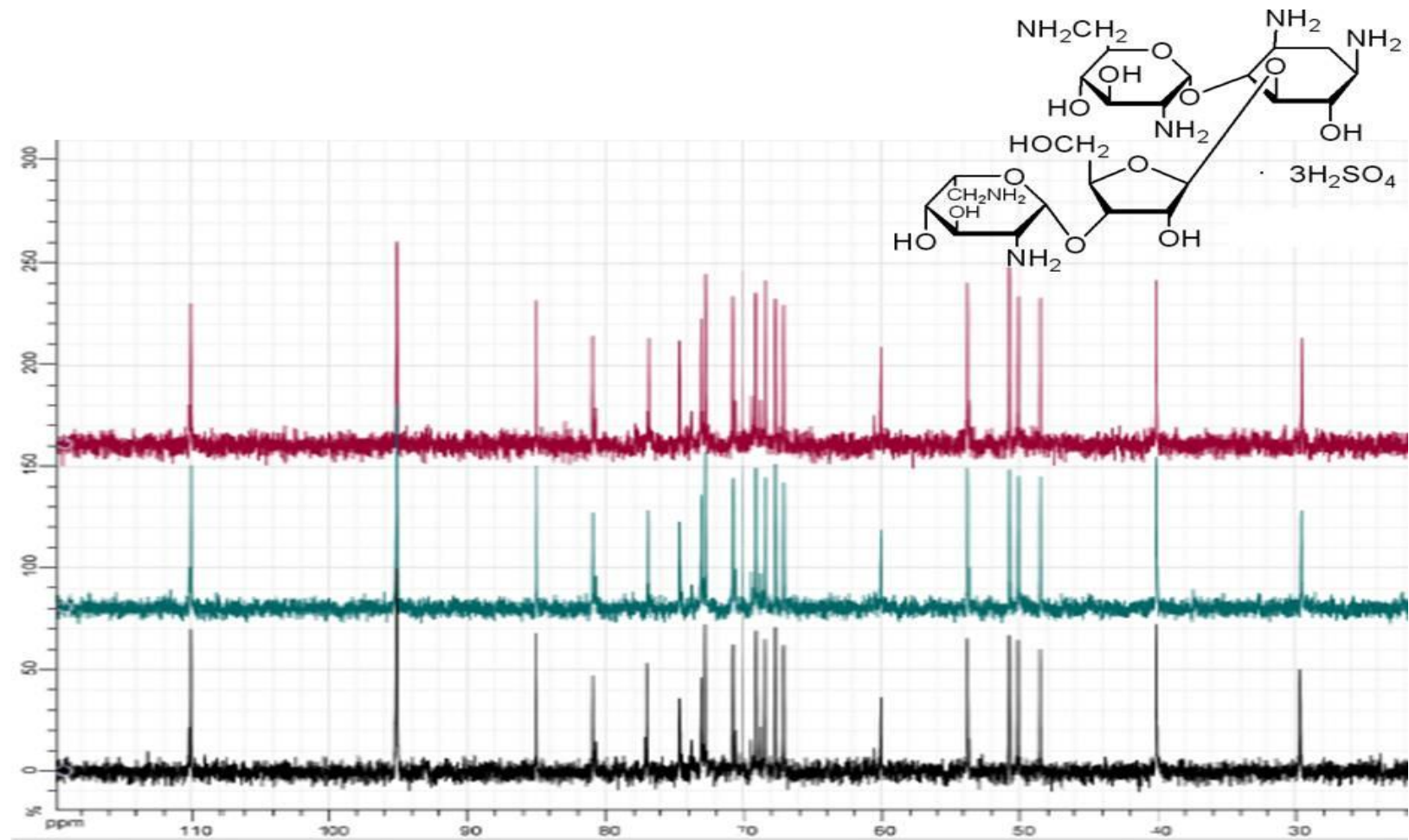
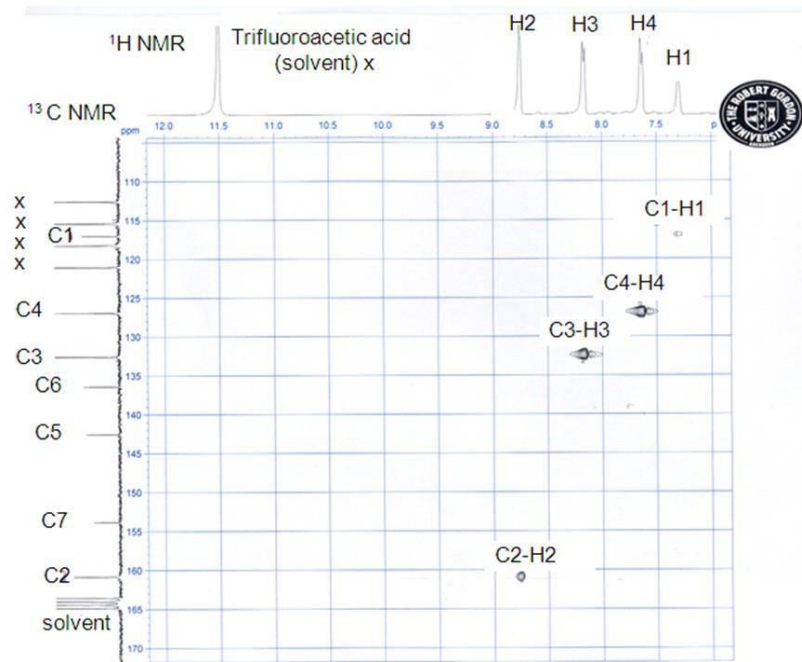


Figure 5.5 ^1H NMR spectra of silver sulfadiazine (SS) dissolved in TFA-d. (—) non-irradiated compound, (—) irradiated with 25.0 kGy \pm 10 % and (—) irradiated with 40.0 kGy \pm 10 %. Below (a): ^{13}C - ^1H heteronuclear single quantum coherence (HSQC) NMR spectrum of SS.

(a)



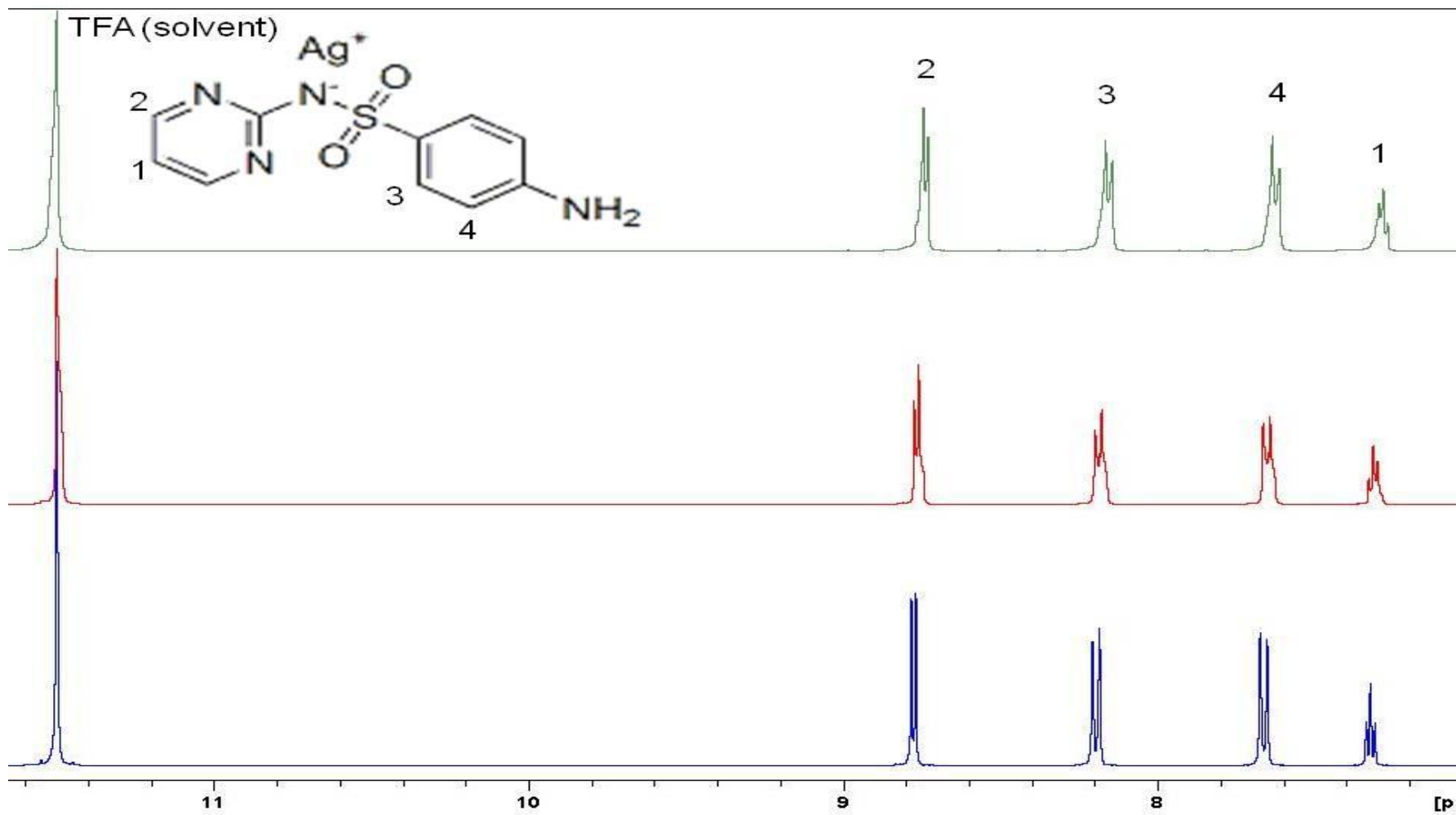


Figure 5.6 Plots of natural logarithm (\ln) of shear stress (σ) as a function of \ln shear rate ($\dot{\gamma}$) for pre-lyophilised gels prepared from non-irradiated and irradiated (25 kGy and 40 kGy) polymers. (a) 2 % w/v GG, (b) 3 % KAG w/v, (c) 5 % w/v SA, (d) 1.5 % w/v XG and (e) SA-KAG (1:1 ratio). (Note the major decrease in viscosity for irradiated samples of GG, KAG, SA and SA-KAG, but not for XG).

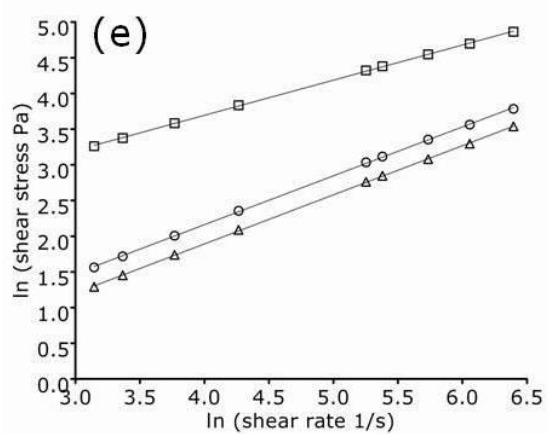
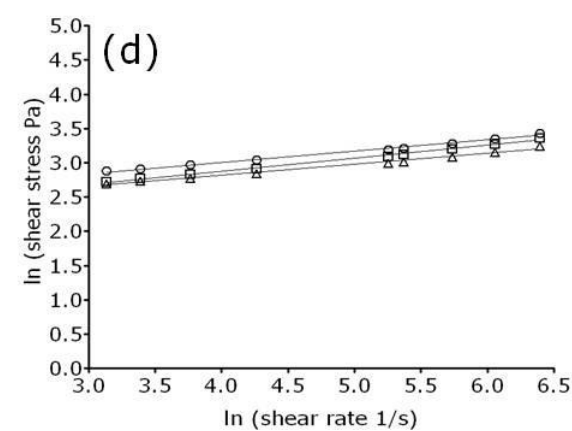
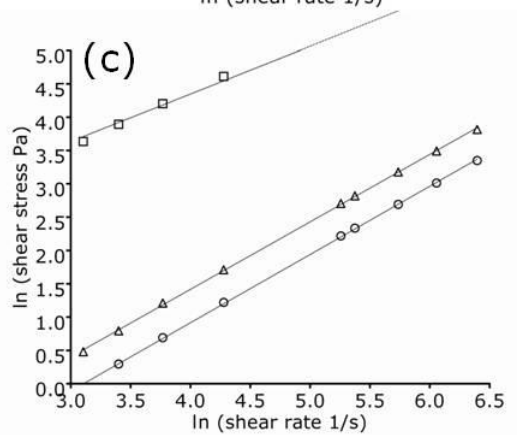
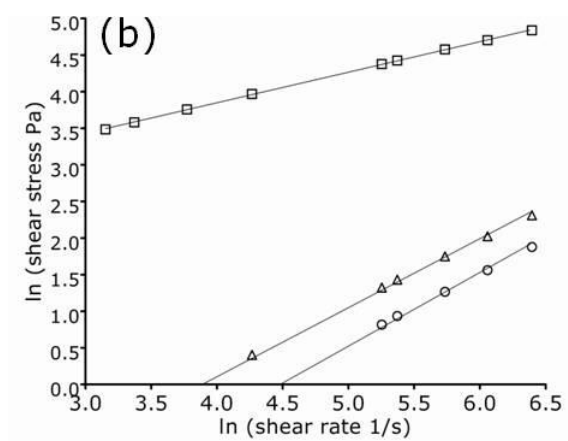
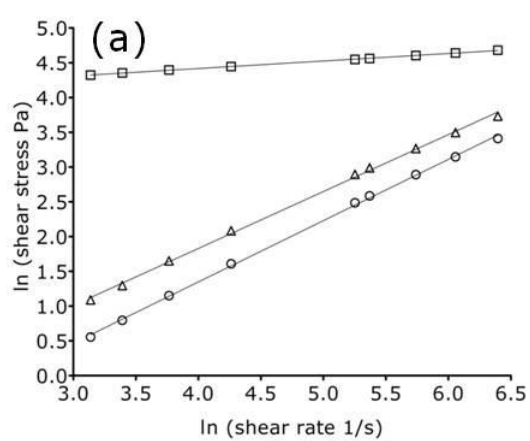


Table 5.5 Viscosity coefficients and yield stresses of pre-lyophilised gels prepared with irradiated (25 kGy and 40 kGy) and non-irradiated polymers, as analysed with the Herschel-Bulkley model (n=3, SEM).

Raw polymers	Non irradiated	Irradiated doses	
	η' (σ_0)	η' (σ_0)	
	0 kGy	25 kGy	40 kGy
2 % w/v GG	82.21± 5.41 (95.87 ± 2.31)	0.49 ± 0.17 (0.00 ± 0.00)	0.22 ± 0.01 (0.00 ± 0.00)
1.5 % w/v XG	2.86 ± 0.12 (23.61 ± 0.68)	1.40 ± 0.06 (19.96 ± 0.33)	2.50 ± 0.32 (22.16 ± 3.41)
5.0 % w/v SA	18.17 ± 0.70 (0.00 ± 0.00)	0.09 ± 0.01 (0.00 ± 0.00)	0.05 ± 0.01 (0.00 ± 0.00)
3.0 % w/v KAG	12.89 ± 0.93 (0.00 ± 0.00)	0.06 ± 0.01 (0.00 ± 0.00)	0.02 ± 0.00 (0.00 ± 0.00)
SA-KAG (1:1)	7.75 ± 0.64 (86.34 ± 5.19)	0.48 ± 0.03 (0.00 ± 0.00)	0.74 ± 0.10 (0.00 ± 0.00)

Figure 5.7 Plots of natural logarithm (\ln) of shear stress (σ) as a function of \ln shear rate ($\dot{\gamma}$) of post-lyophilised 3 % w/v KAG gels containing different antimicrobials, non-irradiated and irradiated (25 kGy and 40 kGy). (a) 3 % w/v KAG (control antimicrobial free), (b) 0.5 % w/v NS, (c) 0.5 % v/v CHD, (d) 1.0 % v/v PVP-I, (e) 1.0 % w/v SS and (f) 0.2 % w/v Pluronic F68. (Note the different degrees of degradation for antimicrobial gels, in particular impregnated with CHD and PVP-I, compared to antimicrobial free matrix of KAG).

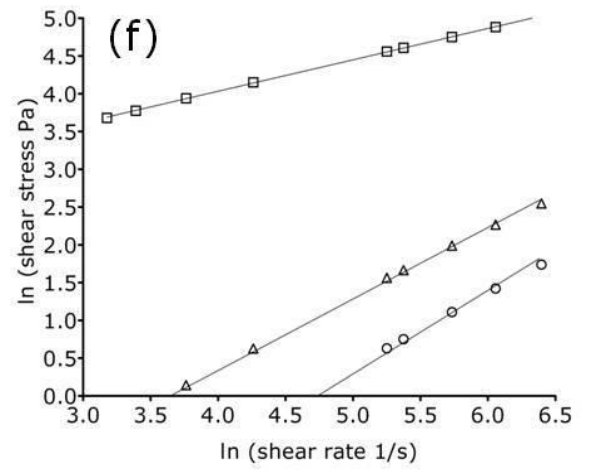
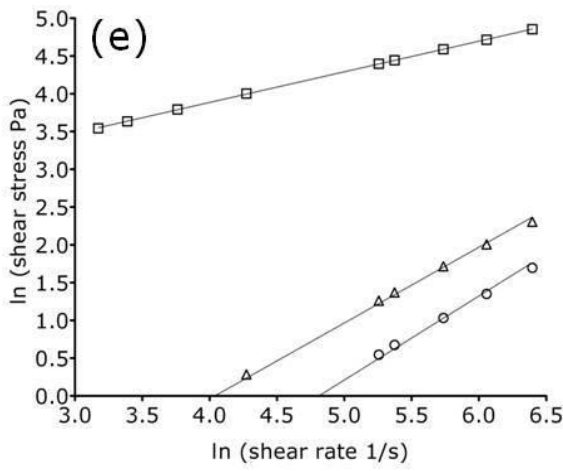
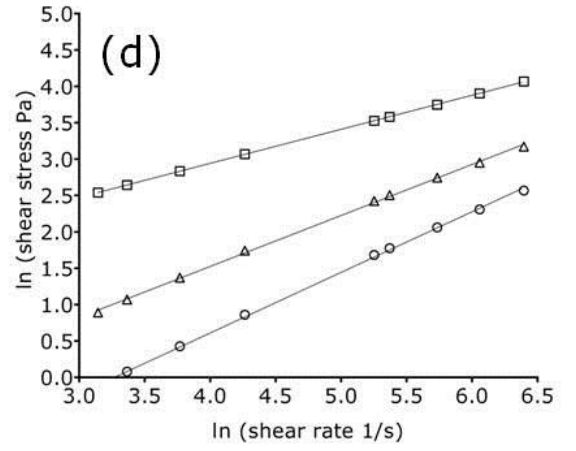
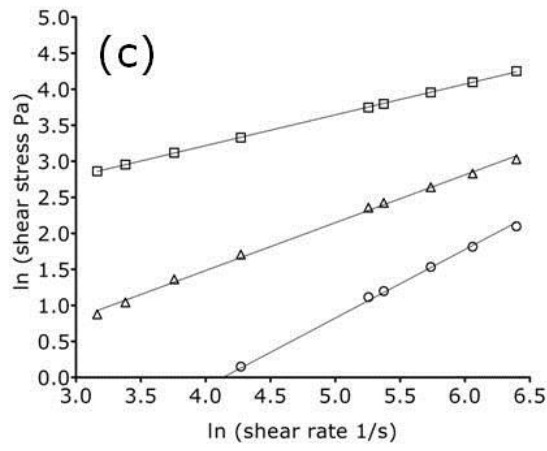
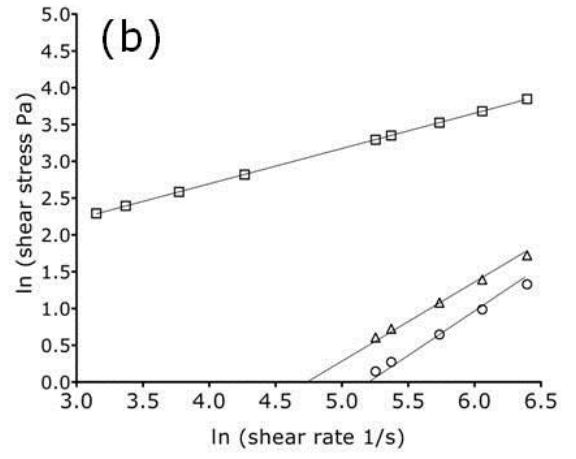
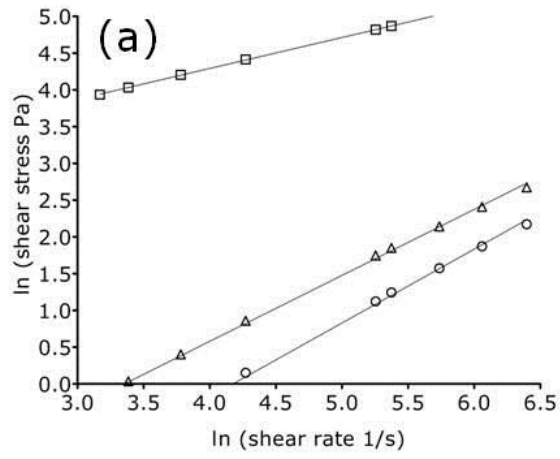


Table 5.6 Viscosity coefficient (η') of KAG pre-lyophilised antimicrobial gels and reconstituted post-lyophilised wafers irradiated and/or non-irradiated, as analysed with the Herschel-Bulkley model (n=3, SEM).

3.0 % w/v KAG wafers	Non-irradiated		Irradiated wafers	
	Pre-lyophilised gels	Post-lyophilised gels	25 kGy	40 kGy
KAG	12.89 ± 0.93	15.26 ± 1.81	0.09 ± 0.01	0.03 ± 0.00
NS	1.56 ± 0.10	2.19 ± 0.94	0.01 ± 0.00	0.01 ± 0.00
CHD	3.79 ± 0.30	3.71 ± 1.53	0.72 ± 0.13	0.04 ± 0.02
PVP-I	4.09 ± 0.34	2.82 ± 0.15	0.50 ± 0.05	0.10 ± 0.03
SS	6.48 ± 0.33	11.36 ± 0.44	0.04 ± 0.00	0.01 ± 0.00
F68	7.40 ± 0.55	17.80 ± 2.61	0.07 ± 0.01	0.02 ± 0.00

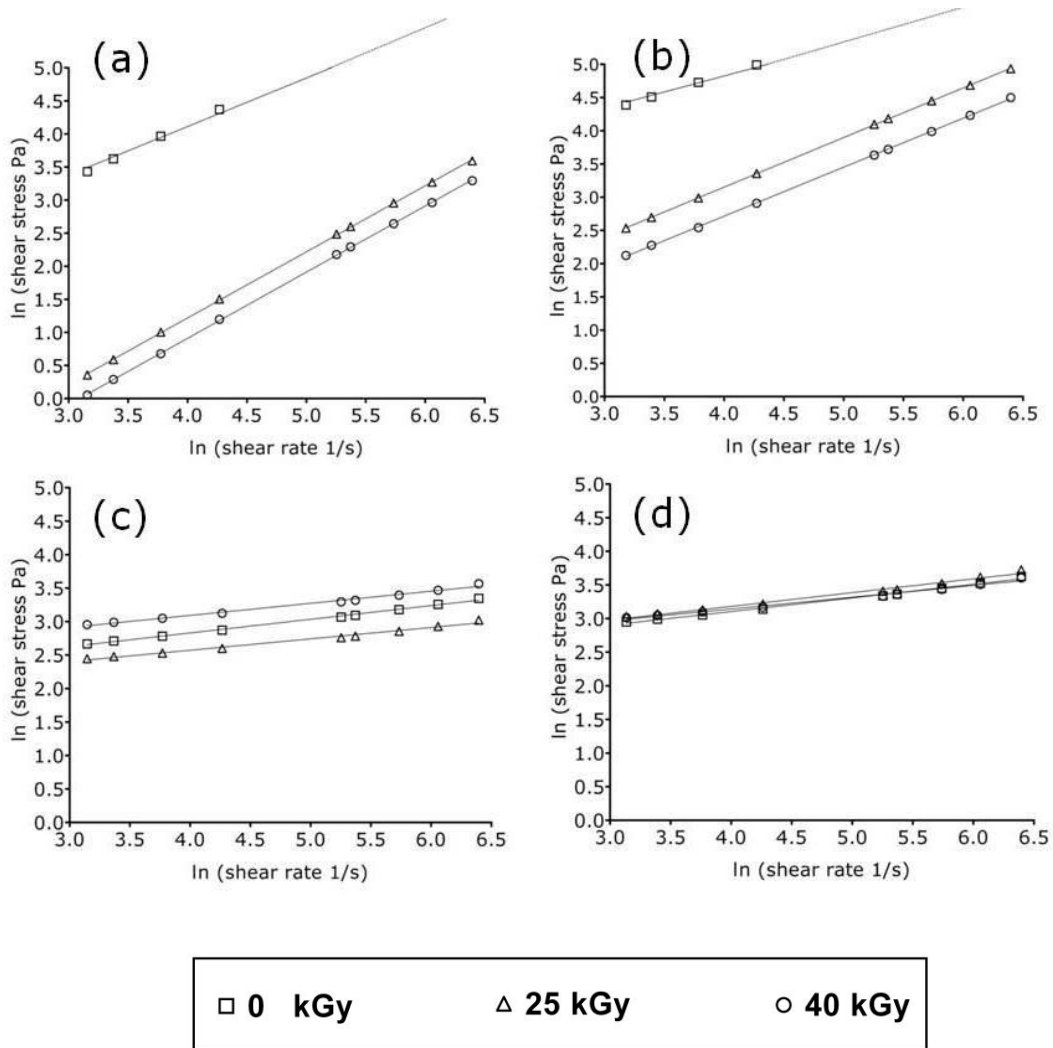


Figure 5.8 Plots of natural logarithm (\ln) of shear stress (σ) as a function of \ln shear rate (γ) for post-lyophilised gels (non-irradiated and/or irradiated with 25.0 kGy \pm 10 % and 40.0 kGy \pm 10 %): (a) 5 % w/v SA (CHD-free), (b) 5 % w/v SA-CHD, (c) 1.5 % w/v XG (CHD-free) and (d) 1.5 % w/v XG-CHD.

Table 5.7 Rheological properties, viscosity coefficient (η') and yield stress (σ_0) of reconstituted, post-lyophilised irradiated (25 kGy and 40 kGy) and non-irradiated antimicrobial-free wafers, prepared from different biopolymers, as analysed using the Herschel-Bulkley model (n=3, SEM). (Post-lyophilised non-irradiated samples of GG did not produce a homogenous gel, rendering rheological measurements infeasible).

Control wafers	Non irradiated	Irradiated doses	
	η' (σ_0)	η' (σ_0)	η' (σ_0)
	0 kGy	25 kGy	40 kGy
2.0 % w/v GG	- -	0.18 ± 0.03 (0.00 ± 0.00)	0.05 ± 0.01 (0.00 ± 0.00)
1.5 % w/v XG	2.42 ± 0.32 (20.58 ± 1.25)	1.23 ± 0.29 (15.94 ± 0.27)	1.82 ± 0.42 (22.67 ± 4.36)
5.0 % w/v SA	10.95 ± 1.73 (0.00 ± 0.00)	0.083 ± 0.026 (0.00 ± 0.00)	0.06 ± 0.01 (0.00 ± 0.00)
SA-KAG (1:1)	12.69 ± 0.34 (148.9 ± 4.33)	0.49 ± 0.03 (0.00 ± 0.00)	0.24 ± 0.03 (0.00 ± 0.00)

Table 5.8 Rheological properties, viscosity coefficient (η') and yield stress (σ_0) of post-lyophilised irradiated (25 kGy and 40 kGy) and non-irradiated 0.5 % v/v CHD antimicrobial gels, prepared from different biopolymers, as analysed with the Herschel-Bulkley model ($n=3$, SEM). (Post-lyophilised non-irradiated samples of GG did not produce a homogenous gel, rendering rheological measurements infeasible).

CHD (0.5 % v/v) antimicrobial wafers	Non irradiated	Irradiated doses	
	η' (σ_0)	η' (σ_0)	
	0 kGy	25 kGy	40 kGy
2.0 % w/v GG	- -	0.18 ± 0.03 (0.00 ± 0.00)	0.04 ± 0.01 (0.00 ± 0.00)
1.5 % w/v XG	2.46 ± 0.192 (26.5 ± 1.41)	1.66 ± 0.41 (34.25 ± 4.59)	1.50 ± 0.08 (26.51 ± 2.97)
5.0 % w/v SA	44.03 ± 9.72 (0.00 ± 0.00)	0.95 ± 0.35 (0.00 ± 0.00)	0.52 ± 0.01 (0.00 ± 0.00)
SA-KAG (1:1)	10.34 ± 0.59 (170.41 ± 7.76)	2.09 ± 0.36 (0.00 ± 0.00)	0.61 ± 0.03 (0.00 ± 0.00)

Figure 5.9 Expansion and inhibition ratios of irradiated (25 ± 10 kGy and 40 ± 10 kGy) KAG antimicrobial wafers tested with a modified disc diffusion assay against common bacterial strains of infected, non-healing wounds. (n=3 SEM)

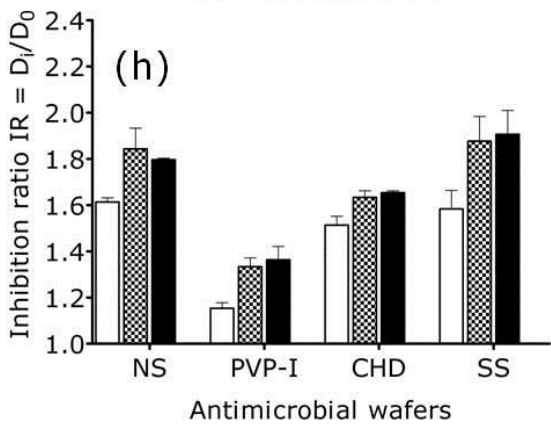
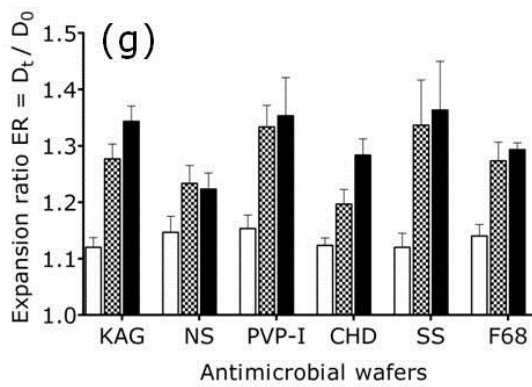
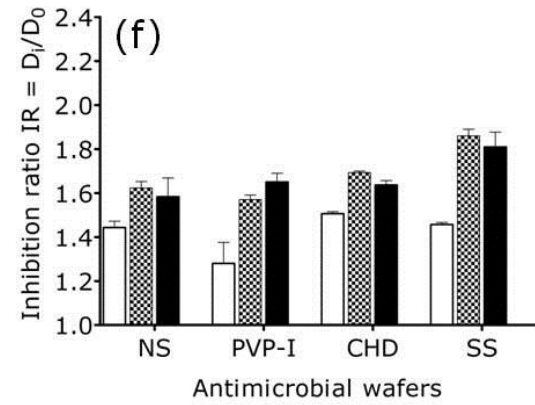
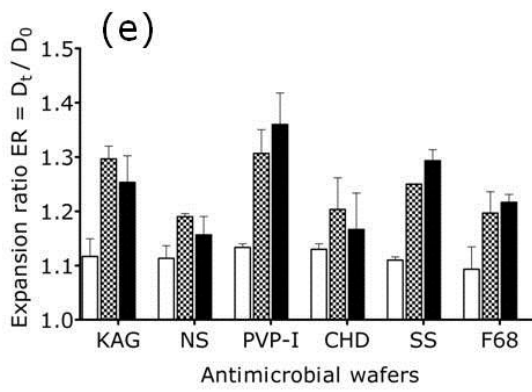
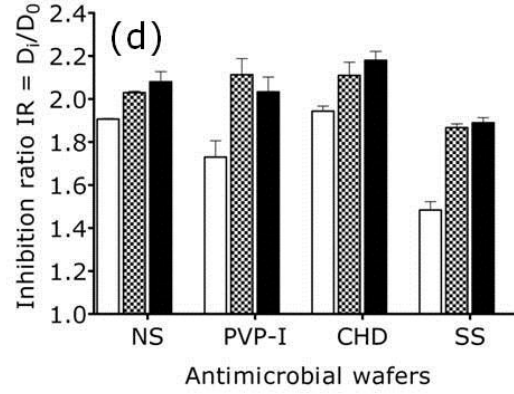
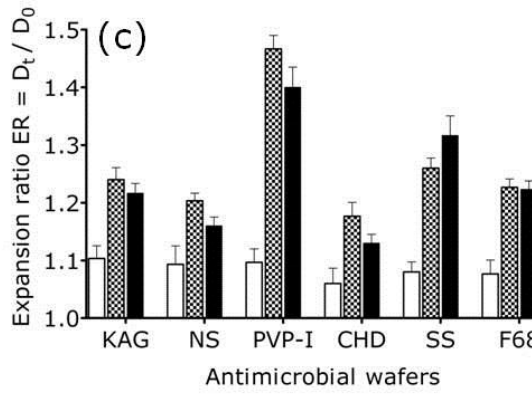
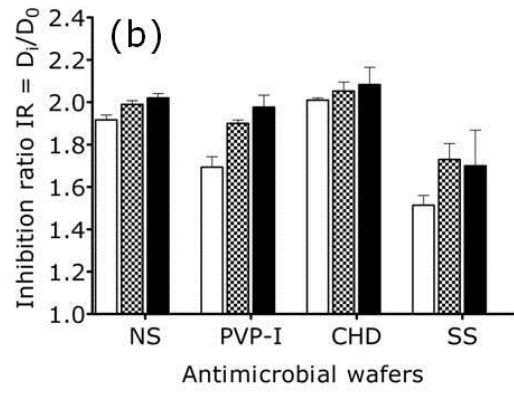
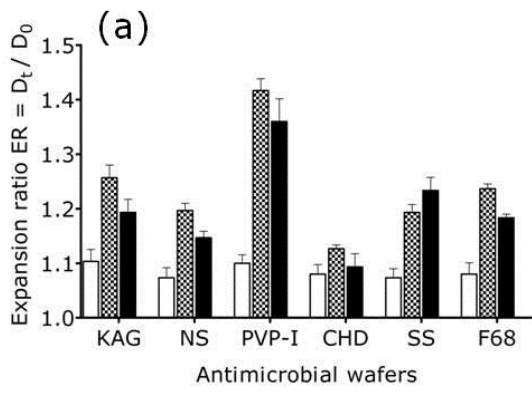
(a), (b) Expansion and inhibition ratio of KAG wafers tested against MRSA

(c), (d) Expansion and inhibition ratio of KAG wafers tested against MSSA

(e), (f) Expansion and inhibition ratio of KAG wafers tested against *E. coli*

(g), (h) Expansion and inhibition ratio of KAG wafers tested against *P. aeruginosa*

(KAG and pluronic F68 control wafers did not demonstrated inhibition zones)



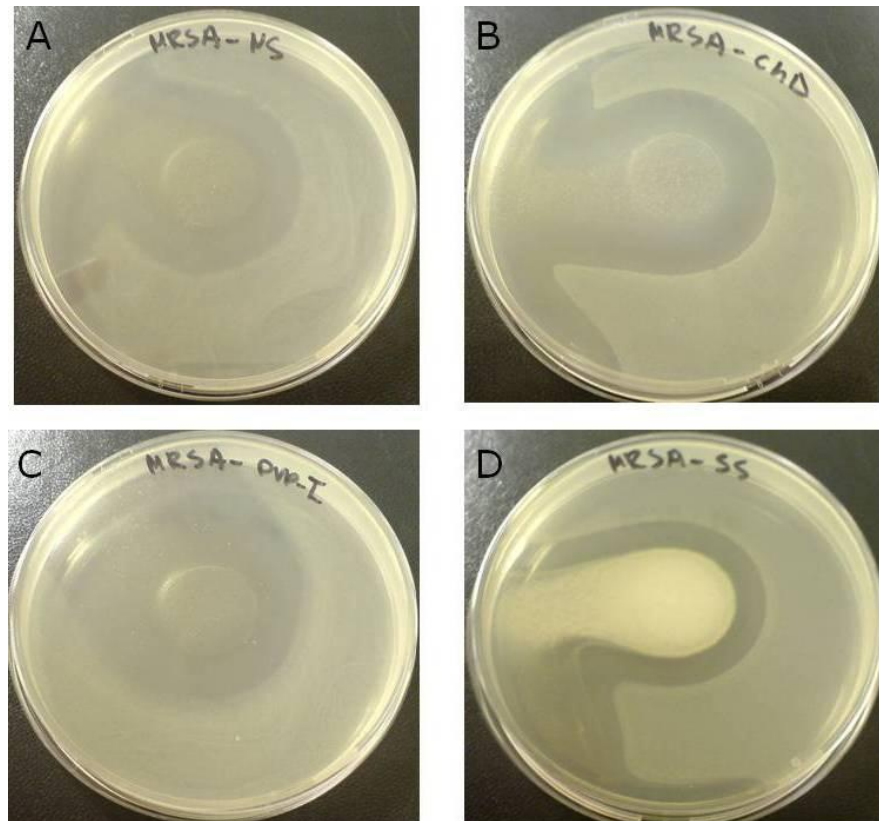


Figure 5.10 Images of irradiated KAG wafers impregnated with clinical concentrations of broad spectrum antimicrobials, tested against MRSA in the modified disc diffusion assay, after 24 hours incubation at 37 °C. **A**-KAG impregnated with 0.5 % w/v NS, **B**-KAG impregnated with 0.5 % v/v CHD, **C**-KAG impregnated with 1.0 % v/v PVP-I and **D**-KAG impregnated with 1.0 % w/v SS. Note the white residue visible in the case of KAG wafers impregnated with CHD (Image B), which was visible for all irradiated CHD impregnated wafers.

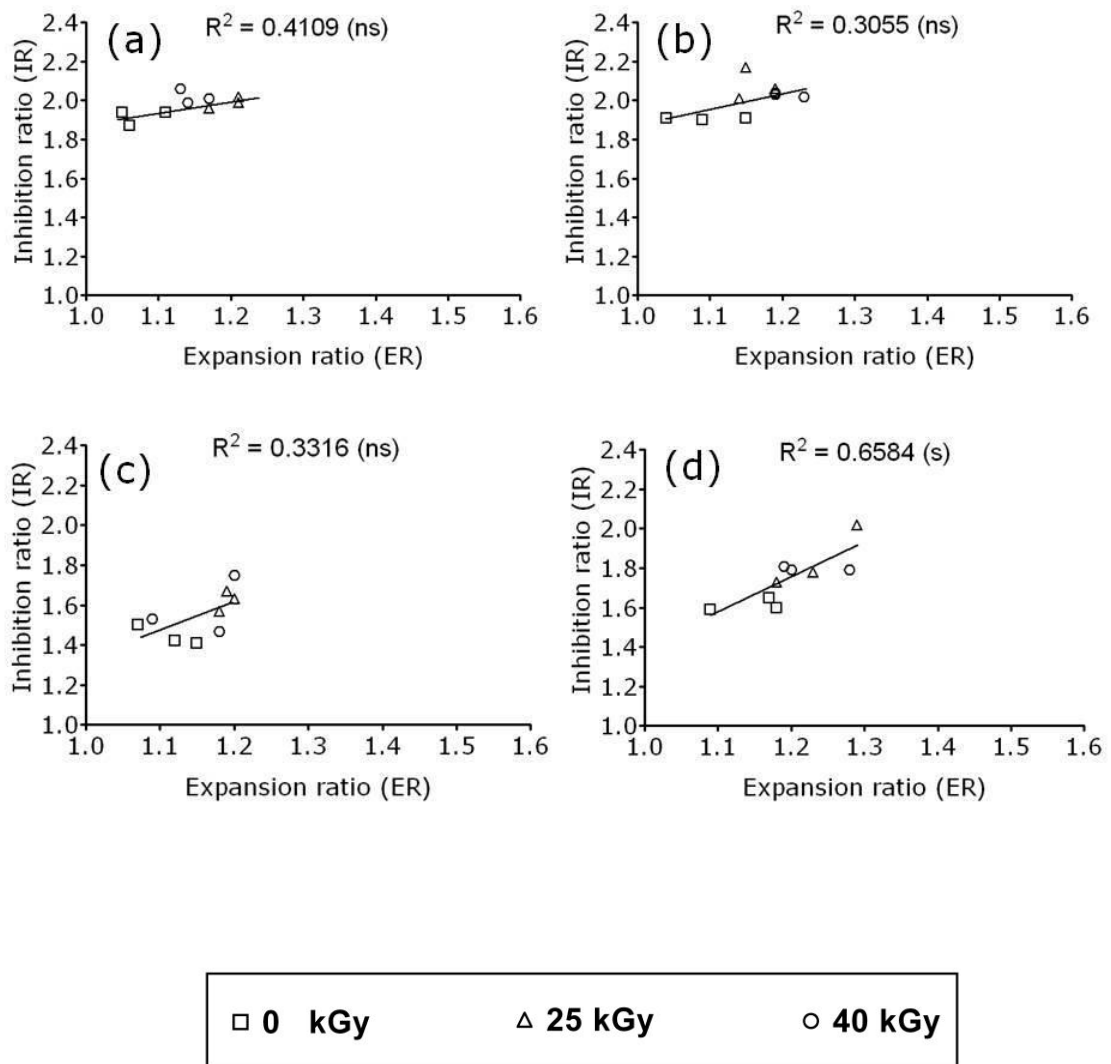


Figure 5.11 Linear regression analysis of inhibition ratio (IR) vs. expansion ratio (ER) of KAG wafers containing (0.5 % w/v) of NS, irradiated at 25.0 kGy and 40.0 kGy \pm 10 %. (a) MRSA, (b) MSSA, (c) *E. coli* and (d) *P. aeruginosa*. (ns)- non significant correlation, (s)- significant correlation

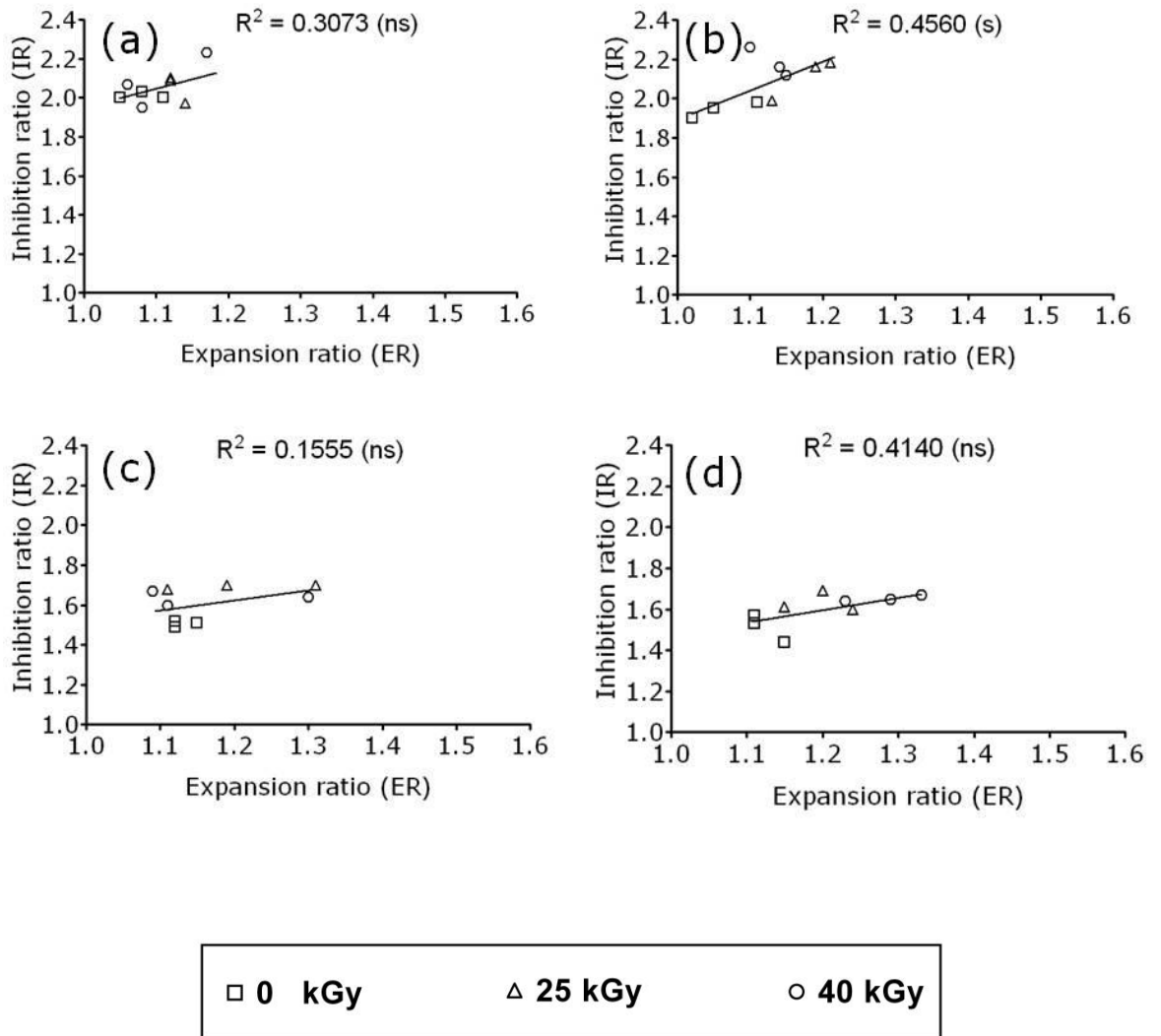


Figure 5.12 Linear regression analysis of inhibition ratio (IR) vs. expansion ratio (ER) of KAG wafers containing (0.5 % v/v) of CHD, irradiated at 25.0 kGy and 40.0 kGy ± 10 %. (a) MRSA, (b) MSSA, (c) *E. coli* and (d) *P. aeruginosa*. (ns)- non significant correlation, (s)- significant correlation

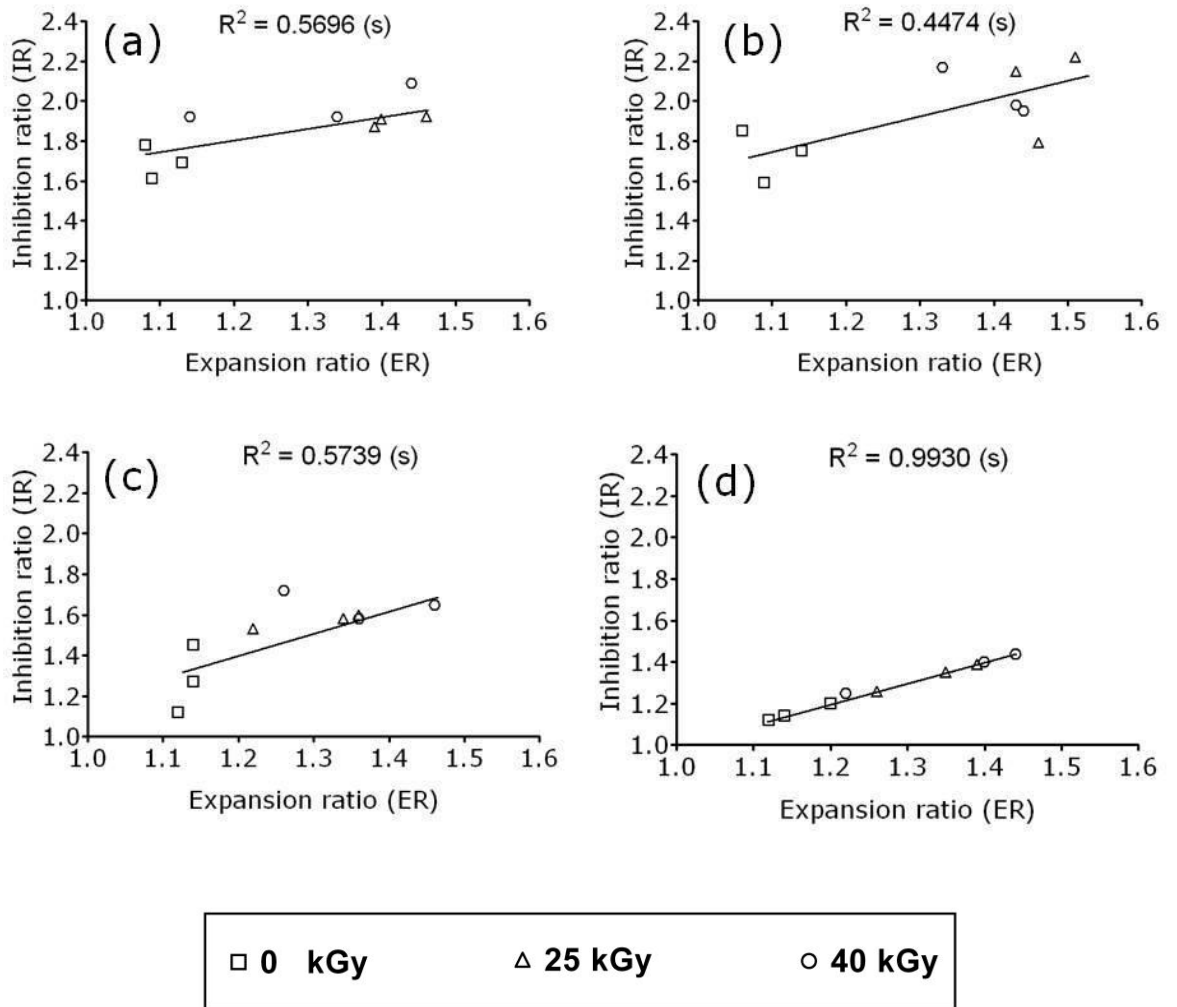


Figure 5.13 Linear regression analysis of inhibition ratio (IR) vs. expansion ratio (ER) of KAG wafers containing (1.0 % v/v) of PVP-I, irradiated at 25.0 kGy and 40.0 kGy \pm 10 %. (a) MRSA, (b) MSSA, (c) *E. coli* and (d) *P. aeruginosa*.

(ns)- non significant correlation, (s)- significant correlation

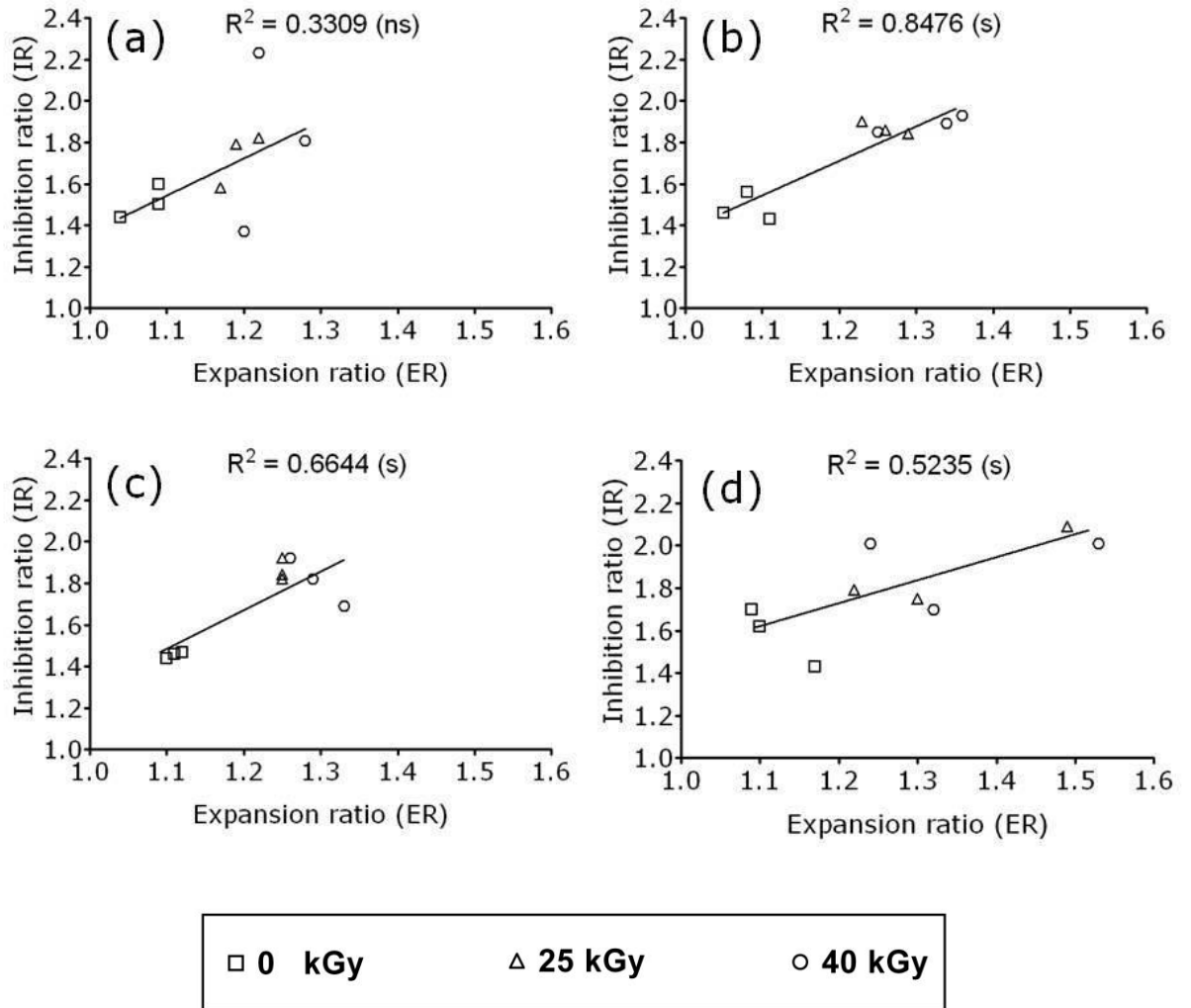


Figure 5.14 Linear regression analysis of inhibition ratio (IR) vs. expansion ratio (ER) of KAG wafers containing (1.0 % w/v) of SS, irradiated at 25.0 kGy and 40.0 kGy \pm 10 %. (a) MRSA, (b) MSSA, (c) *E. coli* and (d) *P. aeruginosa*. (ns)- non significant correlation, (s)- significant correlation

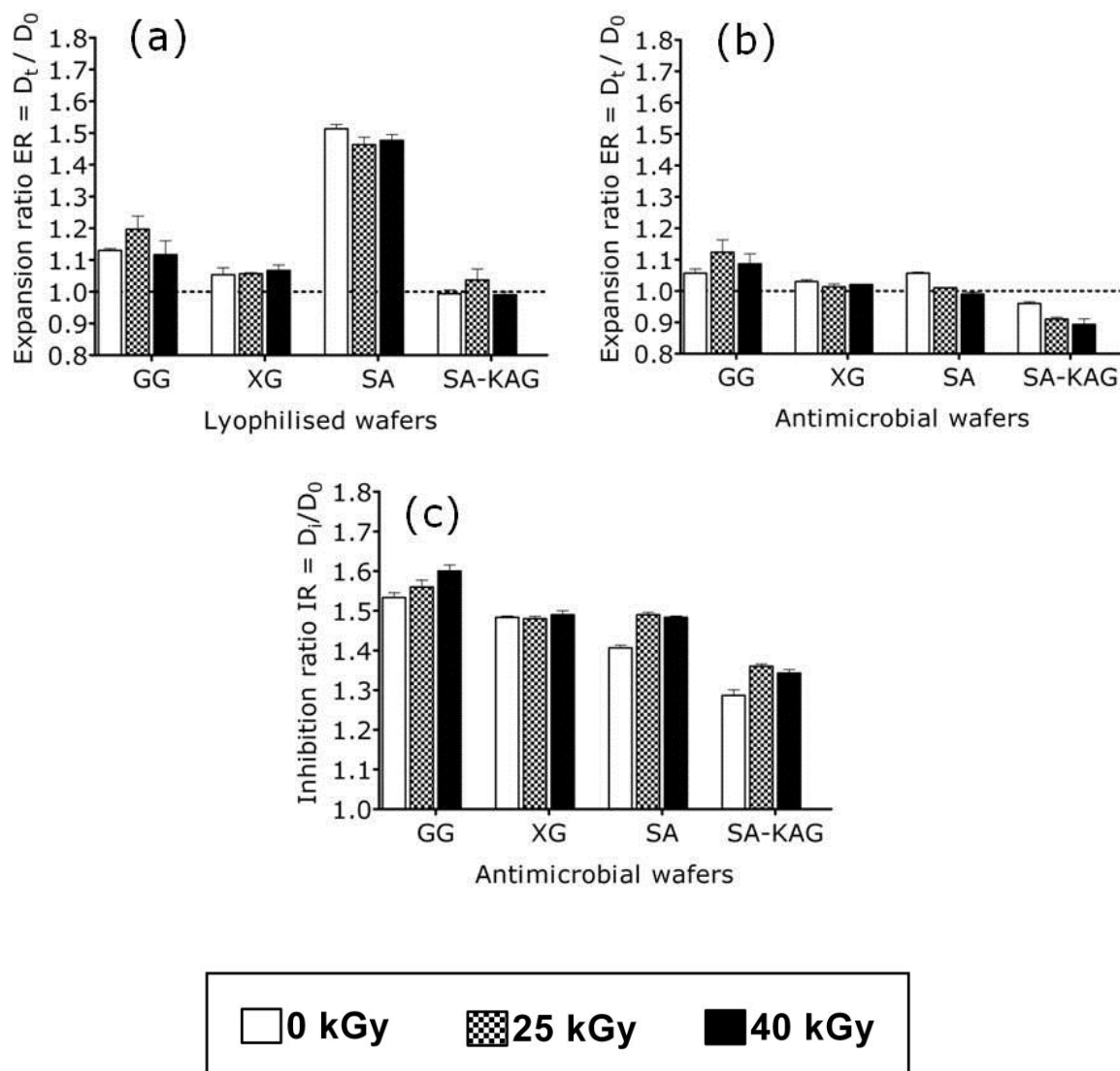


Figure 5.15 Expansion and inhibition ratios of irradiated (25.0 kGy \pm 10 % and/or 40.0 kGy \pm 10 %) wafers prepared with a clinical concentration of CHD (0.5 % v/v) incorporated within different biopolymer matrices, tested in a modified disc diffusion assay against *P. aeruginosa* (n =3, SEM).
 (a) Expansion ratio of controls (CHD-free) lyophilised wafers,
 (b) Expansion ratio of CHD-loaded lyophilised wafers and
 (c) Inhibition ratio of CHD-loaded wafers.

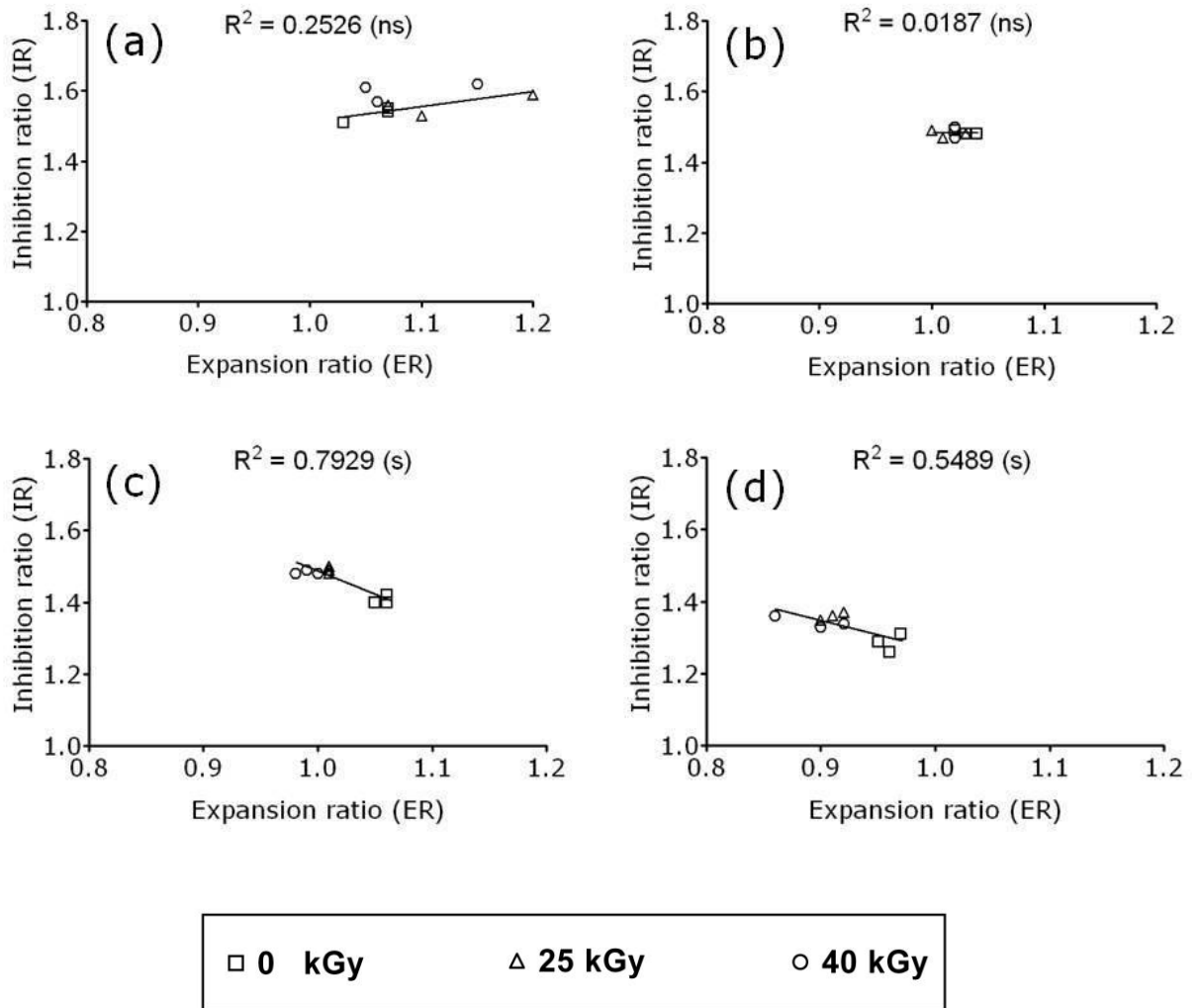


Figure 5.16 Linear regression analysis of inhibition ratio (IR) vs. expansion ratio (ER) of CHD wafers (irradiated and non-irradiated) prepared with different biopolymers, when tested against *P. aeruginosa* on modified disc diffusion assay. (a) GG-CHD, (b) XG-CHD, (c) SA-CHD and (d) SA-KAG-CHD. (ns) – not significant correlation, (s) – significant correlation

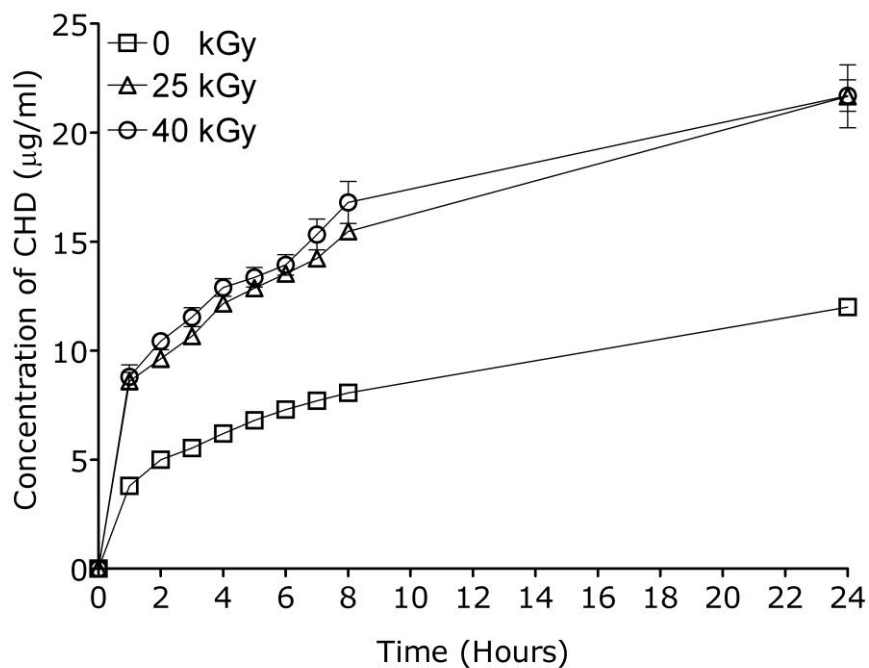


Figure 5.17 Release profiles of SA wafers (irradiated and non-irradiated) impregnated with a clinical concentration of CHD (0.5 % v/v) in NaCl-CaCl₂ dissolution medium (n=3, SEM).

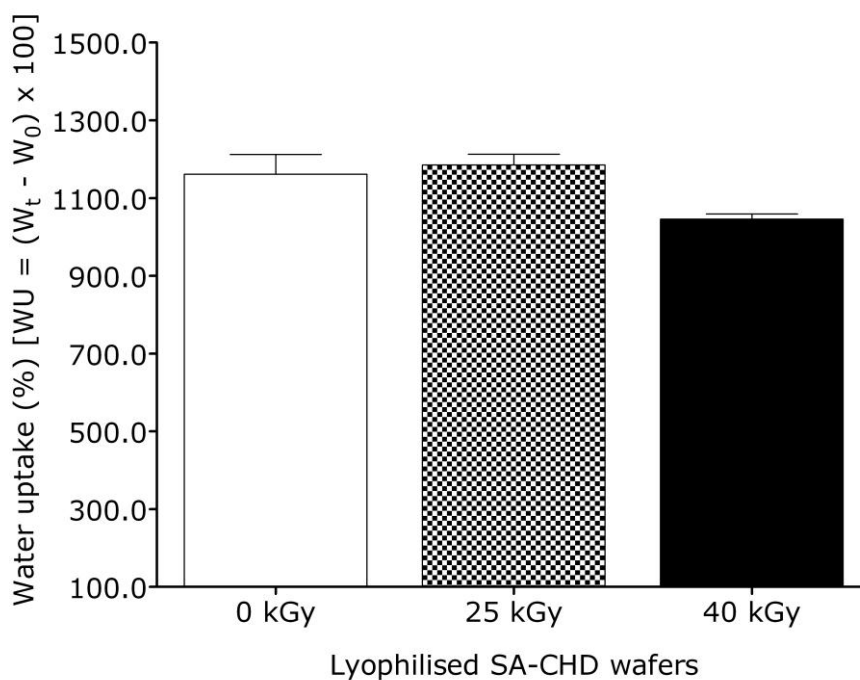


Figure 5.18 Water uptake (%) of rehydrated SA-CHD wafers (irradiated and non-irradiated) at 24 hours, placed on the FSDR (n=3, SEM).

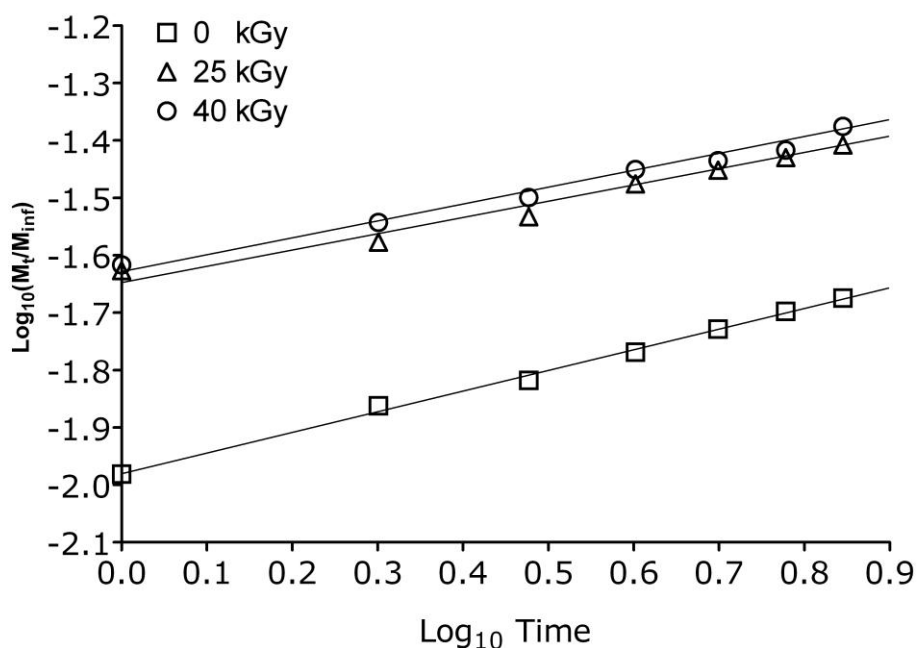


Figure 5.19 Linear regressions of CHD released from irradiated and non-irradiated SA-CHD matrices in NaCl-CaCl₂, as analysed with the Korsmeyer-Peppas model.

Table 5.9 Accumulation of CHD (%) in NaCl-CaCl₂ dissolution medium as released from SA-CHD wafers, impregnated with a clinical concentration of CHD (0.5 % v/v) at 24 hours. Values of the release exponent (n) and the correlation coefficient (R²) of CHD released from irradiated and non-irradiated wafers. All wafers demonstrated Fickian (F) diffusion.

Gamma-Irradiated polymeric wafers of SA-CHD (w/v)	Accumulation of CHD (%) in NaCl-CaCl₂ (pH = 6.5)	Release exponent (n) Correlation coefficient (R²)
0 kGy	3.5 ± 0.04	0.36 ^F (0.9974)
25 kGy	6.2 ± 0.41	0.28 ^F (0.9721)
40 kGy	6.3 ± 0.21	0.29 ^F (0.9746)

5.6 Discussion

Gamma-rays are high energy electromagnetic waves emitted from a radionuclide source such as Cobalt-60 or Cesium-137. They are used commercially to sterilise medical polymers and are attractive for their ability to penetrate packing and destroy endotoxins. Sterilisation by gamma-irradiation involves stable temperatures and easy validation. However, one major limitation of gamma-irradiation is the formation of radiolytic products that usually lead to degradation, alteration in colour and odour for some materials.

The presence of water molecules in the gamma-irradiated material is associated with the production of H_3O^+ and OH^- radicals. According to Zagorski (2004) "radiolytic products of water can be considered as reagents towards added solutes, because in the case of diluted solutions radiation interacts practically with water only, not with solutes". It has been reported that hydroxyl radicals are the main water radiolysis species which interact with polymers and lead to the formation of intermediate reactive compounds. Free radicals, if favourably positioned, can react with each other and form new cross links between separated polymer chains (Rosiak et al. 1995). If not, the final product of irradiated macromolecules will be degraded polymer chains, which is associated with decreased molecular weight. Hydroxyl radicals cause irreversible DNA damage due to a strong oxidant effect and it is this effect that destroys viable bioburden (Silindir and Ozer 2009). Generally doses of 25 - 35 kGy are sufficient to achieve a sterility assurance level (SAL) of 10^{-6} (6-log powers reduction of microbial population) and simultaneously these irradiation doses ensure that either cross-linking or degradation of irradiated polymeric materials will dominate (Baloda et al. 2008; Rosiak et al. 1995).

The validation process for gamma-irradiated products is important as both the level of sterility (absence of viable microorganisms) and the integrity of the final irradiated product are ensured. Microbiological validation of irradiated biopolymers in these studies was performed on TSA and SDA media for the detection of contamination by bacterial and fungal populations, respectively (Table 5.1). It is apparent that the irradiation doses of 25.0 kGy \pm 10 % and 40.0 kGy \pm 10 % were sufficient for elimination of microbial flora present in the polymeric powders of GG and XG. Interestingly, non-irradiated samples of KAG and SA powders did not promote the growth of

microorganisms. This result is likely associated with the pH values of KAG and SA gels. It has been reported that KAG has a high uronic acid content which generates a low pH (4.4 – 4.7) when dispersed in water (Verbeken et al. 2003). This range was verified with pH measurements undertaken in a 3.0 % w/v gel of the KAG batch used in this project (Table 2.1, Chapter 2). The gel of the sodium salt of a low viscosity grade alginic acid, prepared in distilled water (as previously described in Chapter 2, Section 2.5, Table 2.1) generated a slightly basic pH (8.3), which does not present a desirable environment for the growth of microorganisms. A neutral nutritional environment (pH 7.2 ± 0.2) is considered a favourable environment for the growth of the majority of bacterial and fungal species. In addition, it has been reported that polymers of SA and KAG were found to reduce the adhesion of *Streptococcus salivarius* by 98.7 % and 97.9 % respectively (Wilson and Harvey 1989), indicating that the polymeric habitat of either SA or KAG does not present a favourable niche for several bacterial species.

Irradiated wafers maintained their initial cylindrical shape. Microbiological validation of the sterility of non-medicated wafers demonstrated that there was no growth of microorganisms (Table 5.2). Non-irradiated antimicrobial free wafers of KAG, SA, GG and SA-KAG did not present growth of either bacterial or fungal populations. It was apparent that non-irradiated samples of KAG and SA did not demonstrate growth of microorganisms (bacterial and/or fungi) either as raw material or lyophilised wafers. Non-irradiated samples of XG, raw powder and lyophilised wafers, promoted the growth of both bacteria and fungal species. Non-irradiated samples of raw GG showed bacterial contamination, but non-medicated lyophilised wafers of 2 % (w/v) GG did not support the growth of bacterial populations.

Lyophilisation is a common method used to preserve and store collections of microbial cultures; however the freezing rate, storage conditions and moisture content of the lyophilised product can affect the viability of microorganisms. Although the majority of bacteria, yeast and spore-forming fungi can resist the detrimental effect of freezing, the survival rates of lyophilised microorganisms depend on the species and density (Miyamoto-Shinohara et al. 2010; Miyamoto-Shinohara et al. 2008). For example, it has been reported that freeze-dried Gram-positive bacteria demonstrate better

survival rates than Gram-negative strains, due to a thicker cell wall peptidoglycan layer (Miyamoto-Shinohara et al. 2008). All wafers were produced and stored under the same conditions. However, the lack of information about the type and amount of bacterial contaminants present in raw polymers can only lead to speculation with regards to the absence of bacterial contamination of non-irradiated GG wafers. In addition, further investigations are required to examine the effect of considerable amounts of residual water (15 - 20 %) present in lyophilised wafers upon the viability of different bacterial and fungal species.

Microbiological validation of irradiated antimicrobial wafers was undertaken under the same nutritional media and growth conditions (Table 5.3 and 5.4). As expected, there was no growth of microorganisms apparent for irradiated and non-irradiated antimicrobial wafers. The non-irradiated, control wafer containing 0.2 % (w/v) pluronic F68 demonstrated bacterial growth. This is probably associated with bacterial contaminants present in the powder of the non-ionic surfactant, as the raw KAG powder did not present either bacterial or fungal contamination.

Potential changes to the chemical configuration of antimicrobial compounds were assessed with NMR spectroscopy (^1H and/or ^{13}C) as presented in Figures 5.2, 5.4 and 5.5. Irradiated samples of antimicrobials as received were compared to non-irradiated ones. Nuclear configuration of CHD, NS and SS demonstrated that there did not appear to be major structural differences between irradiated samples and non irradiated ones. These results generally suggest that the structural integrity of selected antimicrobial compounds remained unaffected by gamma-irradiation and antimicrobial agents potentially still possess their initial antimicrobial properties.

Previous studies conducted on antimicrobial activity of gamma irradiated (25.0 kGy) common antibiotics that included neomycin sulphate (NS) (Muszynski et al. 2002), revealed that there was a minimal increase of the MIC value for the irradiated antibiotics, the authors concluding that the antimicrobial activity of NS was generally preserved by 96.26 %. (Muszynski et al. 2002). ^{13}C NMR and UV spectrophotometry were essentially inconclusive as to whether there had been any degradation of CHD following gamma-irradiation. The NMR spectra (Figure 5.2) appeared to be the same for irradiated and non-irradiated CHD as no notable shifts in the main resonance

signals were apparent. However, the spectra were very noisy and the appearance of weak resonances due to degradation products may be lost in the background. The UV spectra (Figure 5.3) indicated a slight decrease in the absorbance intensity at the same concentration of both irradiated CHD samples compared with the non-irradiated CHD samples.

It is difficult to conclude if the energy uptake from gamma-rays does or does not influence the antimicrobial activity of such compounds. It has been reported that irradiated, coated-catheters containing small quantities of chlorhexidine, were found less efficacious at preventing bacterial contamination in patients in intensive care units when compared to pre-sterilised chlorhexidine-coated catheters (Sherertz et al. 1996). The latter authors suggested that gamma-rays were likely to have a negative effect on the antimicrobial properties of CHD; however additional experimental studies were required in order to clarify the potential effect of irradiation on the antimicrobial activity of CHD.

Figure 5.4 is the ^{13}C NMR spectra of irradiated and non-irradiated NS. Although of better signal quality than CHD, it is still uncertain if any changes to the chemical configuration of NS have occurred. However, at a glance, it may be safe to conclude that no major changes were apparent.

NMR analysis of SS demonstrated that the structural integrity of this compound remained unaffected by gamma-ray treatment and potentially, the antimicrobial activity of SS is not considerably altered by gamma-irradiation. Reference to Figure 5.5 indicates the downfield regions of the ^1H NMR spectra of irradiated and non-irradiated SS in TFA-d. All the aromatic protons are clearly distinguishable and numbered 1 - 4 (see chemical structure). Assignment of these resonances was possible from the HSQC ^{13}C - ^1H heteronuclear spectrum positioned above [Figure 5.5 (a)]. The ^{13}C NMR component of this HSQC spectrum has three unassigned carbon atoms (not numbered in figure).

Nho *et al.* (2009) have recently reported that cross-linked hydrogels of PVA/PVP/glycerin/antimicrobial, cross-linked by gamma-rays (25.0 kGy), containing 1.0 % silver sulfadiazine (SS) demonstrated slightly decreased antimicrobial activity compared to non-irradiated samples. The latter authors concluded that gamma-rays had a minor effect on the antimicrobial properties

of cross-linked hydrogels impregnated with either silver salts or sodium sulfadiazine.

Although the effect of gamma-rays on the antimicrobial properties of antimicrobial compounds remains ambiguous, it is well known that the absorbance of gamma-irradiation by polymeric materials will instantly lead to chain scission and cross-linking. Both reactions happen simultaneously within the polymeric bulk; however one will usually predominate and result in either degradation or inter-connection of adjacent polymeric chains. Configurational and conformational changes in gamma-irradiated polymer will alter the network structure and affect both swelling and rheological properties. Rheological measurements of irradiated polymers are therefore an essential and reliable gauge of the net effect of ionising radiation on the flow properties of biopolymeric materials.

Rheological analysis of pre-lyophilised irradiated gels was undertaken and compared with pre-lyophilised gels, as presented in Figure 5.6 and Table 5.5. It is apparent that irradiation doses of $25.0 \text{ kGy} \pm 10 \%$ and $40.0 \text{ kGy} \pm 10 \%$ decreased considerably the viscosity of GG, KAG, SA and the binary mixture of SA-KAG. The higher the irradiative dose the greater the reduction in viscosity. The viscosity of XG, however, was not considerably affected. These data suggest that chain scission and degradation dominated within the bulk of GG, KAG and SA which was associated with a dramatic decrease in consistency and yield stress of irradiated biopolymers, while cross-linking reactions were dominant for XG, which was manifest as a slight increase in yield stress. It was evident that pre-lyophilised irradiated gels of GG, KAG and SA, lost their initial ability to form a strong gel network, as samples demonstrated generally Newtonian flow. These results are in agreement with King and Gray (1993), who have reported the degradation of GG and KAG irradiated with a range of gamma-rays $< 10 \text{ kGy}$. Lee *et al.* (2003) have also reported that the effect of increased doses of irradiation on alginate polymers is associated with increased degradation and decreased values of viscosity. In addition, degradation of sodium alginate was enhanced in irradiated polymeric solutions and there was also an associated colour change compared to irradiated samples in the solid state (Sen *et al.* 2010; Nagasawa *et al.* 2000), indicating that the presence of water enhances the degradation effects of gamma-rays upon sodium alginate.

Although the binary mixture of SA-KAG prepared with samples of pre-lyophilised irradiated gels of SA and KAG displayed a notable decrease in consistency (Figure 5.6-e), it is apparent that the viscosity of this synergistic mixture displayed a smaller reduction than the homopolymers. These results indicate that the mechanism of interactions between biopolymers was likely to be unaffected by gamma-irradiation. Degradation of SA and KAG raw materials was increased with increased doses of irradiation. The binary mixture of pre-lyophilised irradiated gels of SA and KAG displayed a higher viscosity at 40.0 kGy than it did at 25.0 kGy. It is difficult to precisely interpret such synergistic behaviour between degraded but interacting polymers, however, a plausible scenario would be that increased amounts of radiolytic products may produce an increased likelihood of increased branching of lower molecular weight fractions of degraded biopolymers. Additional investigations are required to elucidate the effect of gamma-rays on binary polymeric systems.

Rheological properties of post-lyophilised irradiated gels (with and without antimicrobial) were analysed and compared with post-lyophilised gels. Particular attention was given to the antimicrobial impregnated samples as the cascade of events occurring between radical polymer species and antimicrobial compounds are unknown. It is apparent that gamma-irradiation dramatically decreased the viscosity of post-lyophilised irradiated gels of KAG containing antimicrobials (Figure 5.7, Table 5.6). Rheological analysis of post-lyophilised irradiated gels of KAG exhibited Newtonian flow behaviour compared to non-irradiated samples, which were pseudoplastic with no apparent yield stress. However, it was extremely difficult to extrapolate conclusions on the behaviour of irradiated polymer-antimicrobial systems from the calculated values of viscosity coefficient, especially when it is appreciated that incorporation of antimicrobial compounds was already associated with a notable decrease in the viscosity of KAG gels (Chapter 2).

Analysis of rheological continuous flow data as a plot of ' $\ln(\sigma)$ ' as a function of ' $\ln(\dot{\gamma})$ ' permits straightforward and accurate comparison of flow curves in terms of the gradient of the straight line (equivalent to the rate index of pseudoplasticity) and the displacement of the line from the origin, as indicated by the intersect with the ' $\ln(\sigma)$ ' or ' $\dot{\gamma}$ -axis' i.e. the consistency or viscosity coefficient (η'). The higher the line on the graph the 'more viscous'

the sample. Generally, increased doses of gamma-rays increased the degradation of post-lyophilised gels. Interestingly, the degree of degradation between polymer matrices with or without antimicrobial was different. This was particularly true for post-lyophilised irradiated gels of KAG containing CHD and PVP-I, which were degraded to a lesser extent than the KAG control (without antimicrobial). Considering that the inclusion of antimicrobial e.g. CHD, naturally decreased the consistency of KAG gel (Chapter 2), these results indicate that drug polymer interactions occurring between CHD and KAG, were not affected by gamma-rays, as CHD is generally able to withstand irradiation. On the other hand, chain scission and degradation dominated within the bulk of KAG, and degradation of KAG causes the production of radiolysis products, which may generally consist of 'chopped' branches and/or broken backbone residues. Plausibly, free radicals were still able to interact with CHD, where interactions between CHD and degraded KAG hold together the broken branched KAG network resulting in a smaller reduction in consistency.

In the case of irradiated KAG-(PVP-I) systems, a plausible interpretation may be slightly different and more complex, as more than one polymer and additional compounds such as of glycerol, monoxynol-9, sodium phosphate, sodium hydroxide, potassium iodate and citric acid, are also involved. Lugao *et al.* (2002) have reported that irradiation causes cross-linking between PVP chains, where the physicochemical properties of the polymerised PVP network will depend on the presence of additives and irradiation dose. Other authors have also reported the ability of PVP to form of a cross-linked gel network by using a range of gamma-irradiation doses (Benamer *et al.* 2006; Rosiak *et al.* 1990; Rosiak 1994). In addition, it has been reported that gamma-irradiation induces cross-linking between PVP and acrylic acid and/or poly (vinyl alcohol) (Abd Alla *et al.* 2007; Nho *et al.* 2009). Moreover, gamma-rays can induce the diffusivity of inorganic compounds within a polymeric matrix (Mathakari *et al.* 2010). Gamma-irradiation has also been recently utilised for the inclusion of compounds, including antimicrobial compounds, in an expanded polymeric network by radiation grafting (Puiso *et al.* 2011; Gasaymeh *et al.* 2010; Nho *et al.* 2009). Abad *et al.* (2003) have used gamma-rays to synthesise new hydrogels containing blends of PVP and biopolymers such as kappa carrageenan (KC). The latter authors suggested that PVP-KC hydrogels result from cross-

linking of PVP and grafting of KC to PVP, where degraded KC was also physically entangled in the cross-linked PVP network.

Similar to gamma-irradiated blends of PVP-KC, gamma irradiation of KAG-(PVP-I) wafers would result simultaneously in cross-linking of PVP, degradation of KAG and perhaps grafting of KAG to PVP. The combination of these processes may form a KAG-PVP gel network where degraded KAG is physically entangled within the cross-linked PVP and grafted KAG into the PVP backbone. The overall effect could influence the gel fraction (the ratio of weight of swollen gel/ initial weight of polymer) and therefore the swelling behaviour of KAG-(PVP-I) wafer. Abad *et al.* (2003) demonstrated that a higher gel fraction is obtained when pure PVP was irradiated. They suggested that a decreased gel fraction is achieved with increasing concentration of KC, indicating that KC acts as a cross-link inhibitor. In the case of irradiated KAG-(PVP-I) wafers, it is apparent from plot of ' $\ln(\sigma)$ as a function of $\ln(\gamma)$ ' Figure 5.7 (d) that gamma rays induced cross-linking of the iodophore (PVP), and KAG is physically entangled as a semi-interpenetrating polymer network and perhaps grafted to cross-linked PVP. More experiments are needed to elucidate the phenomena taking place.

Rheological analysis of post-lyophilised irradiated gels was undertaken as presented in Figure 5.8, Tables 5.7 and 5.8. It is apparent that chain scission and degradation dominated within the matrices of GG, SA and SA-KAG. Interestingly, although gamma-rays induced a total degradation of post-lyophilised irradiated gel of SA (Figure 5.8-a), the incorporation of CHD in the SA matrix reduced notably the degree of degradation for SA-CHD. These results are in agreement with the behaviour of the KAG-CHD systems previously discussed. In addition, the rheological behaviour of the XG-CHD matrices further supports this scenario, indicating that the presence of CHD immobilises the polymeric chains and/or radiolytic products. Immobilisation of polymeric chains and/or radicals results in a reduction of either polymeric cross-linking and/or chain scission. This phenomenon is apparent in CHD loaded systems of SA and XG compared to CHD-free matrices (Figure 5.8).

The performance of irradiated antimicrobial wafers was tested on a modified disc diffusion assay, previously described (Chapter 2), where the expansion and inhibition ratios of irradiated wafers were compared to non-irradiated specimens. Figure 5.9 presents the data obtained from expansion

and inhibition ratios of KAG antimicrobial wafers tested against MRSA, MSSA, *E. coli* and *P. aeruginosa*. It is apparent that all KAG irradiated wafers expanded more than the non-irradiated ones. The degraded polymeric matrix of KAG was reflected by the increased flow of the re-hydrated wafers, which was associated with total erosion of the cylindrical shape of the lyophilised formulation after 24 hours incubation (Figure 5.10). Interestingly, irradiated wafers impregnated with CHD and PVP-I demonstrated both the lowest and highest expansion ratios, compared to other irradiated antimicrobial loaded KAG wafers. The expansion behaviour demonstrated by irradiated CHD-loaded KAG wafers reflects the rheological behaviour of the KAG-CHD system mentioned above, where the incorporated drug holds together the degraded KAG matrix. The high expansion displayed by the rehydrated matrices of KAG-(PVP-I) is complex to interpret, however such behaviour supports the development of a PVP-I cross-linked system within the degraded KAG matrix. The polymerised, hydrophilic iodophore of PVP-I, swells when placed on the moist agar surface, while the degraded KAG matrix erodes from the outside. Both phenomena occur simultaneously resulting in an increased expansion of irradiated KAG-(PVP-I) discs.

It is apparent that increased inhibition ratios of irradiated KAG wafers are associated with increased expansion ratios of the formulations tested (Figure 5.9-b-d-f-h). Linear regression analysis of expansion ratio (ER) vs. inhibition ratio (IR) for each antimicrobial tested against every bacterial strain (Figures 5.11-14) demonstrated that there was a trend for such a correlation, in some cases. The correlation between ER vs. IR was more evident in the case of SS and PVP-I rather than NS and CHD, indicating that the antimicrobial activity of SS and PVP-I was probably not affected by gamma-irradiation, while NS and CHD lost some of their initial antimicrobial potency. White residues observed around the swollen rehydrated matrices of all CHD-impregnated irradiated wafers support this hypothesis; however, it is difficult to precisely interpret the linear regression analyses of ER vs. IR, as gamma-rays may also have altered the diffusivity and release profiles of drugs embedded in degraded matrices. In addition, drug-polymer interactions, which apparently also influence the expansion ability of the swollen matrix, may also play a key role.

Expansion and inhibition ratios of irradiated CHD-impregnated matrices of GG, XG, SA and SA-KAG demonstrated a different behaviour compared to CHD impregnated wafers of KAG (Figure 5.15). The expansion ratios of antimicrobial-free irradiated wafers showed similar expansion profiles to non-irradiated specimens. This expansion behaviour was particularly expected for XG wafers, rheological properties of which were not altered considerably, however degraded polymers of GG, SA and SA-KAG were expected to demonstrate increased flow on the moist agar surface. This paradox is difficult to interpret as several factors may be at play.

It has been reported that gamma irradiated tablet formulations consisting of polyethylene oxide (PEO) lost the ability to swell and to form a gel layer during dissolution. In addition, irradiated PEO formulations dissolved rapidly decreasing their initial dimensions, while the ability to release the impregnated drug in a sustained manner was totally lost. This behaviour of PEO tablets was associated with considerable chain scission and overall degradation of the polymer matrix by gamma-rays (Maggi et al. 2004). Desai and Park (2006) have reported a similar behaviour for gamma-irradiated chitosan microparticles. The latter authors indicated that increased irradiation doses decreased the swelling capacity and increased the release rate of impregnated drug from irradiated chitosan microparticles.

Depolymerisation of GG, SA and SA-KAG is likely to lead to an inability of the irradiated matrix to swell and form a weak gel network and as a consequence, the rehydrated wafers were expected to show an increased expansion. However, in the case of irradiated CHD-impregnated wafers of SA and SA-KAG, this phenomenon is not evident as the CHD incorporated within the irradiated matrix further restricted the matrix's ability to expand. The ability of impregnated CHD to confine the expansion of wafers was also noted for non-irradiated CHD wafers, previously mentioned in Chapter 3 (Figure 3.5). Although irradiated CHD wafers did not demonstrate an increase in expansion ratio, there was evidence that the restricted expansion was associated with increased inhibition ratios. Linear regression analysis presented in Figure 5.16 (c) and (d) demonstrated that there was an inversely proportional correlation between ER and IR for CHD impregnated wafers of SA and SA-KAG.

Dissolution profiles of irradiated CHD-loaded SA wafers demonstrated that there was a faster release of CHD from the irradiated SA matrices, where the accumulation of CHD at 24 hours almost doubled for the irradiated wafers compared to non-irradiated SA wafers (Figure 5.17, Table 5.9). In addition, increased doses of irradiation (40 kGy) slightly decreased the ability to absorb and retain water (Figure 5.18) while increasing the release of CHD from the irradiated matrix. The results are in agreement with the previous work of Maggi *et al.* (2004) and Desai and Park (2006), indicating that irradiated polymers, in which gamma-rays cause degradation and chain scission, generally lose their ability to control water uptake, while they demonstrate a faster release of the impregnated therapeutic compound. However, in the case of polymers where the impregnated drug interacts with the polymeric carrier, the situation is more complex.

Linear regression of CHD released from SA irradiated wafers, analysed with the Korsmeyer-Peppas model (Figure 5.19, Table 5.9) demonstrated that this model represents an appropriate model for release kinetics, from the irradiated polymeric matrices under sink conditions, as correlation coefficients were approximately 0.97. Although, there was almost a 2-fold increase in the accumulation of CHD from the irradiated SA matrices, the calculated release exponent indicated that diffusion of CHD follows Fickian behaviour. These results suggest that the interaction occurring between the impregnated drug (CHD) and the polymer play an important role in the general behaviour of the antimicrobial polymeric matrix, in terms of exhibited flow behaviour (rheological properties), ability to absorb and retain fluids and release of the impregnated antimicrobial compound. The efficacy of antimicrobial polymeric systems depends on the interactions developed within the polymeric matrix between the drug and the polymeric chains. A sound understanding of such interactions is critical to the development, performance and activity of antimicrobial gel formulations intended for the control of infection and management in chronic wounds. An attempt to elucidate and interpret drug polymer interactions between biopolymers and selected broad spectrum antimicrobials is summarised in the next Chapter (6).

Chapter 6
***In silico*, molecular modelling studies on the
components of karaya (KAG) antimicrobial
wafers**

6.1 Aim

Attempt to interpret drug-polymer interactions affecting the rheological behaviour of KAG-antimicrobial complexes by using molecular modelling studies.

6.2 Introduction

Recently, there has been an increasing interest in the investigation and use of natural polymers as drug delivery carriers. Biopolymers such as guar gum, chitosan and karaya gum have been investigated as potential, non-toxic, biocompatible and biodegradable vehicles for therapeutic compounds. However, the design of novel delivery systems such as biopolymeric-drug conjugates appears to be not an easy task, especially when the properties of either biopolymers or their combination with ionised drugs are unknown.

Different types of intermolecular forces may develop between incorporated drugs in polymeric carriers. Some of them include electrostatic interaction, hydrogen bonding, hydrophobic interaction and Van der Waals forces. Electrostatic forces may occur between charged or partly charged ions of molecules and can be either repulsive or attractive, where the degree of ionisation influences the intensity of such interactions. They can be short-ranged (weak) or long-ranged (strong). Hydrophobic interactions are entropic, moderately strong attractive interactions occurring between non-polar groups separated by water. Hydrogen bonding and Van der Waals are generally considered weak attractive interactions which decrease with increasing temperature (Dickinson 1998).

Previous studies have shown that chitosan, a polyionic natural polymer, develops electrostatic interactions when it is used as a carrier of antimicrobials such as with amoxicillin trihydrate and/or amoxicillin sodium (Torre et al. 2003). Bani-Jaber *et al.* (2009) recently reported drug-polymer interactions occurring between chitosan and diclofenac. Heun *et al.* (1998) have investigated drug-polymer interactions occurring between Eudragit RL/RS resin and four model drugs. The latter authors demonstrated excellent correlation between *in silico* data and data obtained from *in vitro* experiments. Generally, molecular modelling studies have proven to be a useful tool in

increasing understanding of the interactions between drugs and their polymeric carriers. In addition there are a plethora of studies reporting a good correlation between experimental data obtained *in vitro* and *in silico* (Subashini et al. 2011; Cairns et al. 2002), indicating that molecular modelling studies provide a reliable method for the investigation and profound understanding of drug-polymer interactions.

However, understanding the relationship between molecular structure and physicochemical properties of polymers is a challenging task, which gets even more complex when the ionised or partly ionised polymer serves as a carrier of an ionised drug. Although there are many reported investigations of the type of interactions occurring between a polymeric carrier and an ionised drug, there is limited information about how the entrapped interactive drug may influence the rheological behaviour of the biopolymer, adhesion properties, water uptake ability and diffusivity of the compound from the ionic polymeric network.

In the current project, selected biopolymers such as sodium alginate, xanthan gum, guar gum and karaya gum have been used as carriers of antimicrobial compounds. These were intended for the formulation of lyophilised antimicrobial wafers that demonstrated initially altered rheological properties when mixed with broad spectrum antimicrobial compounds. The influence of the incorporated drugs was generally reflected on the performance of antimicrobial wafers. For instance, the significant effect of the incorporated drugs on the adhesion properties of the KAG-antimicrobial wafers. In addition, expansion ratios of CHD wafers appeared to be different to those of antimicrobial-free wafers. Moreover, diffusivity of solute CHD was considerably affected by the CHD-polymer interactions occurring within the swollen biohydrogel network. Drug-polymer interactions developed between the entrapped drugs and the polymer network may also be an important factor on the effect of gamma-rays upon the physicochemical properties and performance of the antimicrobial matrix.

Therefore, a brief investigation was undertaken in order to better understand and attempt to interpret the drug polymer interaction developed between a partly ionic biopolymer and incorporated drugs. Molecular modelling studies undertaken focused generally on the molecular behaviour of biopolymeric carrier KAG in association with four different antimicrobial

compounds. Molecular simulation between constructed compounds was initially investigated *in vacuo*, and provided information about macroscopic (thermodynamics and optical properties) and microscopic (molecular motions and intermolecular forces) behaviour of molecules and created complexes.

6.3 Materials and methods

Molecular modelling studies were undertaken to attempt to interpret and decipher the drug polymer - interaction occurring between KAG and selected antimicrobials, when mixed together. Chemical structures of antimicrobials were taken from the supplier (Sigma-Aldrich, UK), and conformation of KAG was based on the information given in the Merck Index (12th edition 1997), Verbeken *et al.* (2003) and De Brito *et al.* (2005). Molecular modelling was carried out on a Silicon Graphic Octane II or Hewlett Packard 3000 series workstation using the Insight-II 2004 graphics interface and Discover 3.0 simulation software (Accelrys, UK). The energy calculations, minimisation and dynamic simulation of biopolymer KAG, NS, CHD and pluronic F68 surfactant were analysed using the cvff force field, while cff91 was used for PVP-I and SS. Models for each antimicrobial and polymer were constructed (Insight-II) and partial atomic charges approximated from a single-point PM3 calculation. Each antimicrobial was docked manually with the polymer. The optimised models were subjected to molecular dynamics simulation (10 ps equilibration and 200 ps production, 1-fs timesteps) with initial atomic velocities taken from a Maxwell-Boltzmann distribution at 300K and 500K. The time-averaged structures from 200 samples taken at 1-ps intervals were minimised. Ligand structures were sampled for conformational averaging *in vacuo*. Atomic trajectories saved every 1 ps were used for conformational averaging, and these structures were finally minimised to an energy convergence criterion of 0.1 kcal mol⁻¹ Å⁻¹. Binding enthalpies were obtained by subtraction of the potential energy of the antimicrobial and polymer from that of the complex:

$$E_{\text{bind}} = [E_{\text{complex}}] - [E_{\text{drug}} + E_{\text{polymer}}]$$

where, E_{bind} = calculated binding enthalpy between antimicrobial and polymer; E_{complex} = potential energy of complex after final minimisation; E_{drug} =

potential energy of antimicrobial after final minimisation and E_{polymer} = potential energy of polymer after final minimisation. Negative values of E_{bind} indicate favourable interactions between the drug and the polymer matrix, while positive values of E_{bind} indicate unfavourable interactions between the polymer and the incorporated drug.

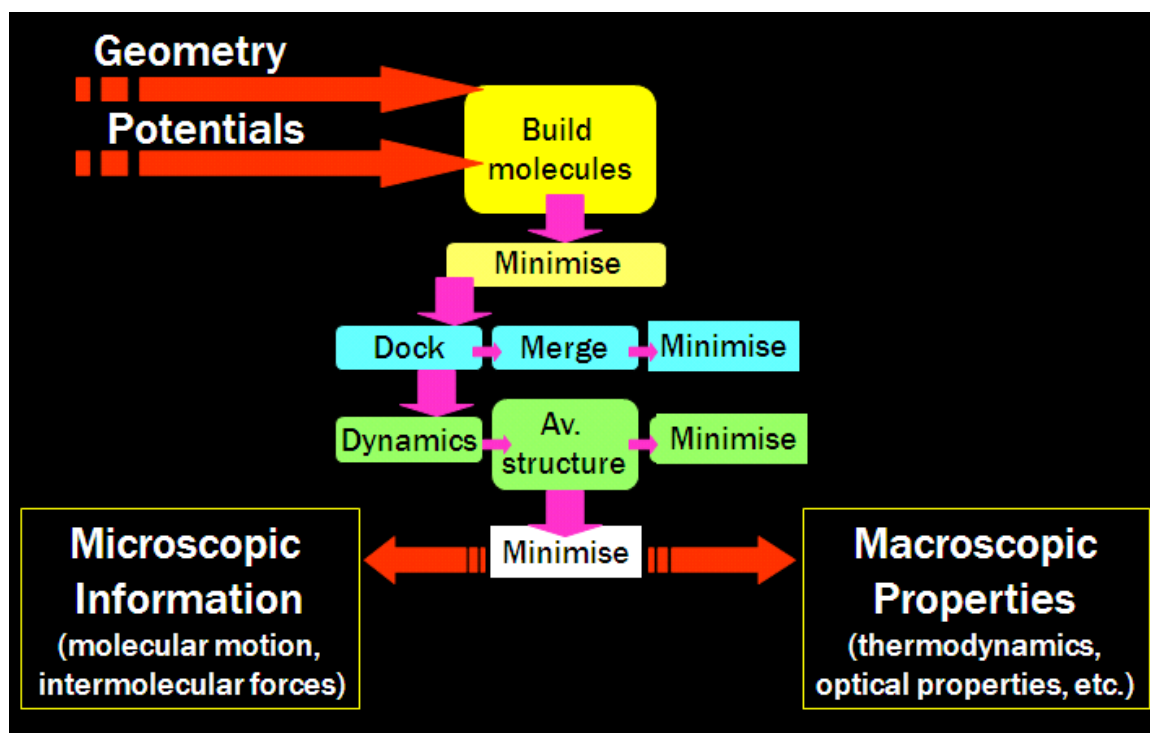


Figure 6.1 Summarised work diagram of the molecular modelling stages:

Build molecules: Construction of molecules based on a specific coordinate system (Cartesian x , y , z) and calculation of potential energy surfaces, which is considered to be the movement on a multi-dimensional surface (Leach 1996).

Minimisation: The minimum energy arrangements of atoms, equivalent to a 'plausible' starting geometry, also known as global energy minimum, which is generally considered to be a stable state of the constructed molecular system (Leach 1996). Polymers have a more complex energy surface profile, compared to small molecules, mainly due to the large number and variety of atoms or sub units that they possess (Figure 6.2).

Dock: Docking is defined as the affinity of molecules with an optimal orientation and energy to form a stable complex (Lengauer and Rarey 1996).

Merge: Permanent unification of minimised structures of constructed molecules (polymer and drugs) in order to form a polymer-drug complex.

Dynamics: Molecular dynamics (MD) is a virtual simulation of constructed minimised molecules and created complexes in order to investigate their conformational space as a function of time. Virtual simulation usually involves the application of realistic temperatures (300 K = 26.85 °C and 500 K = 226.85 °C), allowing simulated structures to become more conformationally flexible and capable of reaching a global energy minimum. During this process mobile molecules generate a trajectory (history of motion) which demonstrates the conformational behaviour of the molecules/complexes and confirms the accuracy of generated values of enthalpies (Leach 1996). It has to be mentioned that the generated values of enthalpies of simulated molecules and created complexes depend on the size of molecules/complex and provided heat.

Average structure: This is a final arrangement of structures generated from the trajectory of the simulated molecules/complexes.

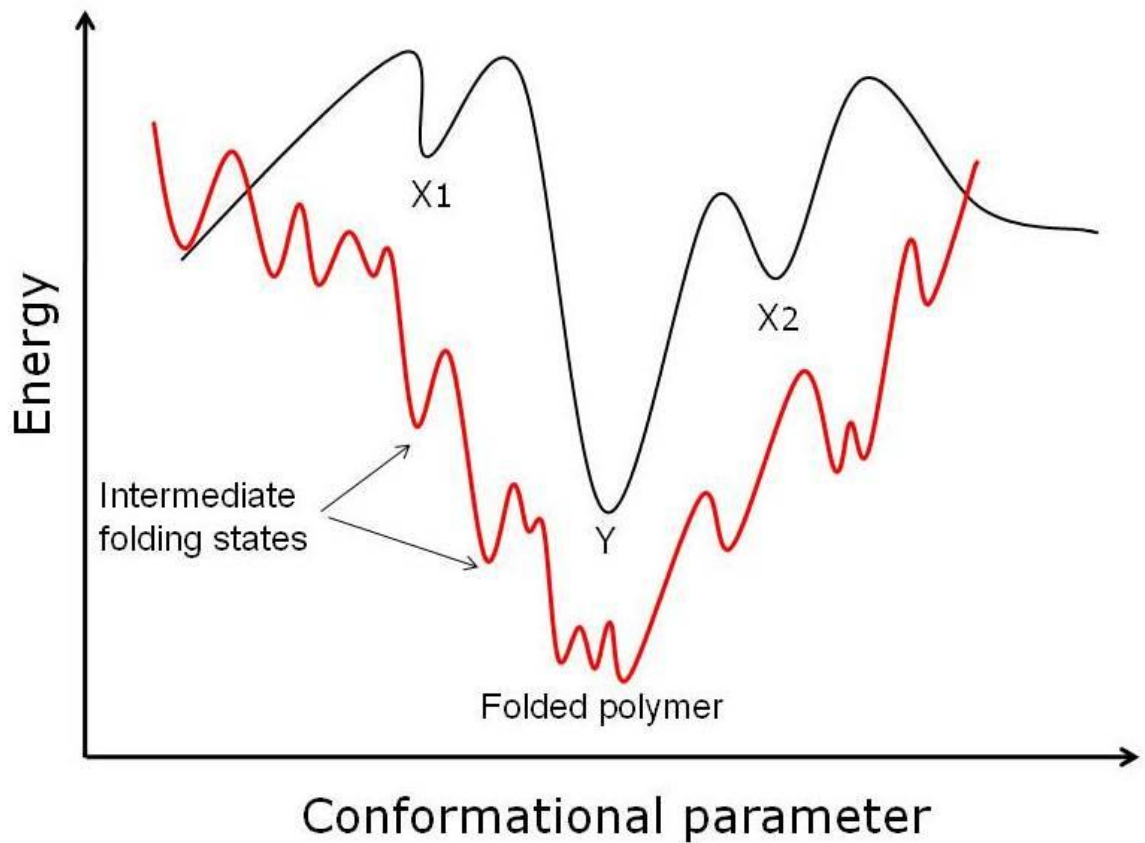


Figure 6.2 A schematic one-dimensional energy surface of small molecules. Minimisation moves downwards the nearest minimum. X_1 , X_2 – local minima, Y – global energy minimum, which can be only reached following molecular modelling simulations (Leach 1996). (–) Folding-energy landscape for a biological heterogeneous polymer (protein) (Frauenfelder and Wolynes 1994).

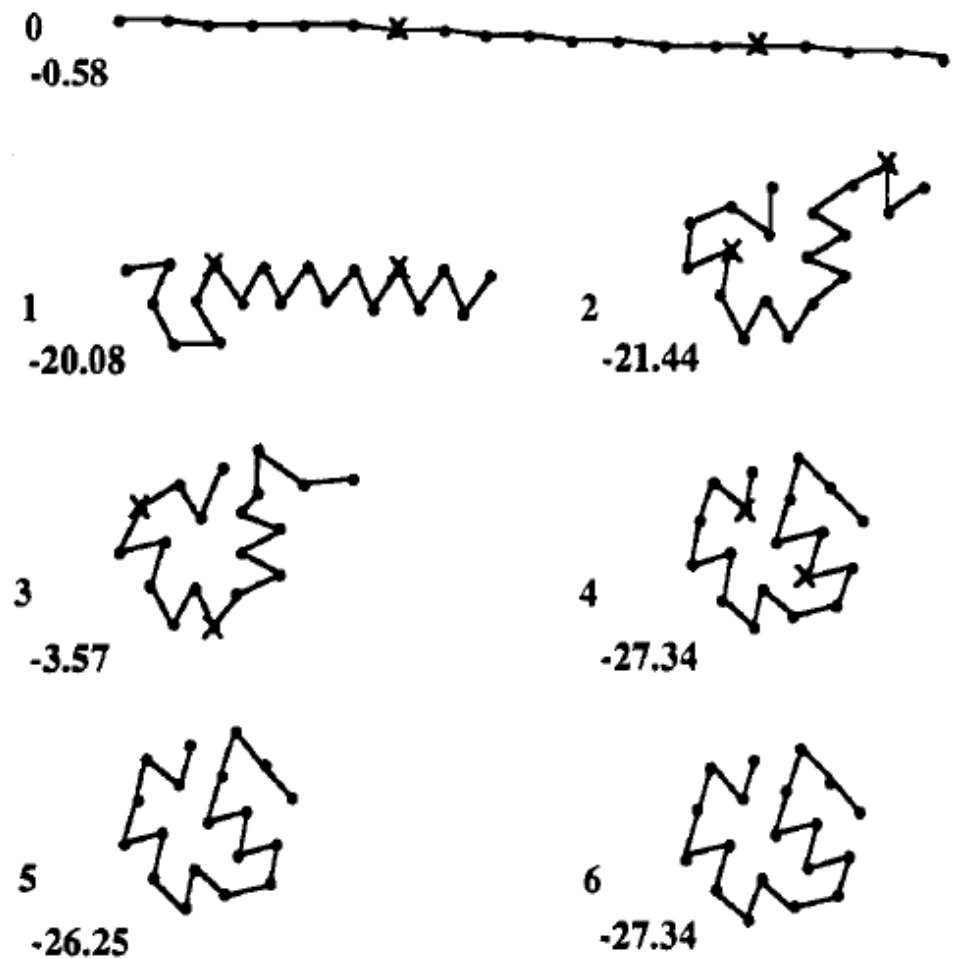


Figure 6.3 Schematic folding pathways of polymers, used to reach a global minimum energy conformation (Adapted from Judson 1992). Note that the conformational variation ability (flexibility) of a polymeric molecule, which can produce different values of minimisation energy (kcal mol⁻¹).

6.4 Results

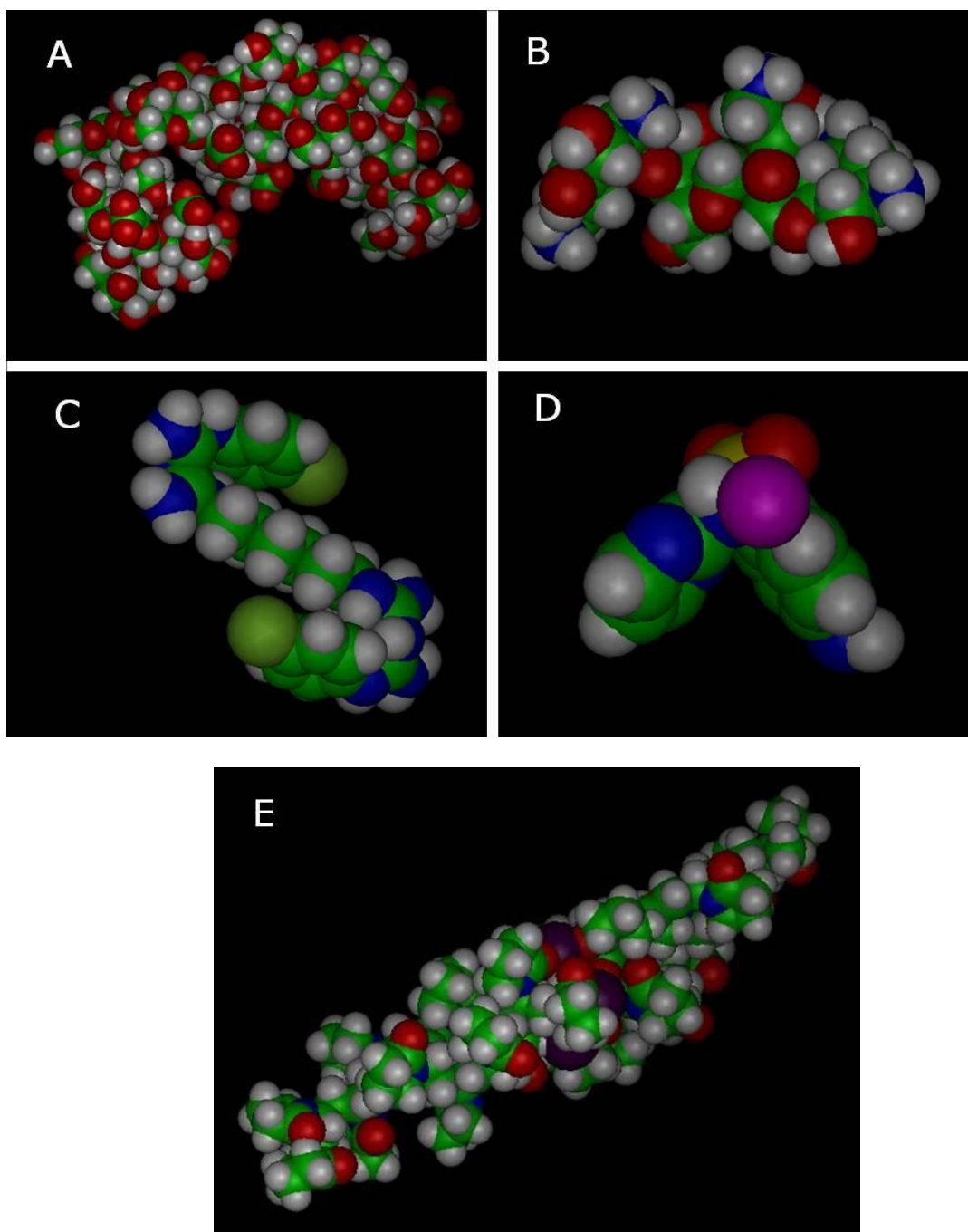


Figure 6.4 Molecular modelling configurations [Corey-Pauling-Koltum (CPK rendering)] of minimised structures of KAG polymer and selected antimicrobials. Note the interesting three dimensional shape of chlorhexidine (CHD) ('Z' structure) and silver sulfadiazine (SS) ('butterfly' structure). Please, note that the structures are not presented at the same magnification. **A** – KAG, **B** – NS, **C** – CHD, **D** – SS and **E** – PVP-I

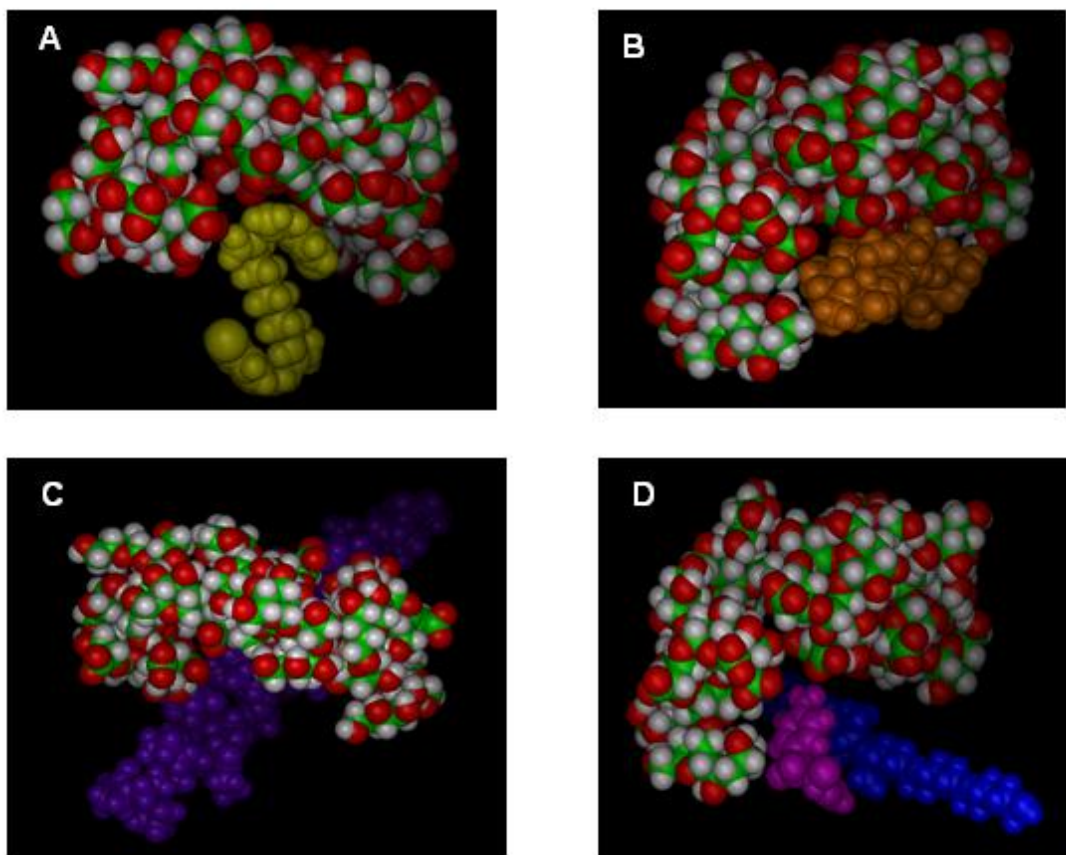


Figure 6.5 Molecular modelling of minimised (CPK rendering) KAG – antimicrobial complexes: **A** – KAG-CHD, **B** –KAG-NS, **C** –KAG-PVP-I and **D** –KAG-SS (with pluronic F68).

Table 6.1 Optimal docking energies of KAG with the incorporated drugs *in vacuo*. Note from the merged complexes above (Figure 6.3) that the most favourable residence of the associated drugs is the 'pocket' created from the structure of KAG. PVP-I and SS-F68 have a higher affinity to KAG compared to CHD and NS, as they possess a higher number of atoms (docking energy is proportional to the number of atoms in molecule).

Complex	Energy of affinity (kcal mol⁻¹)
KAG-CHD	106.08
KAG- NS	667.70
KAG-PVP-I	-956666.00
KAG-SS-F68	-987576.00

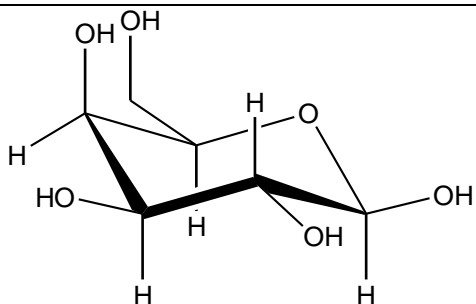
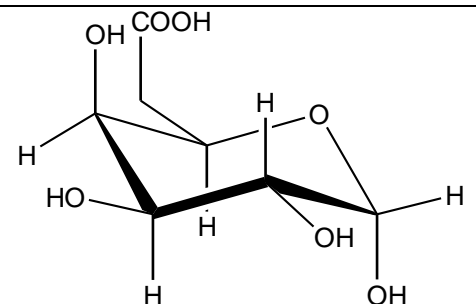
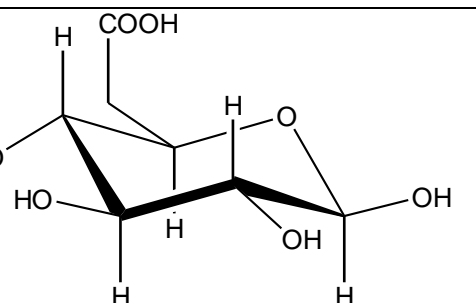
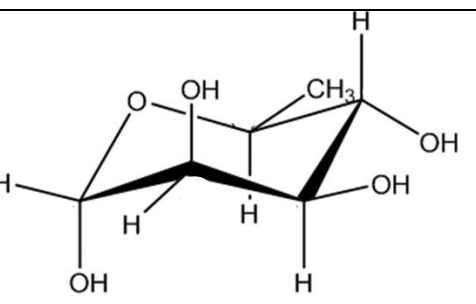
Table 6.2 Binding enthalpies (E_b) of compounds and complexes (1 : 1 ratio) calculated *in vacuo* at 300 K. Note that calculated E_b values of complexes were negative, except of KAG-NS, indicating favourable interactions between karaya gum (KAG) and incorporated drugs.

Molecules	Energy of molecules (kcal mol⁻¹)	Energy of complex KAG/drug (kcal mol⁻¹)	Energy of binding $E_b = E_c - [E_d + E_p]$ (kcal mol⁻¹)
KAG	9171.8		
CHD	22.2	9106.0	-88.0
NS	1412.9	11194.8	610.1
PVP-I	-639.3	5840.4	-2692.1
SS	-69.7		
pluronic F68	2.9	6464.9	-2640.1

Table 6.3 Binding enthalpies (E_b) of compounds and complexes (1: 1 ratio) calculated *in vacuo* at 500 K. Note that calculated E_b values of complexes were negative indicating favourable interactions between karaya gum (KAG) and all incorporated drugs.

Molecules	Energy of molecules (kcal mol⁻¹)	Energy of complex KAG/drug (kcal mol⁻¹)	Energy of binding $E_b = E_c - [E_d + E_p]$ (kcal mol⁻¹)
KAG	9771.3		
CHD	100.9	9823.1	-49.1
NS	1442.8	10602.3	-611.8
PVP-I	-720.0	5631.4	-3419.9
SS	-36.5		
pluronic F68	108.0	6496.5	-3346.3

Table 6.4 Sugars present in karaya gum (KAG).

Sugars	Formula (Molecular weight)
 <p style="text-align: center;">β-D GALACTOPYRANOSE</p>	$C_6H_{12}O_6$ (180.16)
 <p style="text-align: center;">α-D GALACTURONIC ACID</p>	$C_7H_{12}O_7$ (208.17)
 <p style="text-align: center;">β-D GLUCURONIC ACID</p>	$C_7H_{12}O_7$ (208.17)
 <p style="text-align: center;">α-L RHAMNOSE</p>	$C_6H_{12}O_5$ (164.16)

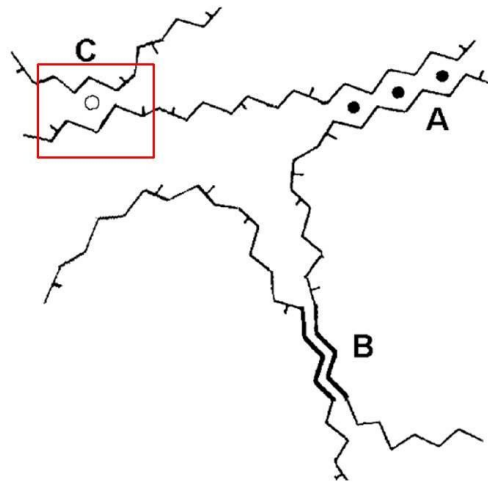


Figure 6.6 Proposed model for *Sterculiaceae* gelation; **A**-ordered ionic interaction between galacturonic acid residues and calcium ions (Ca^{2+}) (the 'egg-box model'), **B** - hydrogen bonding between rhamnose segments, **C** - ionic interaction between two or more galacturonic acid residues of the backbone and /or branches of glucuronic acid (Adopted from Silva et al. 2003).

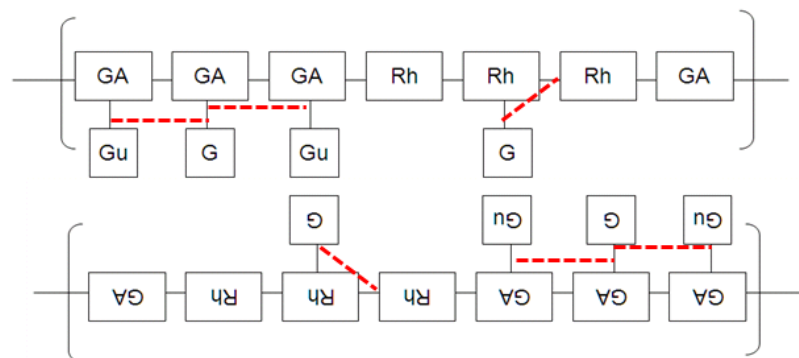


Figure 6.7 A plausible block configuration of karaya gum (KAG) consisting of α -L-rhamnose (Rh) residues linked to 1, 4- α -D-galacturonic acid (GA) backbone and branches linked to 1, 2- linked- β -D-galactopyranose (G), 1, 3-linked- β -D-glucuronic acid (Gu) to the backbone residues. (----) represents the entrapped drug (CHD) within the KAG network (**C** - zone of Figure 6.6), where the antimicrobial compound (which displayed a 'Z' shape) is hooked between the polymer residues, disrupting the 3-D structure of the polymer network, weakening polymer-polymer interactions and resulting in a 'thin' gel network.

6.5 Discussion

Molecular modelling may be generally defined as the investigation and conceptualisation of molecules via physical, mathematical and graphical representations. In other words, molecular modelling is a virtual simulation of molecules or of molecular systems in order to understand and/or predict their behaviour (Schlecht 1998). Although MD is found to be a powerful tool to further understand and also predict the properties of molecules, including polymers, complex biopolymers represent a major challenge when trying to mimic their properties *in silico*. Cross-linking between different chains increases the variations in the constitution and structures of a polymer, which sometimes can have a dramatic affect upon the overall properties of the molecule (Leach 1996).

Karaya gum (KAG) is a complex, partly acetylated branched polymer, which originates from the dry grounded exudate of *Sterculia urens* tree. Analysis of the structure of KAG demonstrated that this biopolymer consists of a backbone of α -D galacturonic acid and α -L rhamnose residues. Branches are linked by 1, 2-linkage of β -D-galactose and/or by 1, 3-linkage of β -D-glucuronic acid (Verbeken et al. 2003). Although the chemical composition of the biopolymer differs with the place of origin and harvested period, it has been reported that generally KAG contains 60 % acetyl free, neutral sugars (galactose and rhamnose) and 40 % acidic residues (glucuronic and galacturonic acids) (De Brito et al. 2005). In addition, it has been reported that KAG contains traces of proteins (approximately 1 %); however protein content was found lower than in other biopolymers of natural gum extracts (Verbeken et al. 2003). There is, therefore, an extensive degree of chemical variation in samples of KAG.

De Brito *et al.* (2005) have investigated the rheological properties of KAG aqueous solutions and demonstrated that KAG forms a relatively strong gel network at concentrations higher than 2 % (w/v). These results are in agreement with the rheological properties of 3 % (w/v) KAG gels investigated in the present project, which have been reported previously (Chapter 2). An aqueous solution of 3 % (w/v) KAG demonstrated a pseudoplastic flow with no yield stress, where the calculated viscosity did not exceeded 13.00 Pa.s. The gelling mechanism of branched, partly ionic biopolymers is a complex process. A gelation model for *Sterculiaceae* has been proposed by Silva *et al.* (2003) as

presented in Figure 6.6 and it has been reported that the presence of acetyl groups, in particular glucuronic and galacturonic acid residues, are essential in the formation of the KAG gel network as they promote the interactions between the polysaccharide chains. In addition, it has been reported that the presence of electrolytes, such as sodium and chloride, decrease the gel strength of aqueous solution of KAG and lead to a less viscous gel (De Brito et al. 2005).

The incorporation of clinical concentrations of broad spectrum antimicrobials in the KAG gel network was associated with a considerable decrease in viscosity (Chapter 2, Table 2.3). Rheological analysis showed that the incorporation of NS and CHD caused a notable decrease in viscosity of KAG, which was approximately 8 times and 3.4 times respectively. The incorporation of PVP-I and SS (prepared with pluronic F68) also decreased the viscosity of KAG gel approximately 2-times. These results indicate that the incorporation of ionic molecules, such as CHD and NS, have a greater affect upon the gel network of KAG. However, it is apparent that the incorporation of non-ionic compounds of either PVP-I and SS (with pluronic F68) also affected the KAG gel network. In the case of PVP-I, the situation appears to be more complex, as small quantities of other compounds included in the standardised commercial solution of PVP-I, such as glycerol, monoxynol-9, sodium phosphate, sodium hydroxide, potassium iodate and citric acid, may also have an additional effect on the KAG gel network.

Molecular modelling studies initiated with the construction of molecules. Drug molecules of CHD, NS and SS were created based on their chemical conformation and therefore the CPK rendering (Figure 6.4) indicates plausible and realistic geometries. PVP-I was constructed as the connection of twelve blocks of polyvinylpyrrolidone (PVP), where four large atoms of iodine were tethered within the PVP matrix. The structure of karaya gum (KAG) was based on a plausible configuration of sugars present in KAG, taken from the existing literature. The final structure of KAG consisted of 30 sugar molecules (Table 6.4) including α -D galactopyranose (20 %), α -L rhamnose (30 %), α -D galacturonic acid (30 %) and β -D glucuronic acid (20 %). Although the actual length of polymer is variable, the KAG molecule was constructed to mimic closely the structure of KAG biopolymer.

Complexes of KAG-drug were constructed as presented in Figure 6.5. It is apparent that the most optimal residence of the incorporated drugs was found to be within the 'pocket' created within the minimised structure of KAG. This pocket arises due to gross folding of the modelled polymer as a result of the minimisation algorithm. According to Mingaleev *et al.* (2002) "conformational flexibility is considered to be a fundamental property of polymers which differentiates them from small molecules and promote their remarkable properties". This ability of polymers is generally mediated from the complex structures of the constituent's sub-units. The energy of a polymeric molecule is a function of a topological arrangement of the sugars. Generally, the energy of polymers is described as a hypersurface, with many energy valleys (or craters) and hills (Figure 6.2), where each of the valleys is indicative of a particular conformational state of the polymer (Frauenfelder and Wolynes 1994). Figure 6.3 presents a schematic folding pathway, which can lead to different conformations and different energy values that a polymeric molecule can possess. In addition, it is apparent from the schematic, one-dimensional energy surface (Figure 6.2) that there is a notable difference between the surface energy profiles of small and polymeric molecules. Therefore, the KAG polymer is expected to display a linear geometry and a high degree of flexibility, dissimilar to the incorporated small drug molecules, which may play a critical role on the calculated binding energy behaviours of the drug-polymer complexes.

The absolute energy of affinity of drugs with the KAG structure ranged from 106.08 – (-987576.00) kcal mol⁻¹ (Table 6.1), but these values are calculated from the number of atoms present. Large molecules consisting of numerous atoms will display an increased energy value. The incorporation of PVP-I and SS-F68 demonstrated the highest energy of affinity. On the other hand, CHD and NS showed positive values of proximity with KAG indicating an unfavourable interaction of KAG to either CHD or NS. However NS demonstrated the highest repulsive behaviour to KAG.

Data obtained from the *in vacuo* simulation at 300 K (Table 6.2) indicated that all incorporated drugs showed a favourable interaction (-ve binding enthalpy) with the KAG, except for NS. The most favourable interaction was displayed from PVP-I and SS (with pluronic F68). Although it was expected that CHD would have shown the most favourable interaction

with KAG, as the cationic structure of CHD would be attracted to the partly anionic KAG residues, calculated enthalpies at 300 K did not represent such a trend. In the case of NS, the incorporated drug demonstrated a positive value of binding energy, indicating unfavourable interaction with the KAG network. The most favourable interactions were obtained with PVP-I and SS-F68. These components are not cationic and are therefore not expected to bind strongly to a partly anionic polymer. The high interaction energy obtained from the molecular modelling suggests that the size of the antimicrobial is important and that hydrophobic effects (interactions which occur between non-polar molecules) are more influential in this type of 'polymer-polymer' interaction.

Molecular dynamics of generated molecules and complexes were also performed at 500 K in order to further simulate the motility of structures (Table 6.3). Generally, the energy of molecules was slightly increased compared to those values obtained at 300 K. Only PVP-I displayed a slightly decreased energy when simulated at 500 K. Interestingly, CHD and F68 increased their energy by 4.5 and 37 times respectively, however, the energy values of complexes remained generally similar. The calculated binding enthalpies for each complex simulated at 500 K, demonstrated that all drugs showed a favourable interaction (-ve binding enthalpy) to the KAG matrix. These results are similar to the calculated binding enthalpies obtained at 300 K, except for NS.

Rheological analysis of KAG antimicrobial gels demonstrated that the viscosity coefficient of gels showed a decreasing trend compared to control (antimicrobial-free gel), where $KAG > SS-F68 > PVP-I > CHD > NS$. These results suggest that the presence of the antimicrobial compound disrupts the three-dimensional polymer network, weakening polymer-polymer interactions and 'thinning' the gel (Figure 6.7). The calculated binding enthalpies determined at either 300 K and 500 K supported this hypothesis i.e. all the complexes displayed negative binding enthalpies, where generally $PVP-I > SS-F68 > NS > CHD$, indicating a favourable interaction with the polymer. The rank order of effect was however different, with the compounds displaying the greatest binding energy demonstrating only a modest drop in viscosity. However, the viscosity lowering appears to be possibly the result of a bulk physical presence of the drug disrupting the close three-dimensional lattice of the polymer.

The differences in rank order may be due to a number of effects and these are listed below:

- Molecular modelling counts best where there are simple molecular interactions occurring between drug and polymer. It may be that 'bulk' effects are not captured well by a technique which relies upon specific atom-atom interactions.
- Some of the structures modelled in this study are large and are very conformationally flexible. It is possible that 100,000 fs of molecular dynamics (MD) was insufficient to capture all available trajectories and that the study could be repeated allowing for a greater production phase of MD (e.g. MD occurring at 600 K for 200,000 fs).
- Similarly, the temperature of the molecular modelling may be insufficient to completely relax the high molecular weight structures found in these polymers. It is reported that the relaxation process in complex biomolecules can be reached under extensive simulation at increased temperatures (Frauenfelder and Wolynes 1994).
- Modelling was carried out '*in vacuo*'. It may be that a better correlation would be obtained if an explicit solvent was employed. There are pitfalls, however, with the use of explicit solvent in that the type of modelling undertaken must be strictly controlled to ensure that sufficient production time is allowed to capture all possible trajectories.

In silico interpretation of interactions taking place within miscible complexes of drugs with polymers is not an easy task. Biopolymers are generally heterogeneous molecules, which are difficult to mimic precisely *in silico*. They possess remarkable properties as thickeners, stabilisers and drug delivery vehicles, mainly due to their ability to form a complex 3-D network in aqueous solution. The chemical variation of biopolymers, however, can lead to unexpected rheological behaviours when used as carriers of charged or non-

charged molecules. Such variations in consistency were noticed in KAG-drug blends. Attempts to decipher and understand the behaviour of KAG-drug conjugates were undertaken using molecular modelling simulation. *In silico* simulations proved to be very useful in conceptualisation and visualisation of the geometries of small drug molecules and *in vitro*, the incorporation of ionic drug molecules had a profound effect on the 3-D gel network of KAG, *in silico* simulations were unable to capture all atom-atom interactions occurring between oppositely charged groups. However, this effect was mainly due to conformational flexibility of the polymeric carrier (KAG) and large drug molecules such as PVP-I and or SS-F68 complexes.

Additional modelling studies are required in order to shed light on the interactive behaviour of biopolymer-drug complexes. These include the investigation of the effects of a longer production phase for the dynamics simulations and the effects of increased temperature during simulations in solvents upon polymer relaxation. Secondly, investigation of polymers under conditions of restraints of mobility and reduced flexibility. Thirdly, investigation of drug-polymer interaction, performed with different docking orientations, with regards to drug's residence (i.e. putting the drug in 'upside down' or outside the polymeric 'pocket') and fourthly, the formation of drug-polymer complexes based on an automatic docking logarithm.

Chapter 7

General discussion

7.1 General discussion and future work

The complex nature of non healing wounds and a poor understanding of the aetiologies that govern impaired healing, represents a challenge for physicians and scientists alike. Chronic wounds are a major cause of disability, social isolation and even mortality for affected individuals. In addition, treatment involves a high economic cost and the risk of spreading hospital and community acquired antimicrobial resistant bacterial strains. Therefore, treatment of chronic, non healing infected wounds represents a great challenge for both patients and healthcare workers in terms of application of a suitably effective therapy.

Chronic wounds result from the inability of the broken skin to follow a well-coordinated and complex physiological healing process, which relies on the overlapping stages of coagulation, inflammation, proliferation and remodelling. In other words, impaired healing results from an imbalance of promoters and inhibitors and disrupted interaction between biochemical mediators with the extracellular matrix (ECM). Instead, the skin restoration process is trapped in an uncontrolled and self-sustained phase of inflammation (Schreml et al. 2010). There are several aetiologies that can delay and/or stop the healing process. They include wound type and pathophysiology, the patient's immune system, age and bacterial infection. Currently, it is not yet well defined which of all the above factors play a primary role in impaired healing as they all interplay, however, infection and bacterial colonisation is considered a common cause of chronic inflammation.

Chronic inflammation is usually caused by persistent bacterial colonisation and infection, as an open ulcer provides a favourable habitat for a variety of bacterial species. The mixed microbiological flora of wounds, in terms of density, diversity and biofilm formation, has been shown to be a common cause of impaired wound healing. Common pathogens of non healing wounds, such as *S. epidermidis*, *S. aureus*, *Porphyromonas* spp, *Peptostreptococcus* spp, *Enterococcus* spp, *E. coli*, *P. aeruginosa*, *Clostridium* spp, which arrive from both external and internal environments, adhere to the injured skin tissue (Parker 2000). The protein content of wound exudate provides a nutritional substrate for bacteria to survive and proliferate in an unprotected ulcer (Landis 2008). As a consequence, control of exudate and

inhibition of bacterial infection can provide an effective therapy to control bacterial bioburden and eventually improve wound healing.

Topical treatment of non-healing, infected wounds can provide many advantages with regards to control of wound exudate, optimal moisture of wound bed and local delivery of antimicrobials. In particular, application of self-adhesive, occlusive and gel transforming formulations have proven to be more efficacious than gauzes and/or cotton wool dressings (Jurczak et al. 2007). Hydrophilic, non-toxic, porous lyophilised wafers, prepared from biopolymers, can provide an innovative approach to the management of a wide variety of suppurating wounds (Matthews et al. 2005). In addition, the incorporation of broad spectrum, widely used antimicrobial compounds within the lyophilised matrices can provide a controlled, continuous and targeted delivery of the drug at the site of infection.

In vitro investigation of the properties and antimicrobial efficacy of novel formulations, intended for application in a variety of suppurating wounds, represent a great challenge. Despite the plethora of traditional, modern, advanced and medicated dressings, there is not an established universal *in vitro* wound model. The latter factor is challenged by the fact that non-healing, infected wounds beds display a high variability in terms of tissue pathophysiology, surface abnormalities and polymicrobial contamination (Bowler et al. 2010). In addition, there is restricted information with regards to the amount and the consistency of wound exudate produced from non healing wounds, as exudation varies with wound type, depth, aetiology and healing stage.

The general aim of this project was to formulate and evaluate biopolymeric antimicrobial wafers as a novel technology for infection control in chronic wounds. The work undertaken focused on the antimicrobial efficacy and quantification of the antimicrobial compounds released from the lyophilized matrices of wafers under simulated conditions of exuding wounds. Suitable *in vitro* wound models, existing and original, such as modified disc diffusion, the free stranding dissolution raft (FSDR) and antimicrobial diffusion cell (ADC) were used to assess the efficacy of antimicrobial wafers. Particular emphasis was given to mimicking *in vitro*, conditions of abnormal and contaminated wound exudate and to investigate the activity of antimicrobial compounds released in a sustained fashion. In addition, the effect of gamma-

irradiation, as a well-established sterilisation process, upon the activity, performance and physicochemical properties of antimicrobial wafers and constituent materials was investigated. Moreover, an attempt was made to try to elucidate and understand drug-polymer interactions developed between embedded antimicrobials and selected biopolymers, which play a key role in the general performance of antimicrobial wafers. As a result, this thesis includes novel data conducive with the stated aims as outlined in Chapter 1.

Cohesive and non-friable antimicrobial wafers were successfully formulated using a variety of natural polymers such as xanthan gum (XG), guar gum (GG), sodium alginate (SA) and karaya gum (KAG), impregnated with clinical concentration of either neomycin sulphate (NS), chlorhexidine digluconate (CHD), povidone iodine (PVP-I) or silver sulfadiazine (SS). In addition, binary mixtures of natural polymers led to novel synergistic interactions of gels as reported in Chapter 2 (Table 2.2). The original rheological properties of SA-KAG gel were quantified and the mixture used as a dual polymeric carrier of CHD.

Mixtures of antimicrobial compounds with natural polymers can be compatible or non-compatible. Incompatibility was determined as the formation of polymeric aggregations and the inability of the polymer to form a homogenous gel. For example, XG and SA were found to be incompatible carriers for NS. Incompatibility may be the result of strong attractive and/or strong repulsive interactions developed between mixed compounds. NS is a soluble salt, aqueous solutions of which contain cationic neomycin and anionic sulphate. XG is an anionic polymer, the aqueous solutions of which exhibit phase separation, in the presence of anionic electrolytes, driven by repulsive interactions (Boyd et al. 2009). Similarly, the sodium salt of alginic acid is soluble in water. The presence of oppositely charged electrolytes in the mixed solutions of SA and NS are likely to lead to long-range attractive and/or repulsive interactions that result in aggregation of the polymer. Interestingly, compatible combinations of biopolymers with selected drugs altered the flow behaviours of the gels. This was associated with a considerable increase or decrease in apparent viscosity or yield stress. Rheological measurements undertaken provided a reliable and essential method to quantify the flow properties of controls and antimicrobial pre-lyophilised gels.

The combination of KAG with either NS, CHD, PVP-I or SS led to considerably decreased consistency of the KAG gel. The decrease in consistency was likely associated with interactions developed between KAG and incorporated antimicrobial compounds. Cationic compounds of CHD and NS caused a greater decrease in viscosity of KAG compared to SS and PVP-I. This phenomenon was associated with the profound effect of ionised molecules upon the acetylated residues of complex KAG, which have been reported to play a key role in formation of the 3-D gel network of KAG (De Brito et al. 2005). Previous studies have also reported the 'thinning' effect of electrolytes upon the flow behaviour of KAG (De Brito et al. 2005).

Although, reduced consistency of KAG antimicrobial gel was expected to be associated with an increased expansion ratio of the wafers, that was not apparent in the case of KAG antimicrobial wafers tested in a modified disc diffusion assay. The expansion of KAG antimicrobial wafers on a seeded agar substrate was mainly governed by equilibrium conditions created in the incubated Petri dish. The main factors that influence the expansion of wafers include hydrophilicity, rate of hydration, rate of evaporation, polymer chain entanglements developed at the interface of wafer and gel substrate and drug-polymer interactions (n.b. when referring to such interactions, the term 'drug' may be conveniently substituted for 'antimicrobial compound').

The incorporation of CHD within the biopolymeric matrices of SA, XG and SA-KAG generally improved the flow properties of the gels. In particular, the combination of CHD with SA or binary combination of SA-KAG led to a considerable increase in apparent viscosity and yield stress, respectively. Improved flow properties of pre-lyophilised gels of SA, XG and SA-KAG were associated with a notable decrease in the expansion ratio of CHD wafers. Similar behaviour for SA and XG lyophilised formulations, rheological properties of which were improved with additions of methylcellulose (MC), was observed by Matthews *et al.* (2005). These results suggest that flow behaviour of pre-lyophilised gels is directly related to the expansion ratio of the re-hydrated wafer. In addition, enhanced rheological properties of an antimicrobial gel may prove beneficial for the *in vivo* performance of the antimicrobial wafer. It has been reported that enhanced flow behaviour of polymeric carriers generally ensures prolonged retention times at the site of

application, and accurately delivered doses of therapeutic agents, hence improved efficacy (Andrews and Jones 2006).

Analysis of adhesive properties of lyophilised wafers were undertaken using a soft, modified agar surface prepared with the same quantities of sodium, calcium and chloride electrolytes found in wound exudate. Work of adhesion of KAG wafers was similar for all articles and range from 0.27 ± 0.016 – 0.37 ± 0.022 N.mm, where antimicrobial wafers exhibited slightly lower values compared to controls. It was evident that the incorporation of antimicrobials caused a drop in viscosity and a significant decrease in tensile stress (peak detachment force/cm²) for the medicated wafers, in particular for PVP-I, compared to controls, as reported in Chapter 2 (Figure 2.8). These results suggest that a smaller force was required to detach antimicrobial wafers from the model surface; however, the drop in viscosity of KAG-antimicrobial gels was not proportional to the reduced tensile strength exhibited from the antimicrobial KAG wafers. Other factors such as porosity (matrix microstructure) and wettability can also influence adhesion of wafers. Although all KAG wafers demonstrated highly porous microstructures, visualised using scanning electron microscopy (S.E.M), there was an apparent difference between polymeric matrices containing different antimicrobials. The matrix of KAG impregnated with 1.0 % PVP-I, in particular, demonstrated small and semi-formatted pores. The distinctive morphology of the microstructure of PVP-I wafers was likely due to the presence of additives with cryoprotective properties such as glycerol.

Although the incorporation of CHD within the matrix of different biopolymers generally improved the rheological properties of the gels, adhesive properties (work of adhesion and tensile strength) of CHD wafers were slightly decreased compared to CHD-free wafers. These results suggest that the embedded CHD had a considerable affect on the wettability of the biopolymers. Analysis of the water uptake capacity undertaken with the FSDR, as reported in Chapter 4 (Figure 4.5), demonstrated that CHD-loaded wafers had a decreased ability to retain water compared to CHD-free matrices. Visualisation of the geometry of CHD, using molecular modelling studies, indicated a symmetrical 'Z' shape compound, which could be easily hooked between flexible and interactive branches of biopolymers (Figure 7.1). This plausible ability of CHD may have a profound affect on the 3-D gel network, by

minimising the volumetric capacity of compartments formed by the cross-linking and therefore the ability of the polymer matrix to retain water.

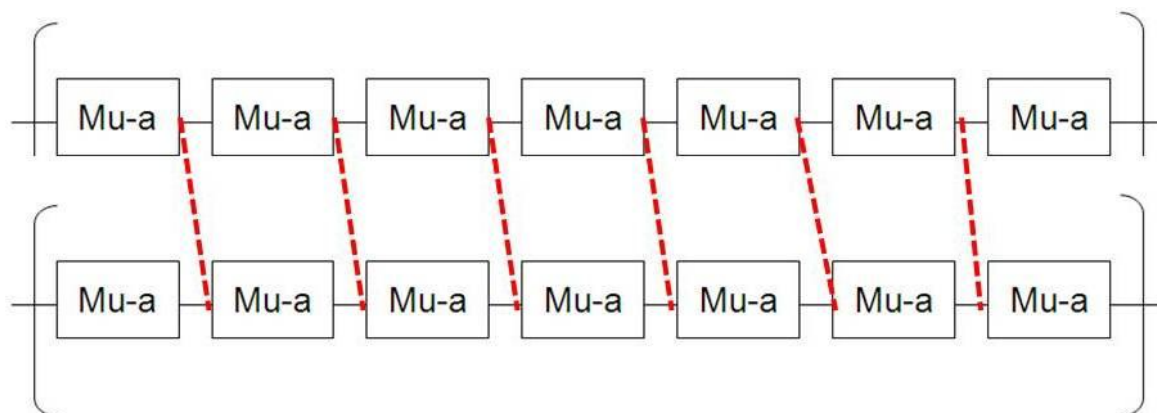


Figure 7.1 A plausible block configuration of sodium alginate consisting of 1,4-linked-β-D mannuronic acid residues (Mu-a), also known as polymannuronate, linearly linked. (---) represent the interlinked CHD between linear chains of SA. This ability of CHD is likely mediated from the 'Z' shape geometry of the cationic drug which can be electrostatically attracted to the negatively charged residues of mannuronic acid. The interlinking of the SA network by CHD induced approximately a 2-fold increase in the consistency of SA gel.

CHD interlinked between the polymeric chains of the carrier probably has a profound affect on the mobility of these chains. In addition, CHD impregnated wafers demonstrated smaller expansion ratios than controls. This phenomenon was more apparent for gamma-irradiated CHD wafers. Even though gamma-irradiation totally degraded KAG polymer, the expansion ratio of CHD wafers was generally smaller compared to irradiated controls, reported in Chapter 5 (Figure 5.9). It was evident from the rheological analysis of consistency, plotted as 'ln of shear rate vs. ln of shear stress' reported in Chapter 5 (Figure 5.7-8), that the drop in consistency for post-lyophilised irradiated CHD gels was smaller than the CHD-free, post-lyophilised, irradiated gels. These results indicate that CHD can generally withstand irradiation and

both the geometry and cationic nature of the incorporated drug play key roles in the performance of the polymeric carrier.

Analysis of the release profiles of CHD wafers and gels demonstrated that neither gels nor wafers released 100 % of the incorporated drug. Although this release behaviour was partly due to the equilibrium conditions (e.g. humidity, water uptake and evaporation) created in the FSDR, drug-polymer interaction played a key role in the amounts of CHD released. It was expected that gels would demonstrate a faster release of CHD than wafers, but that was not apparent except in the case of GG gel. Rheological analysis of pre-lyophilised gels of GG demonstrated that the incorporation of CHD had a minor effect on the flow behaviour of the gum. This may indicate that the non-ionic polymer of GG offers a weaker interaction with CHD. The burst release of CHD from the strong gel network of GG (viscosity = 65.49 Pa.s, yield stress = 93.63 Pa) indicates that drug polymer interactions play an important role in the amounts of antimicrobial released and therefore in the activity the antimicrobial matrix.

Analysis of release profiles of SA wafers and gels loaded with CHD demonstrated the restricted ability of SA-matrix to release the incorporated drug. The total amount of CHD accumulated within 24 hours did not exceed 10.7 ± 2.07 % and 3.5 ± 0.04 % for SA-CHD gel and wafer, respectively. The bulk of CHD remained entrapped in the SA polymeric matrix. Inhibition ratios of CHD-loaded wafers further support this scenario, where the CHD impregnated matrices of SA and SA-KAG demonstrated significantly decreased antimicrobial activities, compared with GG, XG and KAG. However, the decrease in inhibition ratios of SA and SA-KAG wafers was affected to some extent by the small expansion that the latter wafers exhibited on the seeded agar surface. The significant, yet moderate correlation ($R^2 = 0.5882$) between expansion and inhibition ratios of CHD wafers indicates that the zone of inhibition created from the diffusion of the drug is proportional to the ability of the polymeric carrier to expand. Therefore, drug-polymer interactions developed within the matrices of antimicrobial wafers play a primary role in both performance and activity of the specimens.

The efficacy of lyophilised wafers is of prime importance, as antimicrobial wafers aim to control and inhibit microbial bioburden in suppurating wounds. The modified disc diffusion assay is a reliable, yet semi-

quantitative method for the initial investigation of the flow and antimicrobial activity of antimicrobial wafers. All wafers demonstrated antimicrobial activity against common wound pathogens, however, the efficacy of antimicrobial varies with the potency of compounds and the intrinsic sensitivity of different microbial species. Interestingly, SS and PVP-I, two potent and rapid bactericidal compounds, exhibited a moderate antimicrobial activity *in vitro* compared to CHD and NS. These results suggest that *in vitro*, other parameters such as the solubility of the compound and the presence of organic nutritional supplements play a detrimental role in the activity of the antimicrobial compounds tested. For instance, the antimicrobial activity of PVP-I was minor against Gram negative species of *E. coli* and *P. aeruginosa* and recent studies have reported that some iodine dressings such as Iodozyme were not effective *in vitro*, when tested against either *E. coli*, *S. aureus* or *P. aeruginosa* in a disc diffusion method (Bradshaw 2011). Other authors have also reported the quenching activity of organic matter upon PVP-I (Messenger et al. 2001). On the other hand, *in vivo*, iodophores and/or iodine dressings are generally reported as very effective antimicrobial treatments in wound management. For example, Fumal et al. (2002) reported that the application of hydrocolloid dressings impregnated with broad spectrum antimicrobial compounds such as silver sulfadiazine (SS), chlorhexidine digluconate (CHD) and povidone iodine (PVP-I), demonstrated similar antimicrobial activity when reducing the bacterial load in chronic leg ulcers. These topical antimicrobials showed different levels of toxicity upon a variety of dermal cells, however, PVP-I was the most effective compound with regards to overall clinical effect (Fumal et al. 2002).

The antimicrobial diffusion cell was designed in order to elucidate and understand the activity of the slowly released broad spectrum antimicrobials such as NS, PVP-I, CHD and SS against a common and dangerous pathogen such as MRSA. The activity of antimicrobials was assessed in the presence of a pseudo-exudate containing similar quantities of electrolytes and protein as found in wound exudate. Data obtained, as reported in Chapter 3 (Figure 3.10), showed that the activity of antimicrobials is altered in the presence of these additives. CHD and PVP-I showed an impaired antimicrobial activity in the presence of protein. In contrast SS and NS enhanced their activity in the pseudo-exudate. The antimicrobial potency of PVP-I was totally lost. These

results are in agreement with previous authors such as Messenger *et al.* (2001) and Pitten *et al.* (2003) who reported the inhibition effect of organic matter on the antimicrobial activity of some antimicrobial compounds including PVP-I and CHD. In addition, these results explained the tolerant nature of *P. aeruginosa* against PVP-I. This opportunistic Gram-negative bacterium possesses the ability to produce a protein layer (Hardegger *et al.* 1994) which makes it able to withstand the lethal effect of PVP-I, as the latter antimicrobial is neutralised in the presence of proteins. However, these results lead to the question as to what makes iodophoric dressings an effective therapy for chronic, non-healing wounds? Recently, Eming *et al.* (2006) have reported the novel role of PVP-I in inhibiting the excessive protease levels in wound fluids obtained from venous ulcers. The latter authors demonstrated that the affinity of PVP-I to proteins leads to inhibition of plasmin and elastase activity, re-establishing the balance between promoters and inhibitors in chronic wound beds. These results suggest that the assessment of protein levels and identification of microbial species in open non-healing ulcers, prior to application of antimicrobial regimes, are important factors for effective treatments.

Despite its poor solubility, silver sulfadiazine (SS) wafers produced a considerable decrease of MRSA populations (approximately 99 %) at 24 hours, when tested with antimicrobial diffusion cell (ADC) assay. It was apparent from the results presented in Chapter 3 (Figure 3.8, 10) that the abundance of chloride ions and protein enhance the solubility of SS, releasing sulphonamide. These results were in agreement with Tsipouras *et al.* (1995) and Fox and Modak (1974) who have reported that disassociation of SS is improved in the presence of human serums that contain both chloride ions and proteins. In addition, these data clearly explain the effect of SS impregnated dressings in burns. The activity of SS dressings in burns is associated with large volumes of wound fluid containing high concentrations of proteins. It has been reported that the albumin fraction in wound fluids exuding from burns range from 69 – 86 % within 32 hours post injury (Lehnhardt *et al.* 2005). The abundance of wound exudate rich in proteins absorbed by SS impregnated dressings, enhance the disassociation of SS and therefore increases the antimicrobial activity of the dressings.

The volume of exudate produced by chronic wounds, protein content and type of microbial species are some of the most important parameters that

should be known prior to the application of any suitable topical antimicrobial therapy. These factors play an important role in the quantities and activity of antimicrobials released from the polymeric dressings. In addition, the use of known quantities of broad spectrum topical antimicrobial compounds is essential in order to inhibit a polymicrobial flora usually present in the majority of chronic wounds. Although the release profiles of CHD from biopolymeric wafers was minimal and ranged from 3.5 ± 0.001 – 17.4 ± 0.39 %, the accumulated concentration exceeded the MIC/MBC values of CHD against the majority of tested strains. Even though most of the antimicrobial remained within the swollen wafer matrix, that in itself did not undermine the use of antimicrobial wafers as effective and contemporary potential dressings, especially when the self-adhesive properties of such formulations are appreciated. In addition, release of small, yet effective quantities of broad spectrum antimicrobials may prove beneficial for dermal tissue, as precise and reduced amounts can minimise the adverse cytotoxic effect of such compounds.

The restoration of broken and infected skin is not an easy task as many factors (internal and external) interplay. Although the majority of modern dressings, including antimicrobial lyophilised wafers, can provide many advantages of the ideal dressing, treatment of chronic wounds will continue to remain a challenge for physicians, formulation scientists and microbiologists. Multidisciplinary approaches to wound management may provide novel combination treatments of therapeutic compound and /or new materials with poly-therapeutic properties (e.g. both pharmacological and antimicrobial). A profound understanding of the healing process and molecular and physiological mechanisms that govern it; the role of microorganisms in the wound bed, in association with available, effective therapeutic agents and unquestionable evidence of their activity in chronic wound therapy; will ensure the success of research in this challenging and interesting area.

7.2 Conclusions and future work

7.2.1 Conclusions

Cohesive, non-friable lyophilised antimicrobial wafers were successfully formulated using a variety of biopolymers miscible with known broad spectrum antimicrobial compounds. The efficacy of antimicrobial wafers was demonstrated *in vitro*, under simulated conditions of suppurating wounds, using modified disc diffusion and an original antimicrobial diffusion cell (ADC). The ADC was shown to be a superior method to disc diffusion for assessing the efficacy of slowly released antimicrobials. It was clear that the activity of antimicrobial compounds changed in the presence of pseudo-exudate. The presence of protein and electrolytes inhibited the antimicrobial activity of PVP-I and CHD, while enhancing the activity of SS and NS against MRSA. The performance of antimicrobial wafers in terms of expansion and release of impregnated drug depended on drug-polymer interactions developed within the gel structures. Gamma-irradiation affected considerably the physicochemical properties of the majority of polymers, except XG, but did not generally affect the antimicrobial properties of lyophilised wafers. However, degraded polymer matrices considerably influenced the general performance of antimicrobial wafers in terms of expansion and faster release of the impregnated drug. Although a variety of methods and disciplines were utilised in the investigation and evaluation of novel antimicrobial wafers, additional research is required to elucidate issues with regards the sequestration and bactericidal activity within the swollen wafer matrix. Finally, additional investigations are required to elucidate the synergistic interactions between natural polymers and antimicrobial compounds ('drug-polymer interactions'). The physical stability of lyophilised wafers is also of great interest.

7.2.2 Future work

(a) To quantify the amount of bacteria absorbed by lyophilised matrices. Bowler *et al.* (1999) has used an *in vitro* wound model to quantify the bacterial sequestering capacity of absorbent dressings.

(b) To examine bacterial immobilisation within the swollen matrix of biopolymeric formulations, medicated and/or non medicated. Walker *et al.* (2003) have visualised encapsulated bacterial populations within carboxymethylated cellulose (AQUACEL[®]) and alginate dressings using scanning electron microscopy (S.E.M). It is necessary, to visualise entrapped populations of common wound pathogens and to assess the bactericidal activity of biopolymeric dressings (with or without containment of antimicrobial) upon immobilised microorganisms. Newman *et al.* (2006) investigated the efficacy of Hydrofiber[®] wound dressings, which had absorbed different concentrations of *S. aureus* and *P. aeruginosa*, using rapid confocal laser scanning microscopy (RCLSM) and BacLight[™] fluorescent dyes.

(c) Analysis of the conformability and occlusiveness of biopolymeric lyophilised wafers using an *in vitro* shallow microbial wound model (Bowler *et al.* 2010).

(d) Analysis of the elasticity of wafers prepared with different biopolymers and the effect of impregnated antimicrobials on the elasticity and conformability of lyophilised wafers.

(e) Physicochemical characterisation of polymer-polymer and polymer-drug interactions using Fourier transform infrared spectroscopy (FTIR) and Fourier transform Raman spectroscopy (FTRS). Sarisuta *et al.* (1999) and Puttipatkhachorn *et al.* (2001) have used FTIR to investigate interactions developed between impregnated drugs and polymeric vehicles.

(f) To investigate the physical stability of lyophilised formulations at different temperatures and humidities. Physical stability of lyophilised formulations can be assessed in environmental simulation chambers or by dynamic vapour sorption (DVS) methods (Airaksinen *et al.* 2005). The equilibrium moisture levels at which lyophilised wafers collapse may have implications for stability on storage.

REFERENCES

A

ABAD, V. L., et al., 2003. Properties of radiation synthesised PVP-kappa carrageenan hydrogel blend. *Radiation Physics and Chemistry*, 68 (4), pp. 901-908

ABD ALLA, G. A., et al., 2007. Structure and swelling-release behaviour of poly (vinyl pyrrolidone) (PVP) and acrylic acid (AAc) copolymer hydrogels prepared by gamma irradiation. *European Polymer Journal*, 43 (7), pp. 2987-2998

AGREN, M. S., 1996. Four alginate dressings in the treatment of partial thickness wounds: a comparative study. *British Journal of Plastic Surgery*, 49 (2), pp. 129-134

AGREN, M. S., Mertz, M. P., FRANZEN, L., 1997. A comparative study of three occlusive dressings in the treatment of full-thickness wounds in pigs. *Journal of the American Academy of Dermatology*, 36 (1), pp. 53-8

AIRAKSINEN, S., et al., 2005. Role of water in the physical stability of solid dosage formulations. *Journal of Pharmaceutical Science*, 94 (10), pp. 2147-2165

ALANDEJANI, T., et al., 2009. Effectiveness of honey on *Staphylococcus aureus* and *Pseudomonas aeruginosa* biofilms. *Otolaryngology-Head and Neck Surgery*, 141 (1), pp. 114-118

AMSDEN, B., 1998. Solute diffusion within hydrogels. Mechanisms and models. *Macromolecules*, 31 (23), pp. 8382-8395

ANDREWS, P.G. and JONES, S. D., 2006. Rheological characterisation of bioadhesive binary polymeric systems designed as platforms for drug delivery implants. *Biomacromolecules*, 7 (3), pp. 899-906

AULTON, E. M., 2002. *Pharmaceutics: The science in dosage form design*. 2nd edition. London: Churchill Livingstone. pp. 49-50

AYELLO, A. E and CUDDIGAN, E. J., 2004. Conquer chronic wounds with wound bed preparation. *The Nurse Practitioner*, 29 (3), pp. 8-25

B

BAIRD, D., et al., 2006. Guidance for the hospital management of methicillin-resistant *Staphylococcus aureus*. The Royal College of Physician of Edinburgh, March, pp. 1-15

BALODA, S., et al., 2008. Guide to irradiation and sterilisation validation of single-use bioprocess system. *BioProcess International*, Supplement, pp. 10-22

BANI-JABER, A., et al., 2009. Investigation of drug polymer interaction: evaluation and characterisation of diclofenac-chitosan co-precipitate. *Jordan Journal of Pharmaceutical Sciences*, 2 (2), pp. 140-148

- BARRY, A. J., 1986. Procedure for testing antimicrobial agents in agar media: Theoretical considerations. In: LORIAN, V., eds. *Antibiotics in laboratory medicine*. 2nd ed. USA: Waverly Press, Inc. pp. 2-26
- BEDU-ADDU, K.B., 2004. Understanding lyophilisation formulation development. *Pharmaceutical Technology Lyophilisation*, www.pharmatech.com, pp. 10-18
- BENAMER, S., et al 2006. Synthesis and characterisation of hydrogels based on poly(vinyl pyrrolidone). *Nuclear Instruments and Methods in Physics Research B*, 248 (2), pp. 284-290
- BERKELMAN, L. R., et al., 1984. Intrinsic bacterial contamination of a commercial iodophor solution: investigation of the implicated manufacturing plant. *Applied and Environmental Microbiology*, 47 (4), pp. 752-756
- BHENDE, S. and SPANGLER, D., 2004. In vitro assessment of Chlorhexidine gluconate-impregnated polyurethane foam antimicrobial dressings using zone of inhibition assay. *Infection Control and Hospital Epidemiology*, 25 (8), pp. 665-667
- BLAINE, G. M., 1946. Experimental observations on absorbable aliginate products in surgery. *Annals of Surgery*, 125 (1), pp. 102-114
- BOATENG, S. J., et al., 2007. Wound healing dressings and drug delivery systems: a review. *Journal of Pharmaceutical Science*, 97 (8), pp. 2892-2923
- BOATENG, S. J., et al., 2010. Characterisation of freeze-dried wafers and solvent evaporated films as potential drug delivery systems to mucosal surfaces. *International Journal of Pharmaceutics*, 389 (1-2), pp. 24-31
- BOWLER, G. P., et al., 1999. Infection control properties of some wound dressings. *Journal of Wound Care*, 8 (10), pp. 499-502
- BOWLER, P., et al 2010. Dressing conformability and silver containing wound dressings. *Wounds UK*, 6 (2), pp.14-20
- BOWLER, P.G., DUERDEN, I. B., ARMSTRONG, G. D., 2001. Wound microbiology and associated approaches to wound management. *Clinical Microbiology Reviews*, 14 (2), 244-269
- BOYD, J. M., et al., 2009. Strand-like phase separation in mixtures of xanthan gum with anionic polyelectrolytes. *Food Hydrocolloids*, 23 (8), pp. 2458-2467
- BRADSHAW, E. C., 2011. An in vitro comparison of the antimicrobial activity of honey, iodine and silver wound dressings. *Bioscience Horizons*, In Press, pp. 1-10.
- BRANNON-PEPPAS, L., 1997. Biomaterials: Polymers in controlled drug delivery. *Medical plastics and Biomaterials Magazine*, November, <http://www.devicelink.com/mpb/archive/97/11/003.html>

BREDENBERG, S. and NYSTROM, C., 2003. In vitro evaluation of bioadhesion in particulate systems and possible improvement using interactive mixtures. *Journal of Pharmacy and Pharmacology*, 55 (2), pp. 169-177

BULLEN, C. E., et al., 1995. Tissue inhibitors of metalloproteinases-1 decreased and activated gelatinases are increased in chronic wounds. *The Society for Investigative Dermatology*, 104 (2), pp. 236-240

BURKS, I. R., 1998. Povidone-Iodine solution in wound treatment. *Physical Therapy*, 78 (2), pp. 212-218

C

CAIRNS, D., et al., 2002. Molecular modelling and cytotoxicity of substituted anthraquinones as inhibitors of human telomerase. *Bioorganic & Medicinal Chemistry*, 10 (3), pp. 803-807

CHAN, C.W.D., et al., 2007. Maggot debridement therapy in chronic wound care. *Hong Kong Medical Journal*, 13 (5), pp. 382-6

CHURCH, D., et al., 2006. Burn wound infections. *Clinical Microbiology Review*, 19 (2), pp. 403-434

CLOUGH, G., and NOBLE, M., 2003. Microdialysis - a model for studying chronic wounds. *Lower Extremity Wounds*, 2 (4), pp. 233-239

COLLIER, M., 2004. Recognition and management of wound infections. *World Wide Wounds*, www.worldwildwounds.com

COOPER, R. A., MOLAN, P.C., HARDING, K.G., 1999. Antibacterial activity of honey against strains of *Staphylococcus aureus* from infected wounds. *Journal of the Royal Society of Medicines*, 92 (6), pp. 283-285

COOPER, R., 2004. A review of the evidence for the use of topical antimicrobial agents in wound care. *World Wide Wounds*, www.worldwildwounds.com

COX, J. P., et al., 1999. Development and evaluation of a multiple-unit oral sustained release dosage form for S (+)-ibuprofen: preparation and release kinetics. *International Journal of Pharmaceutics*, 193 (1), pp. 73-84

CRAIG, W.A. and SUH, B., 1986. Protein binding and the antimicrobial effects: Methods for the determination of protein binding. In: LORIAN, V., eds. *Antibiotics in laboratory medicine*. 2nd ed. USA: Waverly Press, Inc. pp. 447-514

CUSHNIE, T. P. T. and LAMB, J. A., 2005. Antimicrobial activity of flavonoids. *International Journal of Antimicrobial Agents*, 26 (5), pp. 343-356

CUTTING, F. K., 2003. Wound healing, bacteria and topical therapies. *European Wound Management Association Journal*, 3 (1), pp. 17-19.

CUTTING, K. F., 2003. Wound exudate: composition and functions. *British Journal Community Nursing*, 8 (9) pp. 4-9

CUTTING, K. F., AND WHITE, R. J., 2002. Maceration of the skin and wound bed 1: its nature and causes. *Journal of Wound Care*, 11 (7), pp. 275-8

D

DANARAO, A., et al., 2011. Formulation and evaluation of once a day matrix tablets of cefixime trihydrate. *International Journal of Pharmaceutical Sciences*, 3 (1), pp. 1146-1151

DE BRITO, C. A., et al., 2005. Dynamic rheological study of *Sterculia striata* and karaya polysaccharides in aqueous solution. *Food Hydrocolloids*, 19 (5), pp. 861-867

DESAI, G.K. and PARK, J. H., 2006. Study of gamma-irradiation effects on chitosan microparticles. *Drug Delivery*, 13 (1), pp. 39-50

DHARMARAJAN, T. S and UGALINO, T, J., 2002. Pressure ulcer: clinical features and management. *Hospital Physician*, pp. 64-71

DICKINSON, E., 1998. Stability and rheological implications of electrostatic milk protein-polysaccharide interactions. *Trends in Food Science and Technology*, 9 (10), pp. 347-354

DIEGELMANN, R. F., and EVANS, C. M., 2004. Wound healing: an overview of acute, fibrotic and delayed healing. *Frontiers in Bioscience*, 9 (1), pp. 283-289

DOREMUS, H. R. and JOHNSON, P., 1958. The interaction of small ions with proteins from electrical conductance and transference experiments. *Journal of Physical Chemistry*, 62 (2), pp. 203-209

E

ELSTON, J.W.T., and BARLOW, G.D., 2009. Community-associated MRSA in the United Kingdom. *Journal of Infection*, 59 (3), pp. 149-155

EMING, A. S., et al., 2006. A novel property of Povidone-iodine: inhibition of excessive protease levels in chronic non-healing wounds. *Journal of Investigative Dermatology*, 126 (12), pp. 2731-2733

ENOCH, S and PRICE, P., 2004. Cellular, molecular and biochemical differences in the pathophysiology of healing between acute wounds, chronic wounds and wounds in the aged. *World Wide Wounds*, www.worldwildwounds.com

F

FALANGA, V., 1993. Chronic wounds: pathophysiology and experimental considerations. *The Journal of Investigative Dermatology*, 100 (3), pp. 721-725

FALANGA, V., 2005. Wound healing and its impairment in the diabetic foot. *Lancet*, 366 (12), pp. 1736-43

FAYDI, E., ANDRIEU, J., LAURENT, P., 2001. Experimental study and modelling of the ice crystal morphology of model standard ice cream. Part I: direct

characterisation method and experimental data. *Journal of Food Engineering*, 48 (4), pp. 283-291

FLIKKEMA, E., et al., 1998. Temperature modulated calorimetry of glassy polymers and polymer blends. *Macromolecules*, 31 (3), pp. 892-898

FORD, J., 2004. Sterile pharmaceutical products. In: DENYER, P. S., HODGES, A. N., GORMAN, P. S., eds . Hugo and Russell's Pharmaceutical microbiology, 7th ed. Oxford: Blackwell Science. pp. 323-345

FOX, L. C. and MODAK, M. S., 1974. Mechanism of silver sulfadiazine action on burn wound infection. *Antimicrobial Agents and Chemotherapy*, 5 (6), pp. 582-588

FRANKS, F., 1990. Freeze drying: from empiricism to predictability. *Cryo-Letters*, 11 (7), pp. 93-110

FRANKS, J. P., and MOFFATT, J. C., 1999. Quality of life issues in chronic wound management. *British Journal of Community Nursing*, 4 (6), pp. 283-289

FRAUENFELDER, H. and WOLYNES, G. P., 1994. Biomolecules: where the physics of complexity and simplicity meet. *Physics Today*, 47 (2), pp. 58-64

FRAZEE, W. F., et al., 2005. High prevalence of methicillin-resistant *S. aureus* in emergency department skin and soft tissue infections. *Annals of Emergency Medicine*, 45 (3), pp. 311-320

FUMAL, I., et al., 2002. The beneficial toxicity paradox of antimicrobials in leg ulcer healing impaired by a polymicrobial flora: a proof of concept study. *Dermatology*, 204 (1), pp. 70-74

G

GAO, F., et al., 2010. Hyaluronan oligosaccharides promote excisional wound healing through enhanced angiogenesis. *Matrix Biology*, 29 (2), pp. 107-116

GASAYMEH, S. S., et al., 2010. Synthesis and characterisation of silver/polyvinylpyrrolidone (Ag/PVP) nanoparticles using gamma irradiation technique. *African Physical Review*, 4 (6), pp. 31-41

GIANNELLI, M., et al., 2008. Effect of chlorhexidine digluconate on different cell types; a molecular and ultrastructural investigation. *Toxicology in Vitro*, 22 (2), pp. 308-317

GIMENEZ-MARTIN, E., et al., 2009. Adsorption of chlorhexidine onto cellulosic fibers. *Cellulose*, 16 (3), pp. 467-479

GJØDSBØL, K., et al., 2006. Multiple bacterial species resides in chronic wounds; a longitudinal study. *International Wound Journal*, 3 (3), pp. 225-31

GRZYBOWSKI, J., ANTOS, M., TRAFNY, A. E., 1996. A simple in vitro model to test the efficacy of antimicrobial agents released from dressings. *Journal of Pharmacological and Toxicological Methods*, 36 (2), pp. 73-76

H

HADJIISKI, O.G. and LESSEVA, M. I., 1999. Comparison of four drugs for local treatment of burn wounds. *European Journal of Emerging Medicine*, 6 (1), pp. 41-7

HAMILTON-MILLER, J.M.T. and SHAH, S., 1996. A microbiological assessment of silver fusidate, a novel topical antimicrobial agent. *International Journal of Antimicrobial Agents*, 7 (2), pp. 97-99

HARDEGGER, M., et al., 1994. Cloning and heterologous expression of a gene encoding an alkane-induced extracellular protein involved in alkane assimilation from *Pseudomonas aeruginosa*. *Applied and Environmental Microbiology*, 60 (10), pp. 3679-3687

HEALY, B. and FREEDMAN, A., 2007. ABC of wound healing. *British Medical Journal*, 332 (8), pp. 838-841

HEUN, G., LAMBOV, N., GRÖNING, R., 1998. Experimental and molecular modelling studies on interactions between drugs and Eudragit® RL/RS resin in aqueous environment. *Pharmaceutica Acta Helvetiae*, 73 (1), pp. 57-62

HIRSCH, T., et al., 2010. Evaluation of toxic side effects of clinically used skin antiseptics *in vitro*. *Journal of Surgical Research*, 164 (2), pp. 344-350

HOWELL-JONES, R.S., et al., 2005. A review of the microbiology and, antibiotic usage and resistance in chronic skin wounds. *Journal of Antimicrobial Chemotherapy*, 55 (2), pp. 143-149

I

INABA, A. and ANDERSSON, O., 2007. Multiple glass transitions and two steps crystallisation for the binary system of water and glycerol. *Thermochimica Acta*, 461 (1-2), pp. 44-49

INTERNATIONAL SPECIALITY PRODUCTS, 2004. PVP-Iodine; Povidone iodine antiseptic agent. pp. 1-30

IP, M., et al., 2006. Antimicrobial activity of silver dressings: an *in vitro* comparison. *Journal of Medical Microbiology*, 55 (1), pp. 59-63

J

JAMES, G. A., et al., 2008. Biofilms in chronic wounds. *Wound Repair and Regeneration*, 16 (1), pp. 27-44

JONEIDI-JAFARI, H., et al., 2009. The qualitative and quantitative analysis of protein substitution in human burn wounds. *Journal of Plastic Surgery*, 9 (29), pp. 383-399

JONES, A. and VAUGHAN, D., 2005. Hydrogel dressings in the management of a variety of wound types: a review. *Journal of Orthopaedic Nursing*, 9 (1), pp. S1-S11

JULL, A. B., RODGERS, A., WALKER, N., 2009. Honey as a topical treatment for wounds (Review). *Cochrane Wound Group*, 4, pp. 1-49

JULL, A., et al., 2008. Randomised clinical trial of honey-impregnated dressings for venous leg ulcers. *British Journal of Surgery*, 95 (2), pp. 175-182

JUDSON, S. R., 1992. Teaching polymers to fold. *The Journal of Physical Chemistry*, 96 (25), pp. 10102-10104

JURCZAK, F., et al., 2007. Randomised clinical trial of Hydrofiber dressing with silver versus povidone-iodine gauze in the management of open surgical and traumatic ulcer. *International Wound Journal*, 4 (1), pp. 66-76

JURJUS, A., et al., 2006. Pharmacological modulation of wound healing in experimental burns. *Burns*, 33 (7), pp. 892-907

K

KARAVAS, E., GEORGARAKIS, E., BIKIARIS, D., 2006. Application of PVP/HPMC miscible blends with enhanced mucoadhesive properties for adjusting drug release in predictable pulsatile chronotherapeutics. *European Journal of Pharmaceutics and Biopharmaceutics*, 64 (1), pp. 115-126

KAUTZKY, F., et al., 1996. In vitro cytotoxicity of antimicrobial agents to human keratinocytes. *Journal of the European Academy of Dermatology and Venereology*, 6 (2), pp. 159-166

KAVANAGH, M. G. and ROSS-MURPHY, B. S., 1998. Rheological characterisation of polymer gels. *Polymer Science*, 23, pp. 533-562.

KEAST, D.H., and ORSTED, H., 1998. The basic principles of wound care. *Ostomy Wound Management*, 44 (8), pp. 24-8, 30-1

KELLER, L. K. and FENSKE, A. N., 1998. Use of vitamins A, C, and E and related compounds in dermatology: a review. *Journal of the American Academy of Dermatology*, 39 (1), pp. 611-25

KESWANI, N., CHOUDHARY, S., and KISHORE, N., 2010. Interaction of weakly bound neomycin and lincomycin with bovine and human serum albumin: biophysical approach. *The Journal of Biochemistry*, 148 (1), pp. 71-84

KIRKETERP-MØLLER, K., ZULKOWSKI, K., and JAMES, G., 2011. Chronic wound colonization, infection and biofilms. In: BJARNSHOLT, T., OESTRUP, P. J., and MOSER, C. eds. *Biofilm Infection*, 1st ed. New York: Springer Science + Business Media, LLC. pp. 11-24

KING, K. and GRAY, R., 1993. The effect of gamma irradiation on guar gum, locust bean gum, gum tragacanth and gum karaya. *Food Hydrocolloids*, 6 (6), pp. 559-569

KUMAR, S. M., et al., 2010. Triphala incorporated collagen sponge-a smart biomaterial for infected dermal wound healing. *Journal of Surgical Research*, 158 (1), pp. 162-170

KWAKMAN, P. H., et al., 2010. How honey kills bacteria. *Federation of American Societies for Experimental Biology*, 24 (7), pp. 2576-82

L

LANDIS, J. S., 2008. Chronic wound infection and antimicrobial use. *Advances in Skin and Wound Care*, 21 (11), pp. 531-540

LAO, L. L., et al., 2011. Modelling of drug release from bulk-degrading polymers. *International Journal of Pharmaceutics*, In Press

LEACH, R. A 1996. Molecular modelling principles and applications. Singapore: Addison Wesley Longman Limited, pp. 1-5, 212-215, 314-386

LEE, C. A., et al., 2005. Reversal of silver sulfadiazine-impaired wound healing by epidermal growth factor. *Biomaterials*, 26 (22), pp. 4670-4676

LEE, W. D., et al., 2003. Effect of γ -irradiation on degradation of alginate. *Journal of Agriculture and Food Chemistry*, 51 (16), pp. 4819-4823

LEE, W. R., et al., 2009. The biological effects of topical alginate treatment in an animal model of skin wound healing. *Wound Repair and Regeneration*, 17 (4), pp. 505-10

LEHNHARDT, M., et al., 2005. A qualitative and quantitative analysis of protein loss in human burn wounds. *Burns*, 31 (2), pp. 159-167

LENGAUER, T. and RAREY, M., 1996. Computational methods for biomolecular docking. *Current Opinion in Structural Biology*, 6 (3), pp. 402-406

LIMOVA, M. and TROYER-CAUDLE, J., 2002. Controlled randomised clinical trial of two hydrocolloid dressings in the management of venous insufficiency ulcers. *Journal of Vascular Nursing*, 20 (1), pp. 22-34

LIPSKY, A. B and HOEY, C., 2009. Topical antimicrobial therapy for treating chronic wounds. *Clinical Practice*, 49 (15), 1541-9

LUGAO, B. A., ROGERO, O. S., MALMONGE, M. S., 2002. Rheological behaviour of irradiated wound dressing poly(vinyl pyrrolidone) hydrogels. *Radiation Physics and Chemistry*, 63 (3-6), pp. 543-546

M

MACKAY, D. and MILLER, L. A., 2003. Nutritional support for wound healing. *Alternative Medicine Review*, 8 (4), 359-377

MAEDA, M., et al., 2001. Sustained release of human growth hormone (hGH) from collagen film and evaluation of effect on wound healing in db/db mice. *Journal of Controlled Release*, 77 (3), 261-272

MAGGI, L., et al., 2004. Polymers-gamma ray interaction. Effects of gamma irradiation on modified release drug delivery systems for oral administration. *International Journal of Pharmaceutics*, 269 (2), pp. 343-351

- MANNELLO, F., and RAFFETTO, D. J., 2011. Matrix metalloproteinase activity and glycosaminoglycans in chronic venous disease: the linkage among cell biology, pathology and translational research. *American Journal of Translational Research*, 3 (2), pp. 149-158
- MATHAKARI, L. N., BHORASKAR, N. V., DHOLE, D. S., 2010. Co-60 gamma radiation assisted diffusion of iodine in polypropylene. *Nuclear Instruments and Methods in Physics Research B*, 268 (17-18), pp. 2750-2757
- MATTHEWS, K. H., et al., 2005. Lyophilised wafers as a drug delivery system for wound healing containing methylcellulose as a viscosity modifier. *International Journal of Pharmaceutics*, 289 (1-2), pp. 51-62
- MATTHEWS, K. H., et al., 2006. Gamma-irradiation of lyophilised wound healing wafers. *International Journal of Pharmaceutics*, 313 (1-2), pp. 78-86
- MCDONNELL, G. and RUSSELL, D.A, 1999. Antiseptics and disinfectant: activity, action and resistance. *Clinical Microbiology Review*, 12 (1), pp. 147-179
- MCINNES, F., BAILLIE, J.A., STEVENS, E. N., 2007. The use of simple dynamic mucosal models and confocal microscopy for the evaluation of lyophilised nasal formulations. *Journal of Pharmacy and Pharmacology*, 59 (6), pp. 759-767
- MESSAGER, S., et al., 2001. Determination of the antimicrobial efficacy of several antiseptics tested on skin by an 'ex-vivo' test. *Journal of Medical Microbiology*, 50 (3), pp. 284-292
- MIAN, M., BEGHE, F., MIAN, E., 1992. Collagen as a pharmacological approach in wound healing. *International Journal of Tissue Reaction*, 14 (1-9), pp. 1-9
- MINGALEEV, F. S., et al., 2002. Non-linearity-induced conformational instability and dynamics in biopolymers. *Europhysics Letters*, 59 (3), pp. 403-409
- MIYAMOTO-SHINOHARA, Y., et al., 2008. Survival of freeze-dried bacteria. *Journal of General Applied Microbiology*, 54 (1), pp. 9-24
- MIYAMOTO-SHINOHARA, Y., et al., 2010. Survival of yeast stored after freeze-drying or liquid drying. *Journal of General Applied Microbiology*, 56 (2), pp. 107-119
- MOLAN, C. P., 2001. Honey as a topical antimicrobial agent for treatment of infective wounds. *World Wide Wounds*, www.worldwildwounds.com
- MUSTOE, T. 2004. Understanding chronic wounds: a unifying hypothesis on their pathogenesis and implications for therapy. *The American Journal of Surgery*, 187, pp. 65S- 70S
- MUSZYNSKI, Z., et al., 2002. Sterility and antibacterial activity of some antibiotics sterilised by irradiation. *Acta Poloniae Pharmaceutica*, 59 (6), pp. 433-5

MYCOCK, G., 1985. Methicillin/antiseptic resistant *Staphylococcus aureus*. *The Lancet*, 26, pp. 949-950

N

NAGASAWA, N., et al., 2000. Radiation induced degradation of sodium alginate. *Polymer Degradation and Stability*, 69 (3), pp. 279-285

NEWMAN, R. G., et al., 2006. Visualisation of bacterial sequestration and bactericidal activity within hydrating Hydrofiber® wound dressings. *Biomaterials*, 27 (7), pp. 1129-1139

NHO, C. Y., et al., 2009. Preparation and characterisation of PVA/PVP/glycerine/antimicrobial agent hydrogels using γ -irradiation followed by freeze-thawing. *Korean Journal of Chemical Engineering*, 26 (6), pp. 1675-1678

O

ORYAN, A. and ZAKER, S. R., 1998. Effects of topical application of honey on cutaneous wound healing in rabbits. *Zentralbl Veterinarmed A*, 45 (3), pp. 181-8

P

PARK, S., et al., 2003. Biological characterisation of EDC-crosslinked collagen-hyaluronic acid matrix in dermal tissue restoration. *Biomaterials*, 24 (9), pp. 1631-1641

PARKER, L., 2000. Applying the principles of infection control to wound care. *British Journal of Nursing*, 9 (7), pp. 394-404

PEPPAS, A. N. and BURI, A. P., 1985. Surface, interfacial and molecular aspects of polymer bioadhesion on soft tissues. *Journal of Controlled Release*, 2, pp. 257-275

PERRIE, Y. and RADES, T., 2010. FastTrak: Pharmaceuticals drug delivery and targeting. London: Pharmaceutical Press. pp. 107-108

PIERCE, F. G. and MUSTOE, A. T., 1995. Pharmacologic enhancement of wound healing. *The Annual Review of Medicine*, 46, pp. 467-81

PITTEN, A. F., WERNER, P.H., KRAMER, A., 2003. A standardised test to assess the impact of different organic challenges on the antimicrobial activity of antiseptics. *Journal of Hospital Infection*, 55 (2), pp. 108-115

POON, K.M. V. and BURD, A., 2004. In vitro cytotoxicity of silver: implication for clinical wound care. *Burns*, 30 (2), 140-147

POSNETT, J and FRANKS, P.J., 2008. The burden of chronic wounds. *Nursing Times*, 104 (3), pp. 44-45

PUISO, J., et al., 2011. Modification of Ad-PVP nanocomposites by gamma irradiation. *Material Science and Engineering B, In Press*

PUTTIPIPATKHACHORN, S., et al., 2001. Drug physical state and drug-polymer interactions on drug release from chitosan matrix films. *Journal of Controlled Release*, 75 (1-2), pp. 143-153

R

RAYMENT, A. E., et al., 2008. Attenuation of protease activity in chronic wound fluid with biophosphonate-functionalised hydrogels. *Biomaterials*, 29, pp. 1785-1795

REZA, S., QUADIR, A. M., HAIDER, S. S., 2003. Comparative evaluation of plastic, hydrophobic and hydrophilic polymers as matrices for controlled-release drug delivery. *Journal of Pharmaceutical Science*, 6 (2), pp. 282-291

ROSSI, S., et al., 2007. Wound dressings based on chitosan and hyaluronic acid for the release of chlorhexidine diacetate in skin ulcer therapy. *Pharmaceutical Development and Technology*, 12 (4), pp. 415-422

ROSIK, M. J., et al., 1995. Radiation formation of hydrogels for medical purposes; some remarks and comments. *Radiation Physics and Chemistry*, 46 (2), pp. 161-168

ROSIK, M. J., 1994. Radiation formation of hydrogels for drug delivery. *Journal of Controlled Release*, 31 (1), pp. 9-19

ROSIK, M. J., OLEJNICZAK, J., PEKALA, W., 1990. Fast reaction of irradiated polymers- I. Crosslinking and degradation of polyvinylpyrrolidone. *International Journal of Radiation Application and Instrumentation. Part C. Radiation Physics and Chemistry*, 36 (6), pp. 747-755

S

SARISUTA, N., et al., 1999. Physico-chemical characterisation of interactions between erythromycin and various films polymers. *International Journal of Pharmaceutics*, 186 (2), pp. 109-118

SCHÄFFER, M., WITTE, M., BECKER, H. D., 2002. Models to study ischemia in chronic wounds. *Lower Extremity Wounds*, 1 (2), pp. 104-111

SCHLECHT, F. M., 1998. Molecular modelling on the PC. New York: John Wiley & Sons, Inc., pp. 1-10.

SCHREML, S., et al., 2010. Wound healing in the 21st century. *Journal of the American Academy of Dermatology*, 63 (5), pp. 866-881

SCHULTZ, S. G., LADWIG, G., WYSOCKI, A., 2005. Extracellular matrix: review of its roles in acute and chronic wounds. *World Wide Wounds*, www.worldwildwounds.com

SEN, M., et al., 2010. Effect of G/M ratio on the radiation-induced degradation of sodium alginate. *Radiation Physics and Chemistry*, 79 (3), pp. 279-282

- SHENOY, L.S., et al., 2005. Role of chain entanglements on fibre formation during electrospinning of polymer solutions: good solvent, non-specific polymer-polymer interaction limit. *Polymer*, 46 (10), pp. 3372-3384
- SHERERTZ, J. R., et al., 1996. Gamma radiation-sterilised, triple-lumen catheters coated with low concentration of Chlorhexidine were not efficacious at preventing catheter infections in intensive care unit patients. *Antimicrobial Agents and Chemotherapy*, 40 (9), pp. 1995-1997
- SILINDIR, M. and OZER, Y. A., 2009. Sterilisation methods and the comparison of E-beam sterilisation with gamma radiation sterilisation. *FABAD Journal of Pharmaceutical Science*, 34, pp. 43-53.
- SILVA, D. A., et al., 2003. Effect of mono and divalent salts on gelation of native, Na and deacetylated *Sterculia striata* and *Sterculia urens* polysaccharide gels. *Carbohydrate Polymers*, 54 (2), pp. 229-236
- SINGH, R.R.T., WOOLFSON, D.A. and DONNELLY, F.R., 2010. Investigation of solute permeation across hydrogels composed of poly (methyl vinyl ether-co-maleic acid) and poly (ethylene glycol). *Journal of Pharmacy and Pharmacology*, 62 (7), pp. 829-837
- SUBASHINI, M., et al., 2011. Molecular dynamic simulation of drug uptake by polymer. *Journal of Molecular Modelling*, 17 (5), pp. 1141-1147
- SULLIVAN, P. T., et al., 2001. The pig as a model for human wound healing. *Wound Repair and Regeneration*, 9 (2), pp. 66-76
- T**
- TANG, Q., et al., 2009. Synthesis of polyacrylate/polyethylene glycol interpenetrating network hydrogel and its sorption of heavy-metal ions. *Science and Technology of Advance Materials*, 10 (1), pp. 1-7
- THOMAS, A., HARDING, G. K., MOORE, K., 2000. Alginates from wound dressings activate human macrophages to secrete tumour necrosis factor- α . *Biomaterials*, 21 (17), pp. 1797-1802
- THOMAS, S., 1990. Wound management and dressings. The Pharmaceutical Press, pp. 20-42
- THOMAS, S., 2007. Fluid handling properties of Allevyn dressings. *Wound Management Communications*, pp. 1-8
- THOMAS, S., et al., 1996. The effect of dressings on the production of exudate from venous leg ulcer. *Wounds*, 8 (5), pp. 145-50
- TONKS, A. J., et al., 2003. Honey stimulates inflammatory cytokine production from monocytes. *Cytokine*, 21 (5), pp. 242-247
- TORRE, M. P., et al., 2003. Release of amoxicillin from polyionic complexes of chitosan and poly (acrylic acid). Study of polymer-polymer and polymer-drug interactions within the network structure. *Biomaterials*, 24 (8), pp. 1499-1506

TSIPOURAS, N., RIX, J.C., and BRADY, H. P., 1995. Solubility of silver sulfadiazine in physiological media and relevance to treatment of thermal burns with silver sulfadiazine cream. *Clinical Chemistry*, 41 (1), pp. 87-91

V

VERBEKEN, D., DIERCKX, S., DEWETTINCK, K., 2003. Exudate gums: occurrence, production and applications. *Applied Microbiology Biotechnology*, 63 (1), pp. 10-21

VLACHOU, M., et al., 2001. Swelling properties of various polymers used in controlled release systems. *Journal of Biomaterials Applications*, 16 (2), pp. 125-138

W

WALKER, M., et al., 2003. Scanning electron microscopic examination of bacterial immobilisation in carboxymethyl cellulose (AQUACEL®) and alginate dressings. *Biomaterials*, 24 (5), pp. 883-890

WEBER, J. D., RAASCH, R., RUTALA, A. W., 1999. Nosocomial infections in the ICU: the growing importance of antibiotic-resistance pathogens. *CHEST*, 115 (3), pp. 34-41

WERDIN, F., et al., 2009. Evidence-based management strategies for treatment of chronic wounds. *Journal of Plastic Surgery*, 9 (19), pp. 169-179

WHITE, J. R. and COOPER, R., 2005. Silver sulphadiazine: a review of the evidence. *Wounds UK*, 1 (2), pp. 51-62

WHITE, R and CUTTING, F. K., 2006. Modern exudate management: a review of wound treatments. *World Wide Wounds*, www.worldwildwounds.com

WIDGEROW, A.D., 2008. Persistence of the chronic wound – implicating biofilms. *Wound Healing Southern Africa*, 1 (2), pp. 5-8

WILLIAMS, A., 2003. Transdermal and topical drug delivery: from the theory to the clinical practice. 1st ed. Pharmaceutical Press. pp. 1.1-1.2.3

WILSON, M. and HARVEY, W., 1989. Prevention of bacterial adhesion to denture acrylic. *Journal of Dentistry*, 17 (4), pp. 166-170

WOLCOTT, R. D., RHOADS, D. D., DOWD, E.S., 2008. Biofilms and chronic wound inflammation. *Journal of Wound Care*, 17 (8), pp. 333-341

WOODS, E. J., COCHRANE, C.A., PERCIVAL, S. L., 2009. Prevalence of silver resistance genes in bacteria isolated from human and horse wounds. *Veterinary Microbiology*, 138 (3-4), pp. 325-329

www.dressings.org

www.greatvistachemicals.com

www.pubchem.ncbi.nlm.nih.gov

Z

ZAGORSKI, P. Z., 2004. Radiation chemistry of spurs in polymers. International Atomic Energy Agency (IAEA); Advances in Radiation Chemistry of Polymers, November, pp. 21-31